Mammalian Toxicity of Raw and Physico-Chemically Treated Oil Sands Process-Affected Waters

Final Report

Submitted to Alberta Innovates – Energy and Environment Solutions ("AI-EES")

Principle Investigator: Dr. Mohamed Gamal El-Din
Co-Investigators: Dr. Miodrag Belosevic
Dr. James Stafford

Report: Final Report
Project Start Date: May 2014
Project End Date: June 2017

July 2017

Executive Summary

Large volumes of oil sands process-affected water (OSPW) have been produced during the bitumen extraction process from the oil sands industry in the Alberta oil sands region. OSPW contains elevated concentrations of total dissolved solids (TDS), metals, and organic acids naturally present in bitumen. OSPW is currently stored in tailings ponds for its reuse in the bitumen extraction process, process cooling, and material hydro-transport. As a part of the industry's reclamation plan, OSPW in tailings ponds will be treated and eventually be developed into terrestrial and/or aquatic habitat upon mine closure.

Several treatment approaches have been investigated to treat and reclaim OSPW. Biological treatment strategies that rely on natural or managed microbiological degradation are likely too slow to keep up with the rapid expansion of the industry, particularly if discharge (i.e., release) of reclaimed OSPW into the receiving environment is required. In this research, a more sustainable solution is proposed to accelerate the degradation of naphthenic acids (NAs) and other organic compounds present in OSPW using advanced oxidation processes (AOPs) such as ozonation and ozone/hydrogen peroxide (peroxone) treatment. If successful, this would enable the return of reclaimed OSPW to natural systems sooner. Previous studies have reported that ozonation is effective to degrade the acid-extractable fraction (AEF) and increase the OSPW biodegradability. Ozonation has also been found to reduce the OSPW toxicity towards *Vibrio fischeri* and attenuate the developmental toxicity to early life stages of the fathead minnow (*Pimephales promelas*).

Little research has been carried out regarding the OSPW and NA toxicity in mammals. Our previous findings indicate that a concentration-dependent acute and sub-chronic OSPW immunotoxicity in fish and mammals can be significantly reduced by ozone treatment. Since OSPW organic fraction (OSPW-OF) contains a variety of other potentially toxic chemicals in addition to NAs (e.g., polyaromatic hydrocarbons; PAHs), it is not known whether the toxic effects of OSPW-OF are due solely to NAs or other toxic compounds in the organic fractions of OSPW or a combination of both.

The main objective of this research was to compare the possible toxic effects of the whole OSPW and OSPW-OF on the development and reproduction of mammals. Specifically, *in vitro* (mammalian cell lines) and *in vivo* (mouse model system) were used to examine the effects of OSPW-OF and whether advanced oxidation treatment (i.e., ozonation) decreased the toxicity of OSPW-OF.

Characterization of OSPW Matrices

Our study started with the characterization of OSPW before and after treatment by determining the main physico-chemical parameters. In addition, the AEF in OSPW was analyzed by Fourier transform infrared spectroscopy (FT-IR), while classical NAs (i.e., O_2-NAs) and oxidized NAs (O_x-NAs) were semi-quantified using ultra-performance liquid chromatography

time-of-flight mass spectrometry (UPLC-TOF-MS). Ion mobility spectroscopy (IMS) was applied to raw and treated OSPW samples to provide qualitative information of NA species. UPLC-TOF-MS results indicated that the organics in raw OSPW mainly contained classical NAs, oxidized NAs and sulfur containing NA species (S-NAs). The dominant oxidized species in raw OSPW from Aurora pond were O_3-NAs (i.e., NAs with an additional oxygen atom) and O_4-NAs (i.e., NAs with two additional oxygen atoms) (Figures 3 and 4).

Based on FTICR-MS results (Figure 9), the dominant specie in raw OSPW (Syncrude 2014 OSPW from Mildred Lake Site) were O_2 (30.3%), O_3 (27.9%), and O_4 (24.9%). O_2S (2.7%), O_3S (4.8%), and O_4S (2.1%) were the major sulfur-containing species. O_2N only accounted for 0.6% of the total intensity, while N_2O_x accounted for 3.9% of the total intensity.

Our results also indicated that the separation of NA species using silver-ion solid phase extraction (SPE) is a valuable method to extract individual NA species (Figures 12 and 13) that are of great interest for environmental toxicology and wastewater treatment research, to conduct species-specific studies. Furthermore, the separated NA species could be widely used as the standard materials for environmental monitoring of NAs from various sources and sites.

Ozonation and Peroxone Treatment of OSPW

Ozonation and a peroxone process (i.e., hydrogen peroxide/ozone; H_2O_2:O_3) using mild-ozone doses of 30 and 50 mg/L were investigated. Although our results indicated that 1:2 peroxone was the optimum dose based on its high degradation of NAs, no significant difference in terms of NA degradation was found between peroxone and ozonation. Our finding also showed that the NA degradation rates increased with increased carbon and hydrogen deficiency (Z) numbers (Figure 16). Suppressing the hydroxyl radical (•OH) pathway by adding tert-butyl alcohol (TBA) reduced the NA degradation in all treatments, while molecular ozone contribution was 50% and 34% for classical and oxidized NAs, respectively (Figure 19). Our findings indicate that both molecular ozone and •OH were important pathways for the degradation of NA species. FTICR-MS results showed that ozonation was effective to transform the O_x species in OSPW. The ozonation process reduced the relative abundance of O_2S species, which were not detected after ozonation. In terms of transformation of nitrogen-containing species, a decrease of the relative abundance of N_2O_x to 0.6% after ozonation was found (Figure 19).

Ozone and •OH can be scavenged by the presence of substances such as chloride and carbonate. Metal cations such as ferrous and ferric ions as well as their oxides present in OSPW may increase the formation of •OH, leading to an increase in the overall efficiency of ozonation. Additionally, some organic compounds can promote the decomposition of ozone to •OH. Therefore, different fractions of OSPW may have different reactivity to molecular ozone or radical species. Additional experiments are being conducted to evaluate the potential for using indigenous transition metal ions and their oxides present in OSPW to generate •OH. By improving the ozonation performance, we will target the most recalcitrant contaminants in OSPW.

***In Vitro* Studies Using Mammalian Cell Lines**

We used several assays to further explore OSPW toxicity and to directly compare the toxic effects induced by raw OSPW and OSPW-OF based on their relative NA content at the cellular level. By examining the survival, growth, gene expression, and functional activities of a representative mammalian immune cell (i.e., mouse macrophages), we observed that the raw OSPW was significantly more harmful at NA concentrations ranging from 10-18 mg/L, compared to OSPW-OF. These data strongly suggest that at NA doses at the lower range reported in tailings ponds (i.e., <20 mg/L), the complex mixture of inorganic and organic components may significantly contribute to toxicity in the non-fractionated raw OSPW.

Specifically, our results show that raw OSPW had a dramatic inhibitory effect on the growth rate of mouse macrophages (Figure 22), and at the highest doses tested (i.e., 12-18 mg/L) raw OSPW was significantly toxic and caused cell lysis (Figures 23 and 25). This resulted in an overall reduction in total cell numbers (Figure 24), an effect that we did not observe when the cells were exposed to equivalent doses of OSPW-OF. At the dose of 10 mg/L NAs, raw OSPW did not significantly affect the numbers of immune cells in culture (Figure 24); however, the exposed cells displayed a dramatic alteration in their cell morphologies that featured a ruffling of their surfaces leading to the appearance of a frayed plasma membrane with multiple intrusive-like structures that are indicative of membrane degeneration and/or disruption of membrane stability (Figure 26). This suggests that the cells were stressed, which was confirmed by monitoring the expression of selected stress response genes. Specifically, we observed increases in the expression levels of stress genes that are hallmarks of cells experiencing oxidative stress and associated DNA damage (Figure 27).

We also monitored examined the ability of immune cells to secrete important hormones of the immune system called cytokines following OSPW-OF exposures (Figures 28-32). Our results show that raw OSPW at 10 mg/L NAs exhibited differential effects on basal cytokine gene expression and cytokine secretion in resting cells. In addition, raw OSPW had variable influences on the mRNA expression and protein secretion levels in activated cells. Alternatively, OSPW-OF at 10 mg/L NAs demonstrated no significant effects on basal or activated cytokine gene expression or secretion. These data suggest there are factors within raw OSPW that selectively affect cytokine networks in immune cells, which may disrupt immune cell activities causing inflammation-related disturbances. The complexity of these effects requires further investigation but our results also indicate that raw OSPW-exposed macrophages have a reduced ability to engulf bacteria. This suggests that combined with the variable effects on cytokine secretion by mouse macrophages, raw OSPW components can also inhibit phagocytosis (Figure 33), a key antimicrobial defense response of mammalian phagocytes. Overall, we have demonstrated using immune cells that the effects of the yet to be identified OSPW constituents are dose-dependent and that they differentially affect the cell biology of immune cells at the gene, protein, and functional levels.

In conclusion, these results suggest that at the doses tested, raw OSPW but not OSPW-OF components affect the growth, survival, gene expression, protein secretion, and function of

immune cells and our newly optimized cell-based assay systems will be important for further characterizing this phenomenon. While beyond the scope of the present study, identification of the factors in raw OSPW responsible for the selective and specific alteration of immune cell responses needs to be addressed in future studies. The assays developed in this study will be important for characterization of these unknown factors further, and as an *in vitro* bioindicator system, the mouse macrophage cell line has proven to be a valuable model for the rapid (and relatively inexpensive) examination of the toxicity of various OSPW samples.

***In Vivo* Studies Using Mice**

To date, there is little information on the effects of OSPW exposure on development and reproduction of mammals. In this study we examined if OSPW-OF posed a health risk to mammals by means of exposure through their drinking water, specifically during the sensitive stages of gestation and lactation. In acute exposure trials (i.e., two weeks), there were no significant effects of OSPW-OF exposures at all doses tested up to 55 mg/L of NAs on the pregnancy parameters of the exposed mice (Table 6) as well as the maternal body weights (Table 7 and Figure 34). Furthermore, plasma hormone levels, plasma cytokine levels, and stress gene expression analyses (Figures 35-37 and Figures 41-45) showed that overall acute OSPW-OF exposures had very little effects on the exposed animals at OSPW-OF doses of 1 mg/L, 10 mg/L and 55 mg/L of NAs. In another set of trials, mice were sub-chronically exposed (i.e., six weeks) to the same doses of OSPW-OF, which once again suggested that up 55 mg/L there were no significant effects on the general pregnancy parameters of mice, including litter size, sex ratio of the pups, and growth rate of the mice and their pups (Table 8 and Figures 49 and 50). Regarding plasma hormone levels, we found that sub-chronic exposures to 10 mg/L OSPW-OF significantly decreased the plasma levels of aldosterone and progesterone (Figure 51), whereas 55 mg/L OSPW-OF significantly enhances plasma aldosterone levels but reduced progesterone (Figure 52). Estradiol and prolactin levels were unaffected by sub-chronic OSPW-OF exposures at all doses tested. There were minor changes in plasma cytokine levels, however, most cytokine proteins measured were not significantly altered by acute OSPW-OF exposures (Figures 53 and 54). When gene expression studies were performed, we observed that sub-chronic OSPW-OF exposures had variable effects on cytokine and stress gene levels depending on the tissue examined (Figures 55-58). Notably, most genes monitored demonstrated no significant changes in expression levels at all doses examined. It also appeared that sub-chronic exposure of pregnant mice to OSPW-OF (1 mg/L, 10 mg/L, and 55 mg/L) had no overall effects on immune cell numbers or their effector functions after six weeks (Figure 61). Finally, when compared with the control samples, no overt pathological changes were observed after acute or sub-chronic exposures that would be indicative of tissue damage, inflammation, or neoplasia (Figure 62).

In conclusion, the results of the present study suggest the risk of acute and sub-chronic toxicity to small wild mammals exposed to OSPW organic fraction, at indicated NA concentrations, in contaminated drinking water is low. Using mice as the surrogate mammalian model, no significant signs of distress (including death, behaviour changes, loss of body weight, and pregnancy failure) were associated with the oral administration of OSPW-OF, either acutely (2-

week) or sub-chronically (6-week) at the doses up to 55 mg/L NAs. In addition, only minor changes in plasma hormone levels, cytokine gene expression, and cytokine protein secretion at all OSPW-OF doses tested after acute and sub-chronic exposures were observed. Furthermore, although a few stress responsive and detoxification genes were slightly altered in livers of female mice and pups after sub-chronic exposures, no histopathological changes were observed. Finally, immune cells isolated from exposed mice did not demonstrate any change in their antimicrobial activities. Overall, the results of our study suggest that OSPW-OF up to 55 mg/L NAs, even on a repeated oral exposure basis, might be below the threshold required to induce toxicity.

Table of Content

Table of Abbreviations

AEF	Acid-Extractable Fraction
AOPs	Advanced Oxidation Processes
BMDM	Bone-Marrow Derived Macrophages
BOD	Biochemical Oxygen Demand
BTEX	Benzene, Toluene, Ethylbenzene, and Xylenes
BrDU	Bromodeoxyuridine (Ataining Agent)
CHA	Cyclohexanoic Acid
COD	Chemical Oxygen Demand
DCM	Dichloromethane
DNA	Deoxyribonucleic Acid
DO	Dissolved Oxygen
ESI	Electrospray Ionization
FT-IR	Fourier Transformation Infrared Spectroscopy
FTICR-MS	Fourier Transform Ion Cyclotron Resonance Mass Spectrometry
FW	Fetal Weight
GCSF	Granulocyte-Colony Stimulating Factor
GD	Gestation Day
GSTs	Glutathione-S-Transferases
HDPE	High-Density Polyethylene
H_2O_2	Hydrogen Peroxide
IMS	Ion-Mobility Spectroscopy
ISD	Internal Standard
LDH	Lactate Dehydrogenase
LLE	Liquid Liquid Extraction
MTT	3-(4,5-Dimethylthiazol-2-yl)-2,5-Diphenyltetrazolium Bromide
NAs	Naphthenic Acids
•OH	hydroxyl radical
OSPW	Oil Sands Process-Affected Water
OSPW-IF	Inorganic Fraction of Oil Sands Process-Affected Water
OSPW-OF	Organic Fraction of Oil Sands Process-Affected Water
OSPW-O_3	Ozonated Oil Sands Process-Affected Water
O_2-NAs	Classical Naphthenic Acids
O_x-NAs	Oxidized Naphthenic Acids
O_3	Ozone
PAHs	Polycyclic Aromatic Hydrocarbons
PCR	Polymerase Chain Reaction
PW	Placental Weight
ROS	Reactive Oxygen Species
SEM	Scanning Electron Microscopy
SFS	Synchronous Fluorescence Spectroscopy

S-NAs	Sulfur-Containing NA Species
SPE	Solid Phase Extraction
TBA	Tert-Butyl Alcohol
TDS	Total Dissolved Solids
TOC	Total Organic Carbon
TS	Total Solids
UPLC-TOF-MS	Ultra-Performance Liquid Chromatography Time-of-Flight Mass Spectrometry
VEGF	Vascular Endothelial Growth Factor

Glossary

Acid-extractable fraction (AEF): is the acid extractable fraction of organic compounds made insoluble in a solution due to a pH change (by adding acid). The addition of acid reduces the organic compounds solubility in water, so they can be extracted using an organic solvent such as dichloromethane (DCM).

Acute toxicity: describes the adverse effects of a substance that result either from a single exposure or from multiple exposures in a short space of time (usually less than 24 hours). To be described as acute toxicity, the adverse effects should occur within 14 days of the administration of the substance.

Biochemical oxygen demand (BOD): is the amount of oxygen consumed by a sample of water collected in field or at site. It indicates the amount of aerobic life.

Carcinogenicity: is the property of a carcinogen. A carcinogen is any substance, radionuclide, or radiation that is an agent directly involved in causing cancer. This may be due to the ability to damage the genome or to the disruption of cellular metabolic processes. Common examples of non-radioactive carcinogens are inhaled asbestos, certain dioxins, and tobacco smoke. Carcinogens are not necessarily immediately toxic, thus their effect can be insidious.

Cell proliferation: is the increase in cell number as a result of cell growth and division. The accurate assessment of cell number and cell proliferation is useful in many high content assays and is a key readout in cytotoxicity and apoptosis applications.

Chemical oxygen demand (COD): is a test for the amount of organic constituents in a solution, with the logic being all organics can be reduced to carbon dioxide (CO_2) and ammonia with a sufficiently strong oxidizing agent (acid).

Chronic toxicity: describes the development of adverse effects as a result of long term exposure to a contaminant or other stressor, typically at concentrations of the contaminant below acute toxicity and is in contrast to acute toxicity. Adverse effects associated with chronic toxicity can be directly lethal but are more commonly sublethal, including changes in growth, reproduction, or behavior. Chronic toxicity is the ability of a substance or mixture of substances to cause harmful effects over an extended period, usually upon repeated or continuous exposure, sometimes lasting for the entire life of the exposed organism.

Cytokines: are a broad and loose category of small proteins that are important in cell signaling. They are released by cells and affect the behavior of other cells and are produced by a broad range of cells, including immune cells like macrophages, B lymphocytes, T lymphocytes and mast cells, as well as endothelial cells, fibroblasts, and various stromal cells. A given cytokine may be produced by more than one type of cell. They act through receptors, and are especially important in the immune system. Cytokines modulate the balance between humoral and cell-

based immune responses, and they regulate the maturation, growth, and responsiveness of particular cell populations. Some cytokines enhance or inhibit the action of other cytokines in complex ways.

Cytokine secretion assays: Mouse macrophages can constitutively secrete soluble protein molecules called cytokines but often they require stimulation to produce a variety of these cytokine molecules during immune responses. There are many different cytokines and each has a distinct function during immune responses that can range from cellular activation, cellular recruitment, promotion of cellular proliferation, and engagement of antimicrobial activities. One potent activator of macrophages is bacteria (e.g., *E. coli*) and following bacterial stimulation macrophages can be examined for their cytokine secretion abilities as an indicator of their activation status. This approach can be used to determine what effects oil sands process-affected water (OSPW) exposures have on the cytokine secreting activities of RAW 264.7 cells.

C-X-C motif chemokine 10: is a small cytokine belonging to the CXC chemokine (signalling proteins) family. It is an important attractant for other immune cells (i.e., chemoattractant) by bringing them into the inflammatory site.

Developmental toxicity: is any structural or functional alteration, reversible or irreversible, which interferes with homeostasis, normal growth, differentiation, development or behavior of an organism and which is caused by environmental factors and chemicals.

Dissolved organic carbon (DOC): is the amount of carbon in solution that will pass through a fine filter (e.g., 0.22 μm). This is operationally thought to be the dissolved carbon fraction of a water sample.

Down-regulation of immune responses: Any measurable component of an immune cell effector response that is significantly inhibited or reduced relative to untreated control cells. Down-regulated immune responses are measured at doses that do not also significantly reduce immune cell viability such that the quantity of the response being evaluated is not reduced due to an associated decrease in viable cell numbers.

Fourier transformation infrared spectroscopy (FT-IR): is the technique which is used to obtain an infrared spectrum of absorption or emission of a sample. The sample absorbs or emits photons in the infrared wavelengths. The absorption of certain wavelengths is linked to certain functional groups in a molecule such as carboxylic acid, double bounds, hydroxylic groups, etc. and reveals the structural properties of a molecule.

Fourier transform ion cyclotron resonance mass spectrometry (FTICR-MS): is a type of mass analyzer (or mass spectrometer) for determining the mass-to-charge ratio (m/z) of ions based on the cyclotron frequency of the ions in a fixed magnetic field. FTICR-MS provides compositional information (i.e., qualitative analysis) of the naphthenic acids including oxidized species and heteroatomic (S and N) species present in OSPW.

Genotoxicity: describes the property of chemical agents that damages the genetic information within a cell causing mutations, which may lead to cancer. The alteration can have direct or indirect effects on the DNA: the induction of mutations, mistimed event activation, and direct DNA damage leading to mutations. The permanent, heritable changes can affect either somatic cells of the organism or germ cells to be passed on to future generations.

Granulocyte-colony stimulating factor: (G-CSF or GCSF) is a glycoprotein that stimulates the bone marrow to produce granulocytes and stem cells and release them into the bloodstream. Functionally, it is a cytokine and hormone, a type of colony-stimulating factor, and is produced by a number of different tissues. It also stimulates the survival, proliferation, differentiation, and function of neutrophil precursors and mature neutrophils. Therefore, this cytokine is important for the generation of additional immune cells.

Homeostasis: is the property of a system in which variables are regulated so that internal conditions remain stable and relatively constant. Examples of homeostasis include the regulation of temperature and the balance between acidity and alkalinity (pH). It is a process that maintains the stability of the internal environment of an organism in response to changes in external conditions. All living organisms depend on maintaining a complex set of interacting metabolic chemical reactions. From the simplest unicellular organisms to the most complex plants and animals, internal processes operate to keep the conditions within tight limits to allow these reactions to proceed. Homeostatic processes act at the level of the cell, the tissue, and the organ, as well as for the organism as a whole.

Immunomodulatory properties: Any measurable component of an immune cell effector response that is significantly altered relative to untreated control cells. Depending on the measured outcome immunomodulatory properties can result in either the suppression (i.e., down-regulation) or stimulation (i.e., up-regulation) of immune responses. These effects are measured at doses that do not also significantly reduce immune cell viability such that the quantity of the response being evaluated is not reduced due to an associated decrease in viable cell numbers.

Immunotoxicity: is defined as adverse effects on the functioning of the immune system resulting from exposure to chemical substances. Altered immune function may lead to the increased incidence or severity of infectious diseases or cancer, since the immune system's ability to respond adequately to invading agents is suppressed.

Interleukin (IL)-1β: is a member of the interleukin 1 family of cytokines. This cytokine is produced by activated macrophages as a proprotein, which is proteolytically processed to its active form by caspase 1 (CASP1/ICE). This cytokine is an important mediator of the inflammatory response, and is involved in a variety of cellular activities, including cell proliferation, differentiation, and apoptosis. It is an important mediator of the inflammatory response controlling cellular proliferation, differentiation, and apoptosis.

***In vitro* studies:** are performed with cells or biological molecules studied outside their normal biological context. For example, proteins are examined in solution, or cells in artificial culture medium.

***In vivo* studies**: are those in which the effects of various biological entities are tested on whole, living organisms usually animals including humans, and plants as opposed to a partial or dead organism, or those done *in vitro* using test tubes, petri dishes, etc. Examples of investigations *in vivo* include: the pathogenesis of disease by comparing the effects of bacterial infection with the effects of purified bacterial toxins; the development of antibiotics, antiviral drugs, and new drugs generally; and new surgical procedures. Consequently, animal testing and clinical trials are major elements of *in vivo* research. *In vivo* testing is often employed over *in vitro* because it is better suited for observing the overall effects of an experiment on a living subject.

Macrophages: are a type of white blood cell that engulfs and digests cellular debris, foreign substances, microbes, cancer cells, and anything else that does not have the types of proteins specific to the surface of healthy body cells on its surface in a process called phagocytosis. They play a critical role in non-specific defense (innate immunity), and also help initiate specific defense mechanisms (adaptive immunity) by recruiting other immune cells such as lymphocytes.

Macrophage cell-line (RAW 264.7): was originally derived from mouse blood and was established from the ascites of a tumor induced in a male mouse by intraperitoneal injection of Abselon Leukaemia Virus (A-MuLV). These cells are commonly used in metabolic, inflammation and apoptosis studies and can be obtained from the American Type Culture Collection (ATCC; Rockville, MD, USA).

Naphthenic acids (NAs): are a group of alkyl-substituted of aliphatic and alicyclic carboxylic acids and are natural constituents in many petroleum sources. NAs have empirical formulas of $C_nH_{(2n+Z)}O_x$ or $C_nH_{(2n+Z)}O_yS$, where n is the carbon number ($7 \leq n \leq 26$), Z is zero or a negative even integer ($0 \leq |Z| \leq 18$) that specifies the hydrogen deficiency resulting from ring or unsaturated bonding formation, and x and y represent the number of oxygen atoms ($2 \leq x \leq 5$, and $2 \leq y \leq 4$). x=2 for classical NAs (O_2-NAs) and $x \geq 3$ for oxidized NAs (O_x-NAs). Classical NAs from petroleum refineries are predominantly aliphatic acids, while oil sands NAs are predominantly alicyclic acids. Additionally, there is evidence that oil sands NAs include adamantane acids and pentacyclic diamantane acids, aromatic NAs, oxidized NAs and heteroatomic (nitrogen and sulphur) NAs.

Necrosis: is a form of cell injury that results in the premature death of cells in living tissue by autolysis. It is caused by factors external to the cell or tissue, such as infection, toxins, or trauma that result in the unregulated digestion of cell components.

Neurotoxicity: occurs when exposure to toxic substances, alters the normal activity of the nervous system in such a way as to cause damage to nervous tissue. This can eventually disrupt

or even kill neurons, key cells that transmit and process signals in the brain and other parts of the nervous system.

Oil sands process-affected water (OSPW): is a general term used to describe waters that are generated through the mining and extraction of bitumen from oil sands. It is used to describe all waters that are found on site, including groundwater from depressurizing aquifers found within and below the oil sands ore layer; surface water and shallow aquifer water from dewatering activities undertaken to prepare the mine area prior to mining; precipitation and surface water runoff; water collected from dyke seepage control systems; connate water (water that forms part of the ore deposit); and, depending on the operator, effluent from bitumen upgrading facilities. OSPW contains a complex mixture of organics (i.e., carbon containing compounds) and inorganics (no carbon) such as metals and salts.

Phagocytosis: is the process by which a cell—often a phagocyte or a protist—engulfs a solid particle to form an internal vesicle known as a phagosome. In multicellular animals, the process has been adapted to eliminate debris and pathogens.

Polycyclic aromatic hydrocarbons (PAHs): are groups of hydrocarbons, which are composed of multiple aromatic rings. PAHs are neutral, nonpolar molecules; they are found in fossil fuels (oil and coal) and in tar deposits, and are produced, generally, when insufficient oxygen or other factors result in incomplete combustion of organic matter. Some PAHs have been identified as carcinogenic and mutagenic (as well as teratogenic), and are considered pollutants of concern for the potency of adverse health impacts.

Reproductive toxicity: is a hazard associated with substances that will interfere in some way with normal reproduction. It includes adverse effects on sexual function and fertility in adult males and females, as well as developmental toxicity in the offspring.

Subchronic toxicity: is the ability of a substance to cause effects for an extended period of time, but less than the lifetime of the exposed organism.

Synchronous fluorescence spectroscopy (SFS): is an analytical technique to analyze fluorescent compounds in a solution. Fluorescence is the ability of certain compounds to absorb light of one wavelength and emit light with a different (longer) wavelength. This technique gives information about a single target compound. If several fluorescent compounds are present in a solution, no distinction between compounds can be made, as the excitation/emission wavelengths overlap and change the emission spectrum. Nevertheless, this technique can be used to monitor qualitatively the presence of fluorescence compounds, which include aromatic hydrocarbons.

Total organic carbon (TOC): is the total amount of carbon-containing compounds in water and may be used as a water quality indicator.

Vascular endothelial growth factor (VEGF): is a signal protein produced by cells that stimulates vasculogenesis and angiogenesis. It is part of the system that restores the oxygen supply to tissues when blood circulation is inadequate. VEGF's normal function is to create new blood vessels during embryonic development, new blood vessels after injury, muscle following exercise, and new vessels (collateral circulation) to bypass blocked vessels.

1. Background

Large volumes of oil sands process-affected water (OSPW) are produced by the surface-mining oil sands industry in Alberta. OSPW is stored in tailings containment facilities to ensure it can be recycled for bitumen extraction, process cooling, and hydro-transport of materials. As part of the industry's reclamation plan, tailings containment facilities will eventually be developed into terrestrial or aquatic habitat that can sustain functions similar to natural habitats in the region. Therefore, water treatment approaches are required to increase the OSPW quality to allow its release into the environment for land reclamation.

OSPW is a saline mixture of suspended and dissolved solids, inorganics (metals), and organic compounds (e.g., naphthenic acids; NAs). OSPW is considered brackish water due to high salinity and total dissolved solids (TDS) [1]. OSPW has been reported to cause both acute and sub-chronic toxicity to a variety of organisms, including aquatic invertebrates, fish, amphibians, birds, and mammals [2-5]. For instance, it has been found that the long-term OSPW exposure significantly inhibits feeding behaviour, suppresses growth, and reduces reproductive output of *Daphnia magna* [6]. The exposure of fish to OSPW has been associated with increased levels of oxidative stress [7], fin erosion, virally induced tumors, gill abnormalities (aneurisms), increased skin (epithelial) cell proliferation [8], increased mucous cell proliferation, and gill cell necrosis [9]. Chronic exposure of fish to OSPW has resulted in increased prevalence of tumors, presumably due to decreased immune responsiveness [10].

Since the organic fraction in OSPW contains a variety of other potentially toxic chemicals in addition to NAs (e.g., polycyclic aromatic hydrocarbons (PAHs), phenols and BTEX), it is not known whether the toxic effects of raw OSPW are due solely to NAs, a combination of NAs and other organic toxic compounds or a combination of the organic and inorganic fractions of OSPW. Evidence supports that NAs are among the most acutely toxic chemical classes in OSPW. However, polar neutral organic compounds (i.e., non-carboxylic acid chemical classes that include O_2^+, O^+, OS^+, and NO^+ species) have also been found to contribute to acute toxicity [11]. Recently, Hughes et al. (2017) reported that the toxicity of OSPW to rainbow trout (*Oncorhynchus mykiss*) was due to classical NAs, with the potency of individual compounds increasing as a function of carbon number [12]. Notably, it was found that the toxicity was largely a function of classical NAs with ≥ 17 carbons. Because the dissolved organic compounds in OSPW have potential to alter partitioning and effects of PAHs on aquatic organisms, the interactions among organic compounds that co-exist in OSPW and their effect on OSPW toxicity warrant future research [13].

Little research has been carried out regarding OSPW and NA toxicity in mammals [5, 14-16]. Studies using cells derived from mice have shown that exposing certain kinds of white blood cells, such as bone-marrow derived macrophages, to relatively high concentrations of commercial NAs, as well as the organic constituents of OSPW (OSPW-OF) caused a decrease in the response of those macrophages to infection (antimicrobial responses) and decreased cell proliferation ability upon exposure [14]. *In vivo* studies using mice have shown that acute and in

particular sub-chronic oral exposure to OSPW-OF resulted in significant down-regulation of immune responses, suggesting that these animals would be less successful in fighting off infections. As a result, both the immune gene expression and the functions of immune cells isolated from exposed animals were suppressed [5, 17].

Ozone treatment has been studied as a potential tool to assist in remediation efforts, as it has been shown to degrade the acid-extractable fraction (AEF; organic compounds made insoluble in a solution due to a pH) and increase the OSPW biodegradability [18]. Our previous findings also indicated that the immunotoxic effects were concentration-dependent after both acute and subchronic exposure of fish to OSPW and mammals to OSPW-OF, and that these effects were significantly reduced by ozone treatment [5, 19].

Although ozonation is one of the most efficient advanced oxidation processes (AOPs) to attain the mineralization of refractory and toxic compounds [20], the application of ozonation alone has some limitations as molecular ozone (O_3) reactions are selective and limited to aromatic, unsaturated aliphatic pollutants and some functional groups. A combination of peroxone (hydrogen peroxide/ozone; H_2O_2:O_3) seems to be a suitable alternative to overcome these limitations. The combination of O_3 and H_2O_2 can significantly produce more hydroxyl radicals (•OH) for the degradation of ozone-resistant compounds [21, 22]. H_2O_2 is an initiator for O_3 decomposition; however, high H_2O_2 concentrations should be avoided as it acts as an inhibitor for the O_3 decomposition [23].

2. Objectives

The main objective of this research was to compare the possible toxic effects of the whole OSPW and the organic fraction of OSPW (OSPW-OF) on development and reproduction of mammals. Specifically, the *in vitro* (mammalian cell lines) and *in vivo* (mouse model system) were used to examine the effects of OSPW-OF and whether advanced oxidation treatment (i.e., ozonation) decreased the toxicity of OSPW-OF. The main objectives per research area are presented below.

2.1 Characterization of OSPW

Organic compounds present in OSPW include NAs, PAHs, BTEX, and other species, along with heteroatomic components. Some of these species have not been fully characterized, in particular NAs. Because the molecular structure of organic compounds has been found to be a key factor controlling the OSPW toxicity, the development of analytical methods for the characterization of OSPW is needed. Therefore, the objectives of this component of the research project were:

1) to perform a complete physical and chemical characterization of OSPW matrices before and after ozone-based treatment;

2) to develop advanced analytical methods to identify and characterize NA species, using ion mobility and liquid chromatography/mass spectrometry as well as Fourier transform ion cyclotron resonance mass spectrometry techniques;
3) to develop a method to separate the organic and inorganic fractions in OSPW; and
4) to develop a method using silver-ion (Ag-ion) solid phase extraction (SPE) to separate the different NA species

2.2 Treatment of OSPW

Ozonation has emerged as an efficient treatment process for the oxidation of recalcitrant contaminants. Ozonation is not only effective to degrade organic contaminants, but also to remove inorganic components such as soluble iron and manganese, cyanides and nitrites as well as suspended solids. During ozonation, pollutants such as contaminants of emerging concerns and endocrine disrupters can be oxidized either by molecular O_3 or by •OH formed as a consequence of the O_3 decay. It has been found that the combination of O_3 and hydrogen peroxide (H_2O_2) (i.e., peroxone treatment) can significantly produce more •OH for the degradation of ozone-resistant compounds [21, 22]. The presence of other water constituents such as metal ions, reduced inorganic compounds, and organic matter (i.e., humic acid) in the OSPW matrix, can impact the efficiency of ozonation to degrade target pollutants. Therefore, the objectives of this component of the research program were:

1) to assess the efficiency of ozone and peroxone treatment in terms of NA degradation;
2) to evaluate the influence of carbon (n) and hydrogen deficiency (Z) numbers on the structure reactivity toward classical and oxidized NAs;
3) to understand the oxidation mechanisms during the ozonation and peroxone treatment of OSPW; and
4) To investigate the effect of the OSPW inorganic fraction (OSPW-IF) on the ozonation performance.

2.3 *In Vitro* Studies Using Mammalian Cell Lines

The main goal of our *in vitro* studies was to determine if doses of raw OSPW from Aurora pond, the organic fraction (OSPW-OF), and ozonated raw OSPW (OSPW-O_3) and OSPW-OF (OSPW-O_3-OF) were acutely toxic to cultured mammalian cells. We examined whether the exposure of mammalian cells to OSPW affected their viability (live/dead assays), their proliferation (i.e., divide) *in vitro*, and their stress gene levels. In addition, various physiologically relevant doses of these waters were tested for their immunotoxic effects by determining whether they interfered with two important functions of immune cells; namely bacterial engulfment (i.e., phagocytosis) and the expression and secretion of bioactive protein molecules called cytokines. Establishment of this testing methodology was required for standardized *in vitro* assessments of OSPW-mediated acute toxicity and OSPW-mediated immunotoxicity. Using these protocols in the future will enable the evaluation of OSPWs from different mining sites allowing for direct comparisons between different OSPW sources and their associated treatments.

2.4 *In Vivo* Studies Using Mice

The main goal of our *in vivo* studies was to determine whether the OSPW-OF induced reproductive toxicity and/or immunotoxic effects during pregnancy and lactation of mice. In addition, we also examined whether ozonation of the whole OSPW and OSPW-OF influenced its potential reproductive toxicity and/or immunotoxic effects. Completion of this objective was important for the establishment of a series of *in vivo*-based protocols required for conducting further OSPW toxicity assessment in mammals.

3. Materials and Methods

3.1 OSPW Sampling and Analyses

OSPW samples from different sources were used in this research. For the mammalian toxicity tests, OSPW was collected from Syncrude Aurora pond in 2013. For the treatment assessments using ozonation, OSPW samples were obtained from Syncrude's Mildred Lake Tailings Facility in 2014 and Shell OSPW obtained from Muskeg River Mine External Tailings Facility in 2015. Upon delivery, the OSPW samples were stored in high density polyethylene (HDPE) barrels in a cold room at 4°C until use. Prior to use, the OSPW samples were analyzed for a suite of water quality and chemical parameters, including total organic carbon (TOC), biochemical oxygen demand (BOD), and chemical oxygen demand (COD), among other parameters. These parameters were measured using the Standard Methods [24].

To characterize the organic compounds present in OSPW, the following techniques were used:

- Fourier transform infrared spectroscopy (FT-IR) to measure AEF;
- Ultra-performance liquid chromatography time-of-flight mass spectrometry (UPLC-TOF-MS) to semi-quantify classical (O_2-NAs) and oxidized NAs (O_x-NAs);
- Ion-mobility spectrometry (IMS) to separate and identify classical NAs, oxidized NAs, and S-NAs (i.e., qualitative analysis);
- Fourier transform ion cyclotron resonance mass spectrometry (FTICR-MS) to provide compositional information of the NAs including O_x species and heteroatomic (S and N) species (qualitative analysis); and
- Synchronous fluorescence spectroscopy (SFS) for the semi-quantitative analysis of fluorophore organic compounds (i.e., compounds that can re-emit light upon light excitation).

3.1.1 FT-IR analysis

The quantification of AEF was conducted using a Nicolet 8700 FTIR spectrometer. The fixed path length of KBr liquid cell was 3 mm. Purge gas generator from Parker Balston Model 75-52 was used while running the samples. Omnic Software was used to acquire and process the spectrum. The sample spectrum was recorded for 128 scans after a 7-minute purge. The peak height or absorbance was recorded at both wavelengths of 1743 and 1706 cm^{-1}, which correspond to the characteristic adsorption band of the monomeric and dimeric forms of carboxylic groups. The concentration of AEF in the OSPW samples was calculated based on a

prepared calibration curve using a commercial mixture of NAs (Fluka) as standard and the total of recorded peak heights [25]. All samples were analyzed in duplicate.

AEF was prepared by acidifying OSPW to pH 2 and extracted two times with dichloromethane (DCM) in a separation funnel. Volume ratios were 1 volume sample to 0.5 volume DCM. After separation, DCM was evaporated, leaving the extracted acid-extractable organics. The AEF was then analyzed using FT-IR. Prior to the FT-IR analyses, the extracted acid-extractable organics were reconstituted with a known mass of DCM.

3.1.2 UPLC-TOF-MS analysis

Because NAs are a mixture of hundreds of cyclopentyl and cyclohexyl carboxylic acids, a full quantification method for NAs is not currently available given the lack of standard compounds for every individual NA species. Studies attempting to analyzed NAs have established a representative response factor for OSPW NAs in order to perform a semi-quantification of total NAs, based on the assumption that NAs are a class of carboxylic acids with close properties (e.g., pKa) and ionization efficiencies [26, 27].

In our study, NAs were semi-quantified using an UPLC-TOF-MS system (Synapt G2, Waters, Milford, MA). A 1-mL volume of OSPW sample was centrifuged at 10000 rpm for 10 min. The injection solution was prepared with 500 µL of the supernatant, 100 µL of 4.0 mg/L internal standard (ISD; myristic acid-1-^{13}C) in methanol, and 400 µL methanol to reach a final sample volume of 1 mL. Chromatographic separations were performed using a Waters UPLC Phenyl BEH column (1.7 µm, 150 mm × 1 mm), with mobile phases of 10 mM ammonium acetate in water (A), 10 mM ammonium acetate in 50/50 methanol/acetonitrile (B), and the injection volume of 10 µL. The elution gradient was 0−2 min, 1% B; 2−3 min, increased from 1% to 60% B; 3−7 min, from 60% to 70% B; 7−13 min, from 70% to 95% B; 13−14 min, from 95% to 1% B, and hold 1% B until 20 min to equilibrate column with a flow rate of 100 µL/min. The column temperature was set at 50 °C while the sample temperature was set at 10 °C. The samples were analyzed using the UPLC-TOF-MS with the TOF analyzer in high-resolution mode (mass resolution is 40000) and the investigated mass range of 100-600 (m/z). The electrospray ionization (ESI) source was operated in negative ion mode to measure the NAs. Data acquisition was controlled using MassLynx (Waters) and data extraction from spectra was performed using TargetLynx (Waters). This method was developed previously for NA semi-quantification based on the signal of a compound versus the signal of spiked internal standard [18, 26].

The detected classical and oxidized NAs were based on the general empirical formula $C_nH_{2n+Z}O_x$ (x =2 for classical NAs; x = 3 for O_3-NAs, x = 4 for O_4-NAs, x = 5 for O_5-NAs, and x = 6 for O_6-NAs), with carbon number ranging from 7 to 26 and Z number from 0 to -18. Exact masses of NAs (m/z = ± 0.001) that fit the empirical formula $C_nH_{2n+Z}O_x$ were calculated for entirely combinations of carbon = 7 to 26, Z = 0 to -18 and x = 2 to 4 during the data analyses.

Each individual NA species concentration (C_{NAs}) was estimated using Equation 1. It was assumed that the ionization efficiency of NA species, are similar to the internal standard (ISD) during the process of ion evaporation.

$$C_{(NAs)}=\frac{Area_{(NAs)}}{Area_{(ISD)}}\times C_{ISD} \quad (1)$$

In Equation 1, $C_{(NAs)}$ is the concentration of the NA species, C_{ISD} is the concentration of the internal standard, $Area_{(NAs)}$ and $Area_{(ISD)}$ are the areas under the curve for the NA species and internal standard, respectively.

OSPW is a complex mixture, containing thousands of NA species. Due to the complexity of NA analysis (i.e., hundreds of NA species are analyzed for each sample), in this study we did not use replication of samples as a way of quality control for UPLC-TOF-MS analyses. Instead, we used raw OSPW (i.e., untreated OSPW) as a quality control to monitor the repeatability of the results. Standards were also applied to calibrate the accuracy of the analyzing system. In fact, researchers seldom replicate samples for UPLC-TOFMS analysis since this technique has proved its superiority of constant reliability, accuracy and precision [28-30].

3.1.3 IMS analysis

IMS was conducted in a Tri-Wave® ion-mobility cell of 15 cm long, using nitrogen (purity > 99%) as the drift gas. The IMS consisted of a transfer cell that collected certain amount of ions and a helium gate that released the ions into the ion mobility cell. The number of ions was known and the difference in the number ions had a threshold of 5%. Ions were separated using an electric field (T-wave) that moved the ions in one direction and a gas flow in the counter direction, which drifted the ions based on the cross-collision section.

3.1.4 FTICR-MS analysis

Fourier transform ion cyclotron resonance mass spectrometry (FTICR-MS), Bruker 9.4 T Apex-Qe FTICR-MS from (Bruker Daltonics, Billerica, MA, USA) was used to analyze the samples and estimate the differences in species before and after treatment. The Bruker system was equipped with Bruker Daltonics Data Analysis version 4.0 software to process the raw data which can generate the formulae using the “Smart formula” algorithm. Injection of samples was done through direct infusion at 2.0 µL/min flow rate to an ESI source. Each sample was pretreated using liquid-liquid extraction (LLE) and DCM as the solvent. A subsample (100 mL) of treated and raw water was acidified with sulfuric acid (H_2SO_4) to pH 2 and extracted twice with 50 mL DCM. For negative ESI analysis, each fraction after drying was re-constituted in DCM (1000 mg/L) then a dilution of 500 times was made in isopropyl alcohol (IPA). A final concentration of 2 mg/L was achieved after adding 0.1% (v/v) of ammonium hydroxide (NH_4OH). The collection of the data range was selected between 145-2000 m/z while 10 s was kept as an ion-accumulation time in the external hexapole collision-cell of prior to injection to the ICR cell.

3.1.5 SFS analysis

SFS measurements were performed using a 1-cm cuvette in a Varian Cary Eclipse fluorescence spectrophotometer (Ontario, Canada). The excitation and emission slits were maintained at 5 nm, photomultiplier voltage was 780 mV, offset wavelength was 18 nm, and excitation wavelengths ranged between 200 to 500 nm [31].

3.2 Extraction of OSPW Organic Fraction for Mammalian Toxicity Studies

Multi-steps of LLE using DCM were used to extract the whole organic fraction from raw and ozone-treated OSPW (Syncrude Aurora OSPW 2013). The organic fraction of OSPW (OSPW-OF) was used for various mammalian toxicity studies. Raw and ozonated OSPW samples were first characterized as a baseline for subsequent research.

The organic compounds were isolated from 40 L of OSPW, using a liquid-liquid organic extraction protocol developed in our group (Figure 1) [14]. Specifically, the pH of OSPW was adjusted to 10.5 with sodium hydroxide (NaOH) to ensure that weak organic acids (including NAs) were fully dissolved. OSPW was clarified by centrifugation for 20 min at 15000 g, followed by three rounds of liquid-liquid organic extraction, using 100 mL of DCM per liter of OSPW in each round. DCM (organic phase) was collected after each round and combined. The water phase was then adjusted to pH 2.0 using hydrochloric acid, followed by three additional rounds of DCM extraction. The DCM phase from each round was collected and pooled, followed by the removal of DCM using a rotary evaporator. The resulting organic fraction is known as OSPW-OF. The same extraction protocol was performed on 40 L of distilled water, and the material obtained was used as the control for organic fraction exposure. Once the amount of NAs in the organic fraction was determined by UPLC-TOF-MS (604.66 mg in OSPW-OF), the organic fraction was dissolved in the same amount of distilled water (pH ~10) containing final NAs concentrations of 23.8 mg/mL for OSPW-OF NAs.

3.3 Separation of Classical, Aromatic, Oxidized and Sulfur-Containing NAs

The separation of classical, aromatic, oxidized, and heteroatomic (sulfur-containing) NA species from raw and ozone-treated OSPWs was performed using a silver-ion (Ag-ion) solid phase extraction (SPE) method without requirement of pre-methylation for NAs. Ultra-performance liquid chromatography ion mobility time-of-flight mass spectrometry (UPLC-IM-TOF-MS), which was previously applied in a number of studies for the characterization of OSPW samples, was used to characterize the raw and ozonated OSPWs before SPE and SPE fractions for comparison (e.g., ozonation could remove largely the aromatic NAs that are to be separated via Ag-ion SPE), in order to corroborate the fractionation process for the separation of NA species. The identification of compounds from spectra using accurate mass matching with a mass tolerance of ±1.5 mDa, based on estimated mass errors between measured and calculated masses for NAs, allowed the identification of sulfur-containing NAs from O_2-NAs. The separated NA species facilitated the subsequent tandem mass spectrometry (MS/MS) determination of structural information for different NA species due to the removal of matrix and simplified composition compared to raw OSPW.

The raw and ozonated OSPWs were extracted using Ag-ion SPE tubes for comparative characterization. The ozonated OSPW was prepared from raw OSPW with an utilized ozone dose of 80 mg/L, which was used in previous study [32], by sparging with an ozone generator (WEDECO, GSO-40, Germany).

Pre-extracted sample fraction in hexane was required prior to the Ag-ion SPE process [33]. However, LLE directly using hexane could change the composition of NA species from OSPW

[34]. Thus, the raw and ozonated OSPWs were firstly extracted using DCM. OSPW was mixed uniformly using a motor driven paddle mixer before dividing into 500 mL working aliquots, which were then centrifuged at 10,000 rpm for 10 minutes to remove the suspended particles. Sulfuric acid (H_2SO_4) solution (1.8 M) was added dropwise to adjust the pH of OSPW supernatant (pH 9.4) to 2.0 prior to extraction. In each extraction, a 500-mL sample was extracted with 250 mL DCM (90 mL, 80 mL, and 80 mL sequentially with sample: total solvent = 2:1). The organic layers were separated, combined (~250 mL), and air-dried completely under a fume hood at room temperature. Each fraction was re-dissolved into 10 mL hexane and stored at 4 ºC prior to use.

For Ag-ion SPE, the Ag-ion SPE tube was pre-conditioned using 5 mL acetone for three times and then pre-equilibrated using 5 mL hexane for three times. The OSPW extract (5 mL) was loaded onto the cartridge and then rinsed using 5 mL hexane for three times. SPE fractions were achieved via varying the composition and polarity of eluent solvent mixture, and the elution process was optimized as follows: Fraction 1− Fraction 7 (F1−F7) using 5 mL 97/3 (v/v) hexane/acetone for eluting each fraction, F8−F13 using 5 mL 93/7 (v/v) hexane/acetone for each, F14−F16 using 5 mL 88/12 (v/v) hexane/acetone for each, F17−F19 using 5 mL 82/18 (v/v) hexane/acetone for each, and F20−F22 using 5 mL acetone for each. 100% acetone for F20−F22 was applied to elute out remaining NAs from the SPE cartridge. The SPE fractions were collected in test tubes, which were weighed precisely before use, and air-dried completely in the fume hood at room temperature. The test tubes with dried fractions were weighed again to give the mass of each fraction. Dried fractions were re-dissolved using 1 mL 50/50 acetonitrile/water, with the addition of 1 mg/L myristic acid-1-^{13}C as the internal standard to surrogate the instrument fluctuation in analysis, and stored at 4 ºC prior to analysis.

3.4 Ozonation Experiments

Our first set of experiments focused on the treatment of whole OSPW matrix. Ozonation at high doses is an efficient but costly treatment for the degradation of OSPW NAs. To decrease costs and limit doses, a peroxone (hydrogen peroxide/ozone; H_2O_2:O_3) process using mild-ozone doses of 30 and 50 mg/L was investigated at different H_2O_2:O_3 molar ratios (1:1, 1:2, and 1:3). Ozone and peroxone semi-batch experiments were performed in 4-L vacuum flask reactors at the natural pH of OSPW at room temperature (20 ± 1 °C). Figure 2 shows a schematic of ozonation system. H_2O_2 stock solution of 3,000 mg/L was prepared for the peroxone experiments and the required H_2O_2 dose was added prior to ozone exposure. Treatments included: (a) 30 mg/L utilized ozone dose; (b) 50 mg/L utilized ozone dose; (c) 1:1 peroxone (20 mg/L H_2O_2: 30 mg/L utilized O_3 dose); (d) 1:2 peroxone (11 mg/L H_2O_2 and 30 mg/L utilized O_3 dose); and (e) 1:3 peroxone (10 mg/L H_2O_2 and 50 mg/L utilized O_3 dose). Residual H_2O_2 was quenched at the end of peroxone experiment treatments using bovine liver catalase with 1 µM of H_2O_2 transformed by one unit of catalase per minute.

Ozone was produced by an ozone generator (AGSO 30 Effizon, WEDECO AG Water Technology, Herford, Germany), and monitored throughout the experiments in both the feed and off-gas lines using two identical ozone monitors (HC-500, PCI-WEDECO AG Water Technology, Herford, Germany). After each experiment (around 10 minutes of ozonation with stable feed gas rate)

the OSPW was purged with nitrogen to strip residual ozone to stop further reactions. For the mammalian toxicity tests, ozonation was performed using an utilized ozone dosage of 80 mg/L (high ozone dose), which has been used previously to reduce total NA concentrations of OSPW by over 80% (NAs < 1 mg/L) [18]. Lower ozone concentrations were used in the treatment tests in order to visualize the changes of the different NA species after ozone treatment.

The ozone residual in the reactor was measured using the indigo method. The utilized ozone dose (i.e., amount of ozone reacted with the contaminants in the water phase, including ozone auto-decomposition, per unit water volume) was estimated using Equation 2 [18]:

$$\Delta O_3 = \int_0^t \frac{\left(Q_{G,in}\, C_{G,in} - Q_{G,out}\, C_{G,out}\right)}{V_L} dt - C_L \qquad (2)$$

where ΔO_3 is the amount (mg/L) of the utilized ozone; $Q_{G,in}$ is the feed gas flow rate (L/min); $Q_{G,out}$ is the off-gas flow rate (L/min); $C_{G,in}$ is the ozone concentration (mg/L) in the feed gas; $C_{G,out}$ is the ozone concentration (mg/L) in the off-gas; C_L is the residual ozone concentration (mg/L) in the liquid phase; V_L is the effective reactor volume (L), and t is the ozone contact time (min).

3.5 Effect of the Inorganic Fraction on the Ozonation Performance

We investigated the effect of the OSPW matrix on the ozonation performance by using river water (North Saskatchewan River sampled on July 18th, 2015), ozonated river water (i.e., inorganic fraction only), OSPW (Shell 2015 OSPW), and ozonated OSPW (i.e., OSPW with inorganic fraction only). The samples were filtered using 0.45 µm membrane and then ozonated for 4 hours to remove the organic matters in the samples. An ozone generator (Wedeco, Model GSO-40, Water Technology, Herford, Germany) was used to produce O_3 gas using extra dry high purity oxygen.

Once the organic fractions were removed from the samples, semi-batch ozonation experiments were conducted in 4-L Erlenmeyer flasks by bubbling ozone gas into the samples (Millipore water, ozonated river water, and ozonated OSPW). We spiked cyclohexanoic acid (CHA) as a NA model compound and conducted ozonation tests at three ozone doses (10, 15 and 30 mg/L utilized ozone dose). The initial CHA concentration was 40 mg/L.

We also assessed the influence the individual ions on the ozonation of CHA by conducting batch experiments. A 30-mL glass reactor with a cap to eliminate the headspace was used. The concentration of the different ions is presented in Table 1. CHA was dissolved into sodium carbonate ($NaCO_3$) buffer to obtain a stable pH (8.46). The initial CHA concentration was 25 mg/L and initial ozone concentration was 14.5 mg/L. After 20 min of reaction, the samples were quenched using 1 mL 10% sodium bisulfite ($NaHSO_3$). The CHA concentration was measured using a liquid chromatography single quadrupole mass spectrometry system (ACQUITY UPLC H-Class; Waters).

3.6 *In Vitro* Studies Using Mammalian Cell Lines

The mouse macrophage cell-line (RAW 264.7) was selected for our *in vitro* studies as a representative mammalian immune cell model. This cell line represents a population of immune cells (macrophages) that are distributed throughout the body of an animal, and are key innate cellular defenders against bacterial, viral, fungal, and parasitic pathogens. OSPW-mediated influences on RAW 264.7 cellular viability and/or impairment of their functions also represents an important *in vitro* bioindicator for assessing the effects of different OSPW sources and associated treatment protocols on their acute toxicity and immunomodulatory properties.

3.7 *In Vivo* Studies Using Mice

We performed exposures using two selected doses of OSPW-OF and OSPW-O_3-OF (1 mg/L and 10 mg/L; based on NA content). For these experiments, female Balb/c mice were exposed weekly via gavage during pregnancy (21 days) and lactation (21 days). Samples from pregnant mice were collected on gestation day (GD) 14 and at the end of lactation (6 weeks). The assessment of various parameters, including pregnancy rates, fetal implantations, fetal resorptions, weight gain of pregnant animals, weight of pups at birth and the end of lactation, blood and urine hormone levels (progesterone, prolactin, estrogen, and aldosterone), histological assessments (liver, spleen, intestine, lungs, brain, uterus and placental tissues), examination of immune cell numbers and ratios, mRNA levels of genes encoding select detoxifying enzymes in the liver, and mRNA levels of select immune genes and protein levels of cytokines in the blood were all implemented as broad indicators of physiological changes in mice exposed *in vivo* to OSPW-OF and OSPW-O_3-OF. In total, four independent sets of exposures were conducted to allow for comprehensive statistical comparison of the effects of OSPW-OF and OSPW-O_3-OF on mammalian reproduction and assessment of a number of different immunological parameters.

4. Results and Discussion

4.1 Characterization of OSPW

As shown in Table 2, raw OSPW from Syncrude Aurora pond was turbid water (turbidity = 277.0 NTU). It featured a basic pH (8.41) and contained high alkalinity (644.15 mg/L as $CaCO_3$) and large amount of inorganic ions (e.g., SO_4^{2-}, HCO_3^-, and Cl^-) as well as organic species (TOC= 55.7 mg/L).

IMS is a qualitative analytical method that can be used to characterize the NA groups in different matrices (i.e., OSPW from different oil sands companies) at different treatment conditions. As shown in Figure 3a, the IMS of raw Aurora 2013 OSPW showed three clusters separated by the retention time and the drift time: classical NAs (O_2-NAs), oxidized NAs (O_x-NAs) and sulfur NAs (S-NAs). After ozonation, the samples showed little/no classical NAs and S-NAs given they were preferentially removed in the ozonation process (Figure 3b). Oxidized NAs were significantly removed, indicating the high efficiency of ozonation treatment.

The removal of classical NAs was semi-quantified by UPLC-TOF-MS (Figures 3c and 3d). In raw OSPW, NA concentration was 18.4 mg/L, which decreased to 1.6 mg/L after ozonation, equivalent to 91.2% removal. NAs with carbon number higher than 17 were completely oxidized.

The total concentration of oxidized NAs (i.e., sum of O_3-NAs, O_4-NAs, O_5-NAs, and O_6-NAs) in raw OSPW was 22.91 mg/L, and after ozonation it decreased to 11.00 mg/L, equivalent to 52.0% removal (Figure 4). Specifically, the dominate oxidized species in raw OSPW were O_3-NAs (8.75 mg/L) and O_4-NAs (9.57 mg/L), which were reduced by 48.6% and 57.4%, respectively, after ozonation (Figure 5). The concentration of O_5-NAs was 3.98 mg/L, and was reduced by 54.5%. The concentration of O_6-NAs was 0.62 mg/L, and it almost did not change after ozonation. Because oxidized NAs were both removed and generated during ozonation, their removals were not as high as that achieved for classical NAs.

We also compared the characteristic of different OSPW matrices (Table 3). We found that the concentrations of classical NAs varied from 14.4 mg/L (Shell 2014 OSPW from Muskeg River Mine) to 43.4 mg/L (Syncrude 2014 OSPW Aurora pond) in raw OSPW. High variability was also found for BOD, COD and AEF. These results agreed with previous publications that have indicated that the characteristics of OSPW vary greatly due to different ores, extraction processes, and age [1, 35-37].

As shown by the IMS in Figure 6, oxidized NAs were notably removed, indicating the high efficiency of ozonation and peroxone processes. Overall, higher NA removals were observed using 1:2 peroxone, followed by 50 mg/L ozone, and 30 mg/L ozone. Interestingly, for all treatments, the sulfur containing NA species (S–NAs) were completely reduced indicating no intensities in any clusters of the IMS plots after treatment. Our study clearly shows the ability of peroxone at 50 mg/L ozone dose coupled with 20 mg/L H_2O_2 to degrade both classical NAs and S-NA species.

In raw Shell 2015 OSPW, the concentration of classical NAs was 16.9 mg/L, which decreased to 0.6 mg/L after ozonation, equivalent to 96.4% removal. Similarly, high O_2-NA removals were observed in Syncrude 2014 OSPW after different treatment conditions (Figure 7). Overall, the highest O_2-NA degradations were observed in the 1:2 peroxone treatment with degradation of 91% of NAs.

The total concentration of oxidized NAs (i.e., sum of O_3-NAs and O_4-NAs) in raw Shell 2015 OSPW was 17.7 mg/L, and after ozonation it decreased to 2.3 mg/L, equivalent to 87.2% removal. The dominate oxidized species in raw Shell 2015 OSPW were O_4-NAs (9.1 mg/L) which were reduced to 1.4 mg/L after ozonation (Figure 8). In Syncrude 2014 OSPW, the total concentration of oxidized NAs (i.e., sum of O_3-NAs and O_4-NAs) was 19.3 mg/L, and it decreased to 8.3 mg/L after 1:2 peroxone treatment. After ozonation, the dominant species were oxidized NAs, mainly O_4-NAs.

The relative abundance of different species was determined for Syncrude 2014 OSPW using FTICR-MS (Figure 9). O_x species predominated in raw OSPW, accounting for 85.9% of the total intensity in the negative ESI mode. Among the O_x species in raw OSPW, O_2 (30.3%), O_3 (27.9%), and O_4 (24.9%) were the most abundant, followed by O_5 (2.7%). The dominance of the O_2, O_4, and O_3 species was consistent with previous analyses with FTICR-MS [38]. O_2S (2.7%), O_3S (4.8%), and O_4S (2.1%) were the major sulfur-containing species in raw OSPW. Regarding the nitrogen-containing species, O_2N only accounted for 0.6% of the total intensity, while N_2O_x accounted for 3.9% of the total intensity.

Our FTICR-MS results showed that ozonation was effective to transform the O_x species in OSPW (Figure 9). After ozonation with 50 mg/L utilized O_3 dose, the relative abundance of O_2 was reduced to 16.6%. However, the O_3, O_4, O_5, and O_6 species increased to 33.4%, 35.1%, 8.2% and 0.8%, respectively, indicating a significant shift of organic species distribution to more oxygen-rich species. Ozonation of TBA-spiked OSPW showed that molecular ozone oxidation also decreased the relative abundance of O_2 to 19.2%, and increased the relative abundance of O_4 (33.9%), O_5 (6.6%), and O_6 (0.6%) species. The difference of ozonation performance with and without TBA can be attributed to the •OH oxidation. Most likely, both molecular ozone reaction and •OH oxidation played a key role in transforming the organic species in OSPW.

As shown in Figure 9, the ozonation process significantly reduced the relative abundance of O_2S (not detected after ozonation). Simultaneously, there was an increase of the relative abundance for the other sulfur-containing species. The transformation of sulfur-containing species probably indicated that sulfur-containing species were more reactive than O_x species. Preferential oxidation of sulfur-containing species over O_x species has been reported in previous studies with ozonation [18]. In terms of transformation of nitrogen-containing species, a decrease of the relative abundance of N_2O_x to 0.6% after ozonation and to 3.3% after ozonation + TBA was found.

4.2 Development of Method to Separate the Organic and Inorganic Fractions in OSPW

We also assessed different methods to separate the organic and inorganic fractions from OSPW. We tested HLB cartridge and activated carbon column with different eluents. HLB is a hydrophilic-lipophilic-balanced, water-wettable, reversed-phase universal sorbent for acidic, neutral and basic compounds. HLB is made from a specific ratio of two monomers, the hydrophilic N-vinylpyrrolidone and the lipophilic divinylbenzene. HLB provides superior reversed-phase capacity with a neutral polar “hook” for enhanced retention of polar analytes.

Firstly, methanol was applied to elute organics from the HLB cartridge and activated carbon column. The NA concentrations in the eluents were measured by UPLC-TOF-MS. The result showed that for HLB cartridge, 71.61% classical NAs were recovered by methanol, while only 13.08% classical NAs were recovered for the activated carbon column. This indicates that methanol is more efficient to extract organic matter from the HLB cartridge. Figure 10 shows the recovery rate of classical NAs for the HLB cartridge and activated carbon using methanol for different carbon and –Z numbers. The results indicated that methanol could achieve more

recovery rate with higher carbon and –Z numbers for HLB. Opposite results were observed for activated carbon.

4.3 Silver-Ion Solid Phase Extraction of Naphthenic Acids Species

The silver-ion (Ag-ion) solid phase extraction (SPE) has been applied to fractionate methylated fatty acids via multiple-step elution based on saturation degree or cis/trans molecular structure. Pre-methylation for fatty acids is necessary to modify the molecular polarity, facilitating Ag-ion SPE separation, though other structure-related property (e.g., molecular toxicity) is also changed after methylation. In previous studies, similar methylation to NAs was applied, and based on GC×GC-MS determination, fractionation (hexane/ethyl ether mixture as eluent) of aromatic and nonaromatic (or acyclic) NAs using Ag-ion SPE was found [17, 33]. Though the toxicity of separated aromatic and nonaromatic NAs was assessed towards larvae zebrafish after de-methylation to methylated NAs, the methylation and de-methylation reagents and reactions reduced the accuracy of the toxicity assessment for NA species from OSPW. Apparently, the requirement for methylation in this method was a limitation that not only slowed the entire process but also restrained the application of fractionated products, which were only roughly separated as aromatic and nonaromatic species.

Although our work was not included in the original proposal, this study aimed to achieve the separation of classical, aromatic, oxidized, and sulfur-containing NAs from OSPW using Ag-ion SPE and to verify the composition of fractions using UPLC-IM-TOFMS and MS/MS analysis, contributing to future analytical, toxicological, and engineering studies as well as providing the NA standard material for future comprehensive environmental monitoring of NA contamination from various sources.

OSPW samples before SPE and SPE fractions were characterized using ultra performance liquid chromatography ion mobility time-of-flight mass spectrometry (UPLC-IM-TOF-MS) to corroborate the separation of distinct NA species. The mass spectrum identification applied a mass tolerance of ±1.5 mDa due to the mass errors of NAs were measured within this range, allowing the identification of O_2S-NAs from O_2-NAs. Moreover, separated NA species facilitated the tandem mass spectrometry (MS/MS) characterization of NA compounds due to the removal of matrix and simplified composition. MS/MS results showed that classical, aromatic, oxidized, and sulfur-containing NA compounds were eluted into individual SPE fractions.

In this study, raw and ozonated OSPW samples were first determined by 2D drift time versus retention time separation (Figures 11a and 11b) using UPLC-IM-TOF-MS, and O_x–NA ($2 \le x \le 5$) and O_yS–NA ($2 \le y \le 4$) species were identified using accurate mass matching (Figures 11c and 11d). Panels c and d of Figure 11 show that O_2-NAs were observed with two separated clusters and the lower (in position) cluster was previously verified as being saturated acyclic O_2-NAs using the Merichem NA standard [39]. The upper cluster of O_2-NAs consisted of aromatic O_2-NAs based on the fact that this cluster was clearly separated from the cluster of saturated acyclic O_2-NAs and was greatly consumed during the ozonation process (Figure 11d), as previously reported [29, 39]. The results shown in Figures 11c and 11d indicate that, in general, the polarity of NA compounds follows the order classical O_2-NAs < aromatic O_2-NAs < O_2S-NAs <

O_3-NAs < O_3S-NAs ~ O_4S-NAs < O_4-NAs < O_5-NAs based on the fact that the high polarity of compounds reduces the retention time on a reverse phase column [40]. In addition, few NAs from distinct NA species with similar retention times were actually separated in the drift time dimension.

As shown in Figures 12 and 13, NAs were not detected in fractions F1, F2, F21, or F22 from raw OSPW or F1, F21, or F22 from ozonated OSPW because NAs were either not readily eluted or already completely eluted. NA species were eluted out gradually and separated clearly into SPE fractions, e.g. classical (saturated acyclic) O_2-NAs were separated in fractions F3-F5 and aromatic O_2-NAs in fractions F7-F11 (F7-F11 also contained O_3-NAs) based on the separated position of two clusters in accord with Figure 11c, indicating the physical separation of classical and aromatic O_2-NAs. Similar separation was observed in Figure 13, showing that classical O_2-NAs were separated in F2-F5 and the aromatic O_2-NAs in F8-F10 (F8-F10 also contained O_3-NAs). The disruption of intensity for O_2-NAs (Figure 14a) further confirmed the separation of classical and aromatic O_2-NAs species. It was also found that the consumption of aromatic O_2-NAs in the ozonation process was greater than that of classical O_2-NAs.

O_2S-NAs were eluted into F11-F16 (Figure 12), though some other species were also detected in these fractions, e.g. aromatic O_2-NAs in F11-F13, O_3-NAs in F11-F16, and O_4-NAs in F16. O_2S-NAs were completely consumed during the ozonation process (Figures 13 and 14). The consumption of O_2S-NAs is consistent with previous results of ozonated OSPW before SPE. O_3-NAs were eluted into F8-F16 and O_4-NAs were eluted into F16-F20. A slight amount of O_5-NAs was eluted into F20 of raw OSPW (Figures 12 and 14), though the ozonated OSPW before SPE actually had higher abundance of O_5-NAs than raw OSPW. This is because more oxygen atoms in NAs actually required increasing the eluent solvent polarity (Figures 14a and 14d). The affinity of O_5-NAs to solid phase was too strong to be eluted in current solvent polarity conditions. Slight amounts of O_3S-NAs in F16-F20 (Figures 12 and 14) and O_4S–NAs in F14-F20 (Figures 12, 13 and 14) were observed but not clearly separated. This should be attributed to their strong affinity to solid phase as well as their low initial concentration, prohibiting further investigation. The use of stronger solvent polarity (higher than that of acetone) could help elute the O_5-, O_3S-, and O_4S-NAs.

Overall results indicated that the elution of distinct NAs species into individual SPE fractions (e.g. classical O_2-NAs in F3-F5, aromatic O_2-NAs in F7-11, O_3-NAs in F8-16, O_4-NAs in F16-F20, O_2S-NAs in F11-F16 for SPE fractions from OSPW) was achieved using Ag-ion SPE based on the NA compound polarity (primary) and the molecular size for a few NAs from distinct species but with similar retention time (polarity). Ag-ion SPE separation of OSPW NAs is an important advancement for NA species-specific studies in wastewater treatment and toxicological research. Furthermore, the separated NA species in mg level using this method could be widely used in environmental monitoring programs as standard materials, given commercial NA standard comprised of only classical O_2-NAs, e.g. Merichem NA standard (Merichem Co.) or Fluka NA standard (Sigma Aldrich), and no NA mixture standard has been produced from synthetic chemistry as reported in the published literature.

4.4 Ozonation and Peroxone Treatment of OSPW

Ozone dose is considered one of the key operating factors in ozone processes. However, the efficiency of the ozone process to degrade NAs is influenced by many OSPW parameters such as dissolve organic carbon, pH, and alkalinity. In addition, while the ozone dose increases, the rate of ozone decomposition decreases indicating that applying large ozone doses and/or long ozonation contact times has a limited beneficial impact on the degradation of pollutants such as NAs [41]. Therefore, the determination of optimum ozone dose to achieve required levels of degradation, especially in complex water such as OSPW, is very challenging. Previous study showed that increasing the ozone dose to 100 mg/L led to a sharp decrease of typical OSPW parameters such as AEF [42]. However, for ozone doses greater than 100 mg/L, the removal reached a plateau with very little decreases. Likewise, the authors found that the removal efficiency of various NA species decreased considerably from 50 mg/L up to 170 mg/L [28]. Improving the ozonation efficiency using ozone combined with H_2O_2 is necessary to produce treated OSPW that can be released to the environment.

We investigated the impact of the peroxone treatment process on the degradation of NAs. Various peroxone doses were tested to determine optimal treatment efficiencies that would provide for a cost-effective treatment process. These tests were conducted using the whole OSPW matrix (Syncrude 2014 OSPW from Mildred Lake Site).

4.4.1 Impact of treatments on NA degradation

Figure 15 depicts the profile of the concentration of total NAs (classical NAs + oxidized NAs) for all treatments compared to raw OSPW. Our results indicated a structure-reactivity relationship of the NA degradation processes as represented by the combined impact of carbon (n) and Z numbers. Our results also indicated that 1:2 peroxone (20 mg/L H_2O_2 + 50 mg/L utilized O_3 dose) was very effective in reducing the concentration of total NAs by 63%. The other treatments tested, including 50 mg/L utilized O_3 dose, 1:1 peroxone (20 mg/L H_2O_2 and 30 mg/L O_3 dose), 1:2 peroxone (11 mg/L H_2O_2 and 30 mg/L O_3 dose) and 1:3 peroxone (10 mg/L H_2O_2 and 50 mg/L O_3 dose) achieved less degradation in either total NAs and classical NA species. Regarding the degradation of classical NAs, 50 mg/L O_3 dose, 1:1 peroxone, 1:3 peroxone, and 1:2 peroxone achieved degradation levels of 83, 80, 61, and 47%, respectively.

4.4.2 Impact of treatments on NA carbon (n) and Z numbers

The n and Z numbers of the NAs are indicative for the structure and as a consequence an indication of the reactivity towards oxidation. This provides an interesting set of metrics to assess the efficiency of NA degradation and treatment specificity (Figure 16). Overall, the 1:2 peroxone treatment has the highest degradation rates for the classical NAs and total NAs based on both the n (Figures 16a and 16c) and Z numbers (Figures 16b and 16d) which can be attributed to the elevated production of •OH in this treatment. The higher degradation rates are associated with higher n and Z number in all treatments for the classical NA species and total NAs. This trend is not followed by the Z=0 NAs due to the creation of these species from the oxidation and cleavage of higher n and Z NAs. Overall, a high degradation efficiency (>70%) can be observed for NAs with Z numbers -6 to -18 and n from 7 to 19 for all treatment conditions.

For all treatments, there is a positive correlation between increasing n and increasing degradation for classical NAs and total NAs with 50% or greater degradation for n>10 (O_2-NAs) and n>12 (total NAs) (Figures 16a and 16c). Similarly, there is a positive correlation between increasing Z number and degradation rates (Figures 16b and 16d). The Z≥-12 NAs are preferentially removed in all treatments; with lower Z species degradation rates, remaining high for the NAs (Figure 16b) and being lower and more variable for treatments for the total NAs (Figure 16d). There were lower degradation rates for -6<Z<-10 in total NAs, in contrast, they were higher in NAs (Figures 16b and 16d). This lower degradation rate in total NAs can be attributed to the generation/production of higher oxidized NAs from classical NAs during the oxidation processes, contributing in the total NAs [29]. As for the n, this variation in Z numbers is expected given the formation of higher oxidized NAs during the degradation process. However, the high removal rates for larger Z numbers is due to their larger amount of tertiary carbons, rings and possible double bonds which are more reactive towards oxidation.

To examine the combined impact of carbon and Z numbers, it is useful to identify the degradation rates for NA species at each individual n at different Z values as shown in Figures 16 (e,f,g,h) and Figure 17 for the classical NAs and total NAs, respectively. Overall, the degradation rates showed increasing trend with increasing n for each of the classical NAs and total NAs. It should be noted that there are some negative degradation rates (i.e., formation rates) for the oxidized NAs. This indicates these species were generated during the oxidation treatments.

Interestingly, comparing the NA degradation for 30 mg/L ozone and the 1:1 peroxone treatments at n>13 for Z=-10, -12, -14; n>16 for Z=-8; and n=17 and 18 at Z=-6, the degradation rates decrease after adding H_2O_2 (Figures 16e and 16f). It has been reported that increasing the H_2O_2 concentration might not be advantageous under some conditions given H_2O_2 can possibly self-scavenge itself and/or the •OH can be scavenged by the O_3. This impact of scavenging is in agreement with our decision to use a fixed low H_2O_2 concentration compatible with low ozone doses in order to minimize H_2O_2 scavenging at higher H_2O_2 doses.

The NA species for the 50 mg/L ozone (Figure 16g) and 1:2 peroxone (Figure 16h) had similar high degradation patterns as the other two treatments. All treatments showed similar degradation trends for the total NAs with increased degradation rates with increasing n and decreasing Z for n<20. In addition, the highest degradation trend with decreasing Z number for total NAs was observed for 1:2 peroxone treatment (Figure 17d). The oxidation of NAs by the 1:2 peroxone process resulted in the complete degradation of higher molecular weight NAs (n = 11-26) (Figure 16h).

4.4.3 Impact of the treatments of fluorophore organic compounds

The SFS profiles for raw and treated Syncrude 2014 OSPW are shown in Figure 18. The raw OSPW exhibits three distinctive peaks (labelled I, II, III) that are representative of fluorophore organic compounds groups, having one ring, two rings, and three aromatic rings located at 260-280, 300-315 and 320-330 nm, respectively [49]. Overall, the 1:2 peroxone and 50 mg/L ozone

treatments showed the highest reductions in SFS with complete removals of peaks II and III and marked reductions in peak I (Figure 18).

On the other hand, the 30 mg/L ozone and 1:1 peroxone did not reduce effectively peak I as peaks II and II (Figure 18b). Additionally, the 30 mg/L ozone accomplished higher reductions compared to 1:1 peroxone. 1:1 peroxone still exhibited peaks II and III (reduced relatively) and peak I (unreduced). Reasons for this lower reduction in the 1:1 peroxone are not known. However, it can be attributed to the scavenging of •OH at these oxidants doses as mentioned earlier in the NA degradation or the evidence of the significant role of the molecular ozone rather than the •OH in targeting those type of aromatic compounds. The presence of aromatic compounds associated with high molecular weights NAs can be correlated with SFS due to their fluorescence [43].

The reason of the decrease of fluorescence after ozonation might be due to enhancing the electron withdrawing groups in aromatic compounds that can weaken the structures and break down the chromophoric groups in the aromatic structure [44]. The amount of •OH is expected to be very high at pH 8; therefore, the •OH radical is considered to be the main contributor in reducing these aromatic portion. From Figure 18, it can be observed that the removal of some peaks increased by spiking tert-butyl alcohol (TBA) as an •OH scavenger. For instance, peak III recovered by spiking TBA in 1:2 peroxone (Figure 18a). This can be attributed to a competition between the different scavengers in the real water matrix that can occur with the spiked TBA which turns the reaction pathways through other organic radicals. As well, the typical reaction between ozone and aromatics is hydroxylation that can lead to the generation of phenol while continuously producing •OH that can elevate the degradation efficiency [45].

4.4.4 Impact of the treatments on COD, TOC, BOD, and AEF

Besides the NA removals, other parameters such as COD, TOC, BOD and AEF can be used as markers to assess the treatment capability and efficiency. Overall, our findings showed relatively low removals of AEF, COD and TOC for all treatments (Table 4). The limited removals of COD and TOC can be attributed to the stability of the DOC after being oxidized. In our study, the DOC showed no decrease between the raw and treated OSPW samples. OSPW is a very complex matrix that contains recalcitrant organic matter that may be transformed, not mineralized, from parent compounds to by-products or intermediates [30] under the current treatment conditions.

Despite the lack of complete mineralization, all oxidation treatments did result in increased BOD concentrations compared to untreated OSPW which indicates the increased potential for further treatment of OSPW in using biological processes (Table 4). Our results are consistent to previous studies that reported the positive impact of the ozonation on the growth of microbial population [30].

4.4.5 Sulphur and nitrogen species

As shown in Figure 19, a decrease in abundance of O_2S, O_3S and O_4S species as measured by FTICR-MS after all treatments can be observed, except for 1:1 peroxone. Conversely, by spiking

TBA, the abundance increased and become similar to that of raw OSPW due to the inhibition of one of the significant oxidation pathways (i.e., •OH) (Figure 19). Our findings suggest the change in the distribution of the species by selective transformation from one species to another after oxidation. These findings agree with previous study about the hydroxylation of the O_2S to O_3S and other forms [46, 47].

The abundance of N_2O_x species decreased after ozone treatments. In contrast, peroxone treatments were not effective in reducing these species, even it did increase in one of the peroxone conditions (i.e., slight decrease in 1:2 peroxone and increase in 1:1 peroxone). Spiking TBA with ozone treatments suppressed the •OH that led to an increase again in the abundance of N_2O_x species (Figure 19). The reason of the effective reduction of N_2Ox species in ozone treatments compared to an increase after the 1:1 peroxone and marginal reduction in the 1:2 peroxone can be attributed to two possibilities. The first possibility is the low generation of hydrophilic moieties through oxidation reactions which are less reactive with •OH [48]. The second possibility is the reaction of ozone with ammonia that generates different intermediates. These intermediates can be hydroxylamine (H_2NOH) and hyponitrous acid (HNO and its dimer). Specifically, HNO might decay to N_2O due to its instability and contribute to the increase in the N_2O_x [49].

4.4.6 Effect of •OH scavenger

Our results showed that the transformation of O_2-NAs to other oxidized species was partially inhibited after spiking TBA (Figure 19). Despite the role of the molecular ozone in the transformation of O_2-NAs cannot be ignored, the contribution of •OH can be considered significant. For instance, in both 1:2 peroxone + TBA and 50 mg/L utilized O_3 dose + TBA, the transformation of O_2-NAs was reduced and their abundance reached 44-45% compared to 19% and 24% in 1:2 peroxone and in 50 mg/L utilized O_3 dose, respectively. In contrast, the abundance of O_3-, O_4-, O_5-, and O_6-NA species in 1:2 peroxone + TBA remained unchanged or slightly increased compared to raw OSPW. Suppressing the •OH radical pathway by adding TBA reduced the degradation in all treatments, while molecular ozone contribution was 50% and 34% for O_2-NAs and O_x-NAs, respectively. Therefore, our results confirmed that both molecular ozone reaction and •OH oxidation played important roles in transforming the organics in OSPW.

4.5 Impact of the Inorganic Fraction on the Ozonation Performance

We conducted experiments using river water, ozonated river water (i.e., water with inorganic fraction only), OSPW, and ozonated OSPW (i.e., OSPW with inorganic fraction only) to investigate the effect of the inorganic fraction (IF) on the ozonation performance. We spiked CHA as a NA model compound and conducted the ozonation tests. Table 5 summarizes the characteristics of the different water matrices.

The results indicated higher degradation of CHA in the OSPW matrix containing inorganic fractions, compared to those obtained in Millipore water and river water IF, suggesting a catalytic effect of the OSPW IF matrix on the ozonation performance (Figure 20). At low and medium applied O_3 dose, the utilized O_3 dose was almost the same in different water matrices.

However, at high applied O_3 dose, the highest utilized O_3 dose was observed in the experiments using OSPW IF, while the lowest values were recorded in buffer solutions. Some inorganic composition in both river water and OSPW could consume O_3 and compete with CHA for degradation.

We also investigated the effect of individual ion on the ozonation of CHA. As shown in Figure 21, cations such as Na^+ and Mg^{+2} did not have significant influence on the ozonation of CHA; however, HCO_3^- and Cl^- had a negative effect on the CHA degradation. This result was consistent with previous publications [50, 51]. Cl^- and HCO_3^- are radical scavengers that react with •OH radical, decreasing the levels of •OH radical available to react with CHA.

Ozone and •OH can be scavenged by the presence of substances such as chloride and carbonate. Metal cations such as ferrous and ferric ions as well as their oxides present in OSPW may increase the formation of •OH, leading to an increase in the overall efficiency of ozonation. Additionally, some organic compounds can promote the decomposition of ozone to •OH. Therefore, different fractions of OSPW may have different reactivity to molecular ozone or radical species. Additional experiments are being conducted to evaluate the potential for using indigenous transition metal ions and their oxides present in OSPW to generate •OH by manipulating the OSPW matrix without the addition of secondary organic compounds. By improving the ozonation performance, we will target the most recalcitrant contaminants in OSPW.

4.6 *In Vitro* Studies Using Mammalian Cell Lines

Raw OSPW is a complex mixture of inorganic and organic substances and its principal toxic components have yet to be fully characterized. Previously, we showed *in vitro* that the OSPW-OF caused a concentration-dependent immunotoxicity in mammals. The main goal of this portion of the study was to explore the immunotoxic properties of OSPW in mammals using a series of *in vitro* bioassays. Using the RAW 264.7 mouse macrophage cell line we show that:

i) Raw OSPW was acutely toxic in a dose-dependent manner whereas whole OSPW-organic fraction (OF) was not toxic at the equivalent NA doses tested.
ii) Ozonation of whole OSPW does not ameliorate its acute toxicity.
iii) Exposure of mammalian macrophages to raw OSPW but not OSPW-OF altered their cellular shape and size, which suggests they are experiencing cell stress.
iv) Exposure of macrophages to raw OSPW but not OSPW-OF up-regulated stress genes associated with oxidative stress and DNA damage.
v) Raw OSPW and ozonated raw OSPW (OSPW-O_3) at doses of 10 mg/L NAs significantly modulated cytokine gene levels and the ability of macrophages to secrete important protein biomolecules. This indicates that raw OSPW contains factors that have immunotoxic properties that are not removed after ozonation.
vi) The OSPW-organic fraction and OSPW-ozonated organic fraction at doses of 10 mg/L did not affect mouse macrophage cytokine gene expression and secretion.
vii) The ability of macrophages to engulf bacteria, which is indicative of their antibacterial activities, was negatively affected after exposure to raw OSPW but not

OSPW-OF. This suggests that non-organic components in raw OSPW contribute to the observed immunotoxic effects.

The results of the *in vitro* studies on the toxic effects of different OSPW waters using RAW 264.7 mammalian cell line have been recently published in *Environmental Science & Technology* (doi: 10.1021/asc.est.7b02120).

4.6.1 Detailed overview of *in vitro* results

Cell toxicity: The *in vitro* assessment of OSPW toxicity was first examined by direct exposure of the RAW 264.7 cell line to increasing doses (1-18 mg/L NA concentration) of OSPW samples for 18 h of incubation. Cell proliferation was measured by staining the cells with the fluorescent thymidine analog BrdU, which is incorporated into the DNA of dividing cells. Active incorporation of this compound into the nucleus of dividing cells is also an indirect assessment of their viability as only live proliferating cells can be labeled with the BrdU dye (i.e., increased BrdU staining = increased live/proliferating cells). When compared to the 0 mg/L control, cells exposed to raw OSPW for 18 h had a significantly decreased BrdU staining at doses greater than 8 mg/L (Fig. 22). For example, cells treated with 10 mg/L of whole OSPW had a ~60% reduction in their BrdU staining and at doses of 12 mg/L or higher there was a >90% reduction in BrdU staining (Fig. 22). In comparison, the matched PBS dilution controls did not demonstrate a significant reduction in BrdU staining at 10, 12, and 14 mg/L. However, when the culture media was diluted with PBS to match the ratio of media displacements for the raw OSPW water exposures at 16 and 18 mg/L they had ~55% and ~75% reduction in BrdU staining, which was significantly lower than the undiluted control cells (0 mg/L). In comparison, at all doses tested, OSPW-OF did not significantly reduce the BrdU staining of RAW 264.7 cells after 18 h (Fig. 22).

We examined cell health parameters following OSPW exposures using the MTT assay, which assesses cell metabolic activity. MTT is a tetrazolium salt that is converted by active cellular oxidoreductase enzymes into an insoluble purple colored formazan. Therefore, this colorimetric assay can be used to examine the number of viable cells in culture and is widely used for measuring cytotoxicity. Using this assay, we show that cells exposed to the highest dose of whole OSPW (e.g. 16 and 18 mg/L) for 18 h exhibited a significant reduction in their viability (Fig. 23). The MTT values of the untreated cells (0 mg/L) were normalized to 100% cell viability and in comparison to the control cells, raw OSPW doses of 16 mg/L and 18 mg/L reduced the measured viability levels down to 16% and 5%, respectively (Fig. 23). However, 18 h exposures with OSPW-OF at 1, 10, and 18 mg/L did not significantly reduce cell viability and neither did any of the PBS dilution controls.

The determination of direct cell counts to verify that the MTT viability data correlated with reduced cell numbers following OSPW-mediated toxicity was done. In these experiments, cells were seeded at a density of 2 x 10^4 cells per well and then incubated for 18 h in the presence of various doses of raw OSPW (Fig. 24). Then using the Operetta High-Content Imaging System (PerkinElmer), total cell numbers were determined. This experiment confirmed that the decreased % cell viability measured by MTT correlated with a reduction in viable cell numbers at whole OSPW doses >10 mg/L of NAs. For example, after 18 h of incubation the untreated cell

numbers increased from the original seeding number of 2 x 10^4 cells to ~5 x 10^4 (Fig. 24). Cells treated with raw OSPW at 1-10 mg/L NA concentrations had increased total cell numbers (i.e., from 2 × 10^4 to ~4.5 × 10^4) that exceeded the original seeding density due to expected normal cell proliferation (Fig. 24). However, raw OSPW doses >10 mg/L of NA caused a significant reduction in the total cell numbers below the original seeding density of 2 × 10^4 cells. For example, cells treated with 12, 14, and 16 mg/L of raw OSPW had only ~12,500, ~8,600, and ~6,500 cells per well, respectively, and at the highest dose tested, very few cells (~500) remained in wells (Fig. 24).

To further establish that raw OSPW but not OSPW-OF was directly toxic to mammalian cells we also examined cell cytotoxicity using the lactate dehydrogenase (LDH) assay. LDH is an intracellular enzyme that is released following injury or exposure to toxic substances. Since LDH is a stable enzyme, it can be readily measured to evaluate cell toxicity, and as shown in Figure 25, the exposure of RAW 264.7 cells to whole OSPW (but not OSPW-OF) at 18 mg/L NAs for 18 h caused a significant increase in LDH release (i.e., ~45% vs. ~0.76% cytotoxicity for raw OSPW and OSPW-OF, respectively). At 1 mg/L and 10 mg/L NA doses, no significant LDH levels were detected for all treatment groups after 18 h incubation with whole OSPW. These results indicate that at >10 mg/L NA doses, raw OSPW but not OSPW-OF induced the lysis of RAW 264.7 macrophages.

Cell morphology: We also examined cellular morphology (i.e., the shape and size of cells) using scanning electron microscopy (SEM), as a general 'gross' indicator of OSPW-induced effects on mammalian cells. Shown in Figure 26A are cells exposed to 10 mg/L and 18 mg/L of raw OSPW for 6 h. When compared to the control cells (0 mg/L) and the OSPW-OF treated cells, which have an overall smooth and rounded appearance, cells treated with 10 mg/L OSPW had a 'rougher' surface appearance with multiple membrane intrusions throughout the plasma membrane. When cells were exposed to 18 mg/L raw OSPW for 6 h, the cells displayed an even more dramatic alteration in their overall morphology that featured an extremely ruffled membrane and once again the appearance of numerous membrane intrusions (Fig. 26A). SEM imaging was also performed after 18 h exposures (Fig. 26B) that also showed a change in cellular morphology from smooth cells devoid of intrusions (0 mg/L) to those that had a course surface appearance and multiple plasma membrane intrusion-like structures. These alterations were particularly evident after exposure to 14 mg/L to raw OSPW. Importantly, OSPW-OF exposed cells at the same doses and incubation periods were identical in appearance to the control cells and overall these results further suggest that only whole OSPW contains factors that affect mammalian cell morphology, which indicates that these cells may be undergoing a form of toxicological-associated cell stress response.

Cell stress gene expression: To gain further insights into the OSPW-mediated toxicological-associated cell stress response of mammalian cells, we performed gene expression analyses using a panel of marker genes known to be upregulated during oxidative stress and DNA damage/repair responses. Furthermore, this analysis would provide new molecular markers for OSPW-mediated effects on RAW 264.7 cells prior to the induction of cell toxicity and/or alterations of cell functions. In the presence of increased reactive oxygen species (ROS) cells

activate antioxidant responses to mitigate cellular stress and damage. However, when ROS accumulate beyond the ability of the cells to cope with this disturbance, oxidative stress occurs leading to upregulated expression of genes encoding antioxidant enzymes. One of these genes is called heme oxygenase (decycling) 1 (*Hmox1*) and its induction is associated with cellular protection against ROS-induced injury. In our study, following exposure of cells to 10 mg/L NA of raw OSPW for 6 h and 18 h, we observed a significant up-regulation of heme oxygenase (decycling) 1 (*hmox1)* mRNA levels compared to control (non-exposed cells) (Fig. 27A). In contrast, the exposure of cells for 2 h to raw OSPW did not induce an increase in *hmox1* expression, indicating that duration of exposure influenced the change in the expression of this stress gene. In comparison, treatment of the cells with 10 mg/L of raw OSPW for 2-18 h did not affect the mRNA levels of glutathione S-transferase P1 (*gstp1*) (Fig. 27B) but an early and significant up regulation of the expression of growth arrest and DNA damage (*gadd) 45* following exposure of cells to 10 mg/L of raw OSPW was observed (Fig. 27C). For example, compared to control cells (RQ expression value of ~2.7), the exposure of cells to 10 mg/L of raw OSPW for 2 h dramatically increased the mRNA levels of *gadd45* to RQ value of ~55. The observed 2 h induction of *gadd45* mRNA levels by whole OSPW declined to ~11 and ~13 RQ values after 6 h and 18 h, respectively (Fig. 27C). Finally, the expression of 8-oxoguanine DNA glycosylase (*ogg1*) was not affected by exposure to raw OSPW (Fig. 27D). In fact, based on the expression analysis of several additional stress genes (Fig. 27E), it appears that only *Hmox1* and *Gadd45* are affected by raw OSPW exposure thus implicating these as candidate marker genes for OSPW-induced cellular stress. Importantly, OSPW-OF at the same exposure doses did not affect the expression of any of the genes examined in this study including *Hmox1* and *Gadd45*. Following exposure of cells to 10 mg/L raw OSPW, we observed a significant up-regulation of *Hmox1* expression at 6 h and 18 h, with higher expression occurring after the longer exposure period (Fig. 27A). Exposure for 2 h did not induce an increase in *Hmox1* expression and at all exposure times the control cells (0 mg/L) did not exhibit increased *Hmox1* mRNA levels (Fig. 27A). Alternatively, following exposure of cells to 10 mg/L raw OSPW the expression levels of the glutathione S-transferase P1 (*Gstp1*) gene was not increased (Fig. 27B) suggesting that raw OSPW contains components that selectively induce oxidative stress genes.

Cytokine gene and protein expression: When immune cells are stimulated with pathogens such as bacteria, they activate the gene expression and subsequent secretion of several bioactive molecules called cytokines; these small proteins are vital for the propagation and coordination of ongoing immune responses during inflammatory responses. Alteration of cytokine secretion can augment infectious diseases or can cause inflammation-related tissue damage and subsequent inflammatory diseases. To directly assess the effects of OSPW on cytokine gene expression and secretion, we exposed RAW 264.7 cells to OSPW samples and then examined the cytokine mRNA expression and protein secretion levels before and after stimulation of the cells with bacteria (i.e., *E. coli*). We analyzed several cytokines that all generally function as stimulators of the immune system, which included: (i) interleukin (IL)-1β, an important mediator of the inflammatory response controlling cellular proliferation, differentiation, and apoptosis; (ii) vascular endothelial growth factor (VEGF), a cytokine that stimulates vasculogenesis and angiogenesis required for maintaining the blood supply to cells and tissues; (iii) C-X-C motif cytokine-10 (CXCL-10), a small cytokine-like molecule called a chemokine that

functions as an important attractant for immune cells by inducing the migration of cells into inflammatory sites, and; (iv) granulocyte colony-stimulating factor (G-CSF), is a growth factor which stimulates the bone marrow to produce additional immune cells such as granulocytes and stem cells, which are then released into the blood stream. When unstimulated RAW 264.7 cells were treated with 10 mg/L of raw OSPW for 18 h, a significant up-regulation of *il-1β* mRNA was observed (Fig. 28). In contrast, g-*csf* and *vegf* basal mRNA levels were not significantly different between the dilution controls and the whole OSPW treated cells. Furthermore, *cxcl-10* mRNA levels were significantly lower when the cells were treated with raw OSPW relative to the non-treated controls (Fig. 28).

Next we examined the effects of OSPW treatments on *E. coli*-stimulated RAW 264.7 cells by monitoring their cytokine gene expression levels as well as their cytokine protein secretion activities. As expected *il-1β* mRNA levels were significantly increased after the exposure of RAW 264.7 cells to *E. coli* (Fig. 29A). However, when the cells were pre-treated for 18 h with 10 mg/L of raw OSPW, an observed but not statistically significant reduction in *il-1β* expression at 1 h post bacterial stimulation was observed and no significant reduction in *il-1β* expression was evident at 3 h and 6 h after addition of *E. coli* (Fig. 29A). We then examined IL-1β protein secretion levels by unstimulated and *E. coli*-stimulated cells. As shown in Figure 29B, raw OSPW-treated RAW 264.7 cells secreted no detectable amounts of IL-1β protein if they were not stimulated with bacteria. However, bacteria-stimulated cells incubated in undiluted and diluted culture media, as well as those treated with 10 mg/L OSPW-OF, secreted low levels IL-1β ranging from ~50-100 pg/mL. In contrast, cells treated with 10 mg/L of raw OSPW produced significantly more IL-1β (1294 pg/mL) following bacterial stimulation (Fig. 29B). Therefore, in addition to the enhancement of (*il)-1β* mRNA levels in resting RAW 264.7 cells, raw OSPW but not OSPW-OF also significantly augments the IL-1β secretion abilities of bacteria-stimulated mouse macrophages.

In comparison, *vegf* mRNA levels were not increased after bacterial stimulation and raw OSPW had no effect on *vegf* expression at all time points examined (Fig. 30A). However, RAW 264.7 cells constitutively secrete VEGF into the cell supernatants (Fig. 30B). This activity is not enhanced by bacterial stimulation (Fig. 30B) but surprisingly, VEGF secretion levels were significantly augmented by bacteria-stimulated cells if they were treated with raw OSPW but not OSPW-OF (Fig. 30B). Therefore, although basal and stimulated *vegf* mRNA levels were unaffected by OSPW, as was observed for IL-1β, raw OSPW uniquely augmented the secretion of this cytokine in the presence of bacteria stimulation.

Compared to the resting mRNA expression levels, bacterial stimulation significantly increased *cxcl-10* mRNA expression (Fig. 31A). This increase was evident at all time points but with maximum levels reached at 3 h. Interestingly, when the cells were exposed to 10 mg/L of raw OSPW prior to bacterial stimulation, the 1 h and 3 h increases in *cxcl-10* gene expression were completely abrogated (Fig. 31A). Raw OSPW-treated RAW 264.7 cells also secreted very low amounts of CXCL-10 protein (Fig. 31B), however, following stimulation with *E. coli*, significantly more CXCL-10 protein was detected in the RAW 264.7 supernatants. This also agreed with the induction of *cxcl-10* mRNA expression levels following bacteria stimulations. Finally, when the

bacteria-stimulated cells were exposed to raw OSPW but not OSPW-OF, their CXCL-10 secretion activity was significantly impaired (Fig. 31B). Once again, this result agrees with the inhibitory effects that raw OSPW had on *cxcl-10* mRNA expression levels after bacteria stimulations.

Finally, the last cytokine examined in our study was G-CSF, which although inducible by bacteria stimulation, *g-csf* mRNA levels were unaffected by raw OSPW treatment (Fig. 32A). Furthermore, as was observed for IL-1β and CXCL-10, unstimulated RAW 264.7 cells secreted low levels of G-CSF and this basal secretion was not altered by raw OSPW treatment (Fig. 32B). In agreement with the *g-csf* mRNA induction by stimulation, a significant enhancement of G-CSF secretion activity was also observed in bacteria-stimulated cells but unlike all the other cytokines examined raw OSPW had no effect on the secretion of G-CSF by bacteria-stimulated RAW 264.7 cells (Fig. 32B).

Overall, these results suggest that depending on the cytokine measured, OSPW sample tested, and doses used, a dynamic pattern of OSPW-induced modulation of immune cell cytokine gene expressions and protein secretions were observed indicating there are immunomodulatory factors present in raw OSPW that differentially influence macrophage cytokine levels. These results also demonstrate that OSPW-mediated effects occur at the gene level as early as 1 h after the cells were stimulated with bacteria. We also established that the basal cytokine levels of unstimulated cells are affected by 10 mg/L raw OSPW with differential responses for *IL-1β* (i.e. enhanced) and *Cxcl-10* (i.e., inhibited) expression. No effects were observed after 1 mg/L raw OSPW exposures in all mRNA expression studies and 10 mg/L OSPW-OF treated cells also demonstrated no alteration in cytokine gene expression levels when compared to the 0 mg/L controls.

Quantitative phagocytosis assay: We developed and used a quantitative phagocytosis assay that uses fluorescent-labeled bacterial targets and the Operetta High-Content Imaging System (PerkinElmer) to semi-quantify bacterial engulfment by cells treated with OSPW. In this assay, the bacteria are labeled with a pH sensitive fluorophore that is non-fluorescent at neutral pH levels such as the conditions of the cell culture media. However, when bacteria are phagocytosed by the macrophages they are contained in acidic compartments that activate the fluorophore making the bacteria fluoresce in the green emission channel. Our phagocytosis assay measures the percentage of phagocytic cells in a population based on the numbers of fluorescent (i.e., phagocytic) vs. non-fluorescent (i.e., non-phagocytic) cells. As shown in Figure 33A, many of the control cells (i.e., 0 mg/L) are fluorescent indicating that they are capable of engulfing multiple bacteria. In addition, cells treated with 10 mg/L of raw OSPW also have phagocytic activity. However, when the cells were treated with 14 mg/L of raw OSPW very few fluorescent cells were observed indicating that the RAW 264.7 cells lost their ability to engulf bacteria when exposed to a higher concentration of raw OSPW. Shown in Figure 33B is the quantified phagocytosis data obtained using the Imaging System, which clearly shows that at doses of 14 mg/L (but not 10 mg/L) both raw OSPW and raw OSPW-O_3 significantly impaired the ability of mouse macrophages to phagocytose bacteria. In comparison, OSPW-OF and OSPW-O_3-OF treated cells had similar phagocytic activity as the control group. Overall, these

results indicate that an additional consequence of raw OSPW exposures is the impairment of their innate function of phagocytosis.

4.6.2 Discussion (*in vitro* assessment of toxic effects of different OSPW samples)

We have used an expanded array of *in vitro* cell-based assays to further explore OSPW toxicity and to directly compare the toxic effects induced by whole OSPW and OSPW-OF based on their relative NA content. By examining the viability, gene expression, and functional activities of mouse macrophages, we observed that the raw OSPW was significantly more immunotoxic at NA concentrations ranging from 10-18 mg/L, compared to OSPW-OF. These data strongly suggest that at NA doses at the lower range reported in tailings ponds (i.e., <20 mg/L), the inorganic constituents and/or potential interactions between the inorganic and organic components may significantly contribute to toxicity in the non-fractionated raw OSPW. Data on the additive and/or synergistic effects of various constituents present in raw OSPW are not currently available but should be addressed in future studies.

Our results show that raw OSPW had a dramatic effect on the proliferation of mouse macrophages, and at the highest doses tested (i.e., 12-18 mg/L) it significantly reduced cell viability and promoted cell lysis. This caused a reduction in the total cell numbers, which was not observed after the cells were exposed to equivalent doses of OSPW-OF. At the dose of 10 mg/L NAs, raw OSPW did not significantly affect viable cell numbers; however, the exposed cells displayed a dramatic alteration in their cell morphologies that featured a ruffling of their surfaces leading to the appearance of a frayed plasma membrane with multiple intrusive-like structures that are indicative of membrane degeneration and/or disruption of membrane stability. This suggests that the cells were stressed, which was confirmed by monitoring the expression of selected stress response genes. Specifically, we observed increases in the mRNA expression levels of *hmox1* and the *gadd45* genes when RAW 264.7 cells were exposed to 10 mg/L of raw OSPW but not an equivalent dose of OSPW-OF, which indicates that a possible mode of action for OSPW-induced toxicity includes oxidative stress and associated DNA damage.

We also monitored pro-inflammatory cytokine expression levels after OSPW exposures to provide important information regarding its effects on mammalian macrophages. Our results show that raw OSPW at 10 mg/L NAs exhibited differential effects on basal cytokine gene expression and cytokine secretion in resting cells. In addition, raw OSPW had variable influences on the mRNA expression and protein secretion levels in activated cells. Alternatively, OSPW-OF at 10 mg/L NAs demonstrated no significant effects on basal or activated cytokine gene expression or secretion. These data suggest the presence of immunomodulatory factors within raw OSPW that selectively affect cytokine networks in immune cells, which may disrupt immune cell activities causing inflammation-related disturbances. The complexity of these effects require further investigation but our results indicate that raw OSPW-exposed macrophages have a reduced ability to engulf bacteria, which could translate *in vivo* to a higher incidence of bacterial pathogenesis. This reveals that combined with the variable effects on cytokine secretion by mouse macrophages, raw OSPW components can also inhibit phagocytosis, a key antimicrobial response of mammalian phagocytes. This suggests that the

immunomodulatory effects of as yet unidentified OSPW constituents are dose-dependent and they can differentially affect the cell biology of immune cells at the gene, protein, and functional levels.

4.6.3 Conclusions (*in vitro* toxicity studies)

The results suggest that at the doses tested in this study, raw OSPW but not OSPW-OF components have immunomodulatory properties and our newly optimized *in vitro* cell-based assay systems will be important for further characterizing this phenomenon. We speculate that procedures for the organic fractionation of raw OSPW remove, dilute, or mitigate the immunomodulatory effects of the contaminated water and that inorganic compounds present in the raw OSPW may be partially responsible for the observed effects. It is also possible that the synergistic interactions between organic and inorganic OSPW components are required to perturb immune cell cytokine gene expression/secretion as well as phagocytic responses. While beyond the scope of the present study, identification of the factors in raw OSPW responsible for the selective and specific alteration of immune cell responses needs to be addressed in future studies. The *in vitro* assays developed in this study will be important for characterization of these unknown immunoregulatory factors further, and as an *in vitro* bioindicator system, the RAW 264.7 mammalian macrophage cell line has proven to be a valuable model for the rapid (and relatively inexpensive) examination of the toxicity of various OSPW samples. This will be important for comparative assessments of the toxicity of different OSPW sources.

4.7 *In Vivo* Studies Using Mice

To date, there is little information on the effects of OSPW exposure on development and reproduction of mammals. The objective of this portion of the study was to determine whether OSPW-OF posed a health risk to mammals by means of exposure through their drinking water, specifically during the sensitive stages of gestation and lactation. Mice, as the classical mammalian model organism, were used to test the acute (2-week) and sub-chronic (6-week) toxicity of OSPW-OF. The doses were chosen to accurately reflect the environmental exposures that small mammals could experience if their drinking water was akin to OSPW with NAs at concentrations of 1, 10 and 55 mg/L. Effects on body weight, reproductive performance, hormone production, cytokine gene and protein expression, stress gene analysis, and *ex vivo* immune cell activities as well as the hepatotoxicity were all examined. The results of this study may be directly linked to potential risk associated with OSPW exposures to humans, and facilitate the establishment of guidelines required for the protection of public health.

Overall, we have performed four sets of acute and sub-chronic exposure trials. For each trial, female Balb/c mice were exposed weekly to OSPW-OF by oral gavage administrations during pregnancy (21 days) and lactation (21 days). Samples (e.g. plasma, cells, and tissues) from pregnant mice and pups were then collected on gestation day (GD) 14 (i.e., acute exposure) and at the end of lactation (6 weeks; sub-chronic exposure). For both the acute and sub-chronic exposures, the four treatment groups consisted of six mice that were exposed to saline (i.e. sham controls), OSPW-OF low dose (1mg/L; based on naphthenic acid content), OSPW-OF high dose (10 mg/L), and OSPW-O_3-OF (10 mg/L). We also performed acute and sub-chronic exposures to assess the effects of OSPW-OF exposures at 55 mg/L NAs during pregnancy and

lactation. We completed data collection and analyses on the following four independent exposures using the indicated number of animals:

i) Acute Exposure (GD 14):
   a. Sham control; 6 mice per group x 4 trials = 24 total
   b. OSPW (1 mg/L); 6 mice per group x 4 trials = 24 total
   c. OSPW (10 mg/L); 6 mice per group x 4 trials = 24 total
   d. OSPW-O_3 (10 mg/L); 6 mice per group x 4 trials = 24 total
   e. OSPW-OF (55 mg/L); 8 sham control and 8 exposed = 16 total

ii) Sub-chronic Exposure (6 weeks):
   a. Sham control; 6 mice per group x 4 trials = 24 total
   b. OSPW (1 mg/L); 6 mice per group x 3 trials = 18 total
   c. OSPW (10 mg/L); 6 mice per group x 4 trials = 24 total
   d. OSPW-O_3 (10 mg/L); 6 mice per group x 4 trials = 24 total
   e. OSPW-OF (55 mg/L); 8 sham control and 8 exposed = 16 total

4.7.1 Detailed overview of *in vivo* results

a) Acute exposure (Gestation day 14)

Pregnancy parameters: There were no significant effects of OSPW-OF exposures at all doses tested on the pregnancy parameters of the exposed mice (Table 6). For example, mice exposed to 1 mg/L OSPW-OF, 10 mg/L of OSPW-OF, and 10 mg/L of OSPW-OF-O_3 had pregnancy rates of ~65%, which were no different than the sham control group. Furthermore, in the 55 mg/L OSPW-OF trials, all of the exposed mice became pregnant (Table 6). The average number of fetal embryos per animal was between 8 and 10 for all exposure groups indicating that OSPW-OF exposures do not affect implantation success during pregnancy. Examination of the placenta for spontaneous fetal resorptions (indicative of a fetus that dies *in utero*) also showed no differences between the OSPW-OF treatments and the control group (Table 6). We also examined the health status of the fetus during the acute exposures by measuring placental weight (PW), which is indicative of the maternal nutrient supply during pregnancy, as well as fetal weight (FW) and the proportion of a fetus to a placenta (F/P ratio), which estimates the fetal growth condition. In the control animals, a healthy placenta and a normal fetus weighed approximately 0.099 grams and 0.156 grams, respectively on GD 14. Their weight proportion (F/P) was ~1.588 suggesting that a healthy fetus is approximately 1.6-fold heavier than a normal placenta at mid pregnancy. Notably, there were no observed effects of OSPW-OF exposures at all doses tested on the health status parameters of the fetus (Table 6). Finally, during the acute exposure period, all of the pregnant mice in the control group gained ~8 grams weight in two weeks (~41% weight increase) and there were no significant differences in their weight gain when the control group was compared with the OSPW exposure groups on days 4 and 14 (Fig. 34). Since the body weights of pregnant mice were variable among exposure groups (Table 7), we calculated the weight ratios of fetus/mother (F/M) and placenta/mother (P/M) to avoid the interference of maternal body weight. As shown in Table 7, the P/M and F/M values in the control group were 0.352% and 0.553%, respectively. Therefore, when normal pregnant mouse on gestation day 14 has a body weight of 28 grams, her placenta would weigh 0.352% x 28

grams = 0.099 grams and her pups would weigh 0.553% × 28 grams = 0.155 grams. These two parameters were subsequently used as standards for selection of healthy placenta in the following assessments. Using these indicators, no significant changes were observed when comparing the OSPW-OF exposed animals to the sham controls (Table 7). Overall, our results suggest that acute OSPW-OF exposures up to a dose of 55 mg/L of NAs have no effects on the general pregnancy parameters of exposed mice.

Plasma hormone levels: Plasma hormone levels were measured in pregnant mice after the acute exposure period (Figs. 35 and 36). The hormones measured were: i) progesterone, produced by the ovaries to help the uterus prepare for pregnancy and to help maintain the pregnancy; ii) prolactin**,** produced by the pituitary gland and plays an important role in reproductive health as well as stimulating lactation; iii) estradiol**,** acts as a growth hormone for the reproductive system and plays a role in the maintenance of oocytes in the ovaries, which increases due to production by the placenta and reduced estradiol levels leads to pregnancy loss; and iv) aldosterone**,** is a steroid hormone produced by the adrenal gland that is generally increased during pregnancy as it may play a role in the regulation of gestational hypertension. The average plasma levels of estradiol, aldosterone, progesterone, and prolactin in the sham control mice were 9.48 ng/mL, 35.74 ng/mL, 16.53 pg/mL, and 36.69 pg/mL, respectively, and as shown in Figures 22A-22D, there were no significant differences in the plasma hormone levels of OSPW exposed mice when compared to the control group. In addition, as shown in Figure 23, the higher dose of OSPW-OF (55 mg/L) also had no significant effect on plasma hormone levels. These results suggest that an acute OSPW-OF exposure up to a dose of 55 mg/L of NAs does not significantly affect the plasma hormone levels of pregnant mice on GD 14.

Plasma cytokine levels: Cytokine levels were monitored in the plasma of the pregnant animals following acute OSPW exposures. The 10 mg/L OSPW-OF exposed mice had a significant increase ($p<0.05$) in their plasma CXCL-10 levels, which increased from 24 pg/mL in the control group to 46.1 pg/mL (Fig. 37A). In comparison, the 26.7 pg/mL and 60 pg/mL levels of CXCL-10 in the plasma of 1 mg/L OSPW-OF and 10 mg/L OSPW-O_3-OF exposed animals were not significantly different from the control group (Fig. 37A). Although the average measured level of CXCL-10 in the 10 mg/L OSPW-O_3-OF group was higher than that observed for the 10 mg/L OSPW-OF group (i.e., 60 pg/mL vs. 46.1 pg/mL), its higher level of experimental variability likely affected the calculated statistical significance for this group (Fig. 37A). When compared to the 33.1 pg/mL of CXCL-9 detected in the plasma of the sham control group, mice acutely exposed to 1 mg/L OSPW-OF, 10 mg/L OSPW-OF, and 10 mg/L OSPW-O_3-OF did not have significantly different levels of this protein in their plasma (Fig. 37B). For CXCL-1 levels, mice exposed to 10 mg/L OSPW-OF (but not 1 mg/L OSPW-OF) had significantly higher levels in their plasma (e.g., 138.3 pg/L) when compared to the control levels of 49.2 pg/L (Fig. 37C). Comparatively, the 10 mg/L OSPW-O_3-OF exposed mice plasma levels of 111.6 pg/L were higher but not significantly different than the levels of CXCL-1 observed in the plasma of the control animals. Furthermore, the sham control exposed mice on GD 14 had plasma G-CSF levels of 150 pg/mL and after exposure to 1 mg/L OSPW-OF, 10 mg/L OSPW-OF, and 10 mg/L OSPW-O_3-OF the plasma G-CSF levels were 182.6 pg/mL, 243.2 pg/mL, and 176.4 pg/mL, respectively (Fig. 37D). The 243.2

pg/mL of G-CSF measured in the plasma of 10 mg/L OSPW-OF exposed mice was significantly increased relative to the control levels, whereas in the other exposure groups plasma G-CSF levels were not. Finally, we also monitored the plasma levels of the cytokines IL-1α, IL-2, IL-5, IL-13 (Fig. 37E) as well as the chemokines RANTES, MCP-1, MIP-1α, MIP-1β, and MIP-2 (Fig. 37F) during the acute exposure trials and none these immune proteins were significantly affected in all exposure groups on GD 14. Note: although IL-1β levels were reported in our *in vitro* trials, the levels of this protein were below the detection limit of the assay mouse plasma.

In a separate series of exposure trials, Balb/c mice were also acutely exposed to a higher dose (i.e., 55 mg/L) of OSPW-OF and this showed that only CXCL-10 plasma levels were significantly increased when compared to the sham control animals (Fig. 38). Overall, these results suggest that following acute exposure to 10 mg/L of OSPW-OF there are increased plasma levels of CXCL-10, CXCL-1, and G-CSF on GD 14. However, the lower dose of 1 mg/L OSPW-OF as well as the ozonated OSPW-OF (10 mg/L) did not significantly affect the plasma cytokine levels of pregnant mice. In addition, unlike what we observed for the 10 mg/L OSPW-OF exposures (Fig. 37), a higher exposure dose of OSPW-OF did not dramatically alter plasma cytokine levels (Fig. 38).

Cytokine and stress gene expression: A panel of cytokine, oxidative stress, DNA damage/repair, and pregnancy-associated genes were monitored to determine if acute OSPW-OF exposures affected the mRNA expression profiles of these selected pathways. Following acute exposures, spleen, liver, and placental tissue samples were collected on gestational day 14 and then examined using quantitative PCR for the expression analyses of the selected genes. As shown in Figure 26, the spleens of pregnant mice demonstrated no significant differences in the expression of *cxcl-10* and *il-1β*. However, at 10 mg/L of OSPW-OF there was a significant increase in the expression of *cxcl-10* mRNA, which increased ~1.7-fold relative to the sham control whose expression value was normalized to 1.0 (Fig. 39A). None of the other OSPW-OF exposures affected *cxcl-10* expression in the liver and as seen in the spleen, *il-1β* levels in the liver were no different after OSPW-OF exposures when compared to the control (Fig. 39B). Mice acutely exposed to 55 mg/L of OSPW-OF showed no significant increases in *cxcl-10* or *il-1β* mRNA expression in the liver and spleen (Fig. 40). Therefore, at all doses tested, other than *cxcl-10* expression in the liver (Fig. 39A), OSPW-OF exposure doses ranging from 1 mg/L to 55 mg/L had no significant effect on the basal cytokine expression levels examined.

For stress gene expression, *gstp1* and *hmox1* (oxidative stress) as well as ogg1 (DNA damage/repair) showed no significant change in the livers of animals acutely exposed to 1 mg/L OSPW-OF, 10 mg/L OSPW-OF, and 10 mg/L OSPW-OF-O_3 (Fig. 41). When the highest dose of 55 mg/L of OSPW-OF was used, we observed a significant decrease in the expression of *gstp1* (0.82 fold expression; Fig. 42A) and *ogg1* (0.80; Fig. 42B) but not *hmox1* when compared to the normalized sham control expression levels of 1.0 (Fig. 42C). In the spleen, *gstm1* and *hmox1* (oxidative stress genes) as well as *lig1*, *ung*, and gadd45 remained unchanged relative to the sham control group (Fig. 43). Finally, in the placental tissue, no changes in the expression of selected pregnancy-associated genes (i.e., vascular endothelial growth factor-alpha (*Vegf-α*), placenta growth factor (*Pgf*), estrogen receptor-alpha (*Er-α*), and progesterone receptor (*Pgr*)

were observed between the control and OSPW-OF treatment groups at all OSPW-OF dose tested (Fig. 44 and 45). Similarly, the stress genes *hmox1* and *pcna* were unchanged in placental tissues of mice acutely exposed to dose of OSPW-OF ranging from 1 mg/L to 55 mg/L (Figs. 44 and 45). These results suggest that acute exposures of pregnant mice to OSPW-OF (1 mg/L, 10 mg/L, and 55 mg/mL) had no overall effects on the expression profiles of the majority of selected genes belonging to the pro-inflammatory, stress, and pregnancy pathways at GD 14.

Immune cell numbers and their effector responses: As shown in Figures 46-48, mice acutely exposed to OSPW-OF demonstrated no differences in their ratios of T cell subpopulations, which are displayed as the ratio of T helper (CD4) to cytotoxic T cells (CD8) in their peripheral blood (Fig. 46A). Furthermore, when compared to the sham control animals, those exposed to 1 mg/L OSPW-OF, 10 mg/L OSPW-OF, and 10 mg/L OSPW-OF-O_3 had the same overall proportion of leukocyte sub-populations in their peripheral blood with T cells representing the major leukocyte subpopulation in all groups at ~60% followed by B cells (~18%), NK cells (~5%), and monocytes (~3%). At the higher OSPW-OF acute expose dose of 55 mg/L, CD4/CD8 ratios (Fig. 47A), and the relative proportions of peripheral blood leukocyte subpopulations (Fig. 47B) were once again no different than what was observed in the sham control group. Finally, when isolated cells from the exposed animals were examined for their effector functions, we observed that peritoneal macrophages as well as spleen-derived NK cells showed no significant differences in their ability to produce the antimicrobial compound nitrite or their ability to kill target cells, Figures 48A and 48B, respectively. In summary, it appears that acute exposure of pregnant mice to OSPW-OF (1 mg/L, 10 mg/L, and 55 mg/L) had no overall effects on immune cell numbers or their effector functions after two exposures up to gestational day 14.

b) Sub-chronic exposure (6 weeks)

Pregnancy parameters: As shown in Table 8, there were no significant effects of sub-chronic OSPW exposures on the general pregnancy parameters of exposed mice. For example, mice exposed to 1 mg/L OSPW-OF, 10 mg/L OSPW-OF, and 10 mg/L of OSPW-OF-O_3 had pregnancy rates of ~80%, which were no different from the sham control group. Furthermore, in the 55 mg/L OSPW-OF trials, 63% of exposed mice became pregnant, which was not significantly different than the sham control group (Table 8). The litter size in all groups was on average 6 pups indicating that sub-chronic OSPW-OF exposures also have no effect on litter size. As was observed for the acute exposure trials, the female mice gained weight from ~19.6 grams to ~29.8 grams during the first three weeks post-fertilization, which stabilized for the remainder of the experiment up to GD 42 when the mice weighed on average ~25.4 grams (Fig. 49). Notably, there were no significant effects of OSPW-OF exposures on the weight gain of the female mice in all groups examined (Table 8). The ratio of female to total pups in the litters was also calculated, which showed that out of 153 total pups born, 53% were female (Table 8). When the mice were exposed to 1 mg/L OSPW-OF, 10 mg/L OSPW-OF, and 55 mg/L OSPW-OF, the ratio of female pups in the litter was 66%, 57%, 57%, and 69%, respectively. None of these were significantly different when compared to the litters of the control mice (Table 8). In addition, as shown in Figure 50 the average pup weight over the course of the experiment for the control group increased from ~1.6 grams (at birth, PD1) to ~12.7 grams (at the end of lactation, PD21), which was when the pups weighed nearly half of their mothers (P/M ratio: 50%). The body

weights and P/M ratios were not significantly different than the weight of pups in all of the OSPW-OF exposed groups (Table 8 and Fig. 50). Overall, these results suggest that a sub-chronic OSPW-OF exposure up to a dose of 55 mg/L does not affect the general pregnancy parameters of mice, including litter size, sex ratio of the pups, and growth rate of the pups.

Plasma hormone levels: Plasma hormone levels were measured in pregnant mice after the sub-chronic exposure period (Figs. 51 and 52). The average plasma levels of estradiol, aldosterone, progesterone, and prolactin after six weeks in the sham control mice were 6.9 ng/mL, 51.8 ng/mL, 6.7 pg/mL, and 10.6 pg/mL, respectively, and as shown in Figures 51A-D, there were no significant differences in plasma estradiol or prolactin levels of OSPW exposed mice when compared to the control group (Figs. 51A and 51D). However, exposure to 10 mg/L OSPW-OF significantly reduced plasma aldosterone levels from 51.8 pg/mL in the control down to 21.9 pg/mL; an effect that was not observed at the 1 mg/L OSPW-OF dose or when the mice were sub-chronically exposed to 10 mg/L of OSPW-OF-O_3 (Fig. 51B). A significant reduction in plasma progesterone levels was also observed in the mice exposed to 10 mg/L OSPW-OF and 10 mg/L OSPW-OF-O_3 (Fig. 51D). Comparatively, the higher dose of 55 mg/L OSPW-OF significantly increased plasma aldosterone levels by ~50% (Fig. 52B) and also significantly decreased progesterone levels (Fig. 52C) but this dose had no significant effects on the levels of estradiol or prolactin (Figs. 52A and 52D). Overall these results suggest that sub-chronic exposures to 10 mg/L OSPW-OF significantly decreased the plasma levels of aldosterone and progesterone, whereas 55 mg/L OSPW-OF significantly enhances plasma aldosterone levels but reduces progesterone. Estradiol and prolactin levels were unaffected by sub-chronic OSPW-OF exposures at all doses tested.

Plasma cytokine and chemokine levels: Cytokine and chemokine levels were also monitored in the plasma of the pregnant animals following sub-chronic OSPW exposures (Figs. 53 and 54). At all exposure doses tested (i.e., 1 mg/L, 10 mg/L, and 55 mg/L) and for all cytokine proteins examined, other than CXCL-9 (significantly increased from 37.9 pg/mL in sham control to 66.7 pg/mL after 10 mg/L OSPW-OF exposure; Fig. 53B) there were no significant differences in the plasma protein levels when compared to the control animals.

Cytokine and stress gene expression: A panel of cytokine, oxidative stress, DNA damage/repair, and pregnancy-associated genes were monitored to determine if sub-chronic OSPW-OF exposures affected the mRNA expression profiles of these selected pathways. Following sub-chronic exposures spleen and liver from the adult female mice, as well as liver samples were collected and then examined using quantitative PCR for the expression analyses of the selected genes. As shown in Figure 55, the liver and spleens of female mice demonstrated no significant differences in the expression of *cxcl-10* and *il-1β*. However, the liver *cxcl-10* mRNA expression levels did show an increased trend of expression relative to the controls with 1.60, 1.64, and 1.30-fold increases after exposure to 1 mg/L OSPW-OF, 10 mg/L OSPW-OF, and 10 mg/L OSPW-OF-O_3, respectively (Fig. 55A). Mice sub-chronically exposed to 55 mg/L of OSPW-OF showed no significant changes in *cxcl-10* expression but had a significant decrease in *il-1β* mRNA expression levels in the liver with a fold change of 0.82 relative to the sham control expression value that was normalized to 1.0 (Fig. 56). For stress gene expression levels, *hmox1* (oxidative

stress) but not *gstp1* (oxidative stress) or ogg1 (DNA damage/repair) showed a significant decrease in relative expression when the mice were exposed to 10 mg/L OSPW-OF (Fig. 57C). When the highest dose of 55 mg/L of OSPW-OF was used, we observed no significant changes in the mRNA expression levels of *hmox1*, *gstp1*, or ogg1 (Fig. 58). In the spleen, all of the oxidative stress and DNA damage/repair gene mRNA levels remained unchanged relative to the sham control group (Fig. 59). Finally, in the liver tissue of the pups, *gadd45* expression was significantly increased 1.52-fold after 10 mg/L OSPW-OF exposure relative to the sham control expression value that was normalized to 1.0 (Fig. 60), whereas *lig1* (0.80) and *ogg1* (0.78) mRNA expression levels were significantly decreased after exposure to 10 mg/L OSPW-OF-O3 in pup livers (Fig. 60). These results indicate that sub-chronic OSPW-OF exposures have variable effects on cytokine and stress gene levels depending on the tissue examined and gene measured. Notably, most genes monitored demonstrated no significant changes in expression levels at all doses examined except for a decrease in liver *il-1β* levels (55 mg/L OSPW-OF exposure), decreased liver *hmox1* expression (10 mg/L exposure), and the observed changes in gadd45 (increased) and lig1 (decreased) and ogg1 (decreased) after exposures to 10 mg/L OSPW-OF and 10 mg/L OSPW-OF-O_3, respectively.

Immune cell numbers and their effector responses: As shown in Figures 61-63, mice sub-chronically exposed to OSPW-OF demonstrated no differences in their ratios of T cell subpopulations, which are displayed as the ratio of T helper (CD4) to cytotoxic T cells (CD8) in their peripheral blood (Fig. 61A). Furthermore, when compared to the sham control animals, mice exposed to 1 mg/L OSPW-OF, 10 mg/L OSPW-OF, and 10 mg/L OSPW-OF-O_3 had the same overall proportion of leukocyte sub-populations in their peripheral blood with T cells representing the major leukocyte subpopulation in all groups at ~45% followed by B cells (~18%), NK cells (~11%), and monocytes (~4%). At the higher OSPW-OF acute expose dose of 55 mg/L, CD4/CD8 ratios (Fig. 62A), and the relative proportions of peripheral blood leukocyte subpopulations (Fig. 62B) were once again no different than what was observed in the sham control group. Finally, when isolated cells from the exposed animals were examined for their effector functions, we observed that peritoneal macrophages as well as spleen-derived NK cells showed no significant differences in their ability to produce the antimicrobial compound nitrite or their ability to kill target cells, Figures 63A and 63B, respectively. In summary, it appears that sub-chronic exposure of pregnant mice to OSPW-OF (1 mg/L, 10 mg/L, and 55 mg/L) had no overall effects on immune cell numbers or their effector functions after six exposures up to GD 42.

Pathology: Several tissues (e.g., liver, spleen, intestine, kidney, placenta, brain, and lung from adult mice as well as the spleen and liver tissues from pups) were examined microscopically in a double-blind fashion, by a registered veterinary pathologist (Dr. Nick Nation, Veterinary Pathologist, University of Alberta). When compared with the control samples, no overt pathological changes were observed after acute or sub-chronic exposures that would be indicative of tissue damage, inflammation, or neoplasia for all histological samples examined. Shown in Figures 64A and 64B are the pathology report summaries for both the acute and sub-chronic exposures and in Figure 64C are representative sub-chronic histological images.

4.7.2 Discussion (*in vivo* assessment of toxicity of the organic fraction of OSPW)

Early research by Rogers et al. [16] demonstrated that oral exposure to OSPW-NAEs (60 mg/kg/d) during pre-breeding, breeding and gestation caused impaired embryonic implantation in rats, which was likely associated with the changes in cholesterol availability and a parallel decrease in plasma progesterone (a cholesterol progeny) [16]. However, it should be noted that the exposure dose was 10 times the estimated worst-case daily exposure. In reality, NA concentrations range from ~20 to 80 mg/L in fresh settling basins [52], and ~5 to 40 mg/L in reclamation ponds or experimental wetlands [8, 19, 53, 54]. NA levels in Athabasca River adjacent to the lease sites are typically less than 1 mg/L [1]. In the present study, NAs at 1, 10, and 55 mg/L were selected to investigate the possible toxicity of OSPW-OF at environmentally relevant concentrations. Exposure to OSPW-OF during gestation and lactation at these doses did not cause outward toxicity in mice. The body weight and reproductive performance (pregnancy rate, implantation number, resorption rate, litter size and offspring viability, etc.) in the OSPW-OF treated animals was comparable to controls. Also, the weight of embryos on GD 14 and the growth trend of pups during lactation were not impacted by OSPW-OF exposure. These results indicated that acute and sub-chronic exposures of OSPW-OF containing NAs of 55 mg/L or below did not cause overt maternal toxicity and fetal toxicity.

OSPW-OF did not cause lethality in mice during the 2- and 6- week exposures, and there were no obvious signs of distress such as behaviour changes, loss of body weight, or pregnancy failure. Therefore, changes in mRNA levels of stress genes in the livers might not be indicative of acute toxicity but might be indicators of sub-lethal effects on mice. A suite of gene expression markers were used in our study including *gstp1*, *gstm1*, *hmox1*, *lig1*, ogg1, *gadd45*, *ung* and *pcna*. It is shown that the abundances of transcripts of two glutathione-S-transferases (GSTs) were down regulated in livers of mice exposed to high dose of OSPW-OF (55 mg/L NAs) for two weeks, including *gstp1* and *gstm1*. GSTs are a family of detoxification enzymes that function to protect cells from damage caused by reactive electrophiles by conjugating a variety of endogenous and exogenous compounds (including carcinogens, environmental pollutants, drugs and other xenobiotics) with reduced glutathione to produce less reactive water-soluble compounds and facilitate their elimination [55, 56]. The results found in present study were inconsistent with greater abundance of transcripts of GST in livers of fathead minnows [3] and rainbow trout hepatocytes [57] exposed to OSPW. However, Gagné and colleagues [58] also found that GST enzyme activity in trout hepatocytes was significantly inhibited by exposure to OSPW extracts. It was suggested that some inhibitors like organometallic complexes might be present in the extracts that could block the activity and perhaps also block expression of *gst* [58, 59]. Evidence has shown that organic complexes of some elements in group IVA of the periodic table (e.g., germanium, lead and tin) were potent inhibitors of hepatic GST activity [23]. Since OSPW is complex of a variety of organics and metals (including those from IVA family), it is possible that some organometallic compound(s) extracted by DCM extraction might be the agent(s) responsible for the decreased *gst* gene expression. The changes in gene expression might reflect the protein levels. The down-regulated *gst* transcription could lead to decreased *gst* translation, which could be associated with a compromise in the elimination process of xenobiotics. Interestingly, down-regulation of *gst* only occurred during acute exposures. The gene expression returned to the control level or was slightly elevated (i.e., *gstp1*) after

prolonged exposure. This indicates a possible shift towards a detoxification mechanism under long duration of the stress condition generated by OSPW-OF treatment.

OSPW has been shown to cause oxidative stress, demonstrated by greater concentrations of reactive oxygen species (ROS) and higher expression of genes involved in defending against ROS in fish [58, 60], as well as elevated oxidative stress responsive gene in mammalian cells (i.e., elevated *hmox1* expression in RAW 264.6 cells exposed to OSPW as demonstrated in our *in vitro* study). Interestingly, a 6-week oral exposure of OSPW-OF at 10 mg/L NAs induced a down-regulation of *hmox1* expression in the liver. Similar inhibitory effects have been reported in kidneys of rats [61] and human neutrophils [62] under conditions of oxidative stress. These results suggest that *hmox1* expression is not solely dependent on ROS status in cells. Oxidative stress can damage DNA, and when the DNA damage is irreparable, it can lead to cellular transformation occurs and ultimately to the development of tumors [63]. Recently, there are several studies reporting on the genotoxicity of OSPW. Lacaze and colleagues [64] found primary DNA damage in rainbow trout hepatocytes caused by NAs, in a structure-dependent manner. Though different NAs at the same dose resulted in different DNA damage response patterns, the majority of NAs tested were genotoxic at concentrations lower than those reported in OSPW [64, 65]. DNA damage has also been reported in research by Gagne and colleagues [57, 66] with alterations in transcripts of genes involved in DNA repair and synthesis during cell maintenance such as *lig*, *ung*, and *ogg*. LIG functions in the ligation of newly synthesized DNA strands to the backbone of DNA molecules [66], UNG is an important enzyme that prevents mutagenesis by capturing and removing uracil (a base normally present in RNA) from DNA [67], and OGG is the DNA glycosylase that initiates the base-excision repair (BER) pathway to repair non-bulky oxidative DNA lesions [63]. In previous studies, genotoxicity of OSPW was shown by elevated gene expression of *ung* and *ogg* with decreased *lig* [57, 58, 66]. Similar increase in *ung* transcripts was observed in mice after 6-week exposure to OSPW-OF exposure at 55 mg/L; however, reduced *ogg* expression occurred in the short-term (2-week) treatment. It should be noted that, despite the changes in liver gene expression might be predictive of hepatotoxicity, we did not detect any alterations in liver histology following exposure to OSPW-OF at all doses.

4.7.3 Conclusions (*in vivo* toxicity studies)

In conclusion, based on mice as the surrogate mammalian model, the results of the present study suggest the risk of acute and sub-chronic toxicity to small wild mammals exposed to OSPW organic fraction, at indicated NA concentrations, in contaminated drinking water is low. No significant signs of distress (including death, behaviour changes, loss of body weight, and pregnancy failure) were associated with the oral administration of OSPW-OF to mice, either acutely (2-week) or sub-chronically (6-week) at the doses up to 55 mg/L NAs. In addition, only minor changes in plasma hormone levels, cytokine gene expression, and cytokine protein secretion at all OSPW-OF doses tested after acute and sub-chronic exposures were observed. Furthermore, although a few stress responsive and detoxification genes were slightly altered in livers of female mice and pups after sub-chronic exposures, no histopathological changes in livers were observed. Finally, immune cells isolated from exposed mice did not demonstrate any change in their antimicrobial activities. Overall, the results of our study suggest that OSPW-

OF up to 55 mg/L NAs, even on a repeated oral exposure basis, might be below the threshold required to induce toxicity and more specifically immunotoxic effects in mice.

5. Relevance of the Research Results in Support of Water for Life

There are concerns about the environmental and public health impacts as a result of any possible future release of OSPW into the environment. The potential for breakthrough innovation of this research and its impact on water sustainability and water quality in Alberta include the first comprehensive analysis of the reproductive and immune system effects of whole OSPW and the whole OSPW-OF in mammals. The comprehensive *in vitro* and *in vivo* analysis of the potential immunotoxic effects and reproductive toxicity of whole and fractionated OSPW in mice may be directly linked to potential risk associated with OSPW exposures to humans, allowing regulators to set guidelines for the protection of the environmental and public health.

Our research will also support the development of risk assessments and regulations for the safe release of OSPW into the environment. In addition, OSPW management strategies based on the use of advanced OSPW fractionation and oxidation processes will ensure enhanced protection of aquatic ecosystems and terrestrial animals in the oil sands industrial region. The proposed research is aligned with the following investment priorities articulated by AI-EES:

i) **Healthy Aquatic Ecosystems**: Research on oil sands process water (OSPW) in end pit lakes. The knowledge and methodology developed in this proposed research will enable proper assessment of risk and the effects of OSPW exposure on terrestrial animals that are in close proximity to the established end-pit lakes.

ii) **Water Use Conservation, Efficiency, and Productivity**: Provide risk based decision-making tools for assistance in water regulation. The information gathered in the proposed research will be informative for risk assessment and development of regulations for safe release of OSPW into the environment. Further, the bioindicator assays (especially the developed *in vitro* mammalian cell assays) may be employed for post-treatment monitoring of OSPW, prior to the release into the environment, thereby enhancing public health protection.

iii) **Water Protection**: Ensure safe mine water release and water treatment option. The comprehensive chemical analyses of both organic and inorganic fractions, may allow for development of OSPW fraction-specific treatment strategies for the removal of highly toxic compounds that contribute to OSPW toxicity. The dose-response analysis of toxic effects induced by different OSPW fractions, and the use of ozone and for remediation of OSPW, will allow for the development of treatment strategies for safe release of OSPW into the environment and ultimately protection of public health.

6. List of Important Events and/or Distinctions from the Research Activities

N/A

7. List of Peer-Reviewed Publications

Chao Li, Li Fu, James Stafford, Miodrag Belosevic, and Mohamed Gamal El-Din. The toxicity of oil sands process-affected water (OSPW): A critical review. *The Science of the Total Environment*, 2017, 601-602: 1785-1802. doi: 10.1016/j.scitotenv.2017.06.024.

Li Fu, Chao Li, Dustin Lillico, Nicole Philips, Mohamed Gamal El-Din, and Miodrag Belosevic. Comparison of the acute immunotoxicity of non-fractionated and fractionated oil sands process-affected water using mammalian macrophages. *Environmental Science & Technology*, 2017 (In Press). doi 10.1021/acs.est.7b02120.

Mohamed Meshref, Nikolaus Klamerth, Md. Shahinoor Islam, Kerry N. McPhedran, and Mohamed Gamal El-Din. Understanding the similarities and differences between ozone and peroxone in the degradation of naphthenic acids: Comparative performance for potential treatment. *Chemosphere*, 2017, 180: 149-159.

Mohamed Meshref, Pamela Chelme-Ayala, and Mohamed Gamal El-Din. Fate and abundance of classical and heteroatomic naphthenic acid species after advanced oxidation processes: Insights and indicators of transformation and degradation. *Water Research* (under review; submitted for publication on February 14, 2017; Manuscript ID: WR38593).

Rongfu Huang, Yuan Chen, and Mohamed Gamal El-Din. Silver-ion solid phase extraction separation of classical, aromatic, oxidized, and heteroatomic naphthenic acids from oil sands process-affected water. *Environmental Science & Technology*, 2016, 50(12): 6433-6441. DOI: 10.1021/acs.est.6b01350.

8. List of Popular Articles

N/A

9. List of Presentations at Scientific Meetings, Public Events and Media Appearances

James Stafford, Mohamed Gamal El-Din, and Miodrag Belosevic. Mammalian toxicity of RAW and physico-chemically-treated oil sands process-affected waters (OSPW). Alberta

Innovates-Energy and Environment Solutions, Water Innovation Program Forum, Edmonton, AB, May 24-25, 2016 (Oral Presentation).

James Stafford, Li Fu, Chao Li, Mohamed Gamal El-Din, and Miodrag Belosevic. Effects of oil sands process-affected water exposures on mammalian immune parameters. Canadian Society of Zoologists annual meeting; Invited Symposium Speaker: Parasite Immunology and Environment Section on 'Global drivers for shifts in host-pathogen associations, Winnipeg, MB, May 15-19, 2017 (Oral Presentation).

James Stafford, Li Fu, Chao Li, Dustin Lillico, Rongfu Huang, Mohamed Meshref, Arvinder Singh, Mohamed Gamal El-Din, and Miodrag Belosevic. Toxicity of raw and ozone treated oil sands process-affected waters using mammalian macrophages. COSIA-AI-EES Water Conference. Calgary, AB, March 22-23, 2016 (Oral Presentation).

Li Fu, Chao Li, Dustin Lillico, Arvinder Singh, Rongfu Huang, Nikolaus Klamerth, Mohamed Meshref, James Stafford, Mohamed Gamal El-Din, and Miodrag Belosevic. The Effects of Oil Sands Process-Affected Waters Using Mammalian Cell-Line and Animal Exposures. Alberta Innovates-Energy and Environment Solutions, Water Innovation Program Forum, Edmonton, AB, May 30-31, 2016 (Oral Presentation).

Mohamed Gamal El-Din. Treatment of oil sands process-affected water using ozonation: Process efficiency, NA reactivity, and oxidation mechanisms. Invited Speaker, CivE 728: Water and Wastewater Treatment, University of Alberta, February 09, 2017 (Oral Presentation).

Mohamed Gamal El.-Din. Overview of the oil sands process-affected water treatment with advanced oxidation processes. Canada-Spain Workshop on Advanced Oxidation Processes, Barcelona, Spain, July 07-08, 2016 (Oral Presentation).

Mohamed Meshref, Md. Shahinoor Islam, Nikolaus Klamerth, and Mohamed Gamal El-Din. Impacts of ozone based advanced oxidation processes on the oil sands process-affected water remediation. COSIA-AI-EES Water Conference, Calgary, Alberta, March 22-23, 2016 (Poster Presentation).

Mohamed Meshref, Md. Shahinoor Islam, Nikolaus Klamerth, and Mohamed Gamal El-Din. Relative performance of ozone and peroxone on the degradation of naphthenic acid species in oil sands water. IUVA World Congress & Exhibition, Vancouver, British Columbia, January 31 - February 3, 2016 (Oral Presentation).

Mohamed Meshref, Md. Shahinoor Islam, Nikolaus Klamerth, and Mohamed Gamal El-Din. Impact of ozone and peroxone advanced oxidation process on the degradation of naphthenic acids species and detoxification of oil sands process-affected water. 4th European Conference on Environmental Applications of Advanced Oxidation Processes-EAAOP4, Athens, Greece, October 21-24, 2015 (Oral Presentation).

10. List of Training of Highly Qualified Personnel

Name	Position	Research Activities
Dr. Li Fu	Postdoctoral Fellow	Mammalian toxicity experiments
Mr. Dustin Lillico	Ph.D. Student	Immune cell imaging and phagocytosis
Ms. Chao Li	Ph.D. Student	Mammalian toxicity studies
Ms. Rui Qin	Ph.D. Student	Fractionation and ozonation of OSPW-OF
Mr. Mohamed Meshref	Ph.D. Student	Ozonation and peroxone treatment of OSPW
Dr. Rongfu Huang	Postdoctoral Fellow	Advanced analytical analyses and silver-ion solid phase extraction of NA species
Dr. Nikolaus Klamerth	Postdoctoral Fellow	Coordination and assistance in ozonation and fractionation experiments, period 2014-2015
Dr. Pamela Chelme-Ayala	Research Associate	Coordination and assistance in ozonation and fractionation experiments, period 2016-2017

11. References

[1] E.W. Allen, Process water treatment in Canada's oil sands industry: I. Target pollutants and treatment objectives, J. Environ. Eng. Sci., 7 (2008) 123-138.

[2] M.D. MacKinnon, H. Boerger, Description of two treatment methods for detoxifying oil sands tailings pond water, Water Quality Research Journal of Canada, 21 (1986) 496-512.

[3] S.B. Wiseman, J.C. Anderson, K. Liber, J.P. Giesy, Endocrine disruption and oxidative stress in larvae of *Chironomus dilutus* following short-term exposure to fresh or aged oil sands process-affected water, Aquatic Toxicology, 142 (2013) 414-421.

[4] S.D. Melvin, C.M. Lanctot, P.M. Craig, T.W. Moon, K.M. Peru, J.V. Headley, V.L. Trudeau, Effects of naphthenic acid exposure on development and liver metabolic processes in anuran tadpoles, Environmental Pollution, 177 (2013) 22-27.

[5] E. Garcia-Garcia, J.Q. Ge, A. Oladiran, B. Montgomery, M. Gamal El-Din, L.C. Perez-Estrada, J.L. Stafford, J.W. Martin, M. Belosevic, Ozone treatment ameliorates oil sands process water toxicity to the mammalian immune system, Water Research, 45 (2011) 5849-5857.

[6] E. Lari, S. Wiseman, E. Mohaddes, G. Morandi, H. Alharbi, G.G. Pyle, Determining the effect of oil sands process-affected water on grazing behaviour of *Daphnia magna*, long-term consequences, and mechanism, Chemosphere, 146 (2016) 362-370.

[7] S. Wiseman, H. Yuhe, M. Gamal El-Din, J. Martin, P. Jones, M. Hecker, J. Giesy, Transcriptional responses of male fathead minnows exposed to oil sands process-affected water, Comparative Biochemistry and Physiology - Part C Toxicology & Pharmacology 157 (2013) 227-235.

[8] R. Kavanagh, R. Frank, K. Solomon, G. Van Der Kraak, Reproductive and health assessment of fathead minnows (*Pimephales promelas*) inhabiting a pond containing oil sands process-affected water, Aquatic Toxicology, 130-131 (2013) 201-209.

[9] V. Nero, A. Farwell, A. Lister, G. Van der Kraak, L. Lee, M. Van Meer, D. MacKinnon, G. Dixon, Gill and liver histopathological changes in yellow perch (*Perca flavescens*) and goldfish (*Carassius auratus*) exposed to oil sands process-affected water, Ecotoxicology and Environmental Safety, 63 (2006) 365-377.

[10] M. Hagen, E. Garcia-Garcia, A. Oladiran, M. Karpman, S. Mitchell, M. Gamal El-Din, J. Martin, M. Belosevic, The acute and sub-chronic exposures of goldfish to naphthenic acids induce different host defense responses, Aquatic Toxicology, 109 (2012) 143-149.

[11] G.D. Morandi, S.B. Wiseman, A. Pereira, R. Mankidy, I.G.M. Gault, J.W. Martin, J.P. Giesy, Effects-directed analysis of dissolved organic compounds in oil sands process-affected water, Environmental Science & Technology, 49 (2015) 12395-12404.

[12] S.A. Hughes, A. Mahaffey, B. Shore, J. Baker, B. Kilgour, C. Brown, K.M. Peru, J.V. Headley, H.C. Bailey, Using ultrahigh-resolution mass spectrometry and toxicity identification techniques to characterize the toxicity of oil sands process-affected water: The case for classical naphthenic acids, Environmental Toxicology and Chemistry, (2017) DOI 10.1002/etc.3892.

[13] H.A. Alharbi, G. Morandi, J.P. Giesy, S.B. Wiseman, Effect of oil sands process-affected water on toxicity of retene to earlylife-stages of Japanese medaka (*Oryzias latipes*), Aquatic Toxicology, 176 (2016) 1-9.

[14] E. Garcia-Garcia, J. Pun, L.A. Perez-Estrada, M. Gamal-El Din, D.W. Smith, J.W. Martin, M. Belosevic, Commercial naphthenic acids and the organic fraction of oil sands process water downregulate pro-inflammatory gene expression and macrophage antimicrobial responses, Toxicology letters, 203 (2011) 62-73.

[15] E. Garcia-Garcia, J. Pun, J. Hodgkinson, L.A. Perez-Estrada, M.G. El-Din, D.W. Smith, J.W. Martin, M. Belosevic, Commercial naphthenic acids and the organic fraction of oil sands process water induce different effects on pro-inflammatory gene expression and macrophage phagocytosis in mice, Journal of Applied Toxicology, 32 (2012) 968-979.

[16] V.V. Rogers, M. Wickstrom, K. Liber, M.D. MacKinnon, Acute and subchronic mammalian toxicity of naphthenic acids from oil sands tailings, Toxicological Sciences, 66 (2002) 347-355.

[17] A.G. Scarlett, H.C. Reinardy, T.B. Henry, C.E. West, R.A. Frank, L.M. Hewitt, S.J. Rowland, Acute toxicity of aromatic and non-aromatic fractions of naphthenic acids extracted from oil sands process-affected water to larval zebrafish, Chemosphere, 93 (2013) 415-420.

[18] N. Wang, P. Chelme-Ayala, L. Perez-Estrada, E. Garcia-Garcia, J. Pun, J.W. Martin, M. Belosevic, M. Gamal El-Din, Impact of ozonation on naphthenic acids speciation and toxicity of oil sands process-affected water to *Vibrio fischeri* and mammalian immune system, Environmental Science & Technology, 47 (2013) 6518-6526.

[19] M.O. Hagen, B.A. Katzenback, M.S. Islam, M. Gamal El-Din, M. Belosevic, Analysis of goldfish (*Carassius auratus L.*) innate immune responses after acute and subchronic exposures to oil sands process-affected water, Toxicological Sciences, 138 (2014) 59-68.

[20] F. Beltrán, Ozone reaction kinetics for water and wastewater systems, Lewis Publisher CRC Press, Boca Raton, 2004.

[21] H. Suty, C. De Traversay, M. Cost, Applications of advanced oxidation processes: present and future, Water Science and Technology, 49 (2004) 227-233.

[22] W.T.M. Audenaert, Ozonation and UV/hydrogen peroxide treatment of natural water and secondary wastewater effluent: experimental study and mathematical modelling, Ghent University, Belgium, 2012.
[23] C. Gottschalk, J. Libra, A. Sau, Ozonation of Water and Waste Water : A Practical Guide to Understanding Ozone and its Applications, Wiley-VCH, 2010.
[24] American Public Health Association (APHA), Standard Methods for the Examination of Water and Wastewater, 21st edition. American Water Works Association and Water Environment Federation, Washington, DC, 2005.
[25] A.C. Scott, R.F. Young, P.M. Fedorak, Comparison of GC-MS and FTIR methods for quantifying naphthenic acids in water samples, Chemosphere, 73 (2008) 1258-1264.
[26] R. Huang, N. Sun, P. Chelme-Ayala, K.N. McPhedran, M. Changalov, M. Gamal El-Din, Fractionation of oil sands-process affected water using pH-dependent extractions: A study of dissociation constants for naphthenic acids species, Chemosphere, 127 (2015) 291-296.
[27] R. Hindle, M. Noestheden, K. Peru, J. Headley, Quantitative analysis of naphthenic acids in water by liquid chromatography-accurate mass time-of-flight mass spectrometry, Journal of Chromatography A, 1286 (2013) 166-174.
[28] M.S. Islam, J. Moreira, P. Chelme-Ayala, M. Gamal El-Din, Prediction of naphthenic acid species degradation by kinetic and surrogate models during the ozonation of oil sands process-affected water, Sci. Total Environ., 493 (2014) 282-290.
[29] N. Sun, P. Chelme-Ayala, N. Klamerth, K.N. McPhedran, M.S. Islam, L. Perez-Estrada, P. Drzewicz, B.J. Blunt, M. Reichert, M. Hagen, K.B. Tierney, M. Belosevic, M. Gamal El-Din, Advanced analytical mass spectrometric techniques and bioassays to characterize untreated and ozonated oil sands process-affected water, Environmental Science & Technology, 48 (2014) 11090-11099.
[30] J.W. Martin, T. Barri, X. Han, P.M. Fedorak, M. Gamal El-Din, L. Perez, A.C. Scott, J.T. Jiang, Ozonation of oil sands process-affected water accelerates microbial bioremediation, Environ. Sci. Technol., 44 (2010) 8350-8356.
[31] Z. Shu, C. Li, M. Belosevic, J.R. Bolton, M. Gamal El-Din, Application of a solar UV/chlorine advanced oxidation process to oil sands process-affected water remediation, Environmental Science & Technology, 48 (2014) 9692-9701.
[32] R. Huang, K.N. McPhedran, L. Yang, M. Gamal El-Din, Characterization and distribution of metal and nonmetal elements in the Alberta oil sands region of Canada, Chemosphere, 147 (2016) 218-229.
[33] H.C. Reinardy, A.G. Scarlett, T.B. Henry, C.E. West, L.M. Hewitt, R.A. Frank, S.J. Rowland, Aromatic Naphthenic Acids in Oil Sands Process-Affected Water, Resolved by GCxGC-MS, Only Weakly Induce the Gene for Vitellogenin Production in Zebrafish (*Danio rerio*) Larvae, Environmental Science & Technology, 47 (2013) 6614-6620.
[34] R. Huang, K.N. McPhedran, N. Sun, P. Chelme-Ayala, M. Gamal El-Din, Investigation of the impact of organic solvent type and solution pH on the extraction efficiency of naphthenic acids from oil sands process-affected water, Chemosphere, 146 (2016) 472-477.
[35] J.S. Clemente, N.G.N. Prasad, M.D. MacKinnon, P.M. Fedorak, A statistical comparison of naphthenic acids characterized by gas chromatography-mass spectrometry, Chemosphere, 50 (2003) 1265-1274.

[36] J.S. Clemente, T.W. Yen, P.M. Fedorak, Development of a high performance liquid chromatography method to monitor the biodegradation of naphthenic acids, J. Environ. Eng. Sci., 2 (2003) 177-186.
[37] X.M. Han, M.D. MacKinnon, J.W. Martin, Estimating the *in situ* biodegradation of naphthenic acids in oil sands process waters by HPLC/HRMS, Chemosphere, 76 (2009) 63-70.
[38] K. Zhang, A.S. Pereira, J.W. Martin, Estimates of octanol-water partitioning for thousands of dissolved organic species in oil sands process-affected water, Environ. Sci. Technol., 49 (2015) 8907-8913.
[39] R.F. Huang, K.N. McPhedran, M.G. El-Din, Ultra Performance Liquid Chromatography Ion Mobility Time-of-Flight Mass Spectrometry Characterization of Naphthenic Acids Species from Oil Sands Process-Affected Water, Environmental Science & Technology, 49 (2015) 11737-11745.
[40] L.R. Snyder, J.J. Kirkland, J.W. Dolan, Introduction to Modern Liquid Chromatography, 3rd Edition, Wiley, New Jersey, 2010.
[41] T.A. Ternes, J. Stüber, N. Herrmann, D. McDowell, A. Ried, M. Kampmann, B. Teiser, Ozonation: a tool for removal of pharmaceuticals, contrast media and musk fragrances from wastewater?, Water Research, 37 (2003) 1976-1982.
[42] M. Islam, T. Dong, K. McPhedran, Z. Sheng, Y. Zhang, Y. Liu, M. Gamal El-Din, Impact of ozonation pre-treatment of oil sands process-affected water on the operational performance of a GAC-fluidized bed biofilm reactor, Biodegradation, 25 (2014) 811-823.
[43] R.A. Frank, K. Fischer, R. Kavanagh, B.K. Burnison, G. Arsenault, J.V. Headley, K.M. Peru, G. Van der Kraak, K.R. Solomon, Effect of Carboxylic Acid Content on the Acute Toxicity of Oil Sands Naphthenic Acids, Environ. Sci. Technol., 43 (2009) 266-271.
[44] M.S. Islam, J. Moreira, P. Chelme-Ayala, M. Gamal El-Din, Prediction of naphthenic acid species degradation by kinetic and surrogate models during the ozonation of oil sands process-affected water, Sci. Total Environ., 493 (2014) 282-290.
[45] T. Nothe, H. Fahlenkamp, C. von Sonntag, Ozonation of Wastewater: Rate of Ozone Consumption and Hydroxyl Radical Yield, Environ. Sci. & Technol., 43 (2009) 5990-5995.
[46] D.C. Bressler, P.M. Fedorak, Identification of Disulfides from the Biodegradation of Dibenzothiophene, Applied and Environmental Microbiology, 67 (2001) 5084-5093.
[47] K.G. Kropp, J.T. Andersson, P.M. Fedorak, Biotransformations of Three Dimethyldibenzothiophenes by Pure and Mixed Bacterial Cultures, Environ. Sci. & Technol., 31 (1997) 1547-1554.
[48] O.S. Keen, G. McKay, S.P. Mezyk, K.G. Linden, F.L. Rosario-Ortiz, Identifying the factors that influence the reactivity of effluent organic matter with hydroxyl radicals, Water Res., 50 (2014) 408-419.
[49] U. von Gunten, C. von Sonntag, The Chemistry of Ozone in Water and Wastewater Treatment: From Basic Principles to Applications, IWA Publishing, 2012, 2012.
[50] J.E. Grebel, J.J. Pignatello, W.A. Mitch, Effect of halide ions and carbonates on organic contaminant degradation by hydroxyl radical-based advanced oxidation processes in saline waters. , Environmental Science & Technology, 44 (2010) 6822-6828.

[51] J. Staehelin, J. Hoigné, Decomposition of ozone in water in the presence of oorganic solutes acting as promoters and inhibitors of radical chain reactions, Environ. Sci. Technol. , 19 (1985) 1206-1213.
[52] A. Mahaffey, M. Dubé, Review of the composition and toxicity of oil sands process-affected water, Environmental Reviews, 25 (2017) 97-114.
[53] B.D. Hersikorn, J.J.C. Ciborowski, J.E.G. Smits, The effects of oil sands wetlands on wood frogs (*Rana sylvatica*), Toxicological & Environmental Chemistry, 92 (2010) 1513-1527.
[54] R.J. Kavanagh, R.A. Frank, K.D. Oakes, M.R. Servos, R.F. Young, P.M. Fedorak, M.D. MacKinnon, K.R. Solomon, D.G. Dixon, G. Van Der Kraak, Fathead minnow (Pimephales promelas) reproduction is impaired in aged oil sands process-affected waters, Aquatic Toxicology, 101 (2011) 214-220.
[55] N.H.P. Cnubben, I.M.C.M. Rietjens, H. Wortelboer, J. van Zanden, P.J. van Bladeren, The interplay of glutathione-related processes in antioxidant defense, Environ. Toxicol. Pharmacol., 10 (2001) 141-152.
[56] A. Sharma, A. Pandey, S. Sharma, I. Chatterjee, R. Mehrotra, A. Sehgal, J.K. Sharma, Genetic polymorphism of glutathione S-transferase P1 (GSTP1) in Delhi population and comparison with other global populations, Meta Gene, 2 (2014) 134-142.
[57] F. Gagné, M. Douville, C. André, T. Debenest, A. Talbot, J. Sherry, L.M. Hewitt, R.A. Frank, M.E. McMaster, J. Parrott, G. Bickerton, Differential changes in gene expression in rainbow trout hepatocytes exposed to extracts of oil sands process-affected water and the Athabasca River, Comparative Biochemistry and Physiology Part C: Toxicology & Pharmacology, 155 (2012) 551-559.
[58] F. Gagné, C. André, M. Douville, A. Talbot, J. Parrott, M. McMaster, M. Hewitt, An examination of the toxic properties of water extracts in the vicinity of an oil sand extraction site J. Environ. Monit., 13 (2011) 3075-3086
[59] K.H. Byington, E. Hansbrough, Inhibition of the enzymatic activity of ligandin by organogermanium, organolead or organotin compounds and the biliary excretion of sulfobromophthalein by the rat, Journal of Pharmacology and Experimental Therapeutics, 208 (1979) 248-253.
[60] Y.H. He, S. Patterson, N. Wang, M. Hecker, J.W. Martin, M.G. El-Din, J.P. Giesy, S.B. Wiseman, Toxicity of untreated and ozone-treated oil sands process-affected water (OSPW) to early life stages of the fathead minnow (Pimephales promelas), Water Research, 46 (2012) 6359-6368.
[61] D. Bolati, H. Shimizu, M. Yisireyili, F. Nishijima, T. Niwa, Indoxyl sulfate, a uremic toxin, downregulates renal expression of Nrf2 through activation of NF-κB, BMC Nephrology, 14 (2013) 1-9.
[62] G. Alba, R. El Bekay, P. Chacón, M.E. Reyes, E. Ramos, J. Oliván, J. Jiménez, J.M. López, J. Martín-Nieto, Heme Oxygenase-1 Expression is Down-Regulated by Angiotensin II and Under Hypertension in Human Neutrophils, J. Leukoc. Biol., 84 (2008) 397-405.
[63] H. Sampath, V. Vartanian, M.R. Rollins, K. Sakumi, Y. Nakabeppu, R.S. Lloyd, 8-Oxoguanine DNA Glycosylase (OGG1) Deficiency Increases Susceptibility to Obesity and Metabolic Dysfunction PLOS ONE 5, 7 (2012) e51697.

[64] E. Lacaze, A. Devaux, A. Bruneau, S. Bony, J. Sherry, F. Gagné, Genotoxic potential of several naphthenic acids and a synthetic oil sands process-affected water in rainbow trout (*Oncorhynchus mykiss*), Aquat Toxicol., 152 (2014) 291-299.
[65] J.S. Clemente, P.M. Fedorak, A Review of the Occurrence, Analyses, Toxicity, and Biodegradation of Naphthenic Acids, Chemosphere, 60 (2005) 585-600.
[66] F. Gagné, C. André, P. Turcotte, C. Gagnon, J. Sherry, A. Talbot, A Comparative Toxicogenomic Investigation of Oil Sand Water and Processed Water in Rainbow Trout Hepatocytes, Arch. Environ. Contam. Toxicol., 65 (2013) 309-323.
[67] D.O. Zharkov, G.V. Mechetin, G.A. Nevinsky, Uracil-DNA glycosylase: Structural, thermodynamic and kinetic aspects of lesion search and recognition, Mutation Research/Fundamental and Molecular Mechanisms of Mutagenesis, 685 (2010) 11-20.

Appendix: Tables and Figures

Table 1. Concentration of different ions used in batch ozonation experiments to assess the impact of the inorganic fraction on the ozonation performance.

Ion	Low Concentration (mmol/L)	Medium Concentration (mmol/L)	High Concentration (mmol/L)
$NaNO_3$	4.0	12.0	28.0
$Ca(NO_3)_2$	0.5	1.0	2.0
$Mg(NO_3)_2$	0.5	1.0	2.0
NH_4NO_3	0.1	0.5	1.0
NaCl	4.0	8.0	16.0
$NaHCO_3$	4.0	8.0	16.0
Na_2SO_4	0.5	2.0	6.0
$MnSO_4$	0.005	0.05	0.5

Table 2. Physicochemical measurements for raw and treated OSPW samples (utilized ozone dose = 80 mg/L).

Parameter	Syncrude Aurora OSPW (2013)	
	Raw	Ozonated
pH	8.41	7.39
Turbidity (NTU)	277.00	--
Conductivity (mS/cm)	3.05	--
Redox Potential (mV)	235.60	--
Total Solids (TS) (mg/L)	2083.35	--
Total Dissolved Solids (TDS) (mg/L)	2050.00	--
Total Alkalinity (mg/L as $CaCO_3$)	644.15	--
Hardness (mg/L as $CaCO_3$)	182.50	--
Chemical Oxygen Demand (COD) (mg/L)	224.79	--
Biochemical Oxygen Demand (BOD) (mg/L)	13.61	--
Dissolved Oxygen (DO) (mg/L)	6.88	--
Total Organic Carbon (TOC) (mg C/L)	55.7	--
Acid-Extractable Fraction (AEF) (mg/L)	79.53	--
Classical Naphthenic Acids (NAs) (mg/L)	18.38	1.61
Oxidized NAs (x = 3); O_3-NAs (mg/L)	8.75	4.50
Oxidized NAs (x = 4); O_4-NAs (mg/L)	9.57	4.08
Oxidized NAs (x = 5); O_5-NAs (mg/L)	3.98	1.81
Oxidized NAs (x = 6); O_6-NAs (mg/L)	0.62	0.60
Total Oxidized NAs (mg/L)	22.91	11.00
Chloride (Cl^-) (mg/L)	457.25	--
Sulfate (SO_4-S) (mg/L)	131.80	--

Note: "--" means "measurement not available".

Table 3. Characteristics of different OSPW matrices.

Parameter	Shell 2014 (Muskeg River Mine External Tailings Facility)		Shell 2015 (Muskeg River Mine External Tailings Facility)		Syncrude 2014 (Aurora Pond)		Syncrude 2014 (Mildred Lake Site)	
	Raw	Ozonated (80 mg/L O_3)	Raw	Ozonated (80 mg/L O_3)	Raw	Ozonated (80 mg/L O_3)	Raw	Ozonated (50 mg/L O_3)
pH	9.60	9.25	7.10	7.15	9.62	9.57	8.4 ± 0.1	--
TOC (mg/L)	90.3±7.3	74.4±7.1	51.5±2.8	44.7±0.7	61.8±4.9	67.1±5.8	60.3± 0.2	--
COD (mg/L)	128.6±3.7	136.6±4.2	113.6 ± 0.6	83.7 ± 5.2	177.6 ± 13.6	169.4 ± 21.8	216± 2.1	186.3±1.8
BOD_5 (mg/L)	0.26±0.02	12.1±0.22	1.41±0.25	8.86±0.11	6.05±0.53	17.9±0.74	13.5±0.5	18.2±0.2
O_2-NAs (mg/L)	14.4	1.8	16.9	0.6	43.4	9.2	35.5±0.8	5.8
AEF (mg/L)	48.2±2.7	22.8±2.2	40.8±0.5	9.60±1.3	79.7±1.0	47.2±1.2	71.3± 0.6	39±0.5
Microtox (15 min % inhibition)	58.1±1.0	21.1±2.2	26.4±4.8	No effect	97.0±0.1	48.4±1.4	51.0	29.0

Note: "-" means "measurement not available".

Table 4. Physico-chemical measurements of raw and treated OSPW samples after ozonation and peroxone treatment.

Parameter (mg/L)	Syncrude 2014 OSPW (Mildred Lake Site)				
	Raw	Ozonated (30 mg/L O_3)	Ozonated (50 mg/L O_3)	1:1 Peroxone	1:2 Peroxone
Chemical oxygen demand (COD)	216± 2.1	179.2±2.3	186.3±1.8	200.3±4.1	163.4±3.6
Biochemical oxygen demand (BOD_5)	13.5±0.5	17.9±0.7	18.2±0.2	18±0.4	17.8±0.04
Total organic carbon (TOC)	60.3± 0.2	59.7± 1.6	--	58± 1.6	48.9± 1.4
Dissolved organic carbon (DOC)	39.9±1	41±2.1	40±3.2	44.2± 0.8	40.4± 0.5
Acid-extractable fraction (AEF)	71.3± 0.6	43±0.7	39±0.5	42.4±0.4	17.5±0.5
Classical naphthenic acids (NAs)	35.5±0.8	8.00	5.8	8.1	3.1
Oxidized NAs (O_3-NAs; x = 3)	9.1±0.2	8.2	7.6	8.5	3.7
Oxidized NAs (O_4-NAs; x = 4)	10.2±0.2	6.7	6.6	6.1	4.6

Note: all ozone doses are determined as utilized doses. Utilized ozone dose is the amount of ozone that reacts with the contaminants in the water phase, including ozone auto-decomposition.

Table 5. Properties of the different water matrices used in the experiments to assess the impact of the inorganic fraction on the ozonation performance.

Properties	Raw River Water	Ozonated River Water	Raw OSPW (Shell 2015)	Ozonated OSPW (Shell 2015)
pH	7.80	8.83	8.52	8.90
Conductivity (µs/cm)	280.3	272.9	1316	1155
Total Alkalinity (mg/L as $CaCO_3$)	143.55	149.95	341.45	380.55
Redox Potential(mv)	190.1	162.8	184.3	171.9
COD (mg/L)	--	--	122	--
TOC (mg/L C)	2.02	0.43	25.30	1.65
Anions				
Fluoride (mg/L)	0.07	0.13	3.31	0.81
Chloride (mg/L)	2.74	2.77	121.14	121.97
Nitrite (mg/L)	6.16	5.72	21.48	20.83
Nitrate (mg/L)	0.58	0.56	8.71	2.79
Sulfate (mg/L)	49.25	48.47	179.96	187.64
Bromide (mg/L)	0.15	--	1.15	--
Phosphate (mg/L)	0.12	0.56	0.87	1.26
Cations				
Sodium (mg/L)	4.89	5.22	175.62	204.15
Potassium (mg/L)	1.52	2.89	15.70	13.98
Calcium (mg/L)	79.36	75.92	39.56	37.21
Magnesium (mg/L)	10.51	10.71	10.46	11.45
Copper (mg/L)	3.53	4.21	4.33	0.51
Zinc (mg/L)	0.94	0.98	1.07	0.24
Aluminium (mg/L)	1.69	2.53	2.67	0.45
Silicon (mg/L)	0.83	0.75	1.65	1.59

Note: "-" means "measurement not available".

Table 6. Reproductive parameters examined after acute OSPW-OF exposures of pregnant mice.[1]

	Control	OSPW-OF			OSPW+O_3-OF
	Mean ± SE or Median (n=20)	**1 mg/L (n=15)**	**10 mg/L (n=16)**	**50 mg/L (n=8)**	**Equivalent dilution as 10 mg/L (n=17)**
% Pregnant rate	66.67 ± 7.46	62.5 ± 7.98	66.67 ± 11.79	100	70.83 ± 4.17
# of Embryo	9	9	9	8	10
% Resorption	23.17 ± 4.34	27.43 ± 4.46	32.60 ± 4.53	28.03 ± 5.80	22.29 ± 4.49
Placental weight (g)	0.099 ± 0.002	0.091 ± 0.004	0.098 ± 0.002	0.104 ± 0.002	0.091 ± 0.004
Fetus weight (g)	0.157 ± 0.004	0.162 ± 0.014	0.158 ± 0.005	0.177 ± 0.003	0.156 ± 0.005
Fetus /Placenta weight (F/P)	1.588 ± 0.044	1.769 ± 0.099	1.627 ± 0.058	1.748 ± 0.039	1.736 ± 0.052
Body weight, GD14 (g)	28.52 ± 0.46	27.67 ± 0.36	27.54 ± 0.40	28.75 ± 0.54	29.01 ± 0.60
% weight increase	41.17 ± 1.86	41.25 ± 1.67	39.89 ± 1.51	36.49 ± 3.23	42.62 ± 1.66
Placenta / Maternal body weight (P/M)	0.352 ± 0.011	0.332 ± 0.014	0.356 ± 0.009	0.351 ± 0.011	0.324 ± 0.018
Fetus / Maternal body weight(F/M)	0.553 ± 0.011	0.591 ± 0.054	0.575 ± 0.014	0.615 ± 0.015	0.556 ± 0.025

[1]Gestation day 14 (GD-14) of pregnancy

Table 7. Maternal body weight after acute OSPW-OF exposures.

	Control	OSPW-OF			OSPW+O_3-OF
	Mean ± SE or Median (n=20)	**1 mg/L (n=15)**	**10 mg/L (n=16)**	**50 mg/L (n=8)**	**Equivalent dilution as 10 mg/L (n=17)**
Body weight, GD-1 (g)	20.81 ± 0.29	19.79 ± 0.29	19.68 ± 0.27	20.89 ± 0.17	20.56 ± 0.41
Body weight, GD14 (g)	28.52 ± 0.46	27.67 ± 0.36	27.54 ± 0.40	28.75 ± 0.54	29.01 ± 0.60
% weight increase	41.17 ± 1.86	41.25 ± 1.67	39.89 ± 1.51	36.49 ± 3.23	42.62 ± 1.66
Placenta / Maternal body weight (P/M)	0.352 ± 0.011	0.332 ± 0.014	0.356 ± 0.009	0.351 ± 0.011	0.324 ± 0.018
Fetus / Maternal body weight(F/M)	0.553 ± 0.011	0.591 ± 0.054	0.575 ± 0.014	0.615 ± 0.015	0.556 ± 0.025

Table 8. Reproduction parameters examined during parturition and lactation after sub-chronic OSPW-OF exposures of pregnant mice.

	Control	OSPW-OF			OSPW+O_3-OF
	Mean ± SE or Median (n=26)	**1 mg/L (n=15)**	**10 mg/L (n=18)**	**55 mg/L (n=5)**	**Equivalent dilution as 10 mg/L (n=20)**
% Pregnant rate	80.83 ± 6.40	83.33 ± 9.62	75.00 ± 10.76	62.5	83.33 ± 6.80
Litter size	6	6	5	6	6
% female	58.54 ± 3.20	66.62 ± 7.23	57.18 ± 5.232	69.62± 7.09	57.43 ± 5.68
Maternal Body weight (D4)	19.61 ± 0.26	19.12 ± 0.30	19.30 ± 0.23	20.83 ± 0.35	19.68 ± 0.25
Maternal Body Weight (D25)	29.85 ± 0.58	29.94 ± 0.73	29.20 ± 0.66	32.61 ± 0.94*	30.80 ± 0.59
Maternal Body Weight (GD42)	25.36 ± 0.29	25.17 ± 0.37	24.48 ± 0.29	25.61 ± 0.72	24.87 ± 0.23
Pups body weight (PD1)	1.58 ± 0.04	1.65 ± 0.05	1.64 ± 0.07	1.48 ± 0.07	1.62 ± 0.04
Pups body weight (PD21)	12.73 ± 0.20	12.69 ± 0.30	12.96 ± 0.23	11.80 ± 0.36	13.13 ± 0.21
Pup/maternal weight ratio (%)	50.48 ± 0.91	50.51 ± 1.24	49.90 ± 3.15	46.29 ± 2.27	52.85 ± 0.93

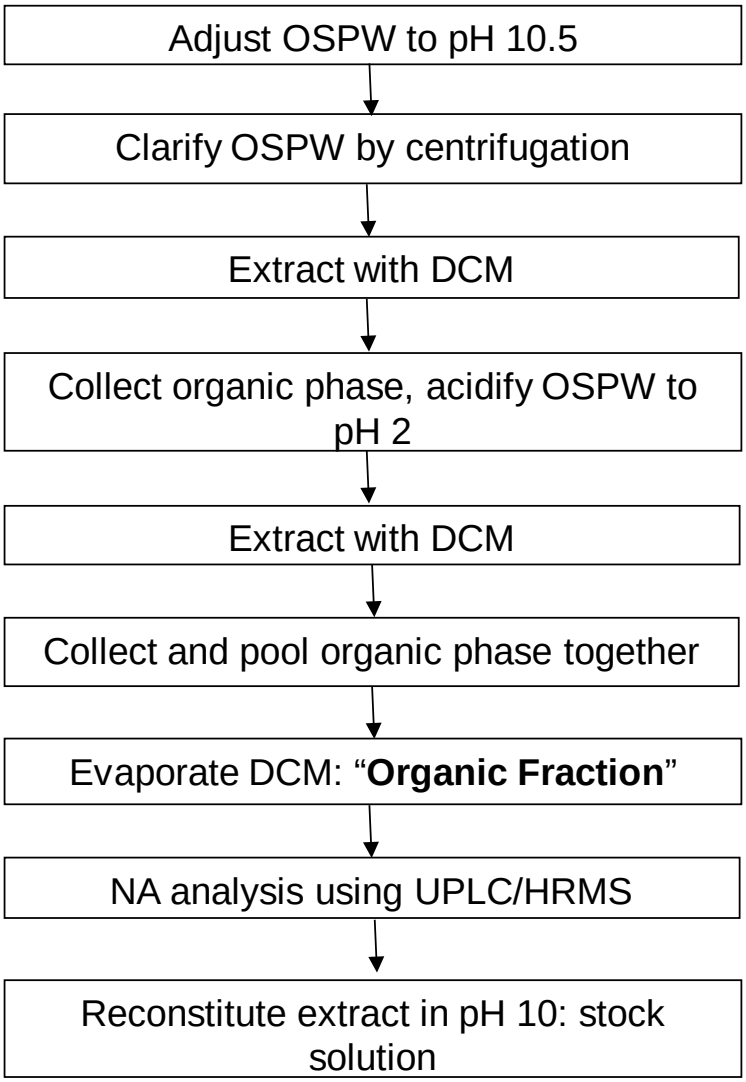

Figure 1. Procedure for extraction of the OSPW organic fraction (OSPW-OF) for mammalian toxicity studies.

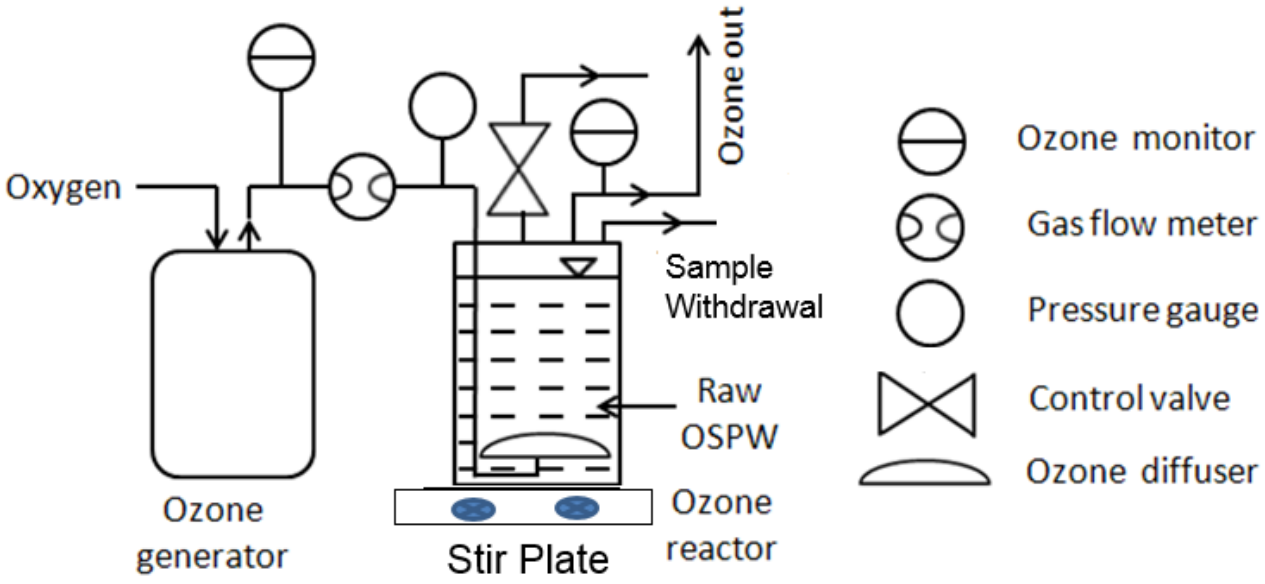

Figure 2. Schematic of ozonation system for a semi-batch reactor.

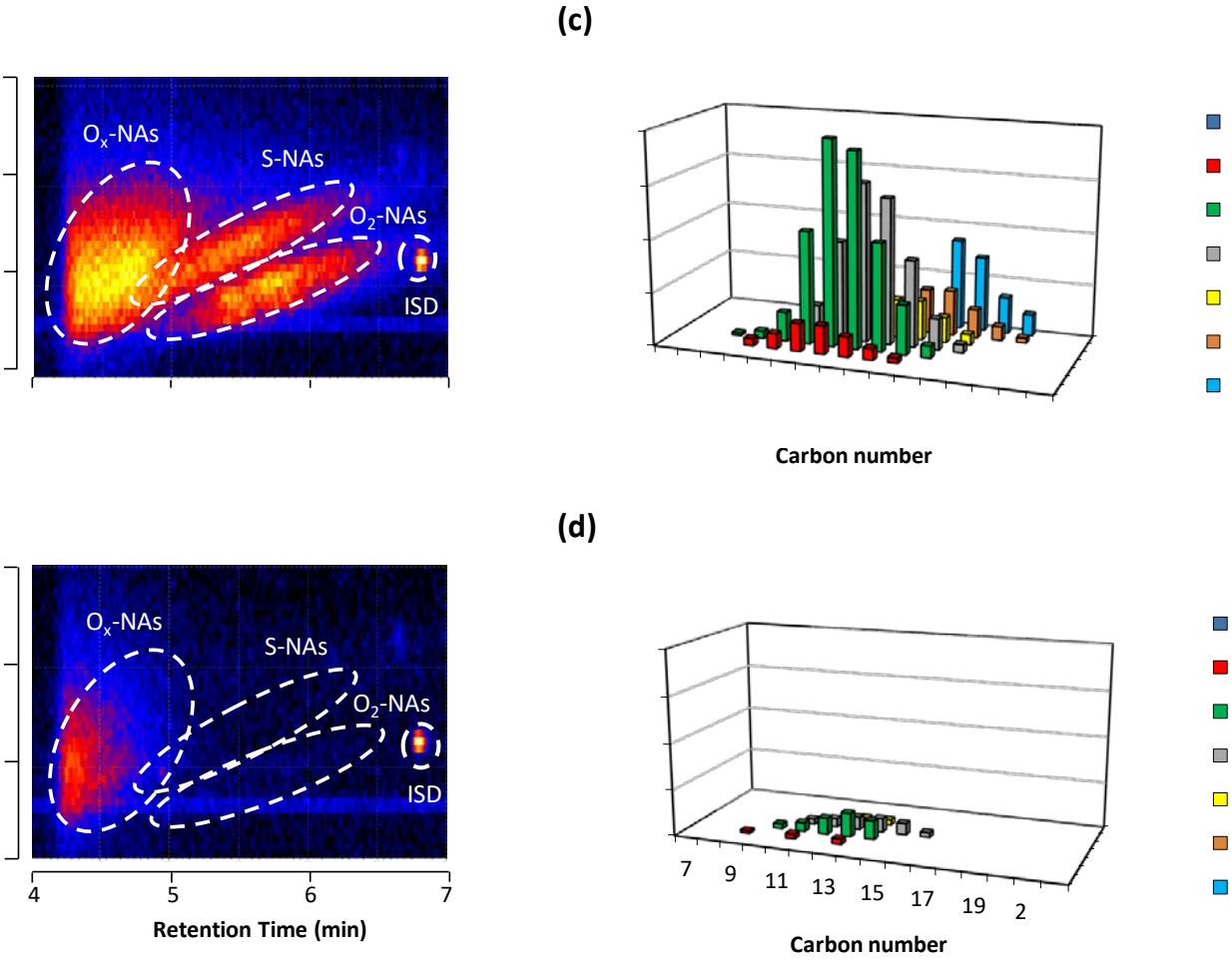

Figure 3. Ion mobility spectra (IMS) for (a) raw OSPW and (b) ozonated OSPW (utilized ozone dose = 80 mg/L). Profiles of classical NAs (i.e., O_2-NAs) based on carbon and Z numbers for (c) raw OSPW and (d) ozonated OSPW (utilized ozone dose = 80 mg/L) (Syncrude 2013 Aurora pond OSPW).

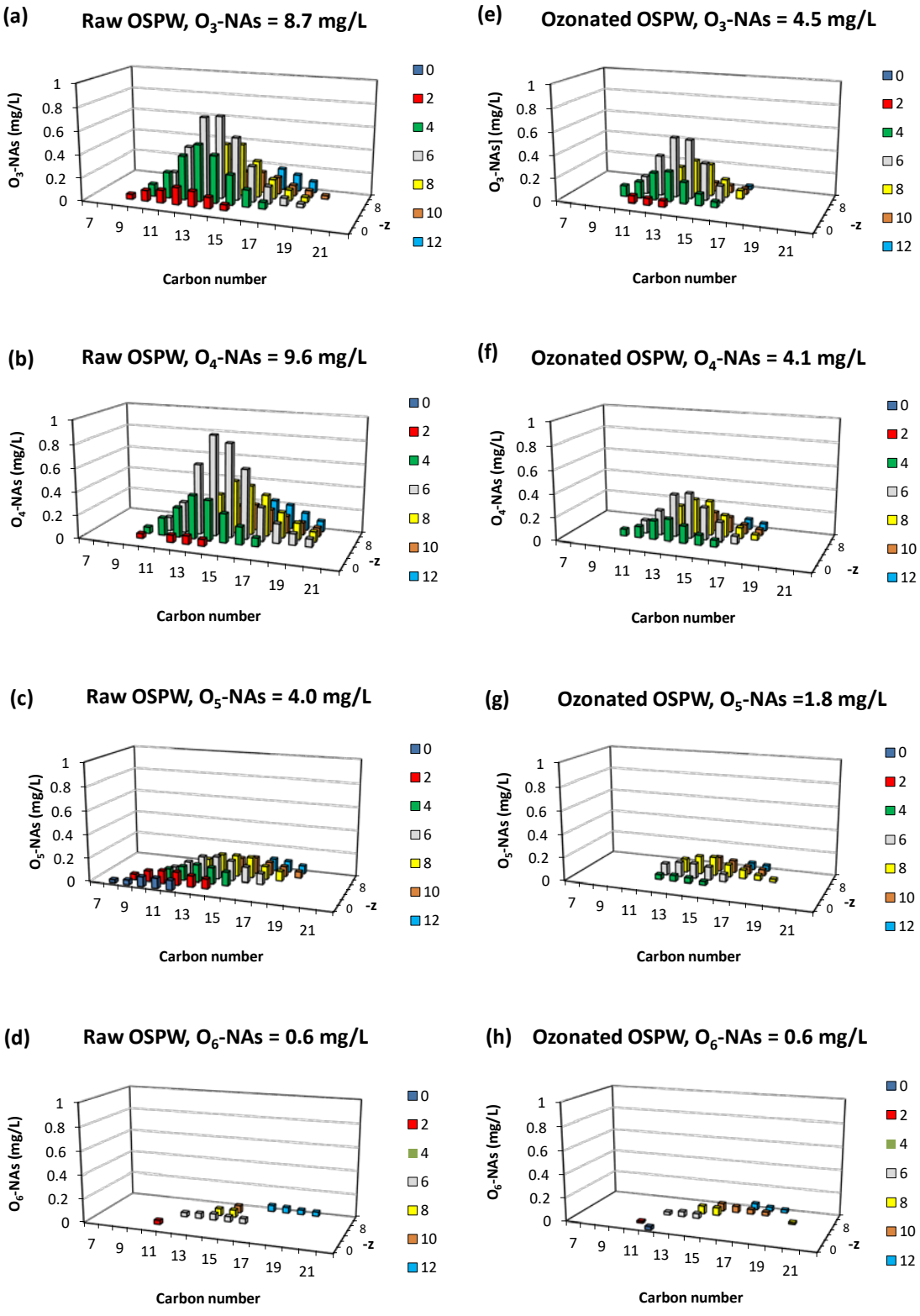

Figure 4. Plots of oxidized NAs (O_3-NAs, O_4-NAs, O_5-NAs, and O_6-NAs) as function of the carbon and z numbers for raw OSPW (a,b,c, and d) and ozonated OSPW (e, f, g, and h) (Syncrude 2013 Aurora pond OSPW).

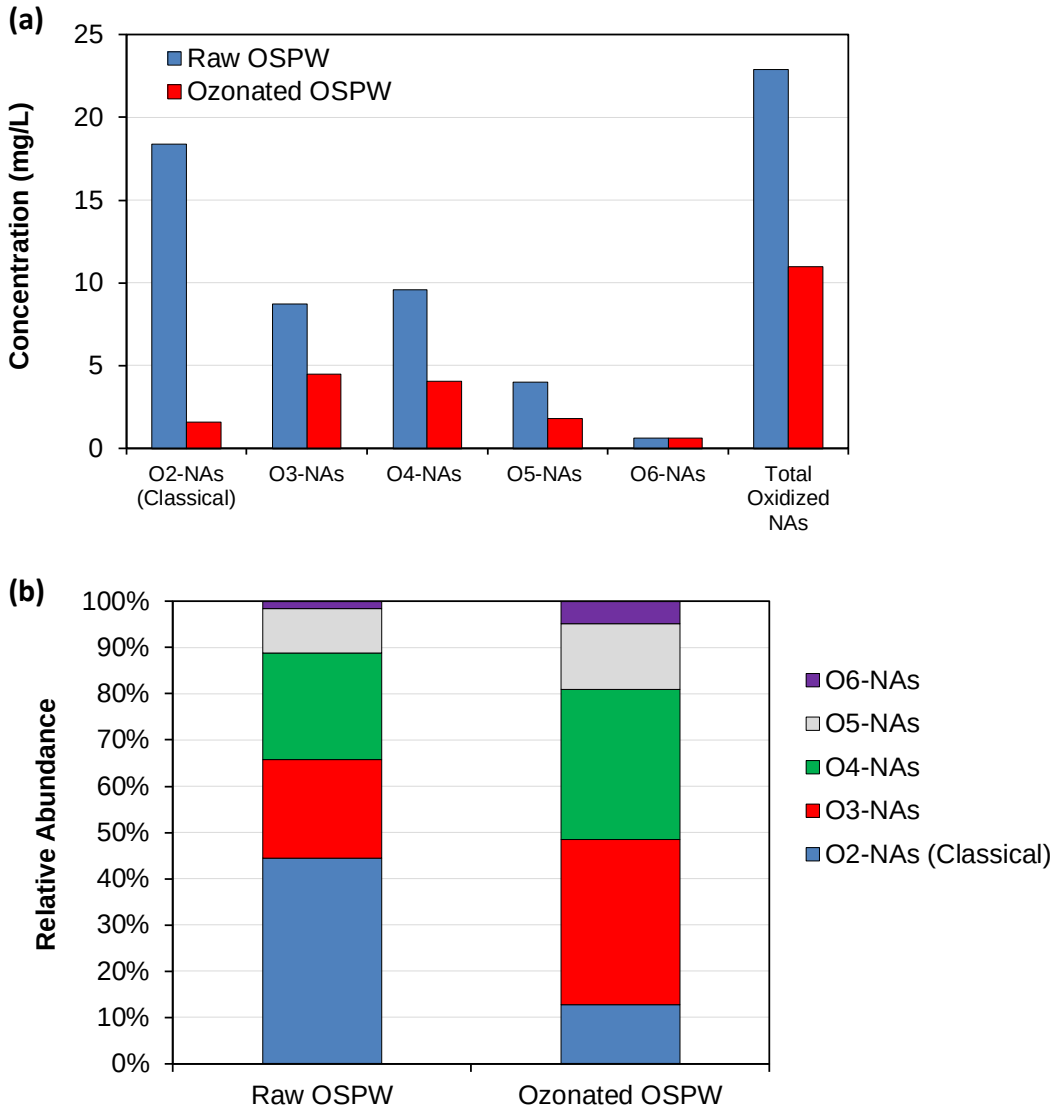

Figure 5. (a) Classical (O_2-NAs) and oxidized NA species (O_3-NAs, O_4-NAs, O_5-NAs, and O_6-NAs) detected in raw and treated OSPW using UPLC-TOFMS. (b) Relative abundance of O_2-NAs and Ox-NAs detected in negative ESI mode (Syncrude 2013 Aurora pond OSPW).

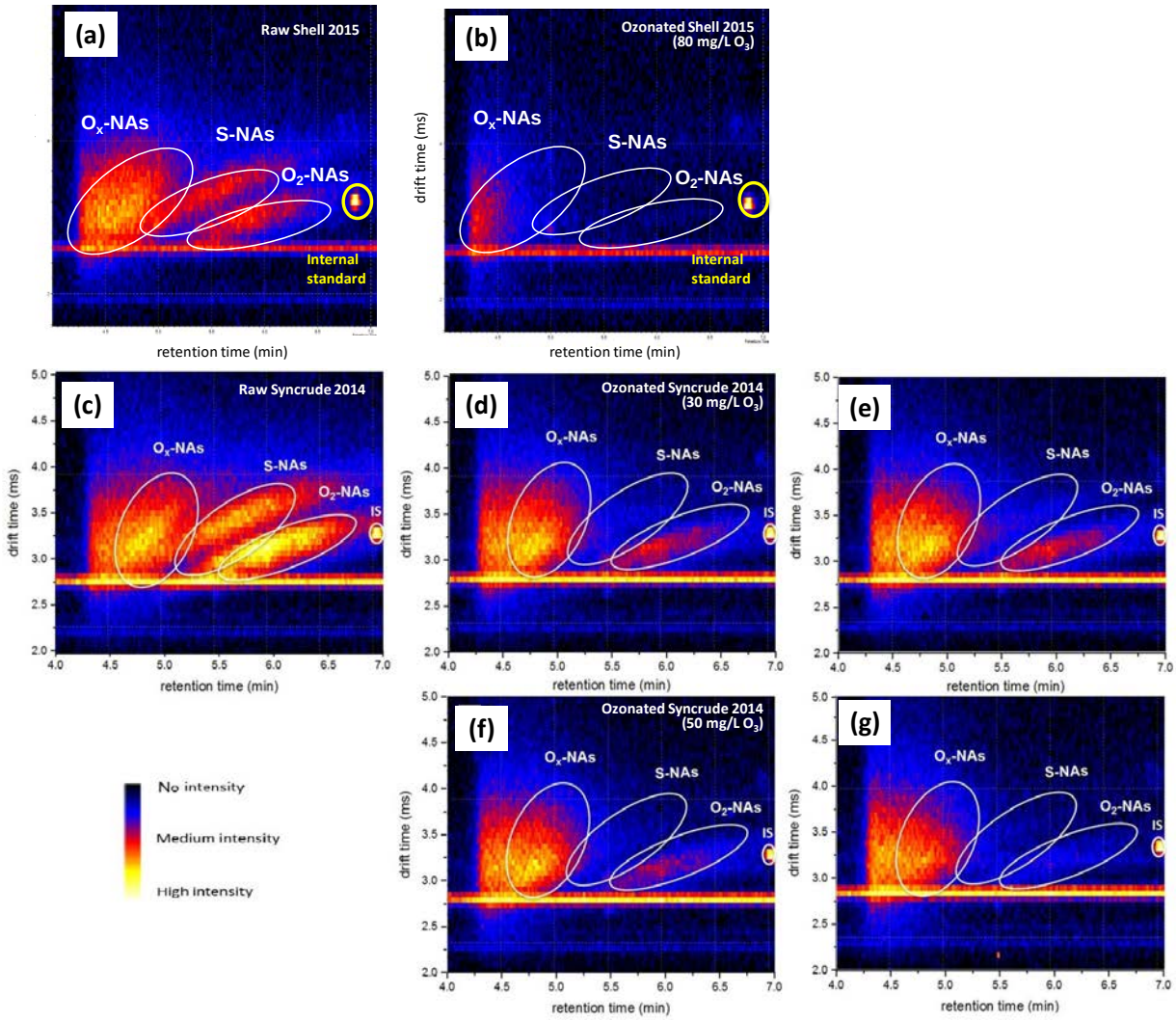

Figure 6. Ion mobility spectra (IMS) for raw and ozonated Shell 2015 OSPW [Muskeg River Mine] (a, b) and Syncrude 2014 OSPW [Mildred Lake Site] (c to g). The bright spot is the internal standard (ISD) which is represented in each plot at $t_R \approx 7$ min and $t_D \approx 3$ ms. The colors specify the relative intensity, with the yellow-colored clusters indicating the peaks areas with high abundance.

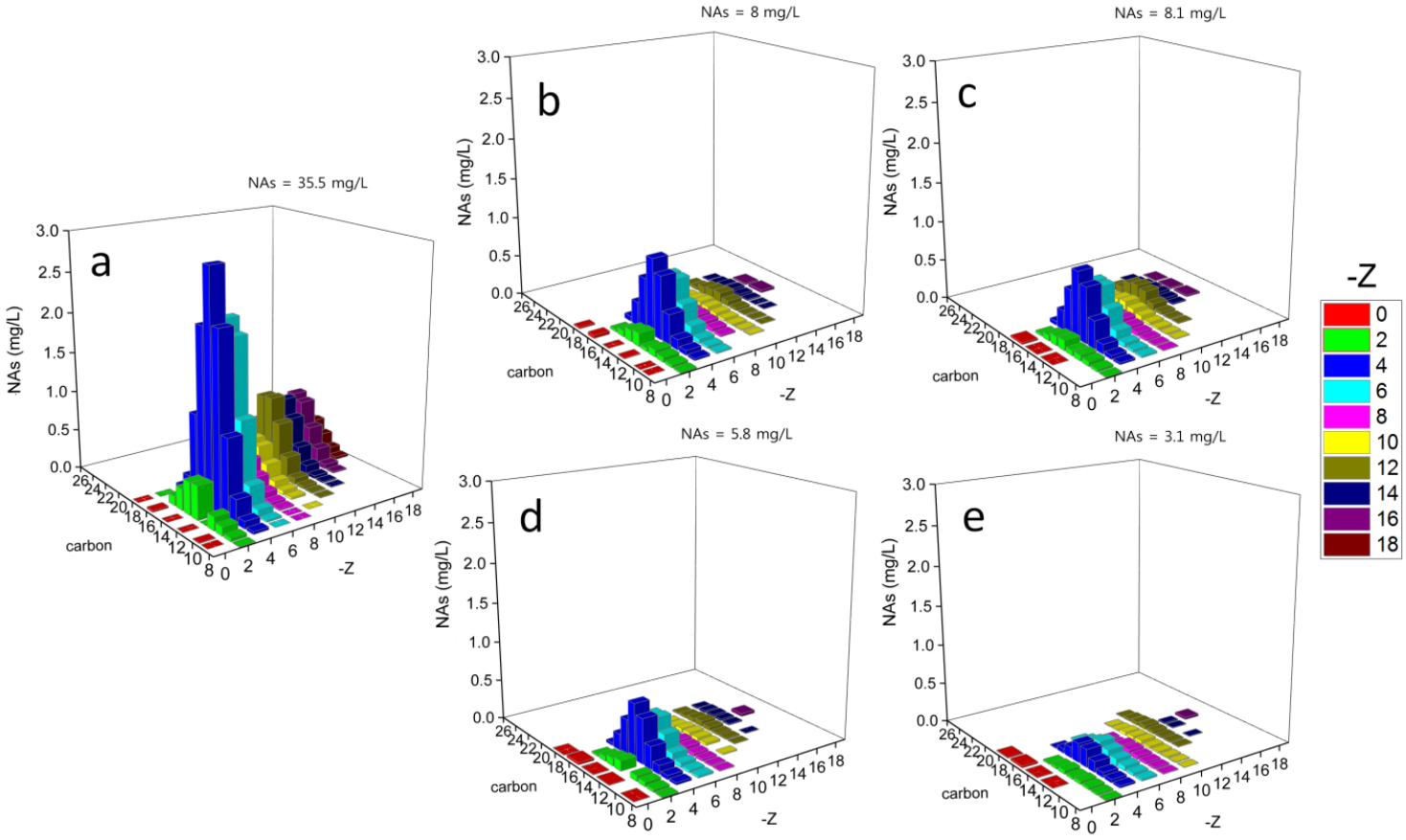

Figure 7. Profile of classical NAs in Syncrude 2014 sample (Mildred Lake Site) before and after treatment: (a) raw OSPW; (b) 30 mg/L ozone; (c) 1:1 peroxone (20 mg/L H_2O_2:30 mg/L O_3); (d) 50 mg/L ozone; and (e) 1:2 peroxone (20 mg/L H_2O_2:50 mg/L O_3). The NA species were semi-quantified using UPLC-TOFMS.

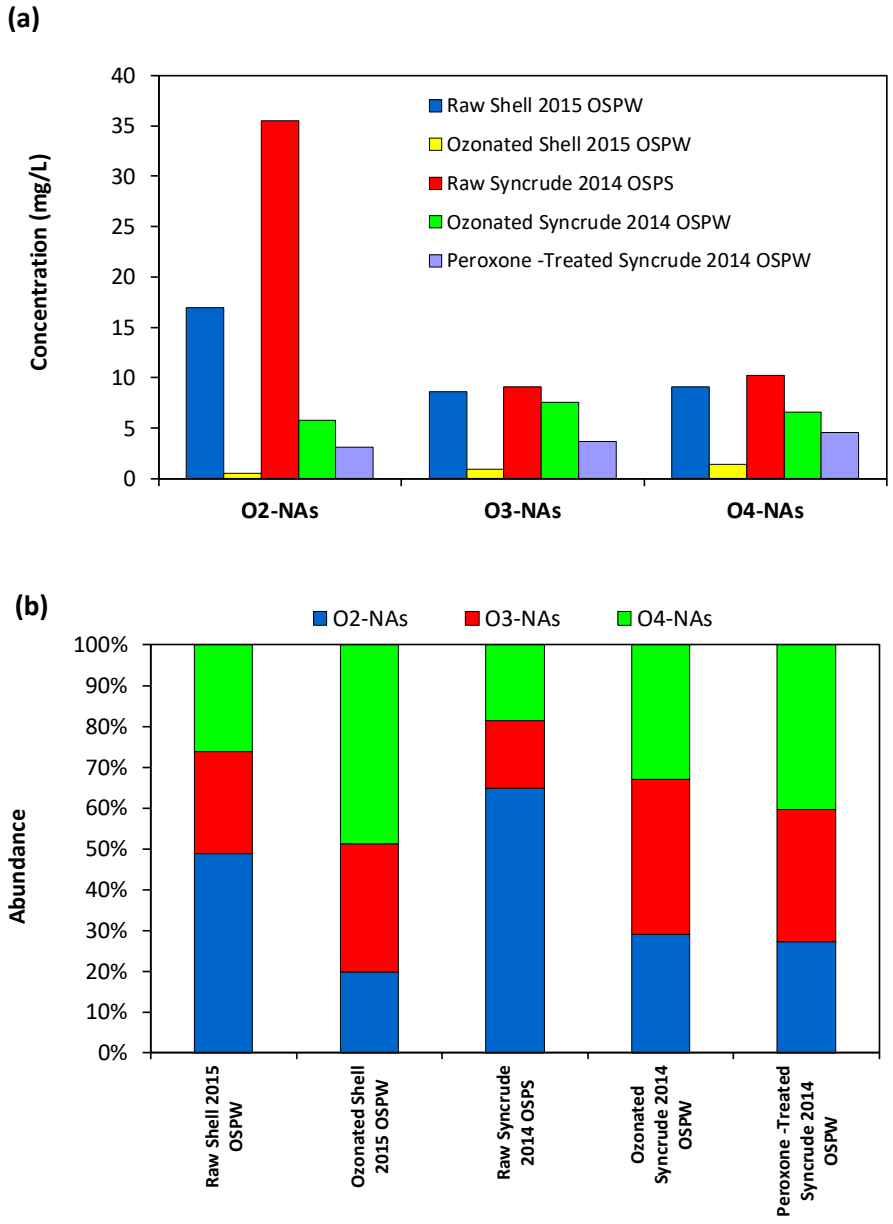

Figure 8. (a) Classical (O_2-NAs) and oxidized NA species (O_3-NAs and O_4-NAs) detected in raw and treated OSPW using UPLC-TOFMS. (b) Relative abundance of O_2-NAs, O_3-NAs, and O_4-NAs detected in negative ESI mode. Ozonated Shell 2015 OSPW [Muskeg River Mine] (80 mg/L utilized O_3 dose); Ozonated Syncrude 2014 OSPW [Mildred Lake Site] (50 mg/L utilized O_3 dose); Peroxone-Treated Syncrude 2014 OSPW (1:2 Peroxone).

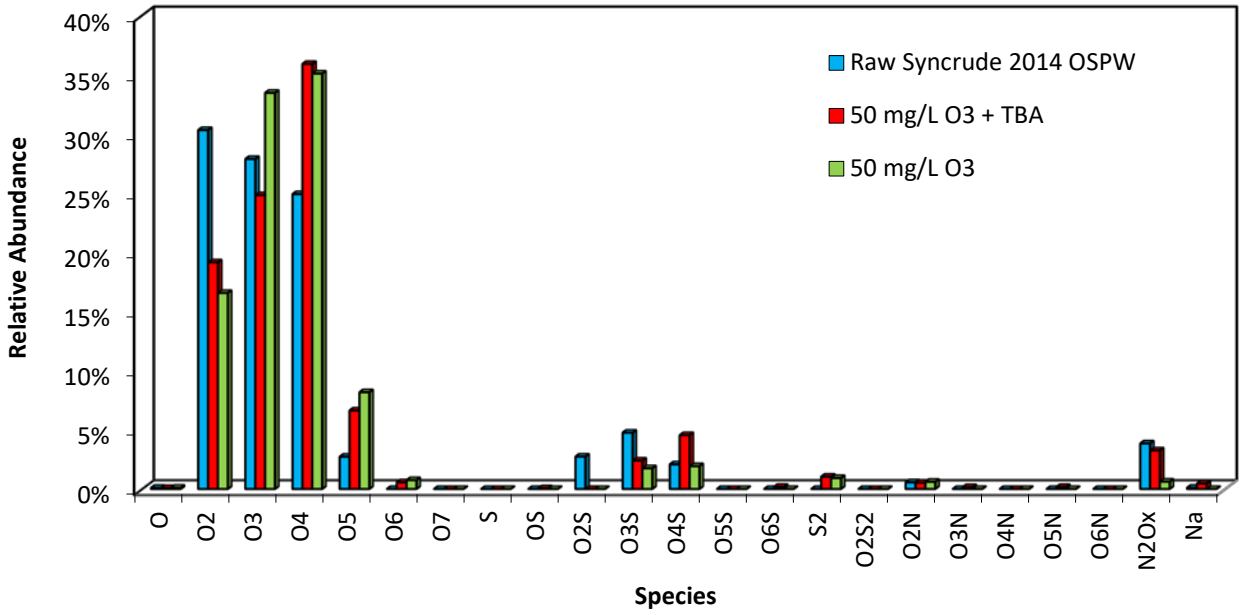

Figure 9. Relative abundance (%) of the different species for raw and ozone-treated OSPWs (50 mg/L O_3) determined using FTICR-MS (Syncrude 2014 OSPW from Mildred Lake Site). Tert-butyl alcohol (TBA) was added as an •OH scavenger.

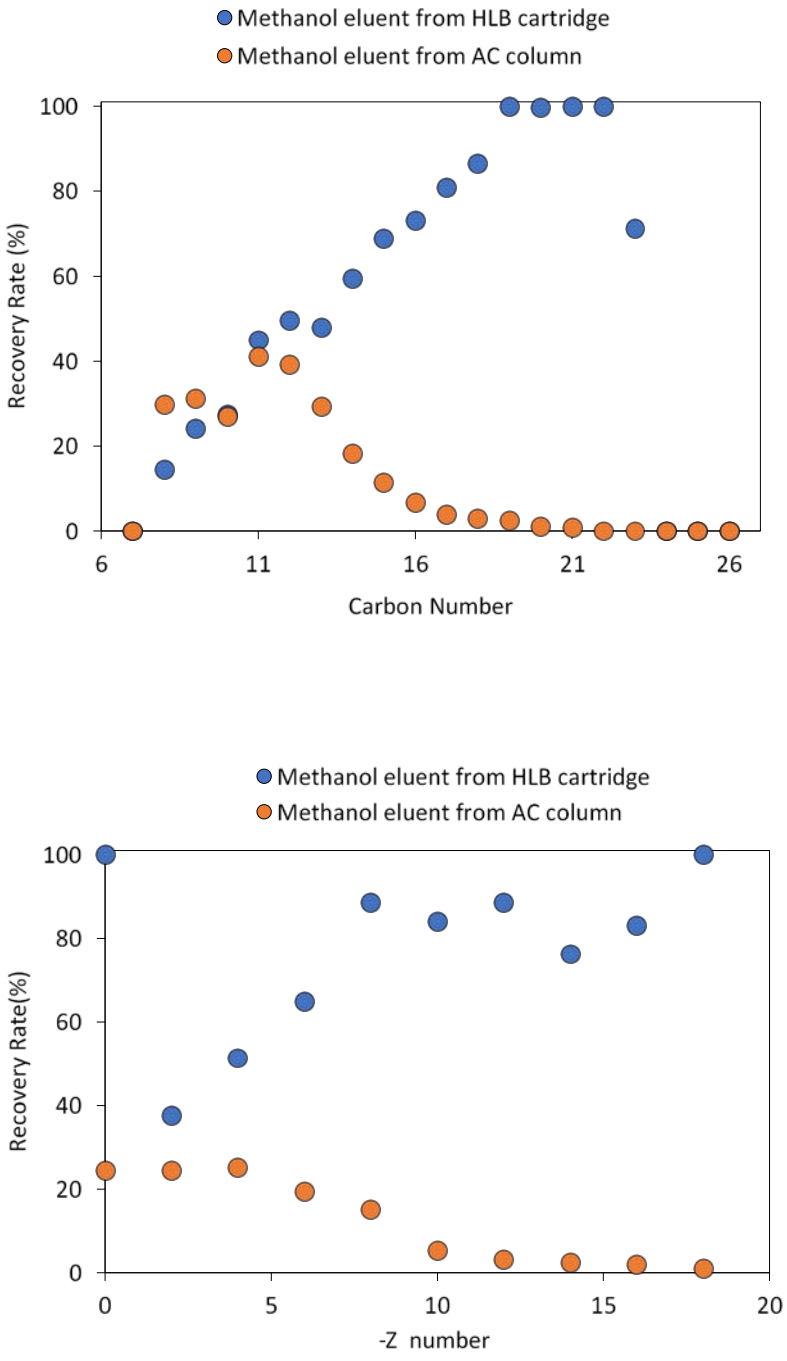

Figure 10. Recovery rate of classical NAs by methanol for HLB cartridge and activated carbon with different carbon and –Z numbers.

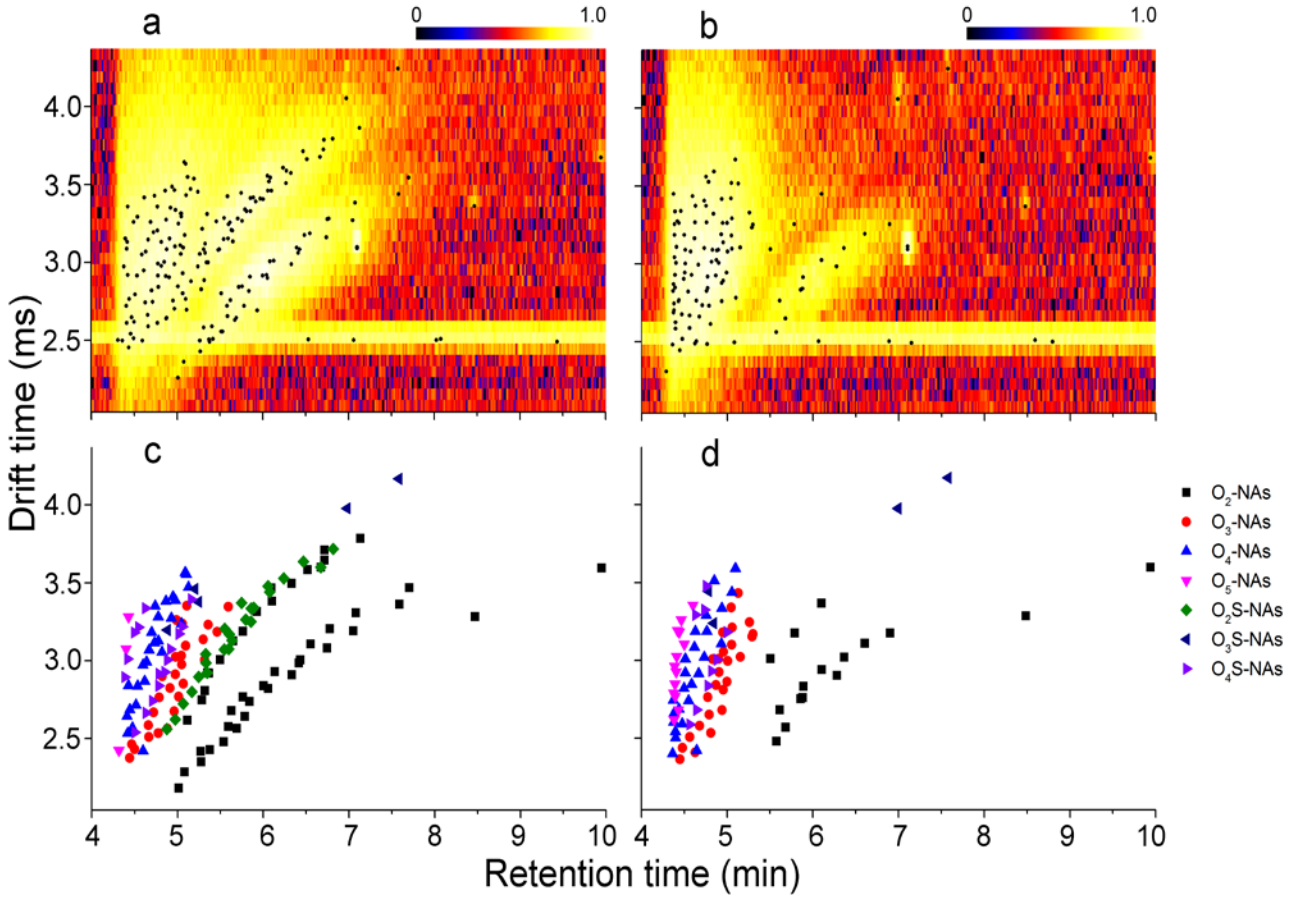

Figure 11. Two-dimensional separation maps for (a) raw and (b) ozonated OSPW. Colors on maps indicate the relative intensity, with light-yellow colored cluster indicating the areas of most abundant peaks. The horizontal strip at 2.5 ms is an artifact of the samples matrix. The spectrum peaks were acquired using DriftScope (Waters Canada) and indicated as black markers. The O_x-NAs ($2 \le x \le 5$) and O_yS-NAs ($2 \le y \le 4$) species were identified based on the match of accurate masses for (c) raw and (d) ozonated OSPW.

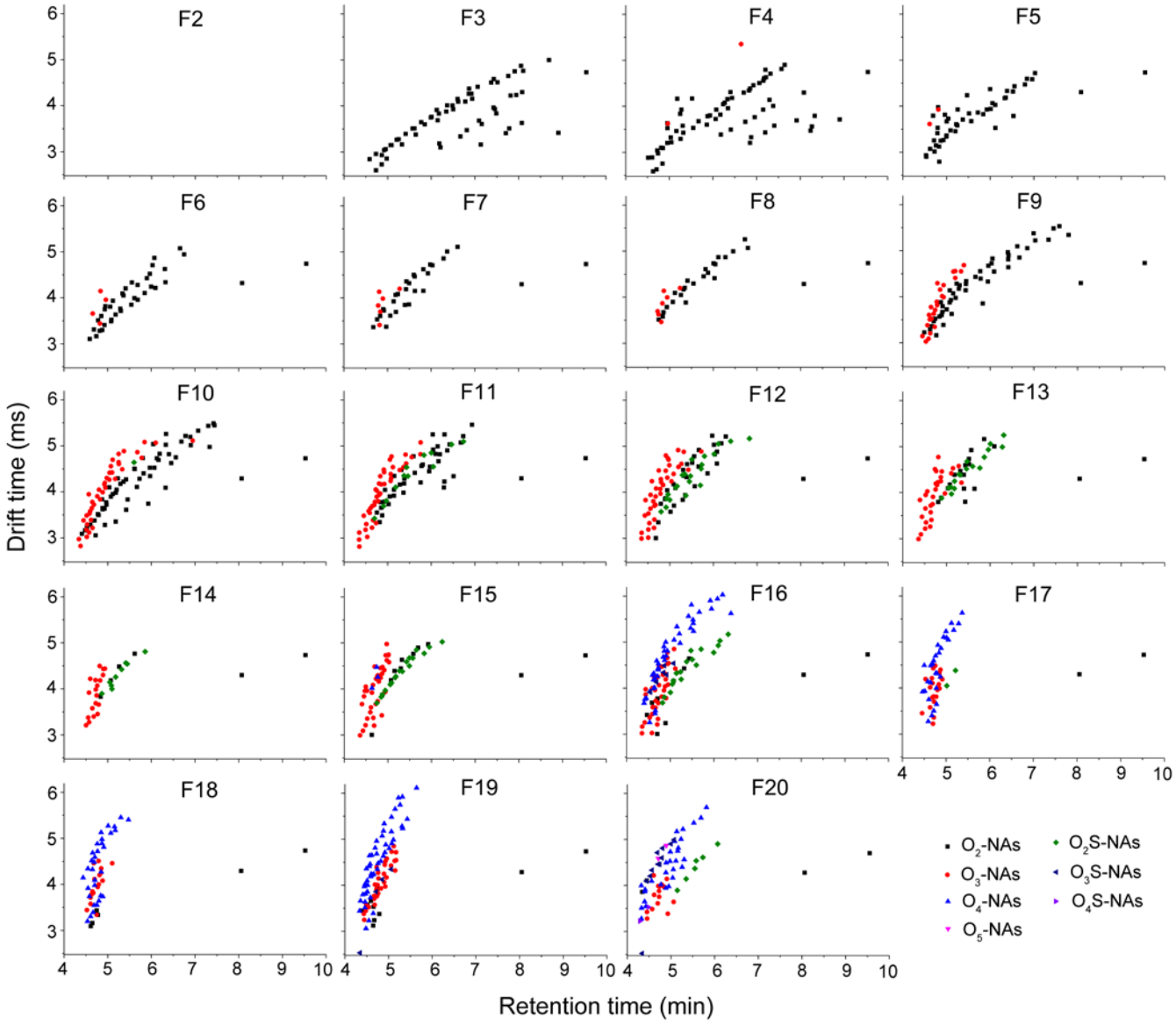

Figure 12. The O_x-NAs ($2 \leq x \leq 5$) and O_yS-NAs ($2 \leq y \leq 4$) species were identified based on the match of accurate masses for Ag-ion SPE fractions F2-F20 from raw OSPW. NAs were not detected in the Ag-ion SPE fractions F1, F2, F21, and F22.

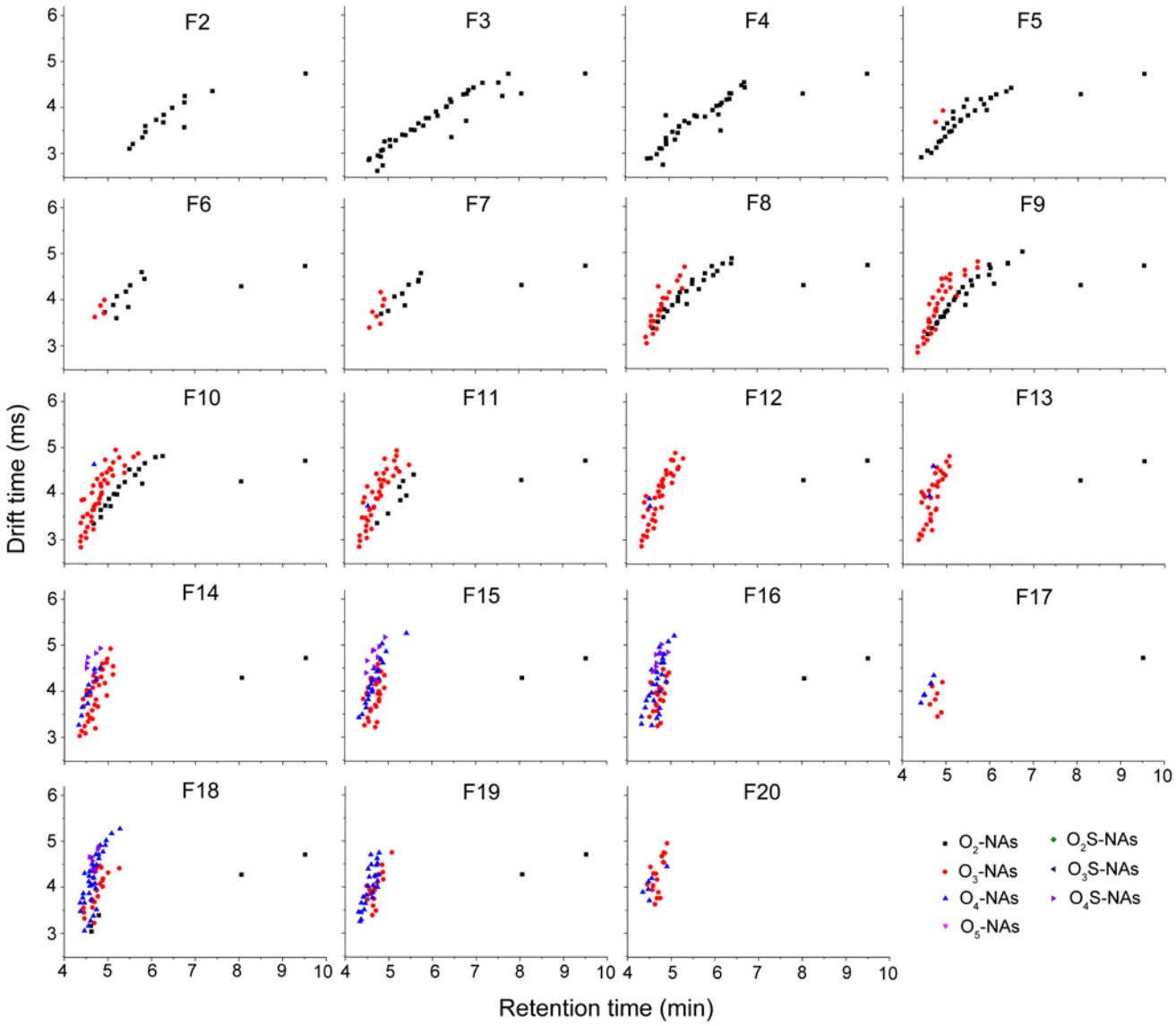

Figure 13. The O_x-NAs ($2 \leq x \leq 5$) and O_yS-NAs ($2 \leq y \leq 4$) species were identified based on the match of accurate masses for Ag-ion SPE fractions F2-F20 from ozonated OSPW. NAs were not detected in the Ag-ion SPE fractions F1, F21, and F22.

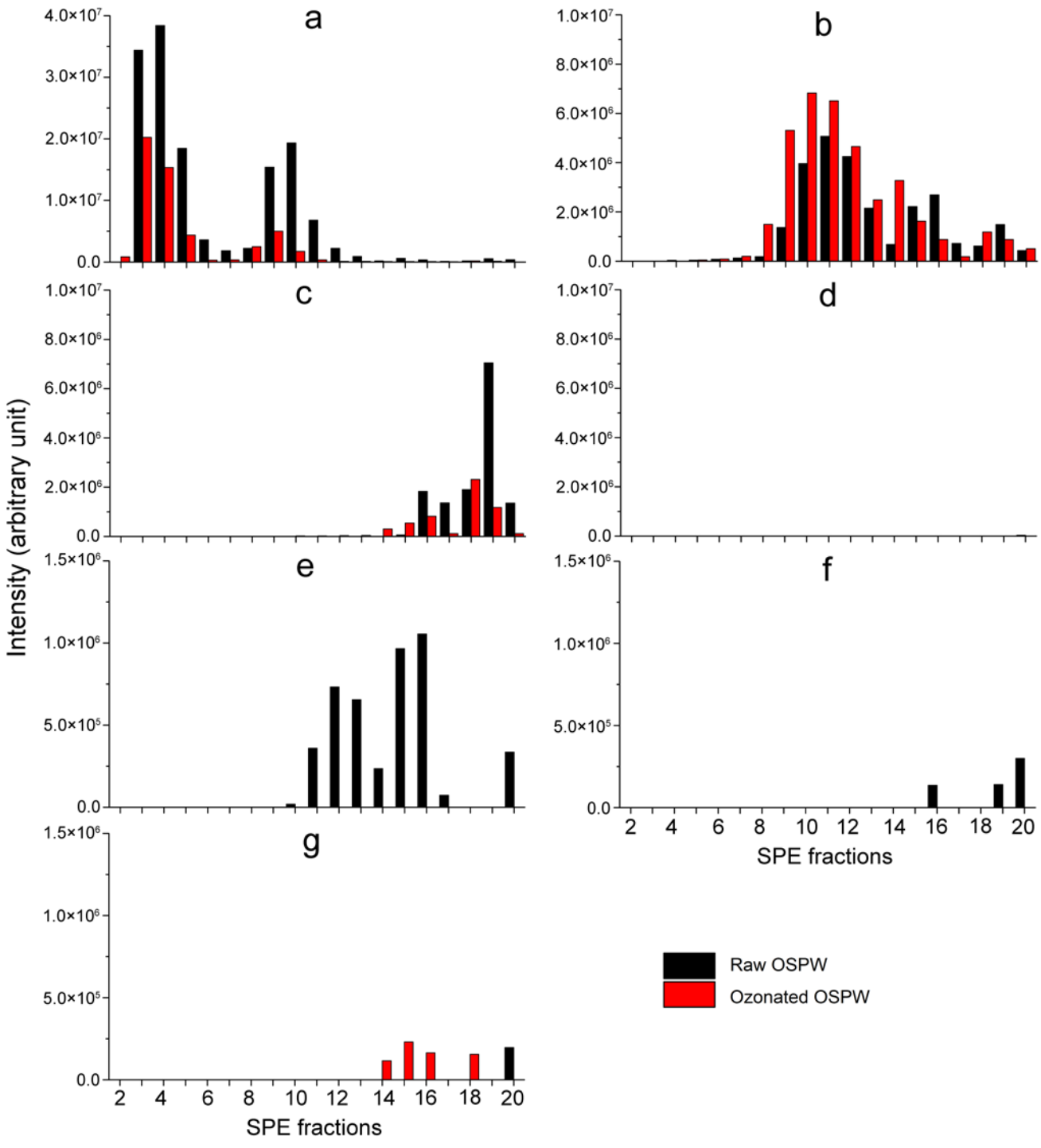

Figure 14. Comparison of intensity for O_2-NAs (a), O_3-NAs (b), O_4-NAs (c), O_5-NAs (d), O_2S-NAs (e), O_3S-NAs (f), and O_4S-NAs (g) in Ag-ion SPE fractions of raw and ozonated OSPWs.

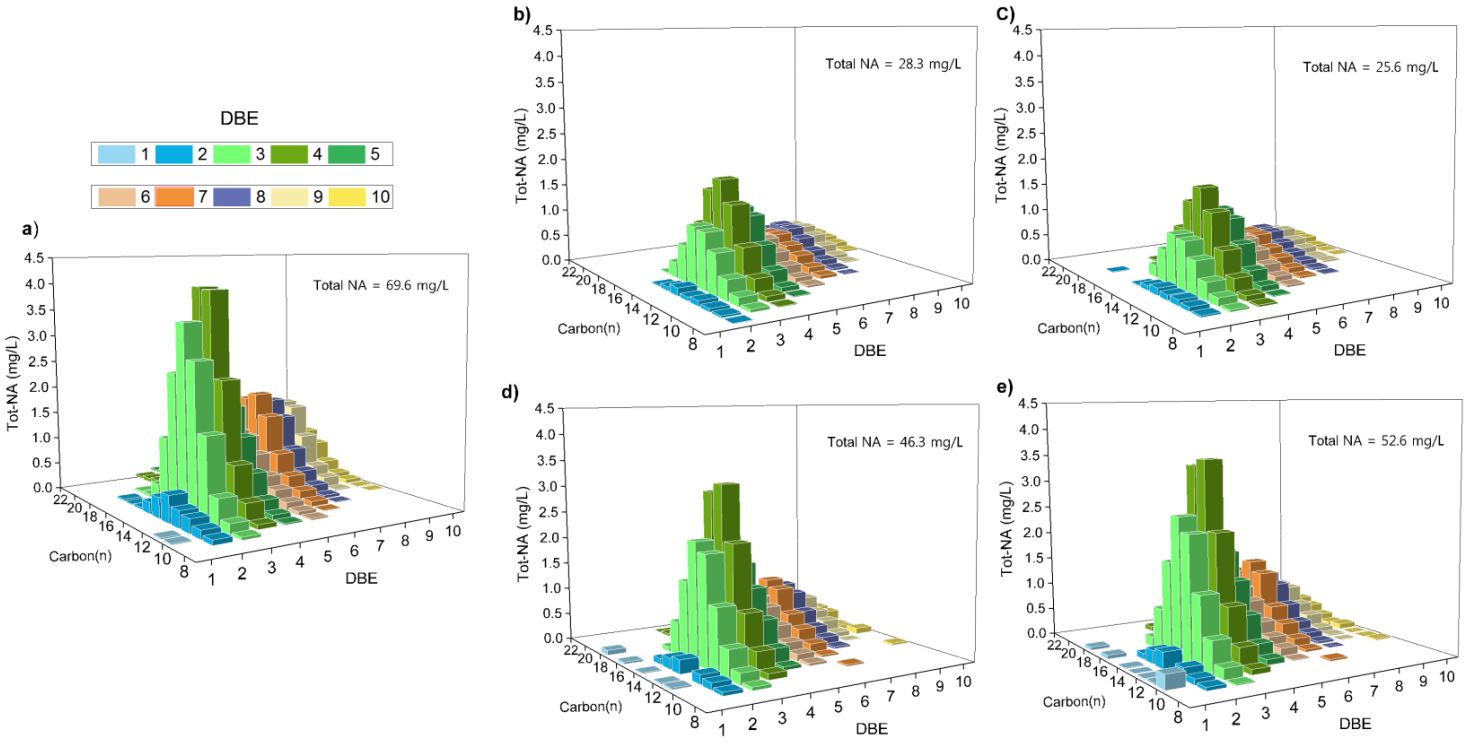

Figure 15. Profiles of total NAs (classical NAs + oxidized NAs) in (a) raw Syncrude 2014 OSPW from Mildred Lake Site; and OSPW treated by (b) 50 mg/L utilized O_3 dose; (c) 1:2 peroxone [20 mg/L H_2O_2 and 50 mg/L utilized O_3 dose]; (d) 1:3 peroxone [10 mg/L H_2O_2 and 50 mg/L utilized O_3 dose]; and (e) 1:2 peroxone [11 mg/L H_2O_2 and 30 mg/L utilized O_3 dose]. NA species were analyzed using UPLC-TOFMS. DBE: double bond equivalent.

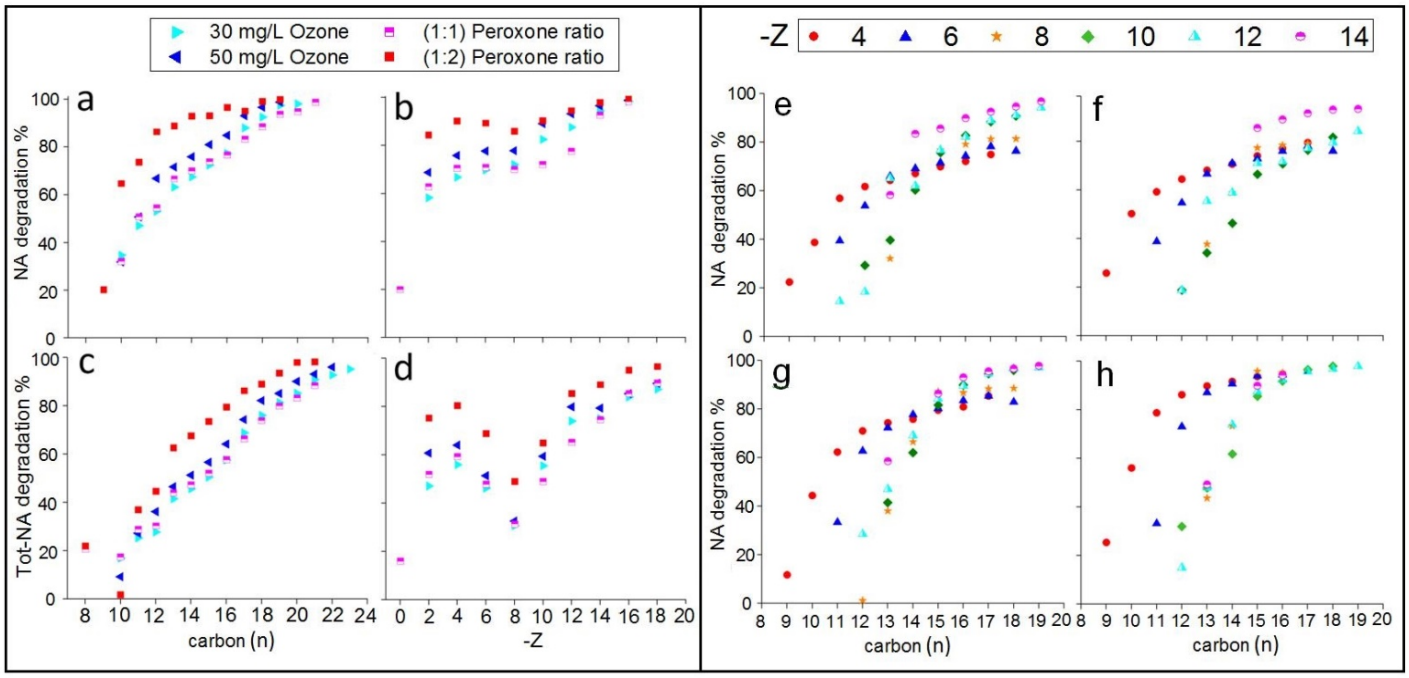

Figure 16. Carbon (n) and Z numbers of NA species after various treatments in terms of: classical NAs (a and b); and total NAs (i.e., NAs + oxidized NAs) (c and d). Combined effects of carbon (n) and Z numbers on classical NAs after various treatments (e) 30 mg/L ozone; (f) 1:1 peroxone (20 mg/L H_2O_2:30 mg/L O_3); (g) 50 mg/L ozone; (h) 1:2 peroxone (20 mg/L H_2O_2:30 mg/L O_3). All ozone doses are determined as utilized doses and the 20 mg/L H_2O_2 is the initial concentration. NA species were analyzed using UPLC-TOFMS (Syncrude 2014 OSPW from Mildred Lake Site).

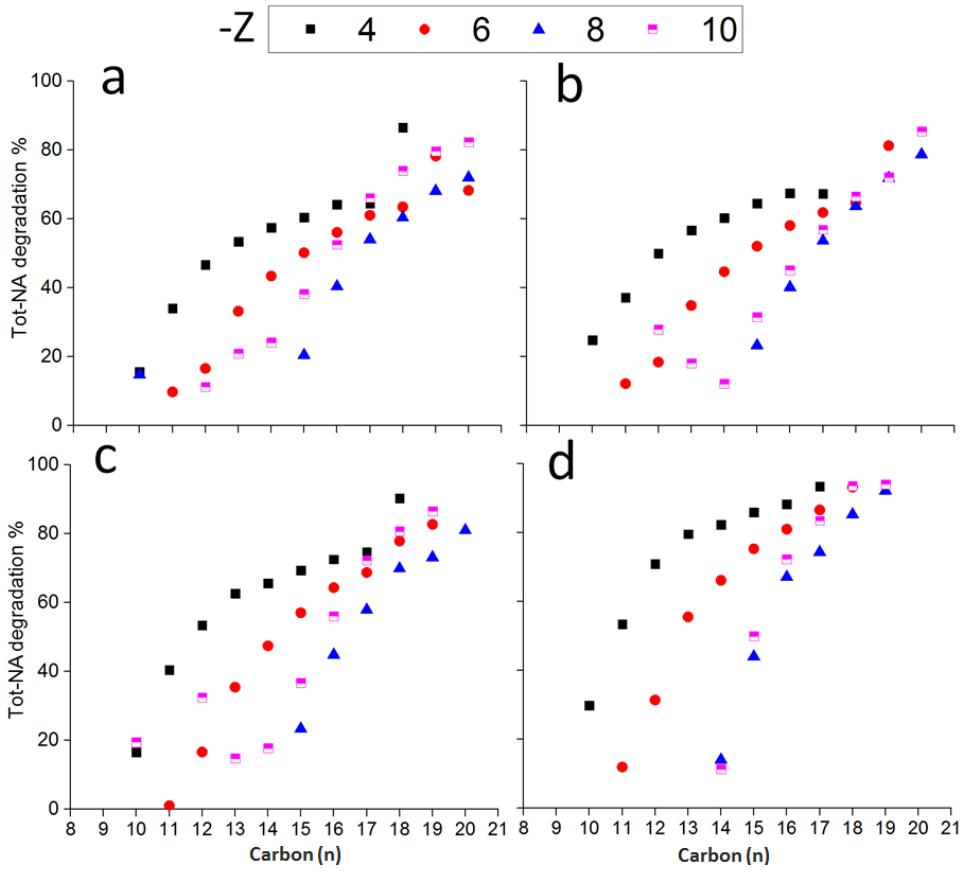

Figure 17. Combined effects of carbon (n) and Z numbers on total NAs (i.e., classical NAs + oxidized NAs) after various treatments: (a) 30 mg/L ozone; (b) 1:1 peroxone (20 mg/L H_2O_2:30 mg/L O_3); (c) 50 mg/L ozone; and (d) 1:2 peroxone (20 mg/L H_2O_2:30 mg/L O_3). All ozone doses are determined as utilized doses and the 20 mg/L H_2O_2 is the initial concentration. NA species were analyzed using UPLC-TOFMS (Syncrude 2014 OSPW from Mildred Lake Site).

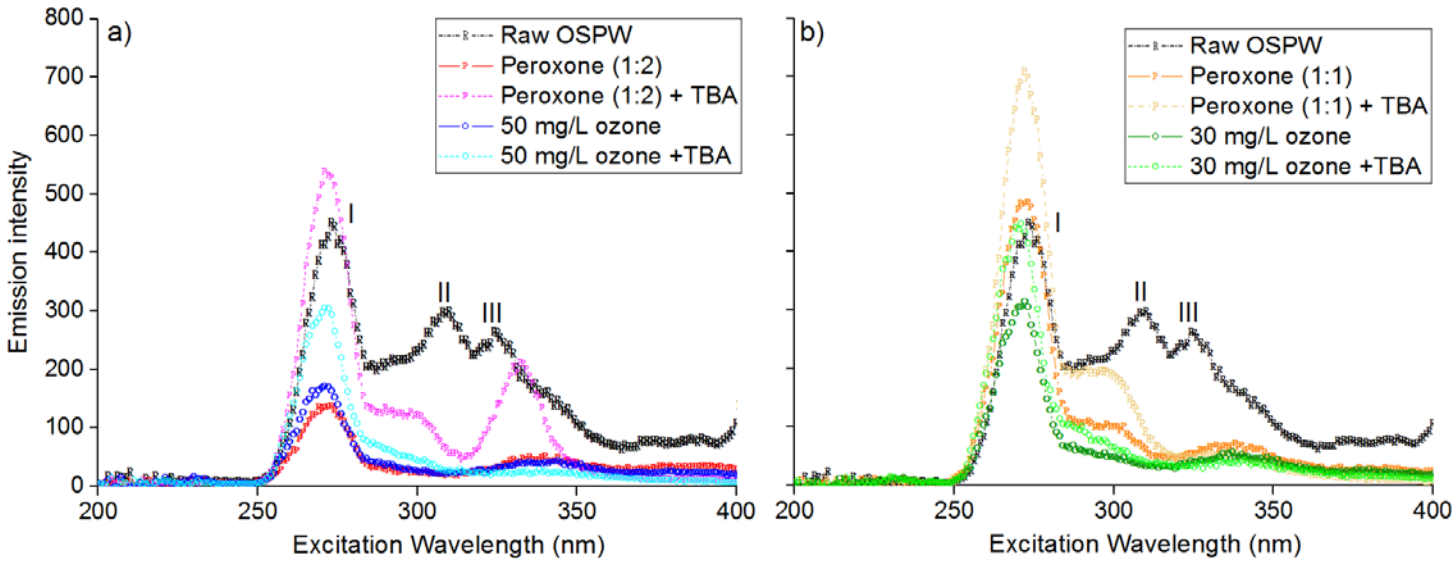

Figure 18. Synchronous fluorescence spectroscopy (SFS) plots after applying different utilized O_3 doses [30 mg/L and 50 mg/L] and peroxone processes at different H_2O_2:O_3 ratios [1:1 and 1:2] with and without adding tert-butyl alcohol (TBA) as a hydroxyl radical (•OH) scavenger. Three distinctive peaks (I, II, III) are representing one ring, two rings, and three aromatics rings, respectively. (Syncrude 2014 OSPW from Mildred Lake Site).

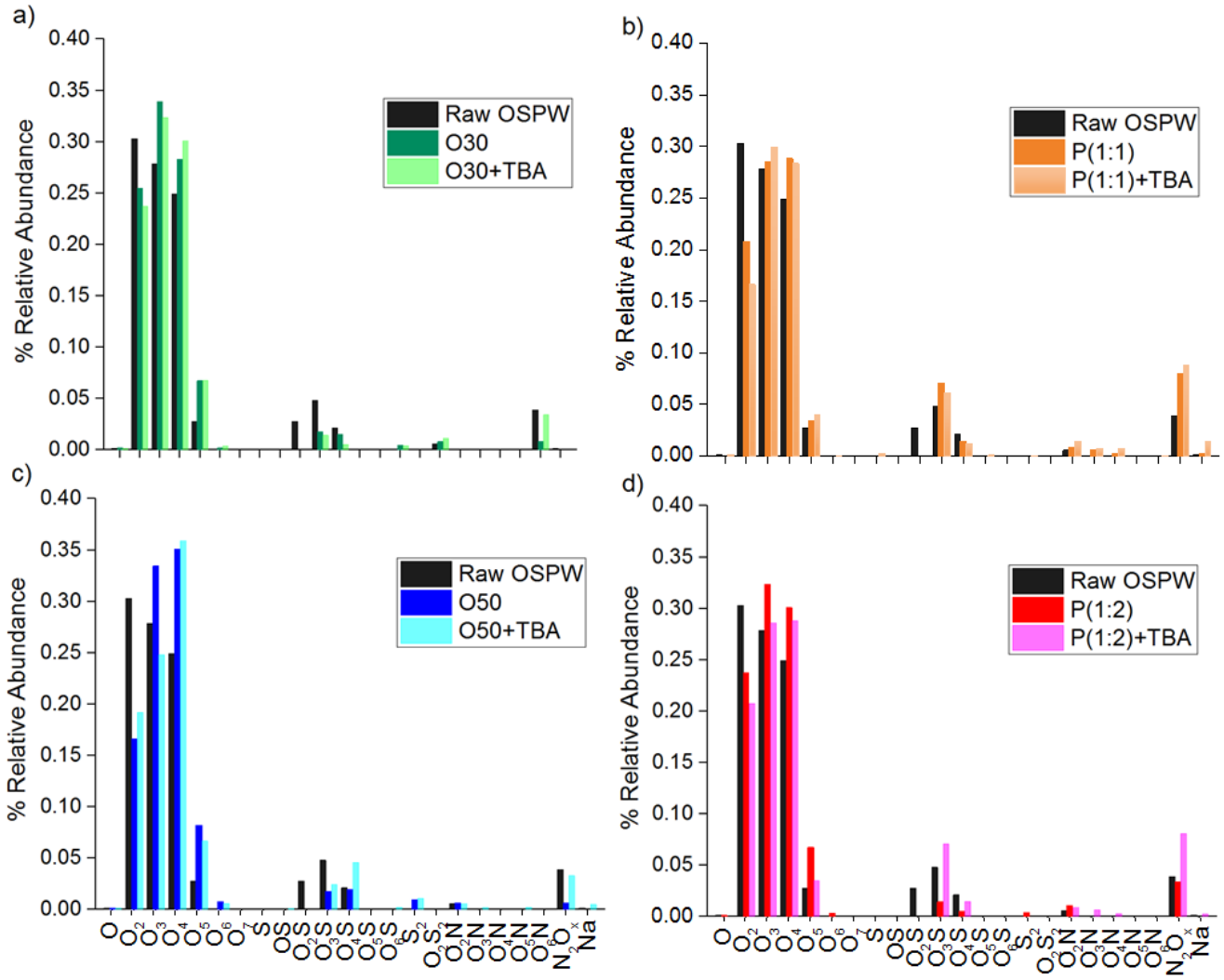

Figure 19. Relative abundance (%) of the different species for raw OSPW as well as treated OSPW at different conditions with and without tert-butyl alcohol (TBA) using FTICR-MS: a) 30 mg/L ozone and 30 mg/L ozone + TBA; b) 1:1 peroxone [P(1:1)] and 1:1 peroxone + TBA; c) 50 mg/L ozone and 50 mg/L ozone + TBA; and d) 1:2 peroxone [P(1:2)] and 1:2 peroxone + TBA. Note: 20 mg/L and 25 mM are the initial concentrations of H_2O_2 and TBA, respectively. H_2O_2 concentration utilized in 1:2 peroxone = 10.2 mg/L and in 1:1 peroxone = 6.9 mg/L. (Syncrude 2014 OSPW from Mildred Lake Site).

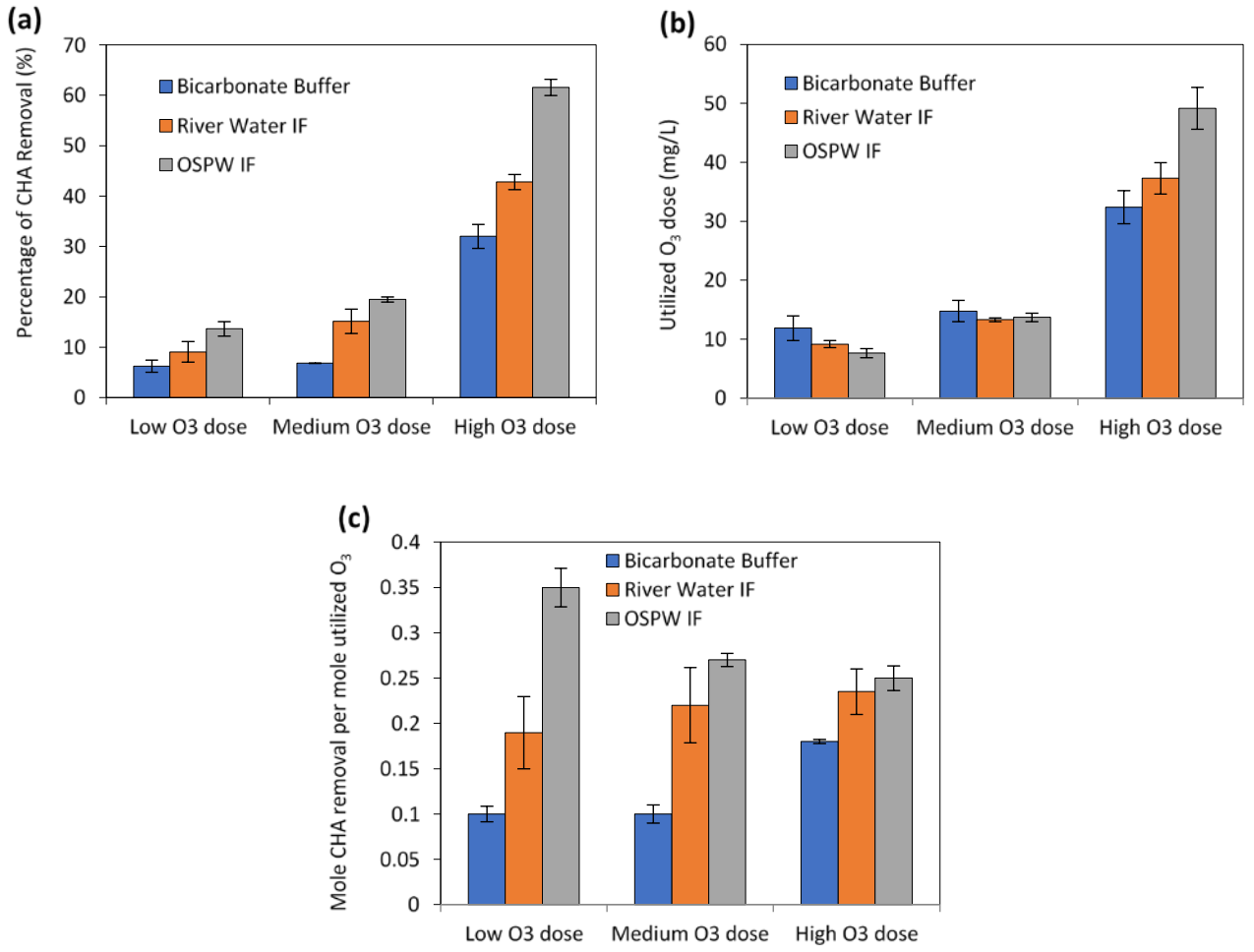

Figure 20. Ozonation of cyclohehanoic acid (CHA) (Initial concentration of 40 mg/L) using different water matrices in semi-batch experiments. Low, medium and high utilized ozone doses were 10, 15 and 30 mg/L, respectively (Shell 2015 OSPW; North Saskatchewan River water 2015). "IF" denotes "inorganic fraction".

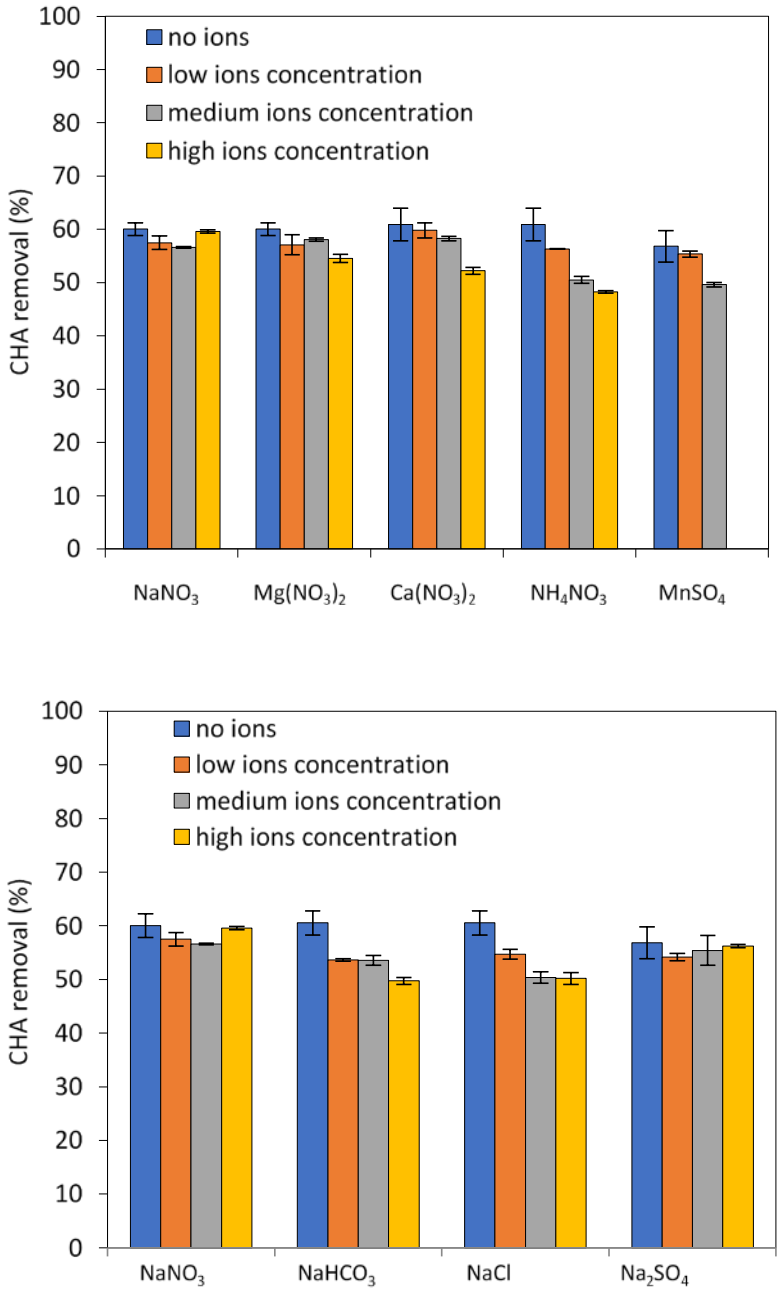

Figure 21. Impact of individual ions on the CHA degradation using batch reactors. Initial CHA concentration = 25 mg/L and initial ozone concentration = 14.5 mg/L.

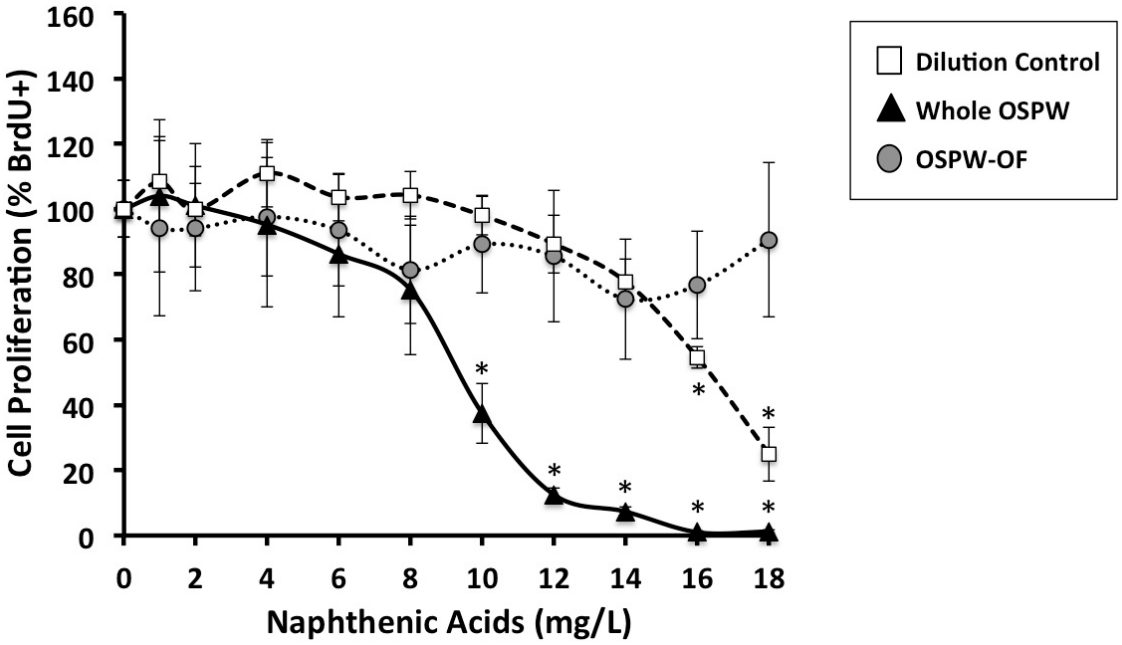

Figure 22. Effects of OSPW treatment on the proliferation of a mouse macrophage cell line. RAW 264.7 cells were expose to the OSPW water samples (Black triangles= whole (raw) OSPW; White squares=dilution controls; Grey circles=OSPW-OF) at NA concentrations ranging from 1 mg/L to 18 mg/mL for 18 h prior to determining cell proliferation activity by BrDU staining. Each point represents the mean ± SEM of three separate experiments and *$p<0.05$ when comparing the various exposures tested to cells incubated in complete media (i.e., 0 mg/L).

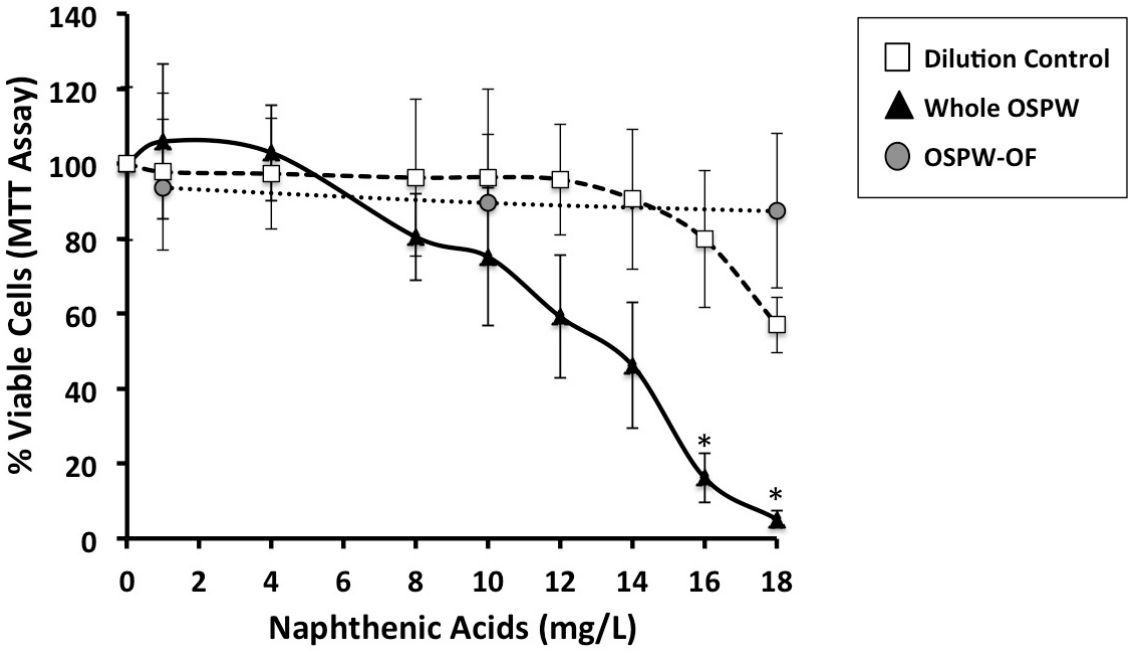

Figure 23. Effects of OSPW treatment on the viability of a mouse macrophage cell line. RAW 264.7 cells were treated with the various OSPW samples (Black triangles= crude (raw) OSPW; White squares=dilution controls; Grey circles=OSPW-OF) at NA concentrations ranging from 1 mg/L to 18 mg/mL for 18 h prior to determining cell viability using the MTT assay. Each point represents the mean ± SEM of three separate experiments and *$p<0.05$ when comparing the various exposures tested to cells incubated in complete media (i.e., 0 mg/L).

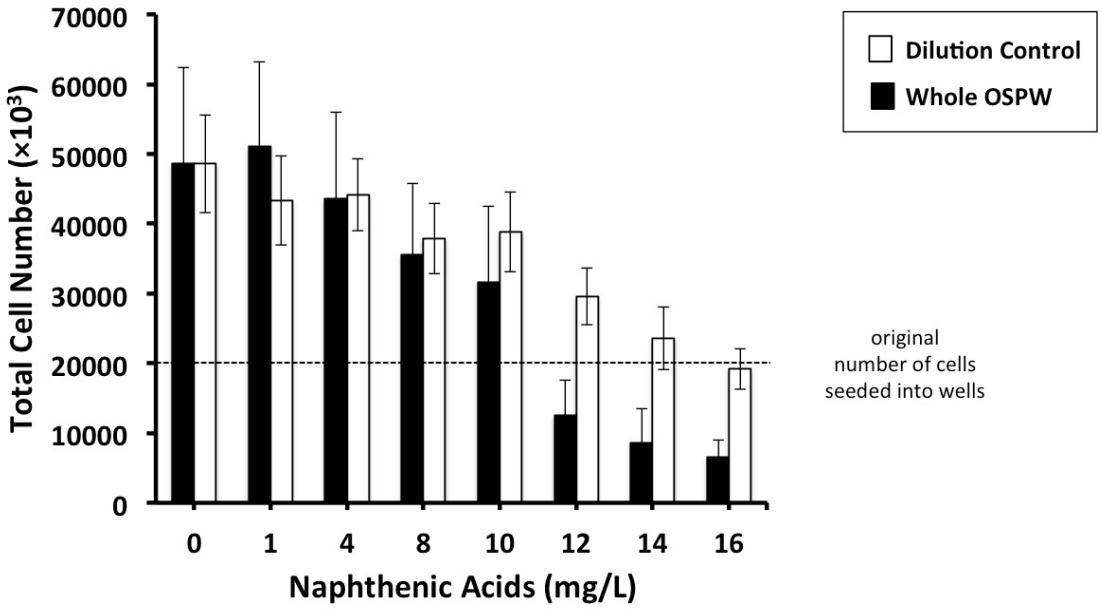

Figure 24. Effects of whole (raw) OSPW treatment on total cell numbers. RAW 264.7 cells ($2x10^4$) were seeded into the wells of a 96-well tissue culture plate and then treated with crude OSPW (0-18 mg/L) for 18 h at 37°C. Following the incubated period, total viable cell counts were performed using the Operetta High Content Imaging System to establish how many cells were in each well. Each bar represents the mean ± SEM of three separate experiments and indicated on the graph with a dashed line is the original cell seeding density prior to exposures. Black bars represent OSPW-treated cells and white bars represent the matched PBS dilution controls.

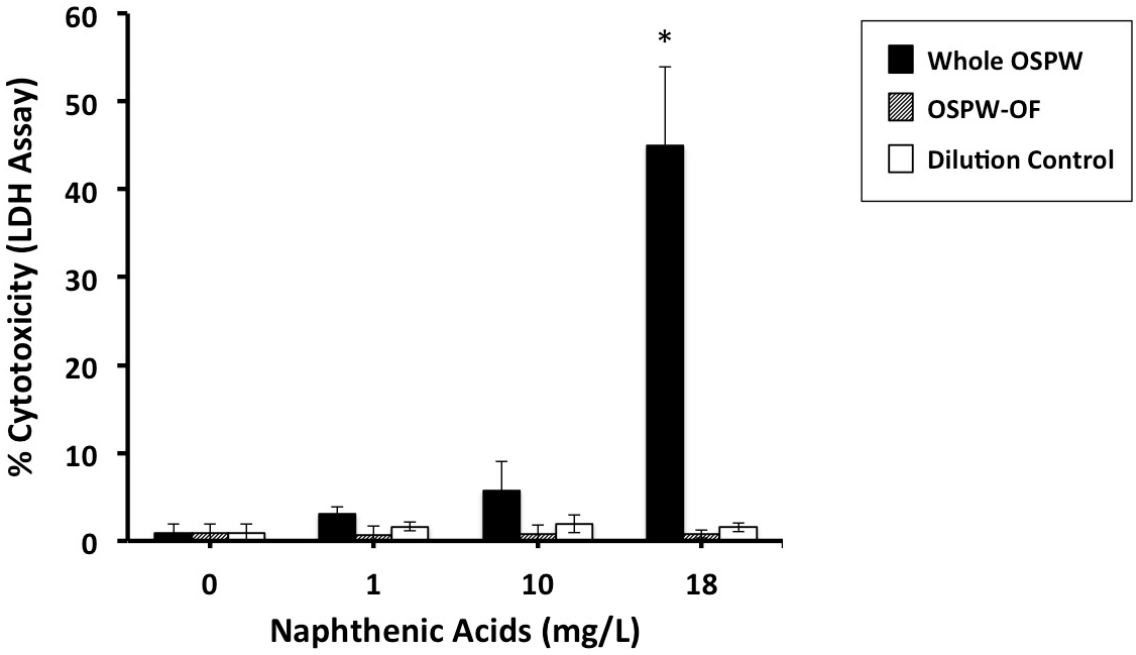

Figure 25. OSPW-induced cytotoxicity of a mouse macrophage cell line. RAW 264.7 cells were treated with whole (raw) OSPW (black bars), OSPW-OF (hatched bars), or matched dilution controls (white bars) at NA concentrations of 1 mg/L, 10 mg/L, and 18 mg/L for 18 h at 37°C. Following the exposures, relative cell lies was determined using the LDH assay. Each point represents the mean ± SEM of three separate experiments and *$p<0.05$ when comparing the various treatments to untreated cells incubated in cell culture media (e.g., 0 mg/L). The % cytotoxicity was calculated as (experimental LDH release – spontaneous LDH release) / (maximum LDH release – spontaneous LDH release) x 100.

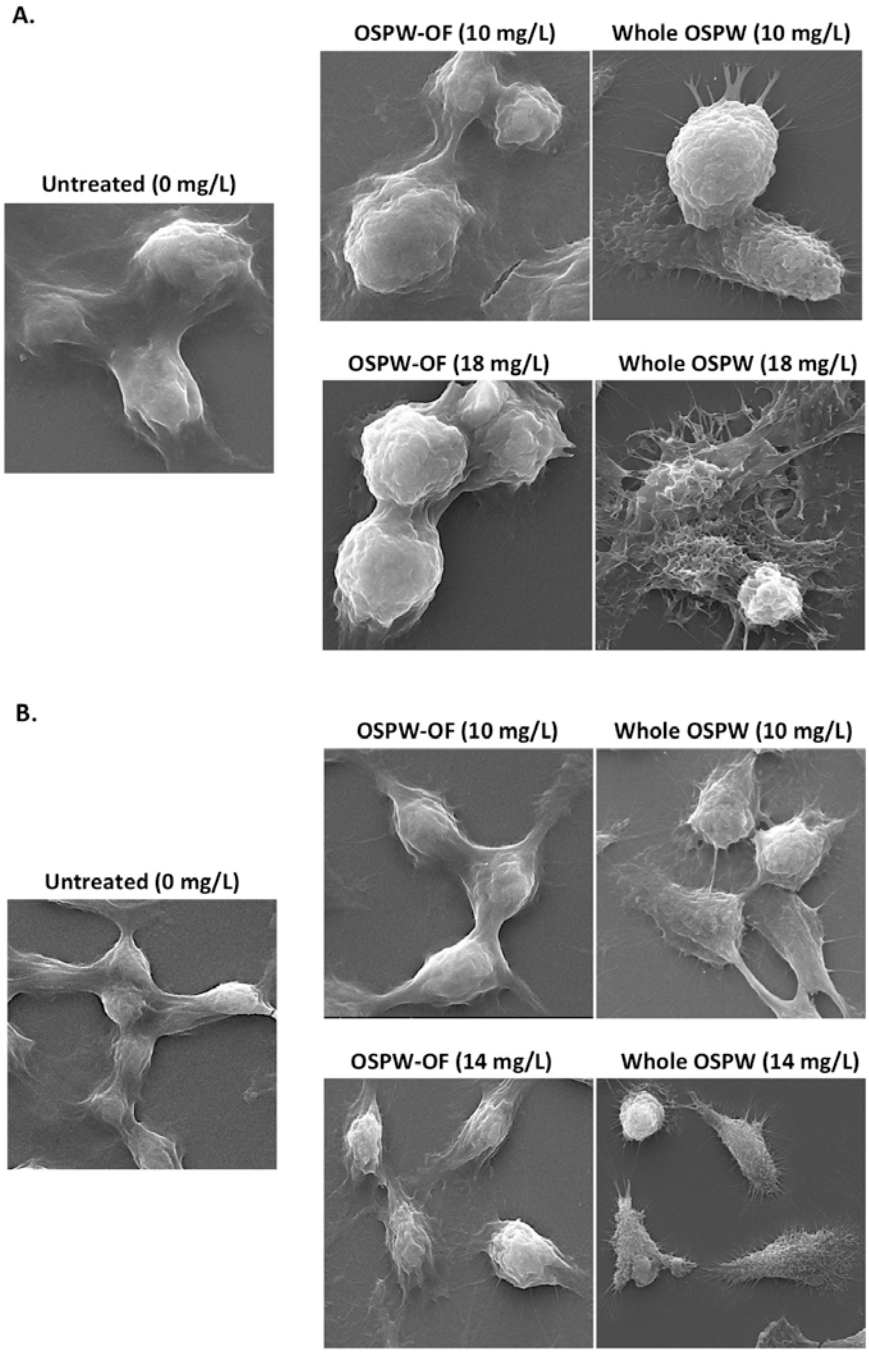

Figure 26. Morphological examinations of an OSPW treated mouse macrophage cell line. RAW 264.7 cells were treated with 10 mg/L or 18 mg/L of whole OSPW for (A) 6 h or 10 mg/L and 14 mg/L of crude (raw) OSPW-OF for (B) for 18 h at 37^{o}C prior to performing morphological examinations using scanning electron microscopy (SEM). Shown are representative panels of the changes in gross cellular morphology of the OSPW exposed cells relative to the untreated control cells. Notably changes in the whole OSPW treated groups include increased ruffling of the cytoplasm and increased spike-like projections on the cell membranes.

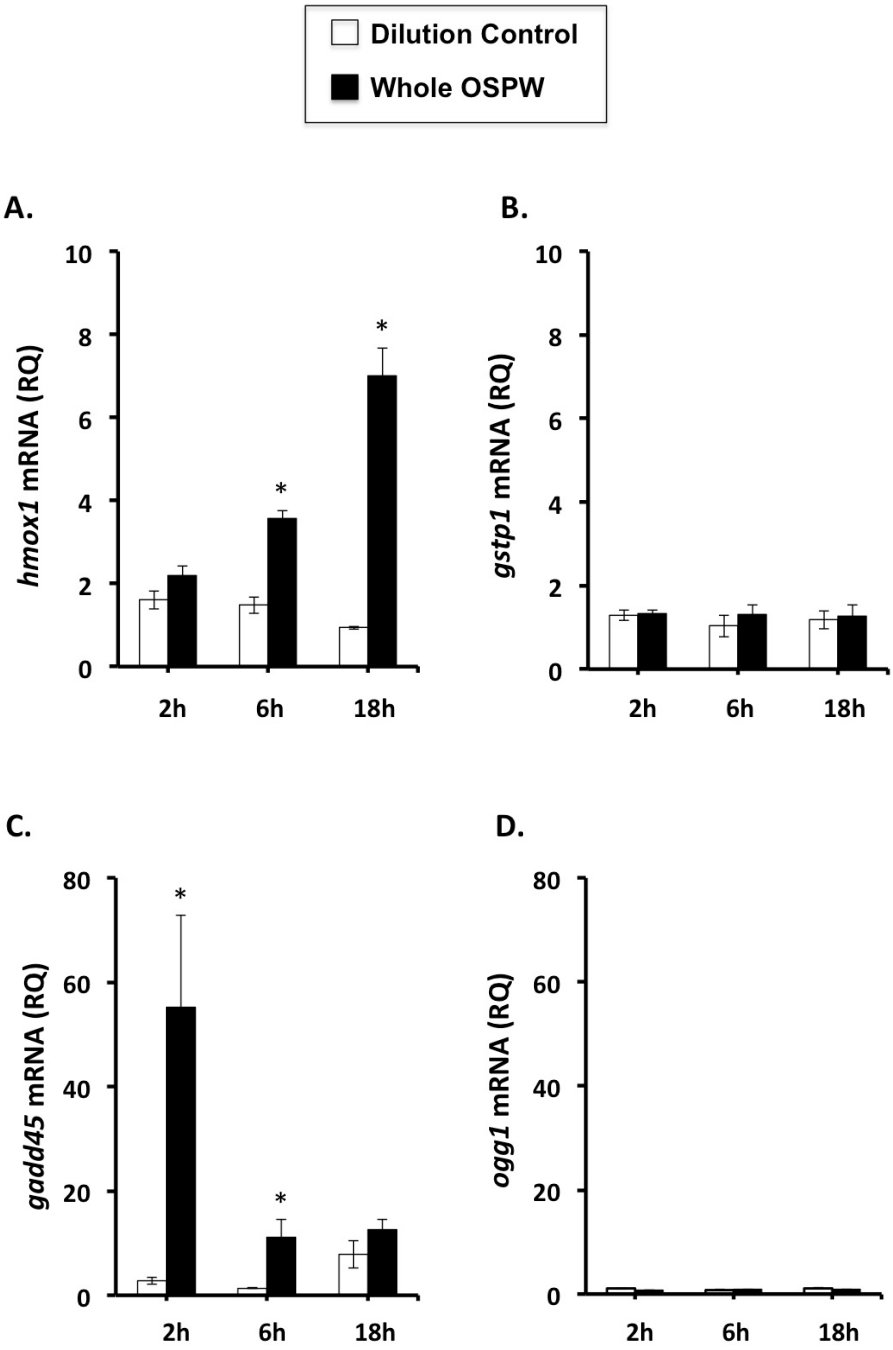
Dilution Control
Whole OSPW
A.
B.
C.
D.
hmox1 mRNA (RQ)
gstp1 mRNA (RQ)
gadd45 mRNA (RQ)
ogg1 mRNA (RQ)
2h
6h
18h
*

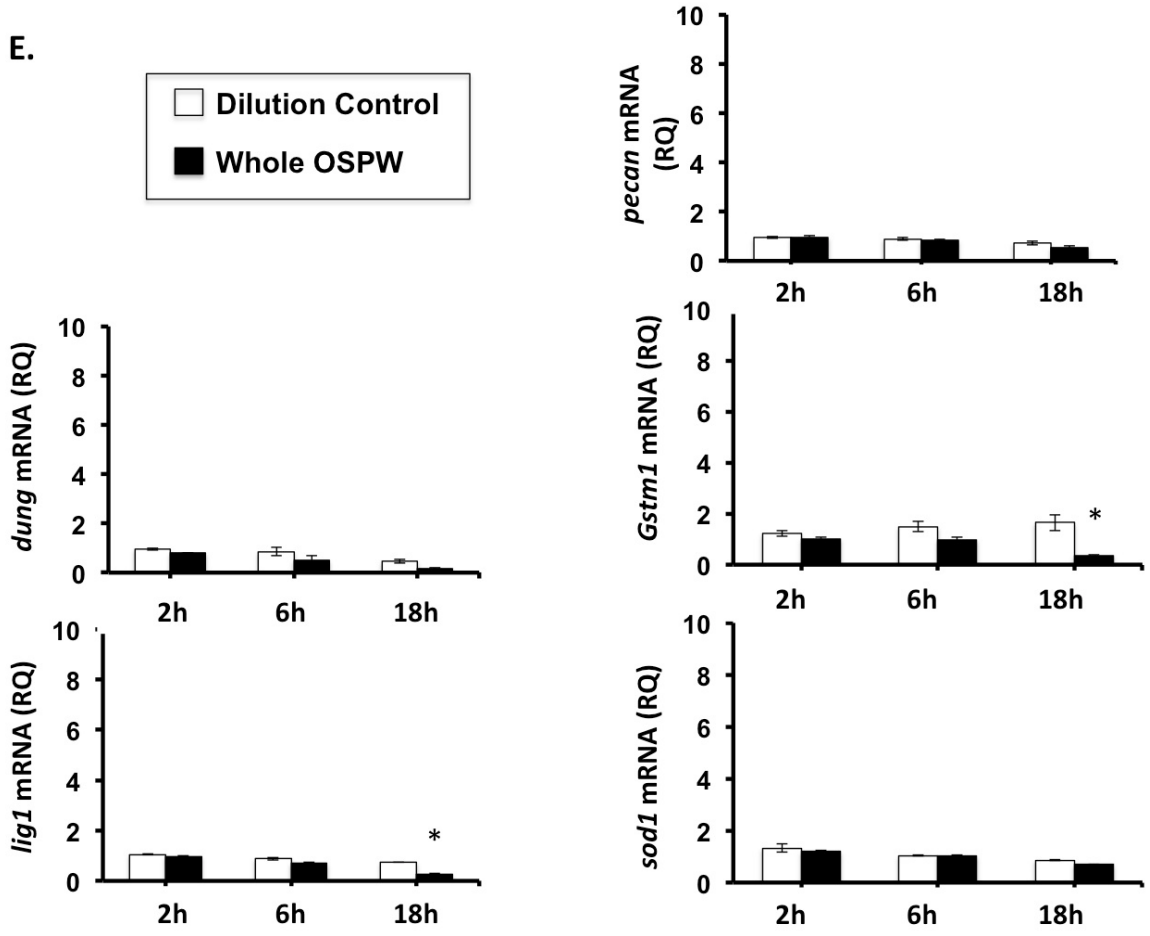

Figure 27. Effects of whole (raw) OSPW treatment on stress gene expression levels of a mouse macrophage cell line. RAW 264.7 cells were treated with 10 mg/L raw OSPW (black bars) or with PBS (white bars) for 2 h, 6 h, and 18 h prior to determining their mRNA expression levels of the oxidative stress genes (A) *hmox1* and (B) *gstp1, the* DNA damage/repair genes (C) *gadd45* and (D) *ogg1* or the other representative stress genes (E) *dung*, *lig1*, *pecan*, *gstm1*, and *sod1* by quantitative PCR. Results are presented as RQ values, which represents their fold differences in expression relative to the normalized control gene *Hrpt1*. Each bar represents the mean ± SEM of three separate experiments and *p<0.05 when comparing the treated cells to the untreated controls at each time point.

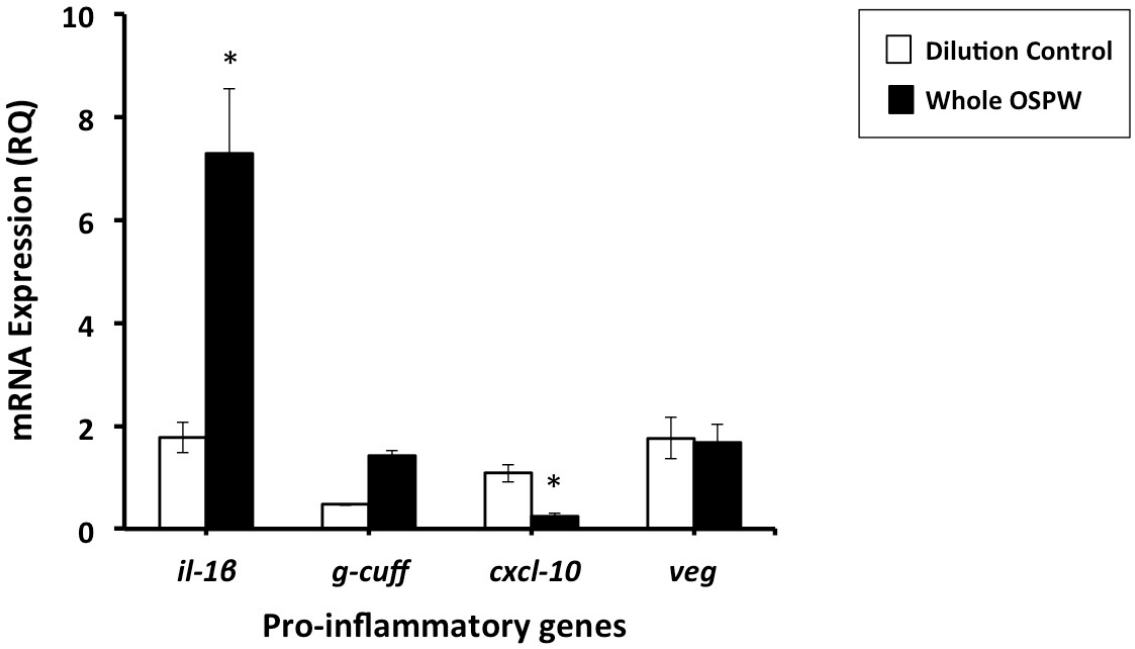

Figure 28. Effects of whole (raw) OSPW treatment on cytokine gene expression levels of resting mouse macrophages. The RAW 264.7 cell line was treated with 10 mg/L raw OSPW for 18 h at 37^{o}C prior to determining their basal mRNA expression levels for the cytokine genes *Il1-β*, *G-cuff*, *Cxcl-10*, and *Veg*. Results are presented as RQ, which represents their fold differences in mRNA expression relative to the normalized control gene *Hrpt1*. Each bar represents the mean ± SEM of three separate experiments and *$p<0.05$ when comparing the treated cells to the untreated controls at each time point.

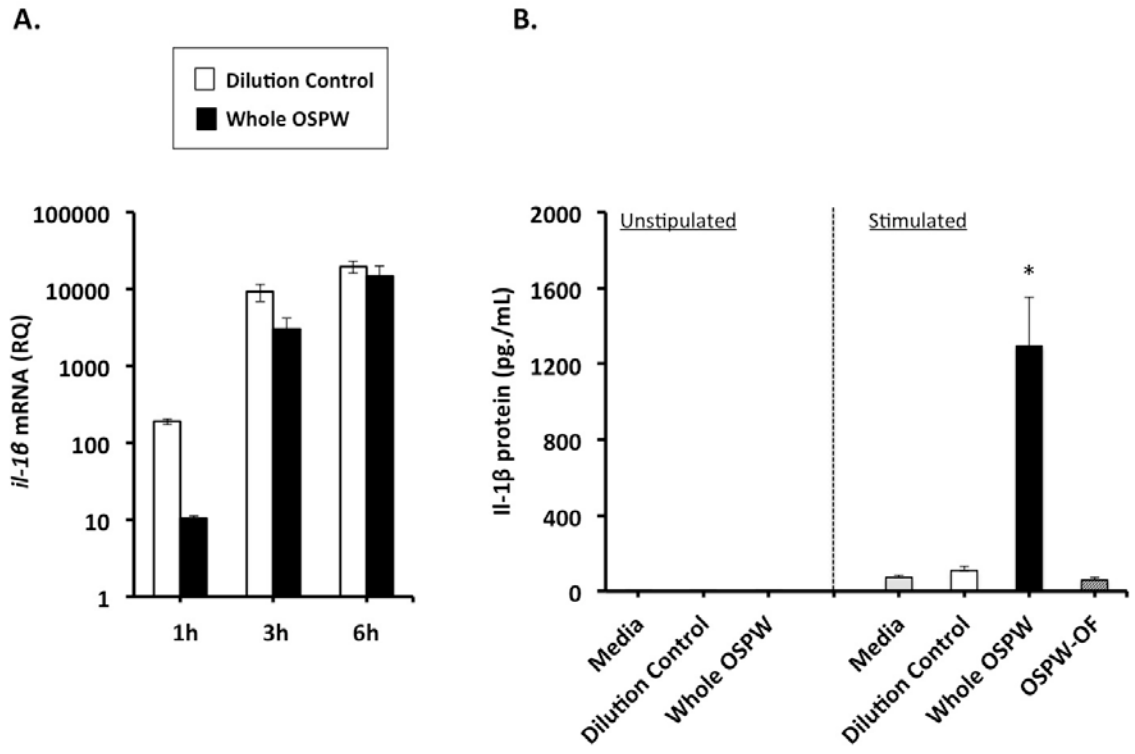

Figure 29. Effects of whole (raw) OSPW treatment on *il1-β* gene and IL-1β protein expression levels of resting and bacteria-stimulated mouse macrophages. (A) the RAW 264.7 cell line was treated with 10 mg/L whole OSPW for 18 h at 37°C prior to determining their expression of *il1-β* mRNA after stimulation with bacteria (i.e., *E. coli*) for 1 h, 3 h, and 6 h. Results for mRNA are presented as RQ, which represents their fold differences in mRNA expression relative to the normalized control gene *Hrpt1*. Each bar represents the mean ± SEM of three separate experiments and *p<0.05 when comparing the treated cells to the untreated controls at each time point. (B) Effects of OSPW treatments on the secretion of IL-1β protein by resting and stimulated mouse macrophages was also determined. The RAW 264.7 cell line was treated for 18h at 37°C with 10 mg/L of raw OSPW (black bars), 10 mg/L of OSPW-OF (hatched bars), the matched 10 mg/L PBS dilution control (white bars), or they were left untreated (i.e., 0 mg/L; grey bars) in complete culture media. Treatments were then removed and the cells were subsequently incubated in complete cell media alone (unstipulated) or in cell media containing 100 µg of *E. coli* bacteria (stimulated). Cells were then incubated for an additional 18 h at 37°C to allow for the secreted cytokines to accumulate in the culture media. Cell supernatants were then collected and examined for the indicated cytokine protein levels using a bead-based antibody capture assay. Each bar represents the mean ± SEM of three separate experiments and *p<0.05 when comparing all treatments with the *E. coli*-stimulated dilution control group (white bar).

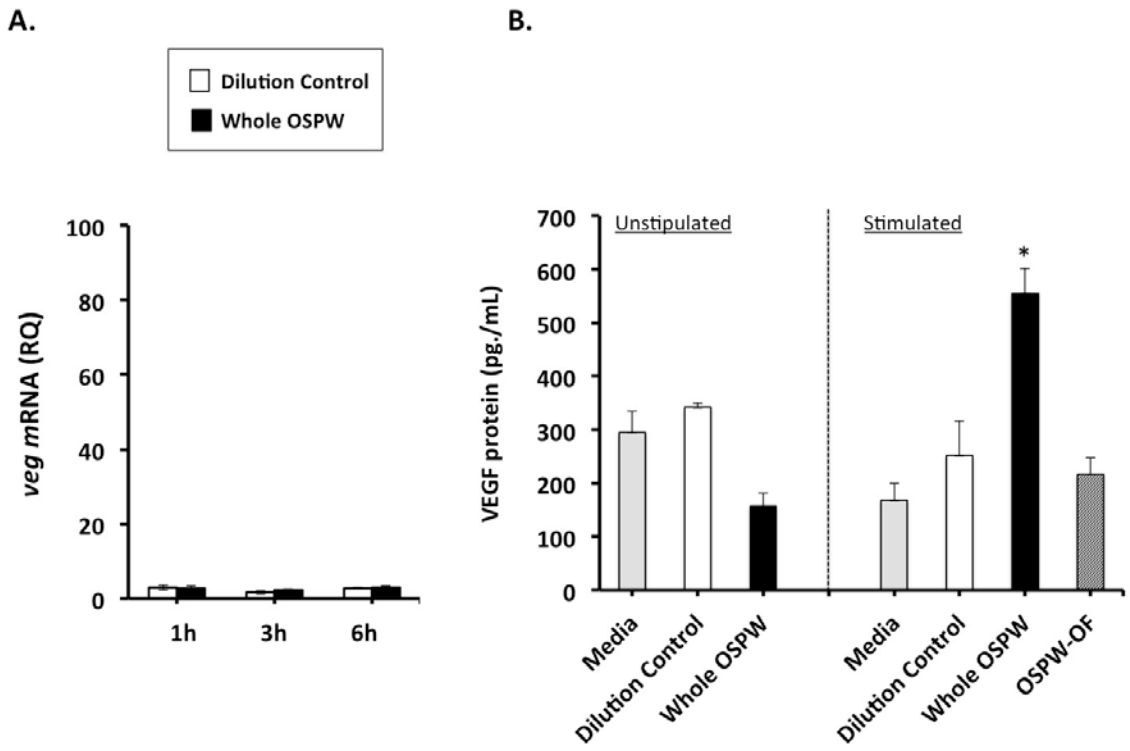

Figure 30. Effects of whole (raw) OSPW treatment on *veg* gene and VEGF protein expression levels of resting and bacteria-stimulated mouse macrophages. (A) the RAW 264.7 cell line was treated with 10 mg/L whole OSPW for 18 h at 37°C prior to determining their expression of *veg* mRNA after stimulation with bacteria (i.e., *E. coli*) for 1 h, 3 h, and 6 h. Results for mRNA are presented as RQ, which represents their fold differences in mRNA expression relative to the normalized control gene *Hrpt1*. Each bar represents the mean ± SEM of three separate experiments and *$p<0.05$ when comparing the treated cells to the untreated controls at each time point. (B) Effects of OSPW treatments on the secretion of VEGF protein by resting and stimulated mouse macrophages was also determined. The RAW 264.7 cell line was treated for 18h at 37°C with 10 mg/L of raw OSPW (black bars), 10 mg/L of OSPW-OF (hatched bars), the matched 10 mg/L PBS dilution control (white bars), or they were left untreated (i.e., 0 mg/L; grey bars) in complete culture media. Treatments were then removed and the cells were subsequently incubated in complete cell media alone (unstipulated) or in cell media containing 100 µg of *E. coli* bacteria (stimulated). Cells were then incubated for an additional 18 h at 37°C to allow for the secreted cytokines to accumulate in the culture media. Cell supernatants were then collected and examined for the indicated cytokine protein levels using a bead-based antibody capture assay. Each bar represents the mean ± SEM of three separate experiments and *$p<0.05$ when comparing all treatments with the *E. coli*-stimulated dilution control group (white bar).

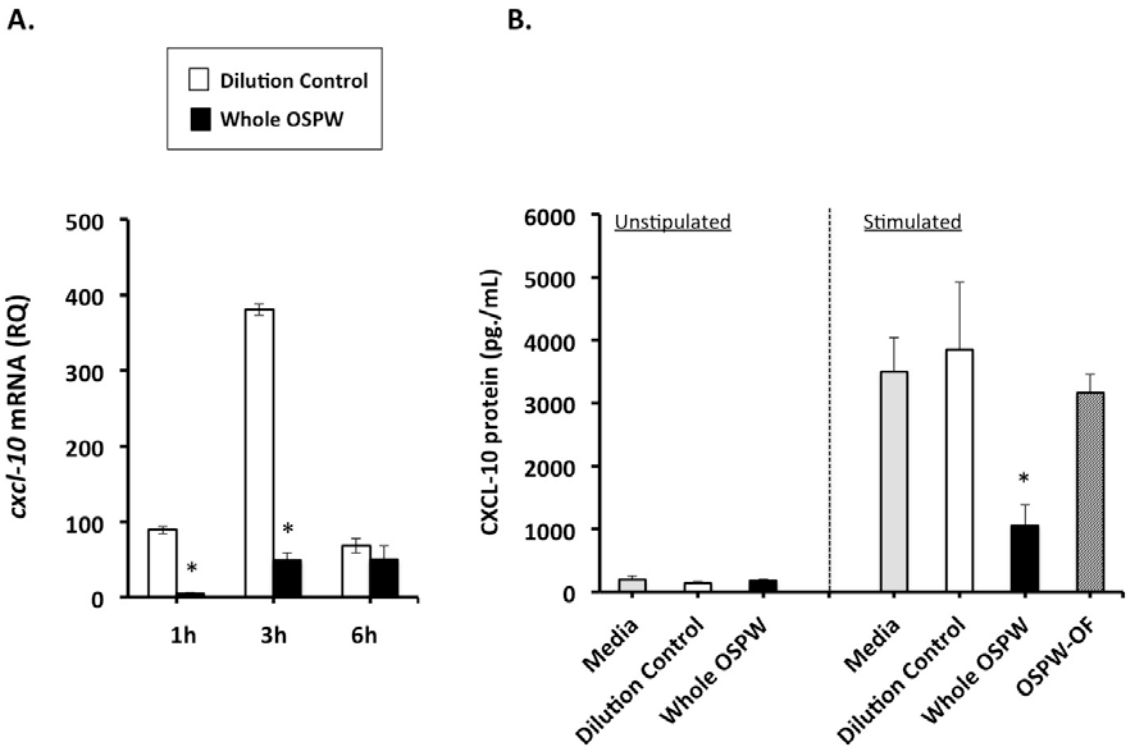

Figure 31. Effects of whole (raw) OSPW treatment on *cxcl-10* gene and CXCL-10 protein expression levels of resting and bacteria-stimulated mouse macrophages. (A) the RAW 264.7 cell line was treated with 10 mg/L whole OSPW for 18 h at 37°C prior to determining their expression of *cxcl-10* mRNA after stimulation with bacteria (i.e., *E. coli*) for 1 h, 3 h, and 6 h. Results for mRNA are presented as RQ, which represents their fold differences in mRNA expression relative to the normalized control gene *Hrpt1*. Each bar represents the mean ± SEM of three separate experiments and *p<0.05 when comparing the treated cells to the untreated controls at each time point. (B) Effects of OSPW treatments on the secretion of CXCL-10 protein by resting and stimulated mouse macrophages was also determined. The RAW 264.7 cell line was treated for 18h at 37°C with 10 mg/L of raw OSPW (black bars), 10 mg/L of OSPW-OF (hatched bars), the matched 10 mg/L PBS dilution control (white bars), or they were left untreated (i.e., 0 mg/L; grey bars) in complete culture media. Treatments were then removed and the cells were subsequently incubated in complete cell media alone (unstipulated) or in cell media containing 100 µg of *E. coli* bacteria (stimulated). Cells were then incubated for an additional 18 h at 37°C to allow for the secreted cytokines to accumulate in the culture media. Cell supernatants were then collected and examined for the indicated cytokine protein levels using a bead-based antibody capture assay. Each bar represents the mean ± SEM of three separate experiments and *p<0.05 when comparing all treatments with the *E. coli*-stimulated dilution control group (white bar).

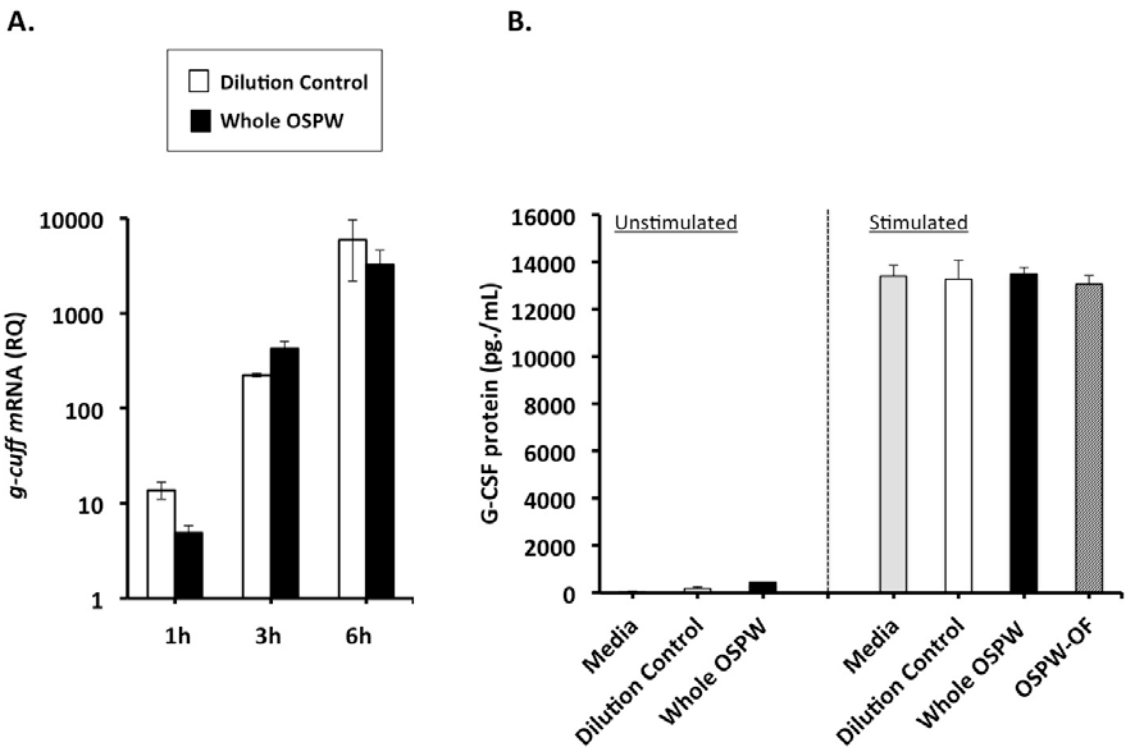

Figure 32. Effects of whole (raw) OSPW treatment on *g-cuff* gene and G-CSF protein expression levels of resting and bacteria-stimulated mouse macrophages. (A) the RAW 264.7 cell line was treated with 10 mg/L whole OSPW for 18 h at 37°C prior to determining their expression of *g-cuff* mRNA after stimulation with bacteria (i.e., *E. coli*) for 1 h, 3 h, and 6 h. Results for mRNA are presented as RQ, which represents their fold differences in mRNA expression relative to the normalized control gene *Hrpt1*. Each bar represents the mean ± SEM of three separate experiments and *p<0.05 when comparing the treated cells to the untreated controls at each time point. (B) Effects of OSPW treatments on the secretion of G-CSF protein by resting and stimulated mouse macrophages was also determined. The RAW 264.7 cell line was treated for 18h at 37°C with 10 mg/L of raw OSPW (black bars), 10 mg/L of OSPW-OF (hatched bars), the matched 10 mg/L PBS dilution control (white bars), or they were left untreated (i.e., 0 mg/L; grey bars) in complete culture media. Treatments were then removed and the cells were subsequently incubated in complete cell media alone (unstipulated) or in cell media containing 100 µg of *E. coli* bacteria (stimulated). Cells were then incubated for an additional 18 h at 37°C to allow for the secreted cytokines to accumulate in the culture media. Cell supernatants were then collected and examined for the indicated cytokine protein levels using a bead-based antibody capture assay. Each bar represents the mean ± SEM of three separate experiments and *p<0.05 when comparing all treatments with the *E. coli*-stimulated dilution control group (white bar).

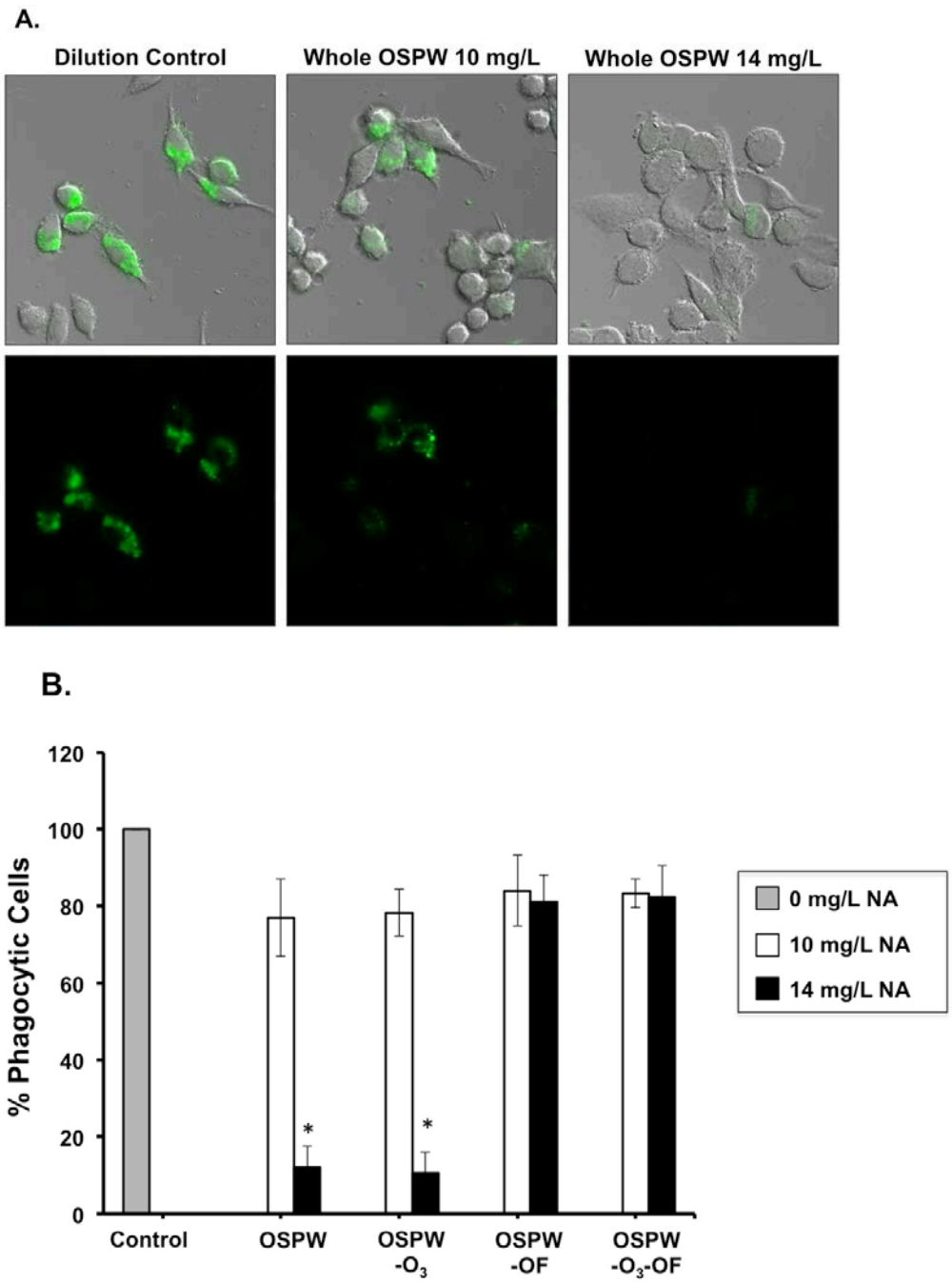

Figure 33. Effects of whole (raw) OSPW exposures on the phagocytic activity of mouse macrophages. RAW 264.7 cells were treated with 10 mg/L or 14 mg/L of whole OSPW for 18 h at 37°C prior to incubating them with fluorescent (prod® green)-labelled *E. coli* for 1 hr. Cells were then visualized microscopically (A) to differential internalized (green) from extracellular non-fluorescent bacteria and the phagocytic activity of the cells was then quantified using the Operetta High Content Imaging System (B). Each bar represents the mean ± SEM of three separate experiments and * represent $p<0.05$ when comparing the 10 mg/L or 14 mg/L raw OSPW treated cells to the untreated control cells (i.e., 0 mg/L).

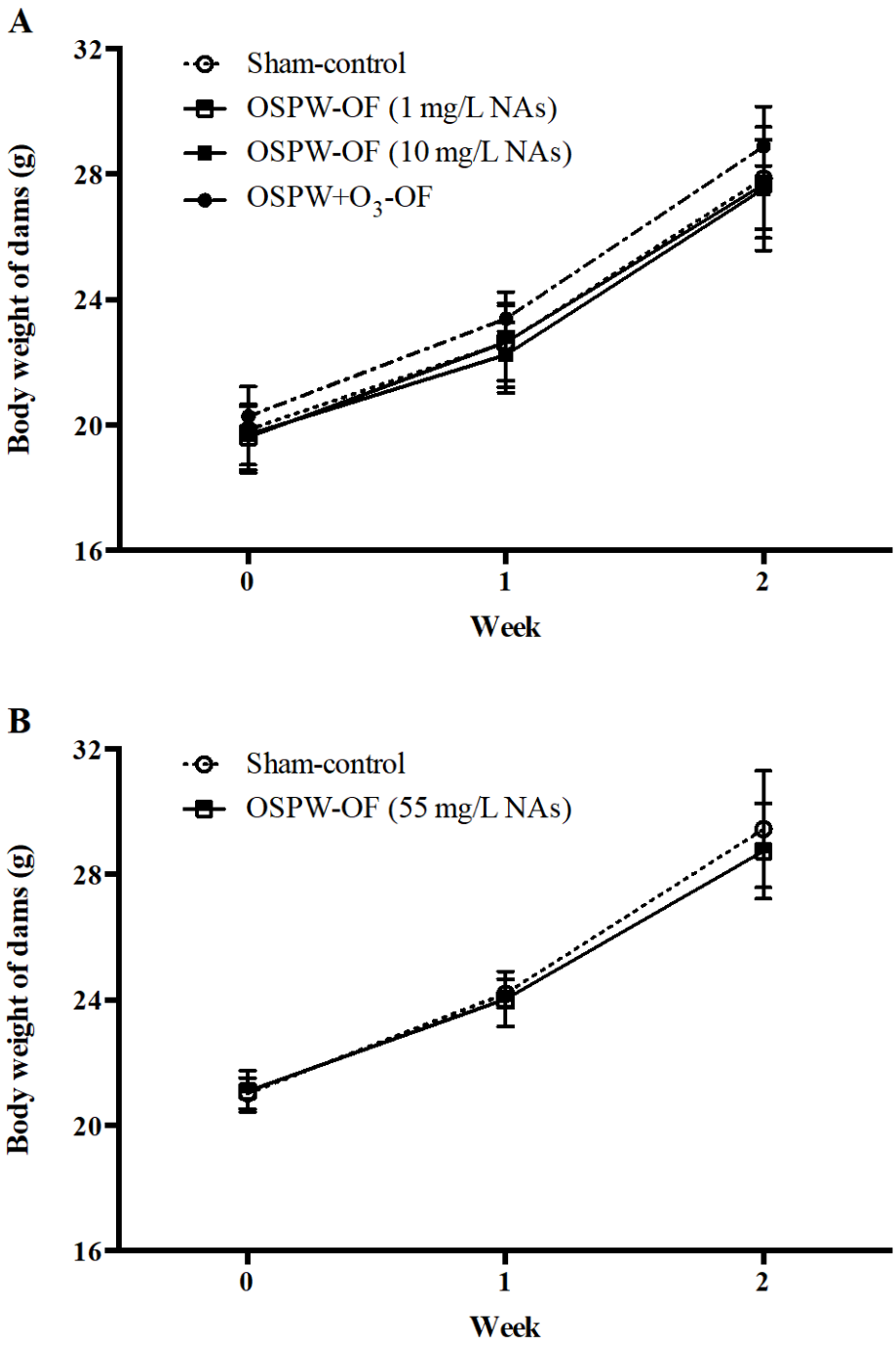

Figure 34. Body weight of female mice during acute exposure. Animals were gavaged weekly with (A) OSPW-OF (1 and 10 mg/L NAs) and OSPW+O_3-OF, or (B) OSPW-OF (55 mg/L NAs) for two weeks beginning on GD 0. Body weight of each mouse was recorded weekly. Date represent mean ± SEM (n=15-16 for A, and 5-8 for B). At each time point, statistical analysis was performed using one-way ANOVA with Dunnett's *post hoc* test for (A) and Student's *T*-test for (B).

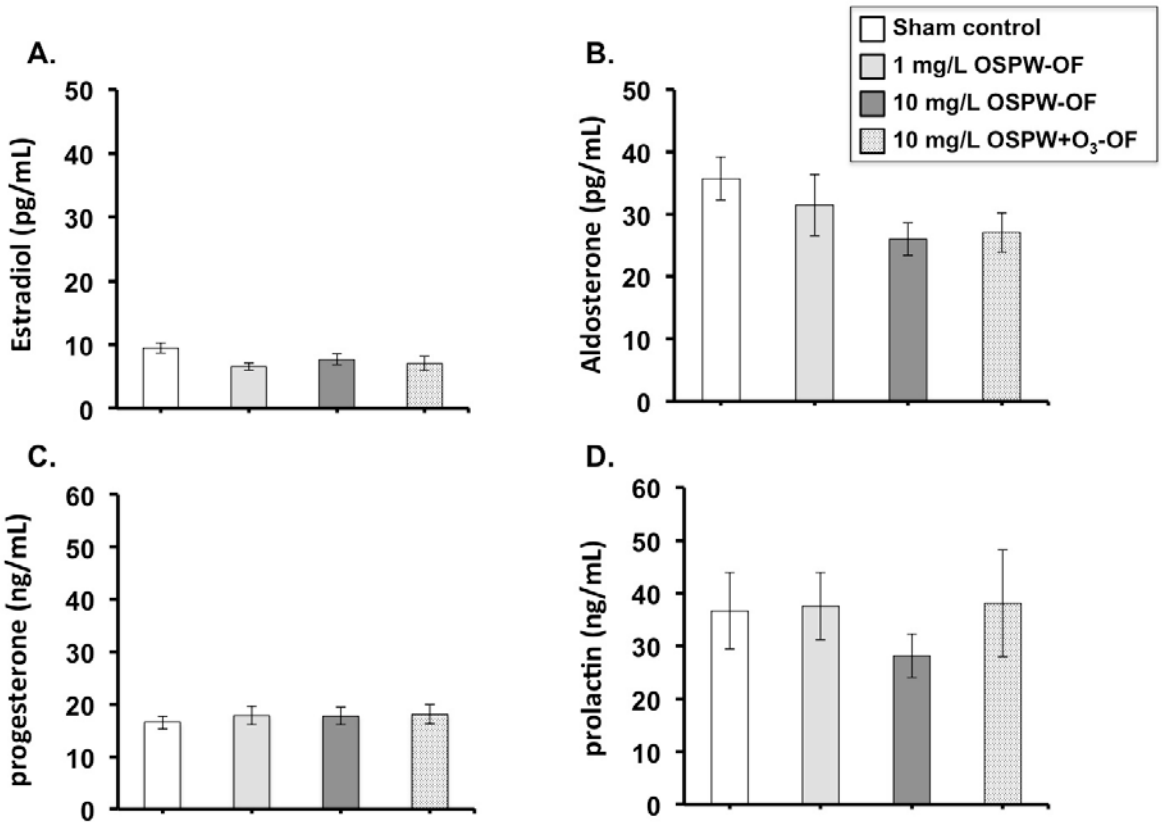

Figure 35. Effects of OSPW-OF acute exposures on the plasma hormone levels in Balb/c mice. (A) Estradiol, (B) Aldosterone, (C) Progesterone, and (D) Prolactin levels were measured in the plasma of pregnant Balb/c mice after two gavage exposures up to gestational day 14. For each experimental group; sham control (0 mg/L; n=17), OSPW-OF 1 mg/L (n=12), OSPW-OF 10 mg/mL (n=11), and OSPW-O_3-OF 10 mg/L (n=12), mouse blood was collected and the plasma and cell pellets were separated prior to the measurement of hormone levels. Each bar represents the mean ± SEM for each group. P values were computed using one-way ANOVA followed by Dunnett's multiple comparisons test. *$p<0.05$ when comparing to sham control.

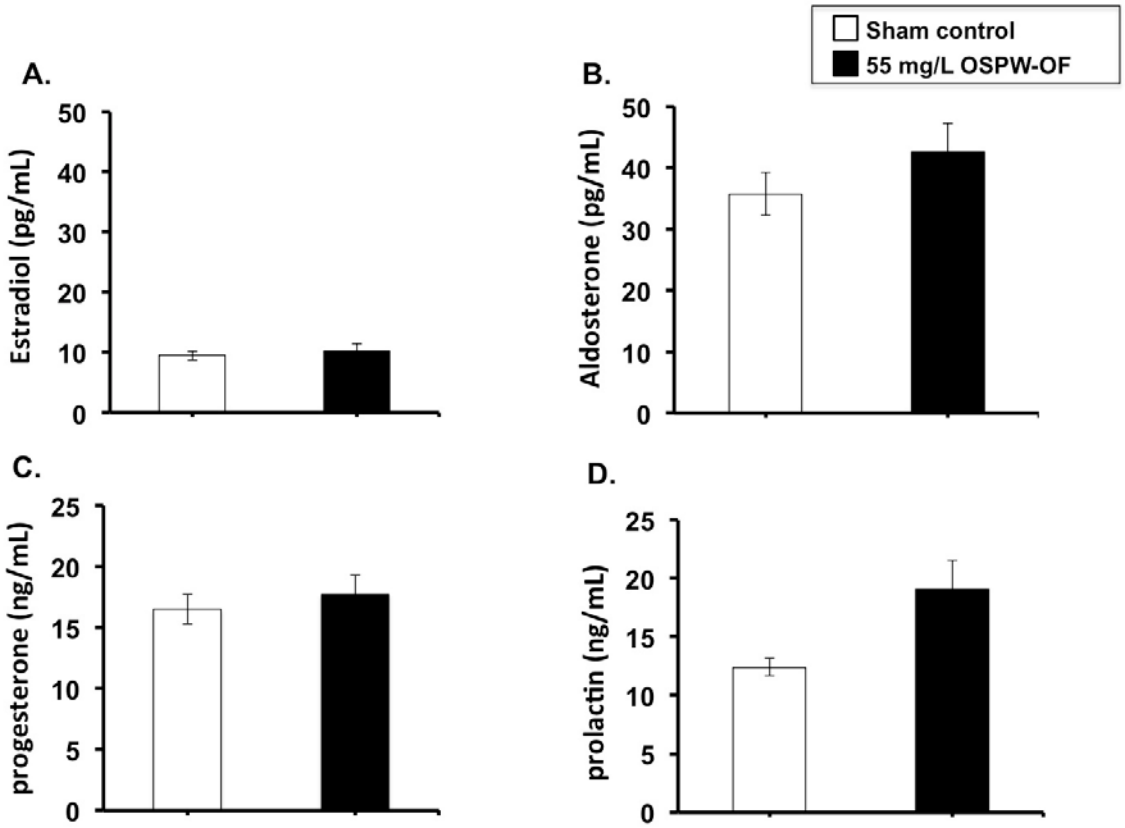

Figure 36. Effects of high dose OSPW-OF acute exposures on the plasma hormone levels in Balb/c mice. (A) Estradiol, (B) Aldosterone, (C) Progesterone, and (D) Prolactin levels were measured in the plasma of pregnant Balb/c mice after two gavage exposures up to gestational day 14. For each experimental group; sham control (0 mg/L; n=5), and OSPW-OF 55 mg/L (n=8), mouse blood was collected and the plasma and cell pellets were separated prior to the measurement of hormone levels. Each bar represents the mean ± SEM for each group. P values were computed using one-way ANOVA followed by Dunnett's multiple comparisons test. *$p<0.05$ when comparing to sham control.

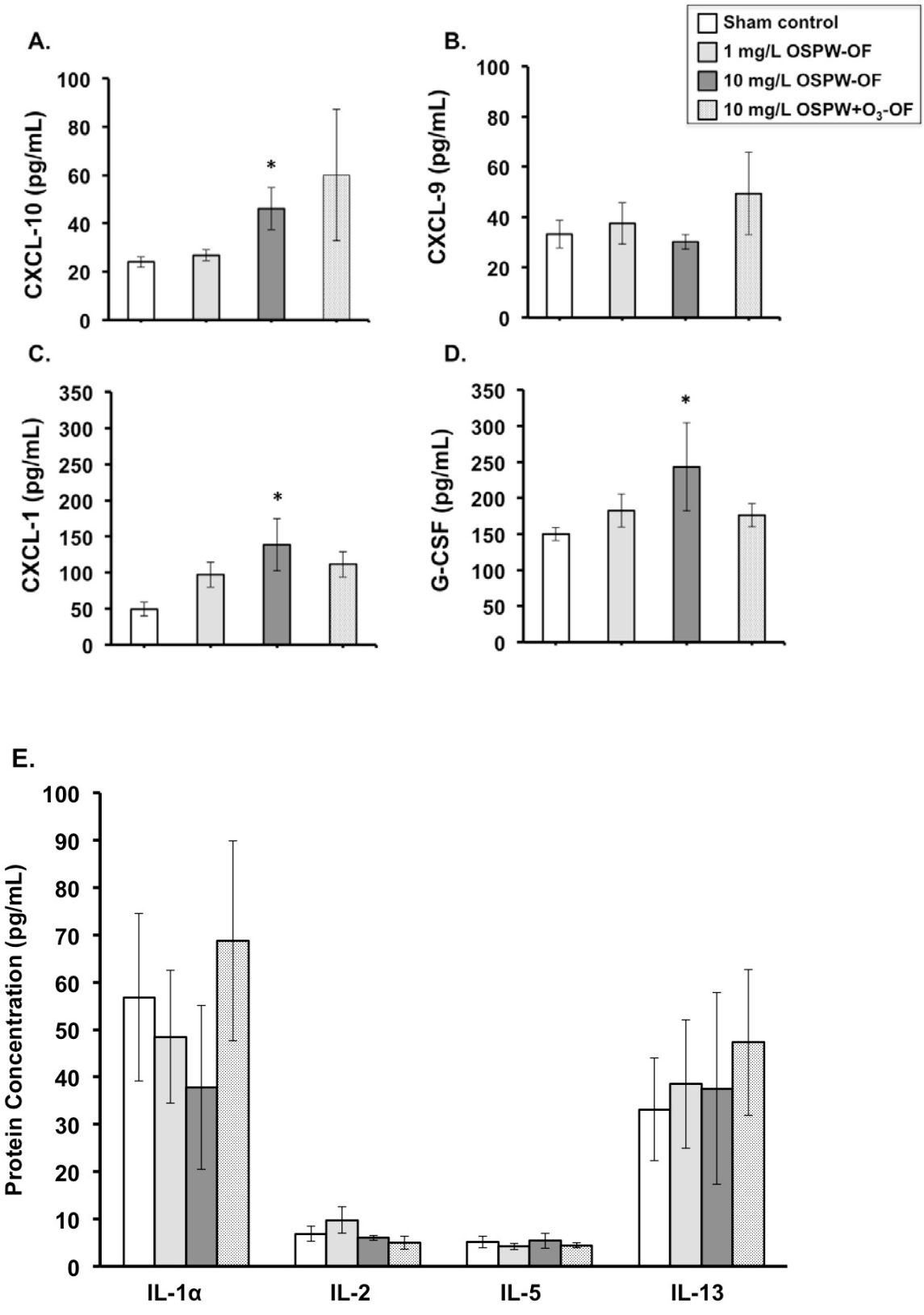
A.
B.
C.
D.
E.
Sham control
1 mg/L OSPW-OF
10 mg/L OSPW-OF
10 mg/L OSPW+O3-OF
CXCL-10 (pg/mL)
CXCL-9 (pg/mL)
CXCL-1 (pg/mL)
G-CSF (pg/mL)
Protein Concentration (pg/mL)
IL-1α
IL-2
IL-5
IL-13
*

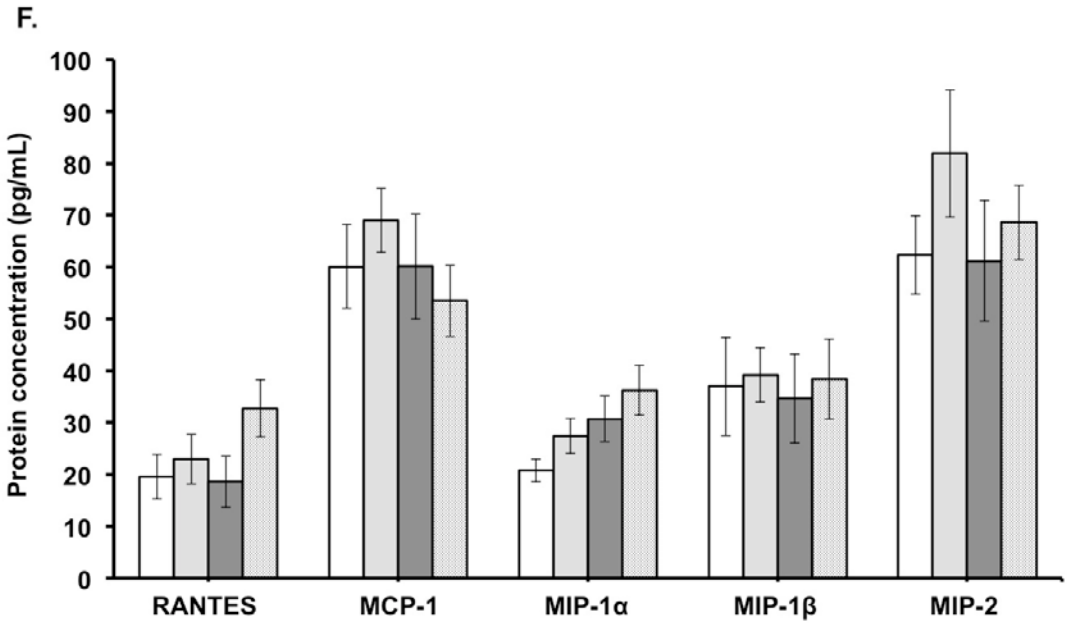

Figure 37. Effects of OSPW-OF acute exposures on the plasma cytokine levels in Balb/c mice. (A) CXCL-10, (B) CXCL-9 (C) CXCL-1, and (D) G-CSF, as well as (E) IL-1α, IL-2, IL-5, IL-13 and (F) RANTES, MCP-1, MIP-1α, MIP-1β, and MIP-2 levels were measured in the plasma of pregnant Balb/c mice after two gavage exposures up to gestational day 14. For each experimental group; sham control (0 mg/L; n=12), OSPW-OF 1 mg/L (n=12), OSPW-OF 10 mg/mL (n=11), and OSPW-O_3-OF 10 mg/L (n=13), mouse blood was collected and the plasma and cell pellets were separated. Plasma samples were then examined for cytokine protein levels using a bead-based antibody capture assay. Each bar represents the mean ± SEM for each group. P values were computed using one-way ANOVA followed by Dunnett's multiple comparisons test. *p<0.05 when comparing to sham control.

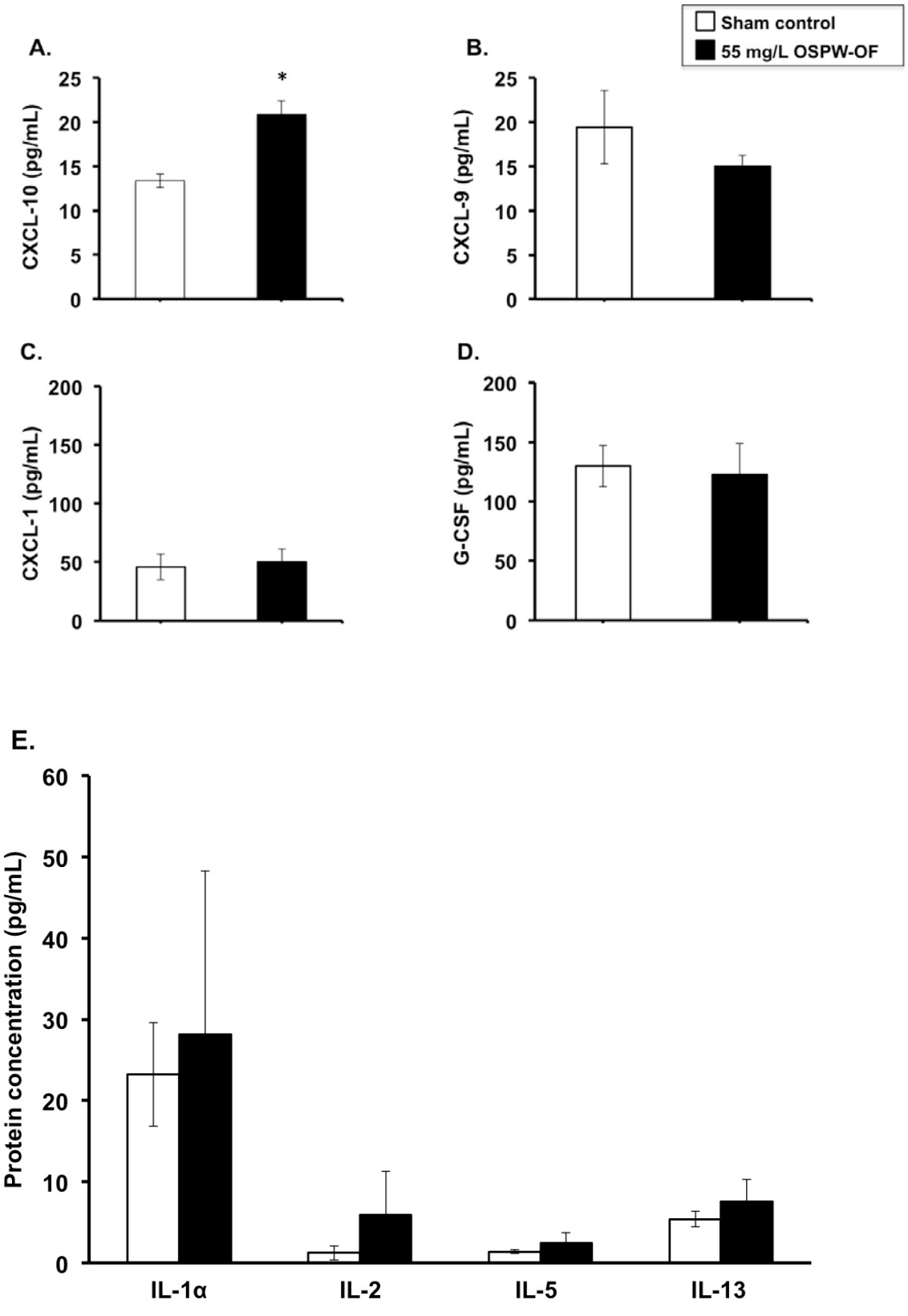
Sham control
55 mg/L OSPW-OF
A.
CXCL-10 (pg/mL)
*
B.
CXCL-9 (pg/mL)
C.
CXCL-1 (pg/mL)
D.
G-CSF (pg/mL)
E.
Protein concentration (pg/mL)
IL-1α
IL-2
IL-5
IL-13

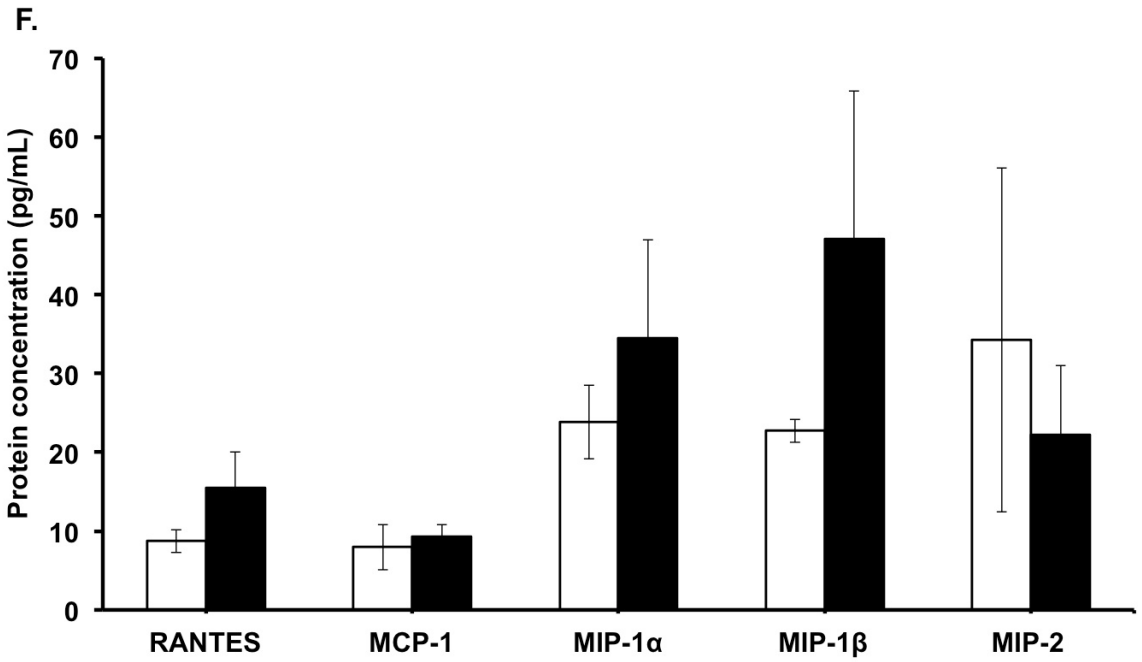

Figure 38. Effects of high dose OSPW-OF acute exposures on the plasma cytokine levels in Balb/c mice. (A) CXCL-10, (B) CXCL-9 (C) CXCL-1, and (D) G-CSF, as well as (E) IL-1α, IL-2, IL-5, IL-13 and (F) RANTES, MCP-1, MIP-1α, MIP-1β, and MIP-2 levels were measured in the plasma of pregnant Balb/c mice after two gavage exposures up to gestational day 14. For each experimental group; sham control (0 mg/L; n=5), and OSPW-OF 55 mg/L (n=8), mouse blood was collected and the plasma and cell pellets were separated. Plasma samples were then examined for cytokine protein levels using a bead-based antibody capture assay. Each bar represents the mean ± SEM for each group. P values were computed using one-way ANOVA followed by Dunnett's multiple comparisons test. *$p<0.05$ when comparing to sham control.

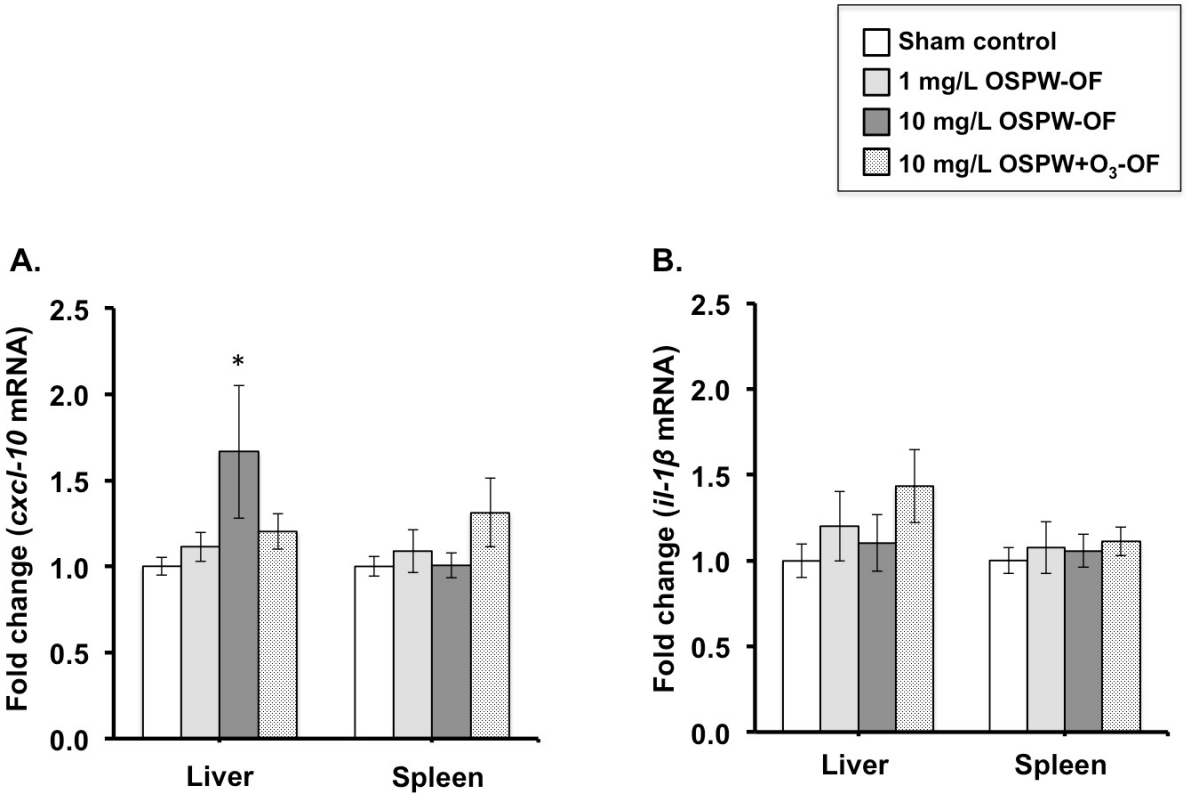

Figure 39. Effects of OSPW-OF acute exposures on the expression of cytokine genes in Balb/c mice. (A) *cxcl-10* and (B) *il-1β* mRNA expression levels were examined in Balb/c liver and spleen tissues by quantitative PCR after two gavage exposures up to gestational day 14. For each experimental group; sham control (0 mg/L; n=7), OSPW-OF 1 mg/L (n=7), OSPW-OF 10 mg/mL (n=6), and OSPW-O_3-OF 10 mg/L (n=8). Each bar represents the mean ± SEM for each group. P values were computed using one-way ANOVA followed by Dunnett's multiple comparisons test. *p<0.05 when comparing to sham control.

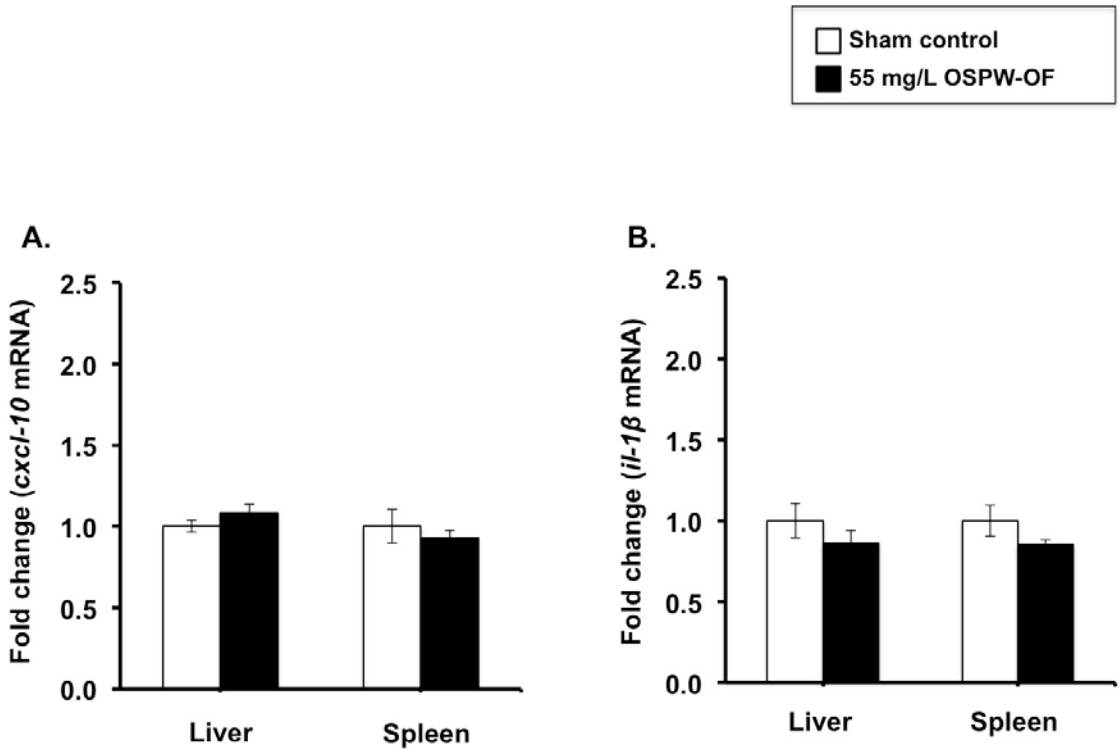

Figure 40. Effects of high dose OSPW-OF acute exposures on the expression of cytokine genes in Balb/c mice. (A) *cxcl-10* and (B) *il-1β* mRNA expression levels were examined in Balb/c liver and spleen tissues by quantitative PCR after two gavage exposures up to gestational day 14. For each experimental group; sham control (0 mg/L; n=5), and OSPW-OF 55 mg/L (n=8). Each bar represents the mean ± SEM for each group. P values were computed using one-way ANOVA followed by Dunnett's multiple comparisons test. *p<0.05 when comparing to sham control.

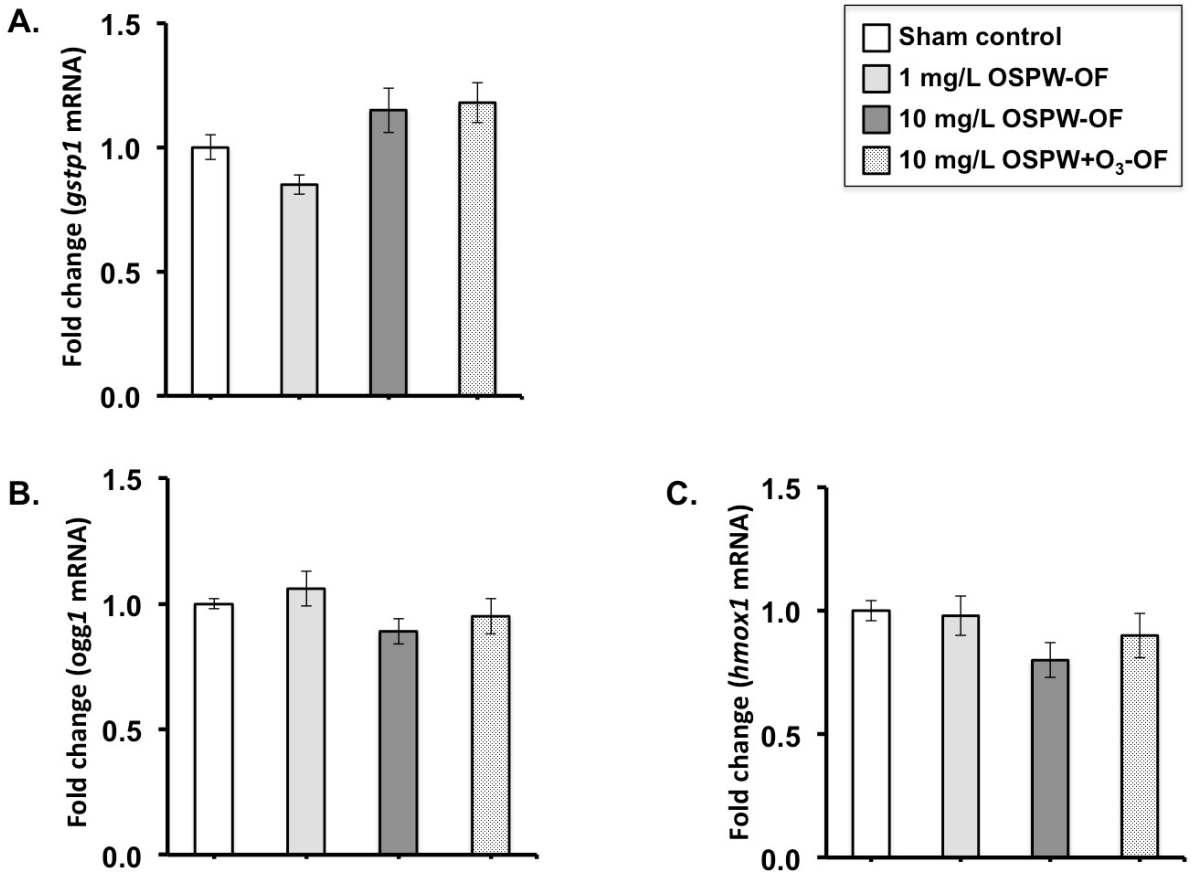

Figure 41. Effects of OSPW-OF acute exposures on the expression of stress genes in the liver of Balb/c mice. (A) *gstp1*, (B) *ogg1*, and (C) *hmox1* mRNA expression levels were examined by quantitative PCR after two gavage exposures up to gestational day 14 in the liver tissue of exposed mice. For each experimental group; sham control (0 mg/L; n=7), OSPW-OF 1 mg/L (n=7), OSPW-OF 10 mg/mL (n=6), and OSPW-O_3-OF 10 mg/L (n=8). Each bar represents the mean ± SEM for each group. P values were computed using one-way ANOVA followed by Dunnett's multiple comparisons test. *$p<0.05$ when comparing to sham control.

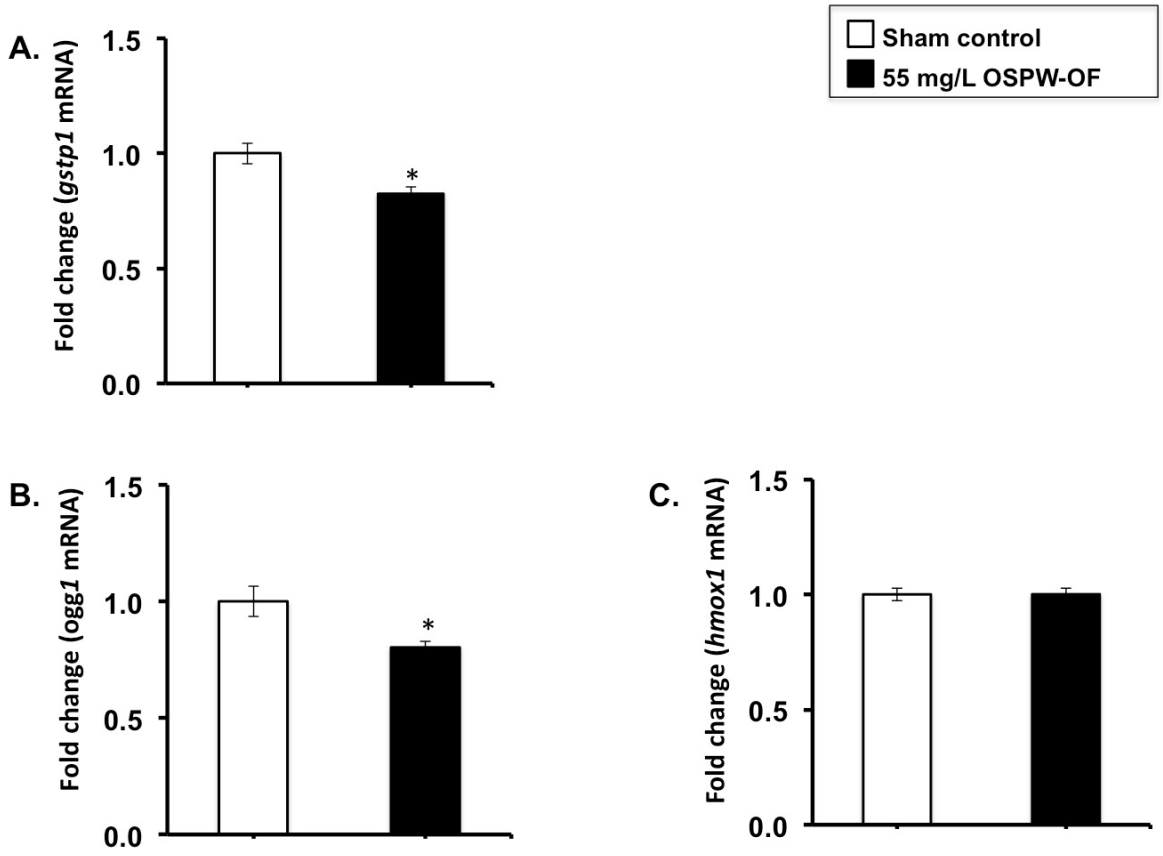

Figure 42. Effects of high dose OSPW-OF acute exposures on the expression of stress genes in the liver of Balb/c mice. (A) *gstp1*, (B) *ogg1*, and (C) *hmox1* mRNA expression levels were examined by quantitative PCR after two gavage exposures up to gestational day 14 in the liver tissue of exposed mice. For each experimental group; sham control (0 mg/L; n=5), and OSPW-OF 55 mg/L (n=8). Each bar represents the mean ± SEM for each group. P values were computed using one-way ANOVA followed by Dunnett's multiple comparisons test. *p<0.05 when comparing to sham control.

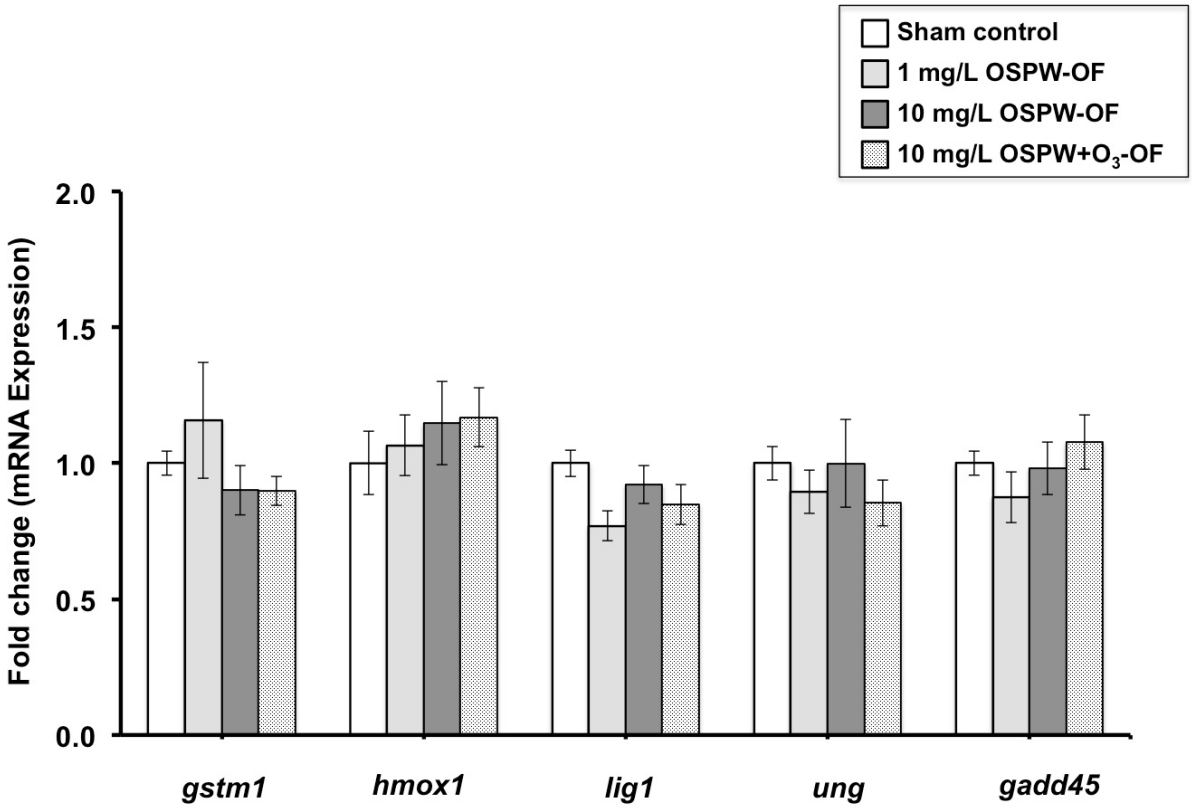

Figure 43. Effects of OSPW-OF acute exposures on the expression of stress genes in the spleen of Balb/c mice. The indicated stress gene mRNA expression levels were examined by quantitative PCR after two gavage exposures up to gestational day 14 in the spleen tissue of exposed mice. For each experimental group; sham control (0 mg/L; n=7), OSPW-OF 1 mg/L (n=7), OSPW-OF 10 mg/mL (n=6), and OSPW-O_3-OF 10 mg/L (n=8). Each bar represents the mean ± SEM for each group. P values were computed using one-way ANOVA followed by Dunnett's multiple comparisons test. *$p<0.05$ when comparing to sham control.

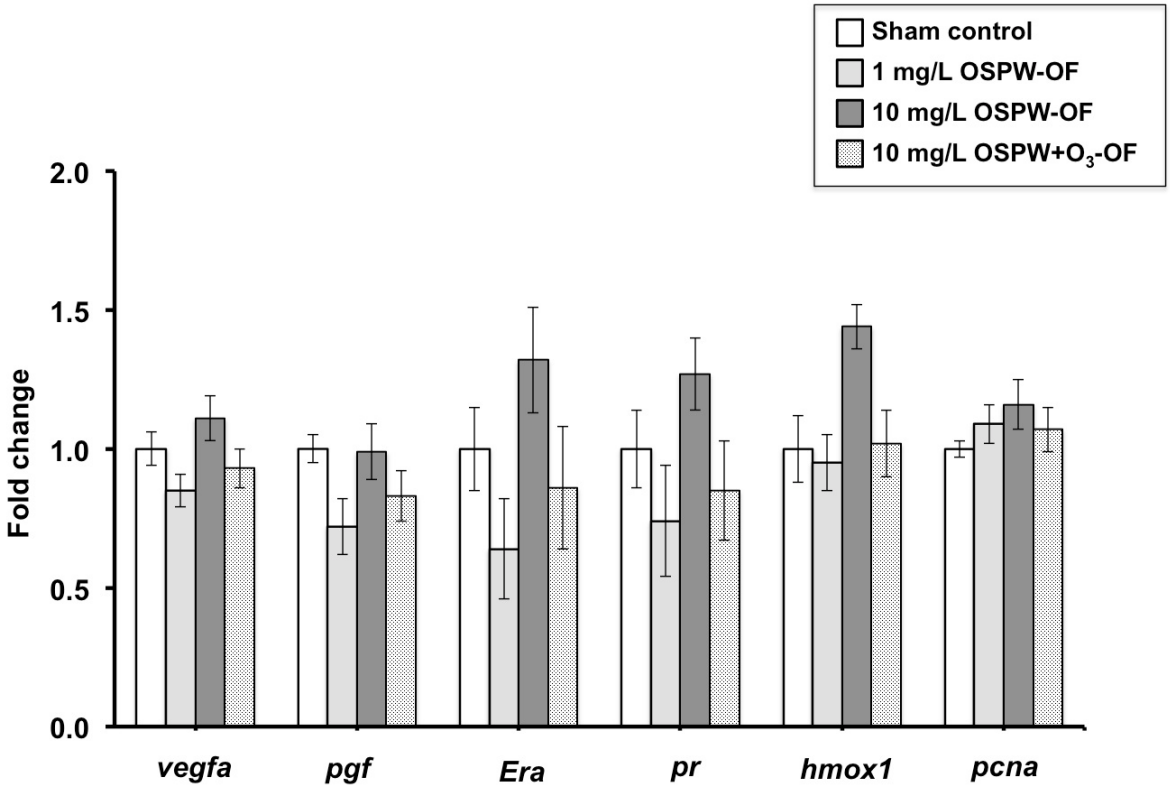

Figure 44. Effects of OSPW-OF acute exposures on the expression of stress genes in the placenta of Balb/c mice. The indicated stress gene mRNA expression levels were examined by quantitative PCR after two gavage exposures up to gestational day 14 in the placental tissue of exposed mice. For each experimental group; sham control (0 mg/L; n=7), OSPW-OF 1 mg/L (n=7), OSPW-OF 10 mg/mL (n=6), and OSPW-O_3-OF 10 mg/L (n=8). Each bar represents the mean ± SEM for each group. P values were computed using one-way ANOVA followed by Dunnett's multiple comparisons test. *$p<0.05$ when comparing to sham control.

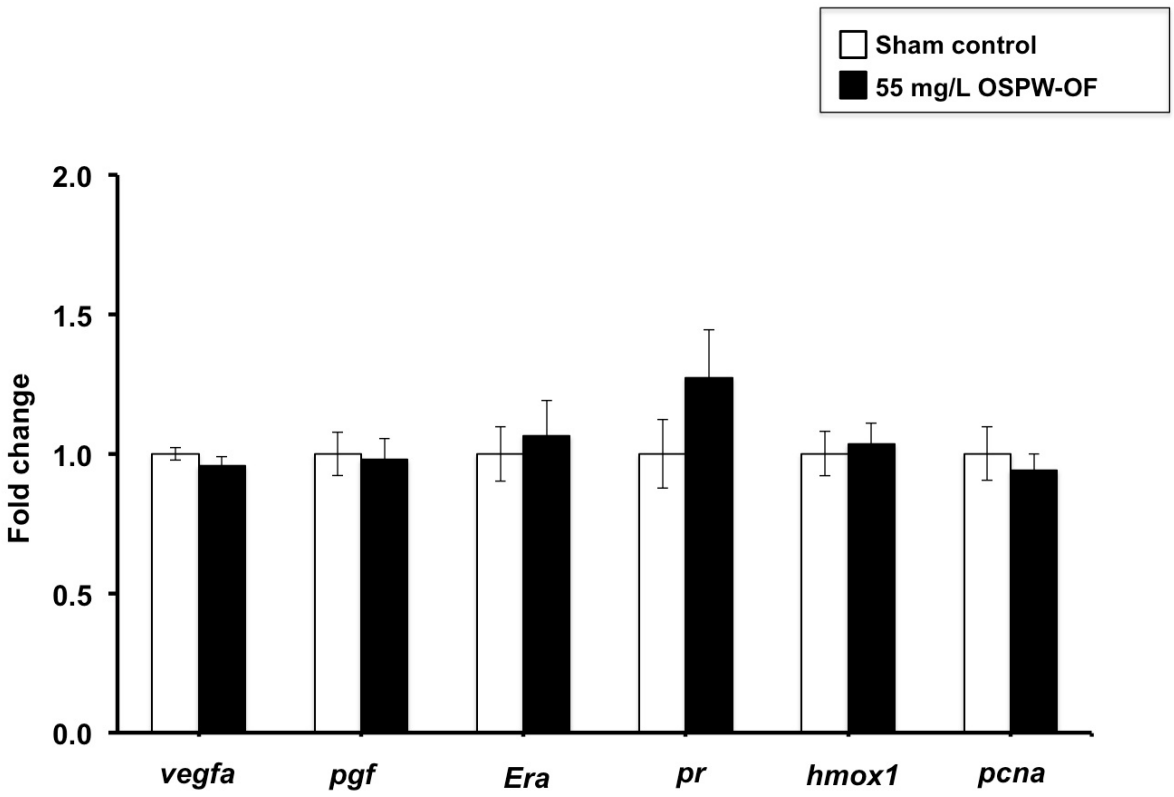

Figure 45. Effects of high dose OSPW-OF acute exposures on the expression of stress genes in the placenta of Balb/c mice. The indicated stress gene mRNA expression levels were examined by quantitative PCR after two gavage exposures up to gestational day 14 in the placental tissue of exposed mice. For each experimental group; sham control (0 mg/L; n=5), and OSPW-OF 55 mg/L (n=8). Each bar represents the mean ± SEM for each group. P values were computed using one-way ANOVA followed by Dunnett's multiple comparisons test. *p<0.05 when comparing to sham control.

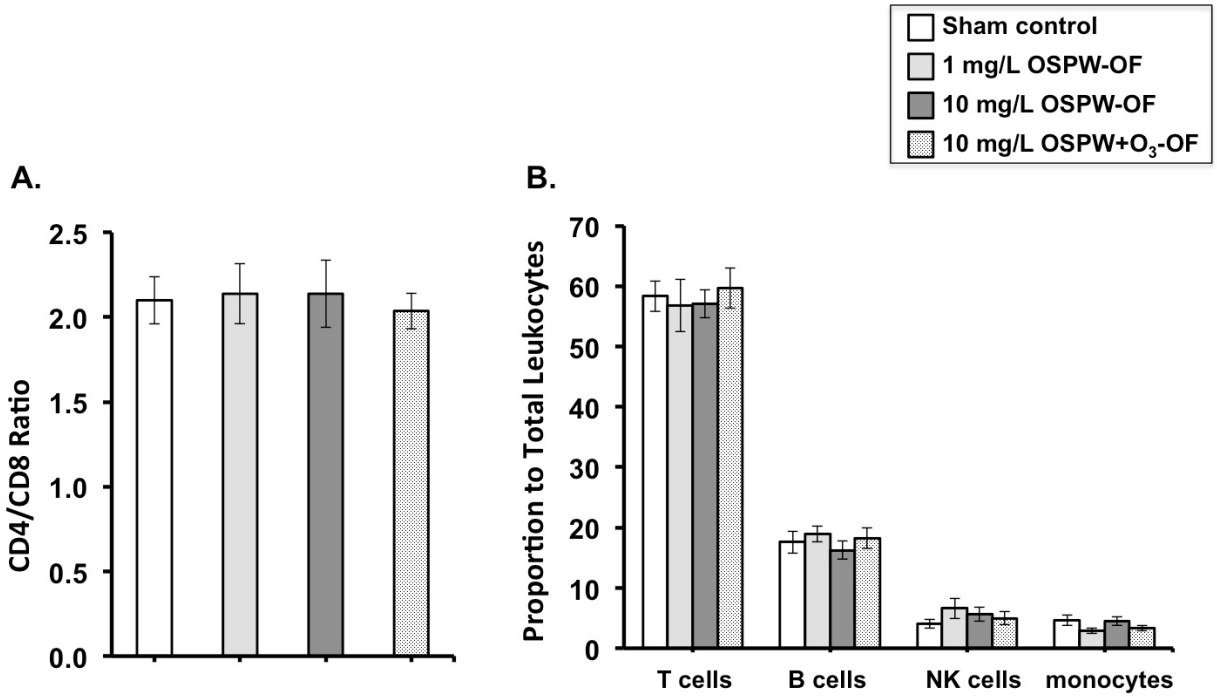

Figure 46. Effects of OSPW-OF acute exposures on peripheral blood immune cell numbers in Balb/c mice. Pregnant mice were exposed for 2 weeks to sham control (n=15), 1 mg/L OSPW-OF (n=12), 10 mg/L OSPW-OF (n=10), or 10 mg/L OSPW-OF-O_3 with (n=14). Peripheral blood mononuclear cells derived from whole blood of the experimental animals each were assessed by staining for the (A) CD4/CD8 ratio (CD45+CD3+CD4+/ CD45+CD3+CD8+), and (B) the proportions of T cells (CD45+CD3+), NK cells (CD45+CD3-DX5-), B cells (CD45+C3-B220+) and monocytes (CD45+CD3-CD11b+Ly6G-) in total leukocytes using BD LSR-Fortessa at Flow Cytometry Facility (University of Alberta). Results are mean ± SEM of the indicated mice each group. P values were computed using one-way ANOVA followed by Dunnett's multiple comparisons test. *$p<0.05$ when comparing to sham control.

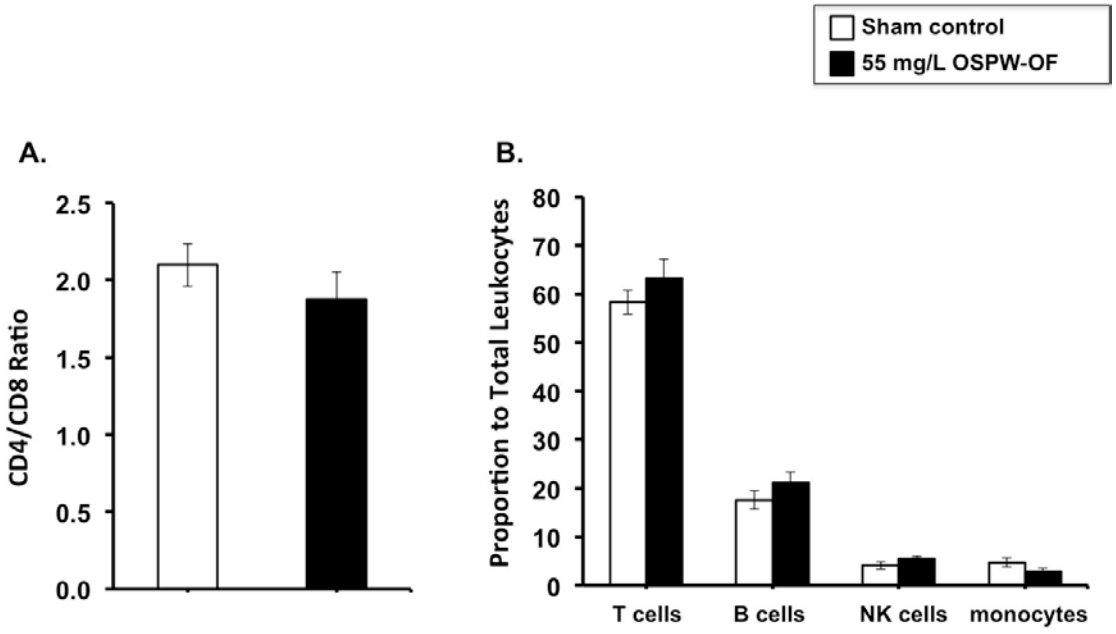

Figure 47. Effects of high dose OSPW-OF acute exposures on peripheral blood immune cell numbers in Balb/c mice. Pregnant mice were exposed for 2 weeks to sham control (n=5), or 55 mg/L OSPW-OF (n=8). Peripheral blood mononuclear cells derived from whole blood of the experimental animals each were assessed by staining for the (A) CD4/CD8 ratio (CD45+CD3+CD4+/ CD45+CD3+CD8+), and (B) the proportions of T cells (CD45+CD3+), NK cells (CD45+CD3-DX5-), B cells (CD45+C3-B220+) and monocytes (CD45+CD3-CD11b+Ly6G-) in total leukocytes using BD LSR-Fortessa at Flow Cytometry Facility (University of Alberta). Results are mean ± SEM of the indicated mice each group. P values were computed using one-way ANOVA followed by Dunnett's multiple comparisons test. *$p<0.05$ when comparing to sham control.

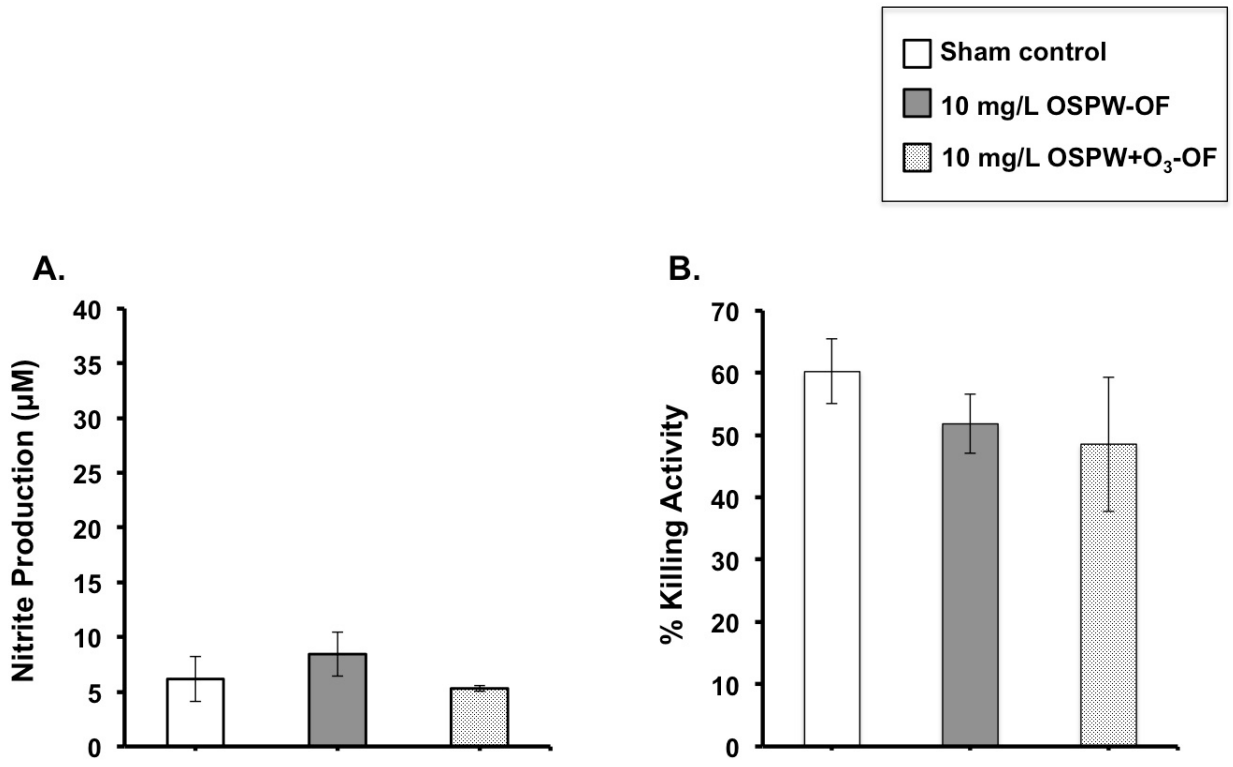

Figure 48. Effects of OSPW-OF acute exposures on *ex vivo* immune cell effector functions in Balb/c mice. Pregnant mice were exposed for 2 weeks to sham control (n=5), 10 mg/L OSPW-OF (n=5), or 10 mg/L OSPW-OF-O_3 (n=6). (A) Peritoneal macrophages were isolated from the exposed mice and then activated with bacterial lipopolysaccharide (LPS) for 18 h, prior to deterination of their nitrite production levels using the Griess reaction (A). Results are mean ± SEM of the indicated mice each group. (B) Splenic natural killer cells were also purified from mice using NK negative isolation kit (Stemcell Technologies, Canada). The target killing activity (i.e. cytotoxicity) of the NK cells was then evaluated using Calcein AM assay. Briefly, NK cells were mixed with Calcein AM-labeled target B cells for 4h. The release of fluorescent calcein from the killed targets then was determined in the cell supernatants using EnSpire 2300 multimode plate reader (PerkinElmer, USA). Results are expressed as percentage of specific killing and demonstrated as mean ± SEM of the indicated mice each group. P values were computed using one-way ANOVA followed by Dunnett's multiple comparisons test. *$p<0.05$ when comparing to sham control.

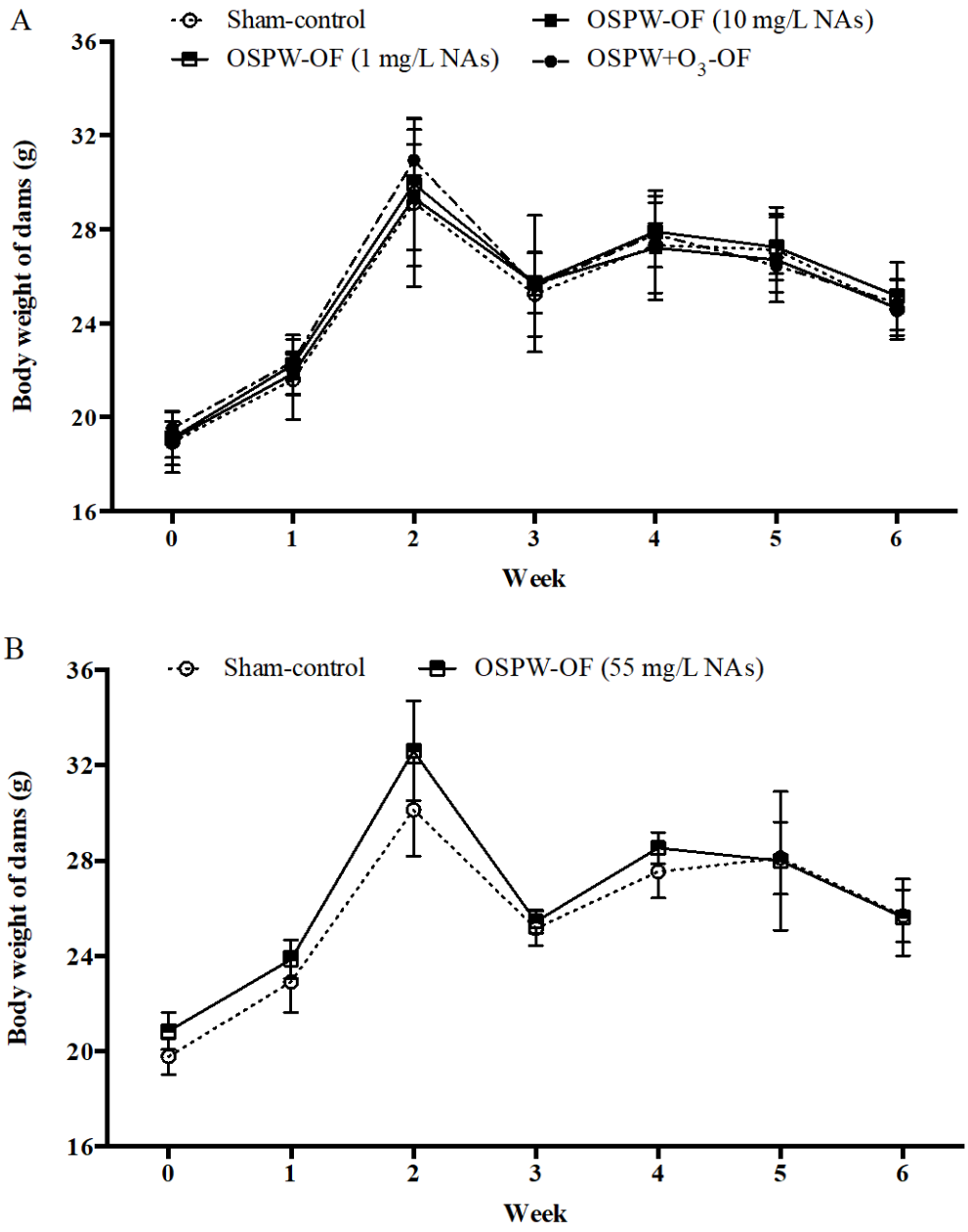

Figure 49. Body weight of female mice during sub-chronic exposure. Animals were gavaged weekly with (A) OSPW-OF (1 and 10 mg/L NAs) and OSPW+O_3-OF, or (B) OSPW-OF (55 mg/L NAs) for six weeks beginning on GD 0. Body weight of each mouse was recorded weekly. Date represent mean ± SEM (n=14-16 for A, and 5-7 for B). At each time point, statistical analysis was performed using one-way ANOVA with Dunnett's *post hoc* test for (A) and Student's *T*-test for (B).

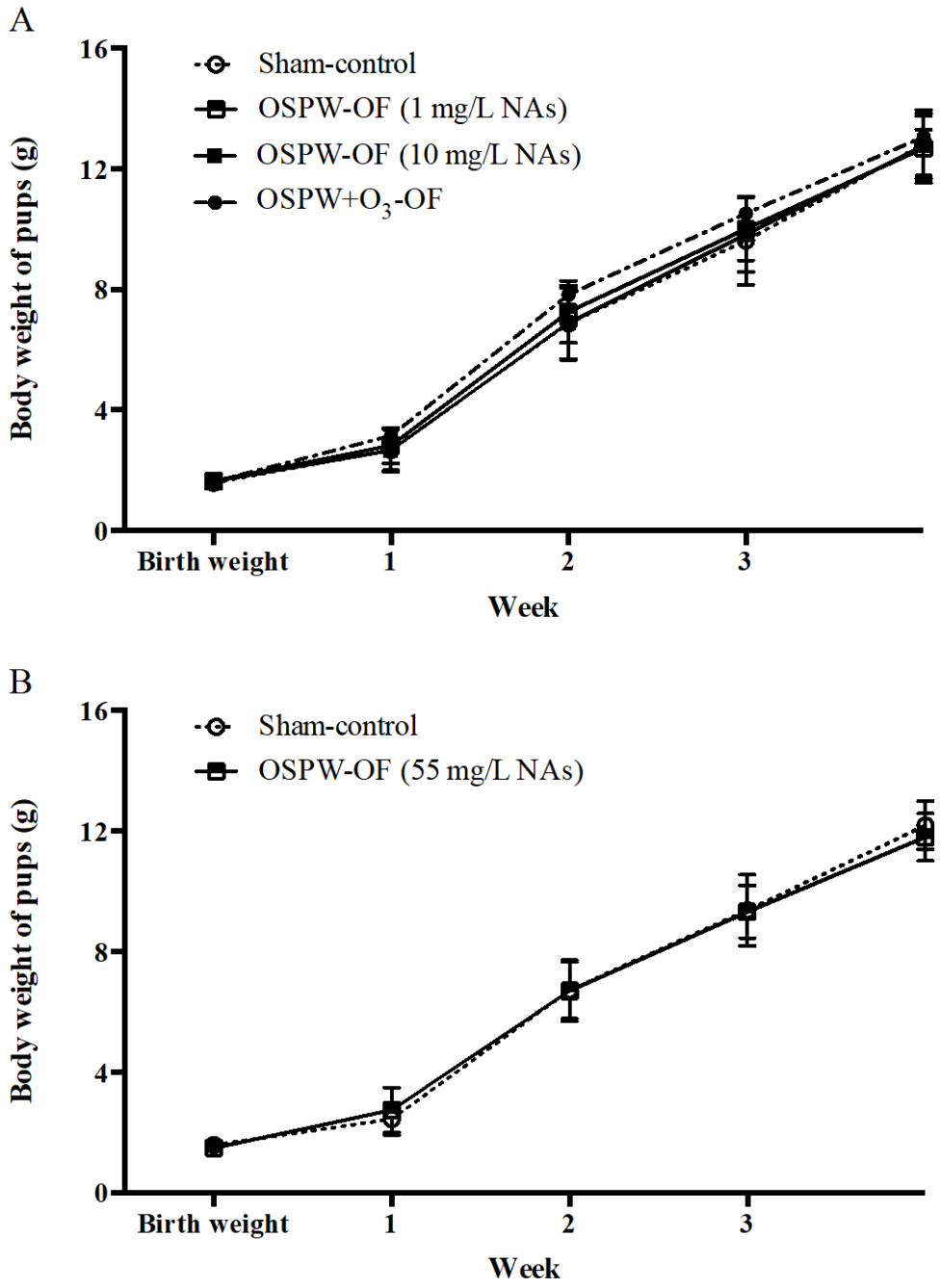

Figure 50. Body weight of pups. Pups were delivered by female mice gavaged with (A) OSPW-OF (1 and 10 mg/L NAs) and OSPW+O_3-OF, or (B) OSPW-OF (55 mg/L NAs) for six weeks beginning on GD 0. Body weight of each pup from each litter was recorded weekly. Date represent mean ± SEM (n=14-16 litters for A, and 5-7 litters for B). At each time point, statistical analysis was performed using one-way ANOVA with Dunnett's *post hoc* test for (A) and Student's *T*-test for (B).

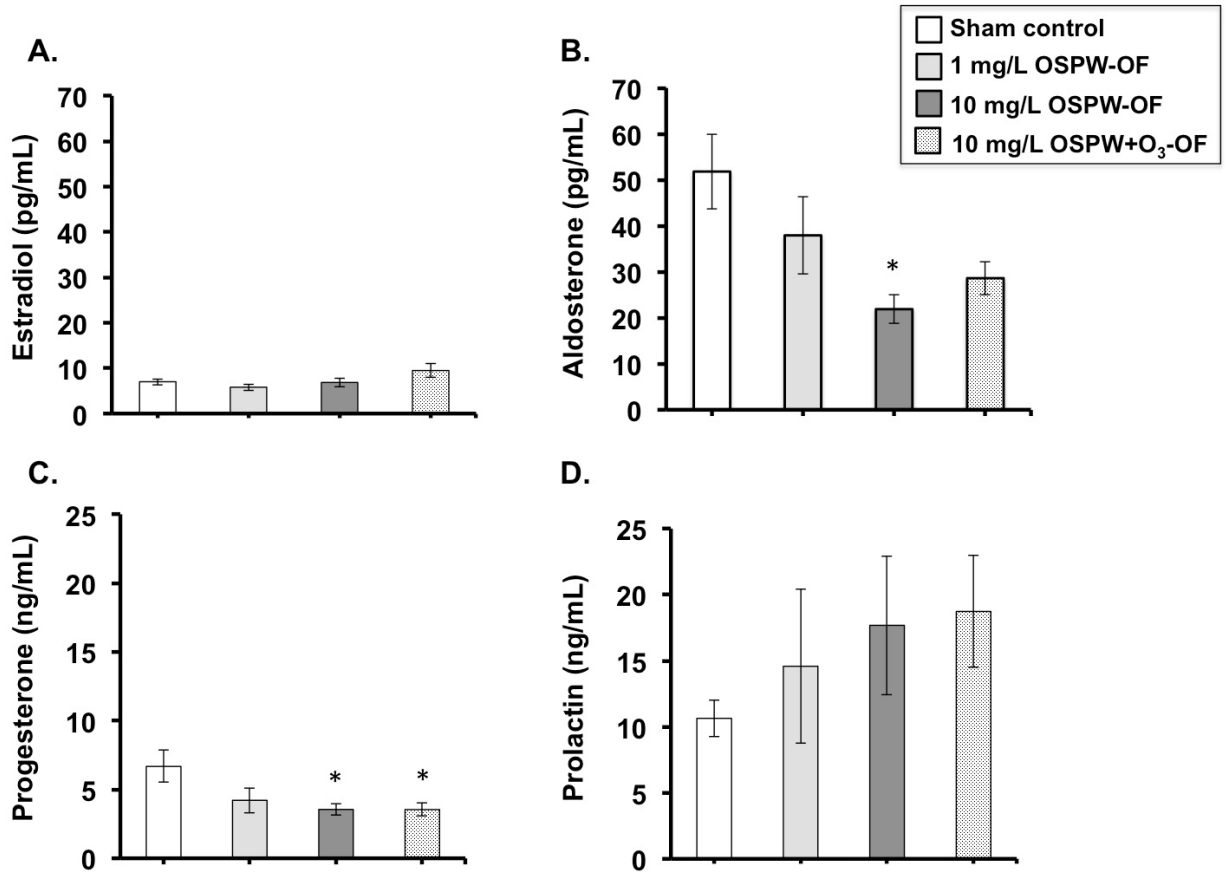

Figure 51. Effects of OSPW-OF sub-chronic exposures on the plasma hormone levels in Balb/c mice. (A) Estradiol, (B) Aldosterone, (C) Progesterone, and (D) Prolactin levels were measured in the plasma of pregnant Balb/c mice after six gavage exposures up to gestational day 42. For each experimental group; sham control (0 mg/L; n=15), OSPW-OF 1 mg/L (n=15), OSPW-OF 10 mg/mL (n=18), and OSPW-O_3-OF 10 mg/L (n=20), mouse blood was collected and the plasma and cell pellets were separated prior to the measurement of hormone levels. Each bar represents the mean ± SEM for each group. P values were computed using one-way ANOVA followed by Dunnett's multiple comparisons test. *$p<0.05$ when comparing to sham control.

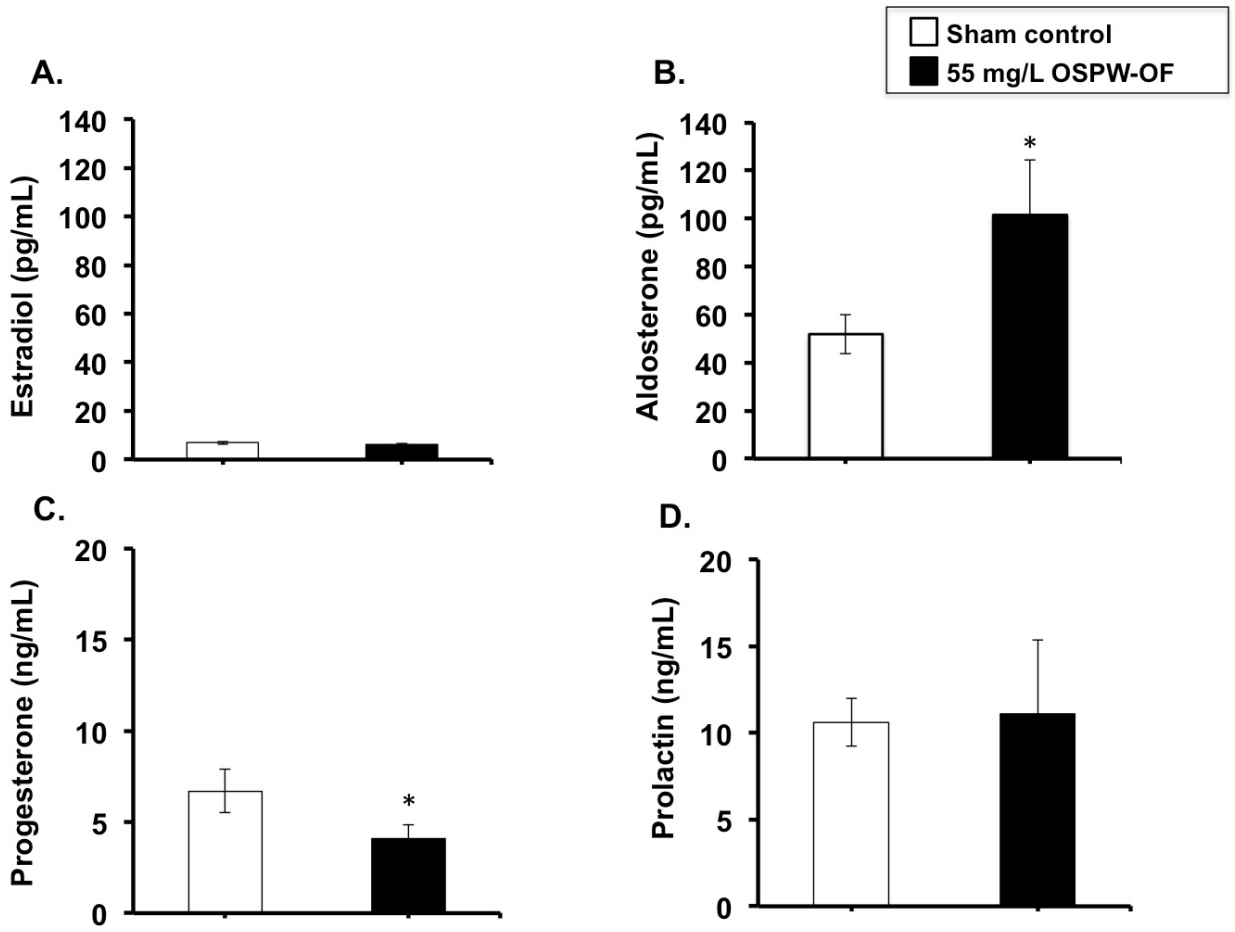

Figure 52. Effects of high dose OSPW-OF sub-chronic exposures on the plasma hormone levels in Balb/c mice. (A) Estradiol, (B) Aldosterone, (C) Progesterone, and (D) Prolactin levels were measured in the plasma of pregnant Balb/c mice after six gavage exposures up to gestational day 42. For each experimental group; sham control (0 mg/L; n=7), and OSPW-OF 55 mg/L (n=5), mouse blood was collected and the plasma and cell pellets were separated prior to the measurement of hormone levels. Each bar represents the mean ± SEM for each group. P values were computed using an unpaired student t test. *$p<0.05$ when comparing to sham control for individual hormones.

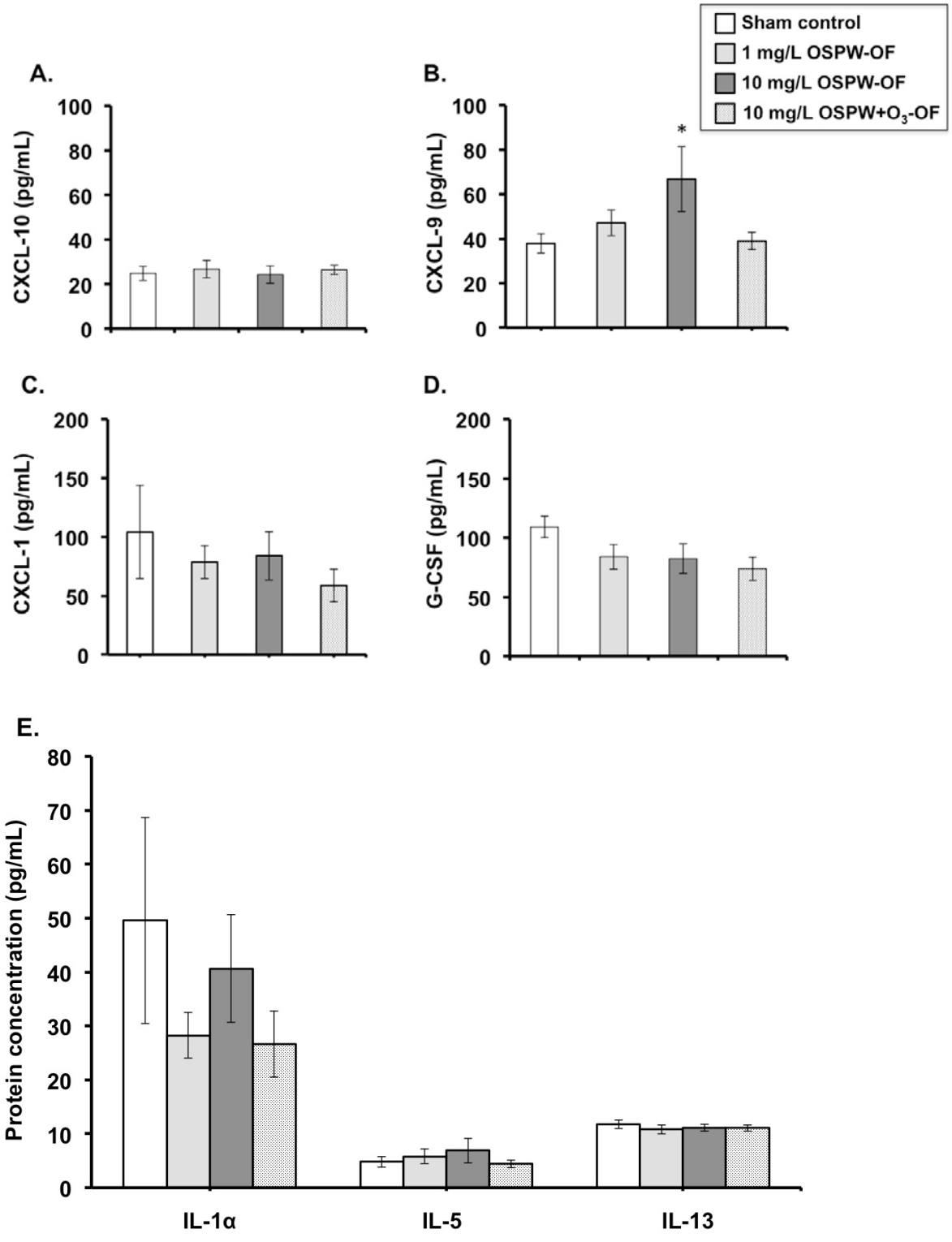
Sham control
1 mg/L OSPW-OF
10 mg/L OSPW-OF
10 mg/L OSPW+O3-OF
A.
CXCL-10 (pg/mL)
B.
CXCL-9 (pg/mL)
*
C.
CXCL-1 (pg/mL)
D.
G-CSF (pg/mL)
E.
Protein concentration (pg/mL)
IL-1α
IL-5
IL-13

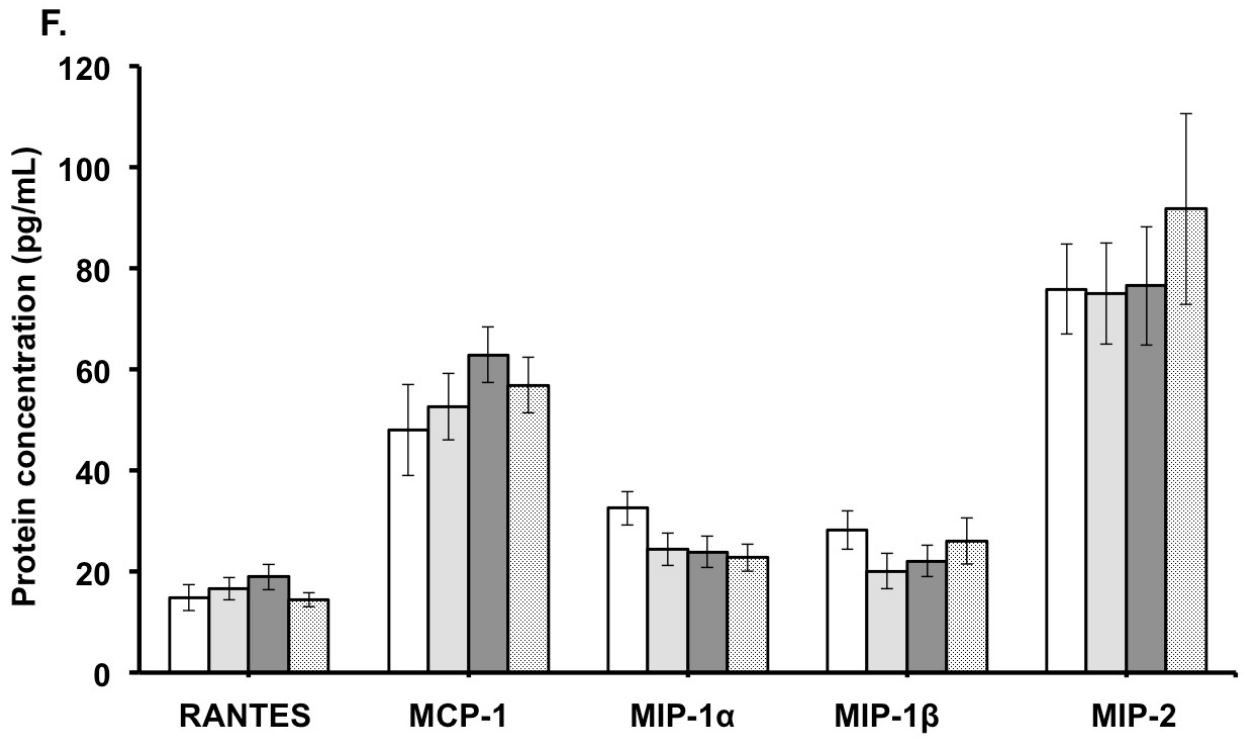

Figure 53. Effects of OSPW-OF sub-chronic exposures on the plasma cytokine levels in Balb/c mice. (A) CXCL-10, (B) CXCL-9 (C) CXCL-1, and (D) G-CSF, as well as (E) IL-1α, IL-5, and IL-13 and (F) RANTES, MCP-1, MIP-1α, MIP-1β, and MIP-2 levels were measured in the plasma of pregnant Balb/c mice after six gavage exposures up to gestational day 42. For each experimental group; sham control (0 mg/L; n=9), OSPW-OF 1 mg/L (n=10), OSPW-OF 10 mg/mL (n=9), and OSPW-O_3-OF 10 mg/L (n=10). Mouse blood was collected and the plasma and cell pellets were separated. Plasma samples were then examined for cytokine protein levels using a bead-based antibody capture assay. Each bar represents the mean ± SEM for each group. P values were computed using one-way ANOVA followed by Dunnett's multiple comparisons test. *$p<0.05$ when comparing to sham control.

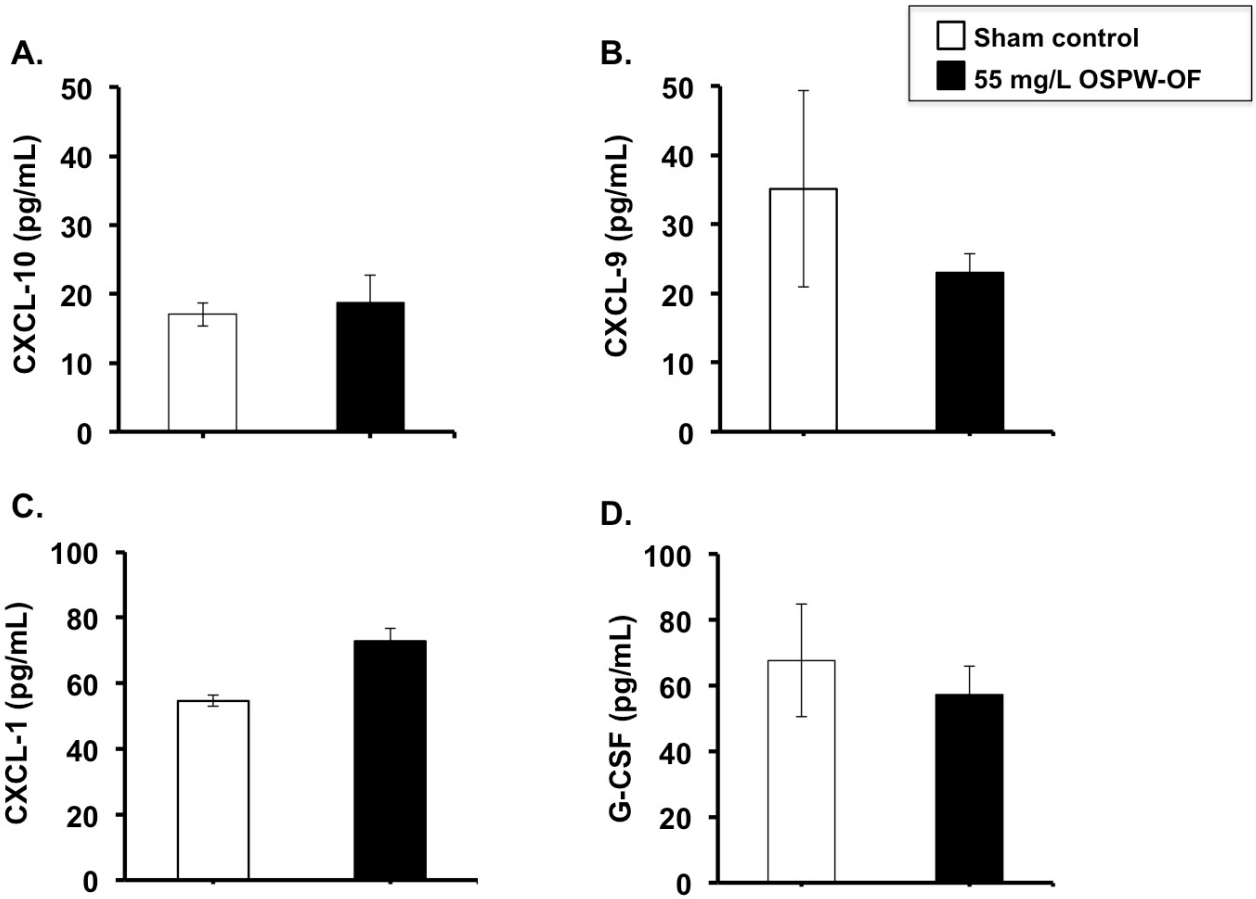
A.
B.
C.
D.
Sham control
55 mg/L OSPW-OF
CXCL-10 (pg/mL)
CXCL-9 (pg/mL)
CXCL-1 (pg/mL)
G-CSF (pg/mL)
0
10
20
30
40
50
60
80
100

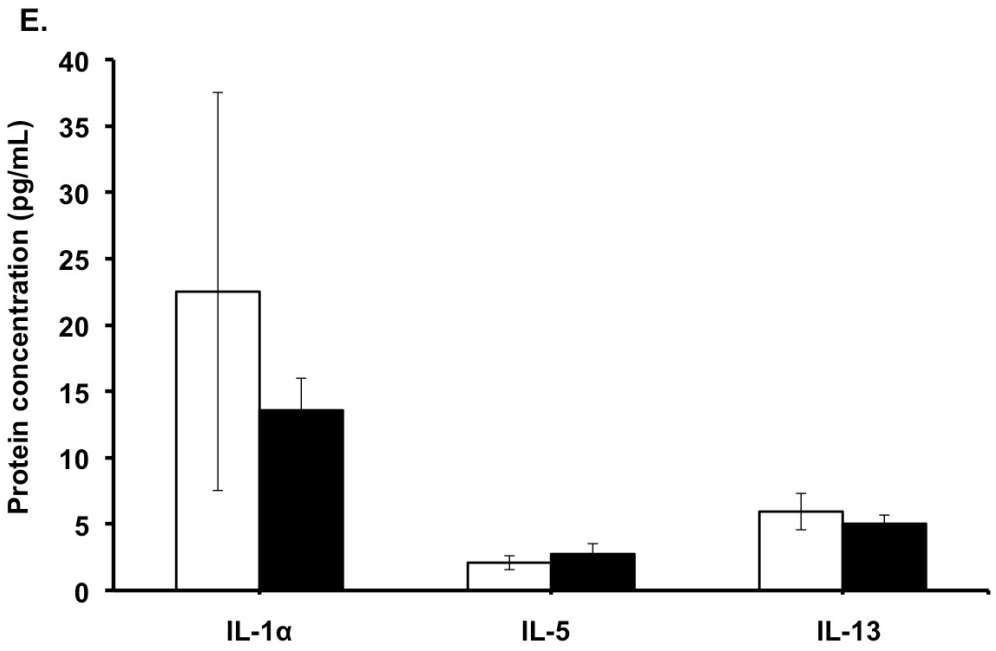

Figure 54. Effects of high dose OSPW-OF sub-chronic exposures on the plasma cytokine levels in Balb/c mice. (A) CXCL-10, (B) CXCL-9 (C) CXCL-1, and (D) G-CSF, as well as (E) IL-1α, IL-5, and IL-13 levels were measured in the plasma of pregnant Balb/c mice after six gavage exposures up to gestational day 42. For each experimental group; sham control (0 mg/L; n=7), and OSPW-OF 55 mg/L (n=5). Mouse blood was collected and the plasma and cell pellets were separated. Plasma samples were then examined for cytokine protein levels using a bead-based antibody capture assay. Each bar represents the mean ± SEM for each group. P values were computed using one-way ANOVA followed by Dunnett's multiple comparisons test. No significance was evident when comparing to sham control.

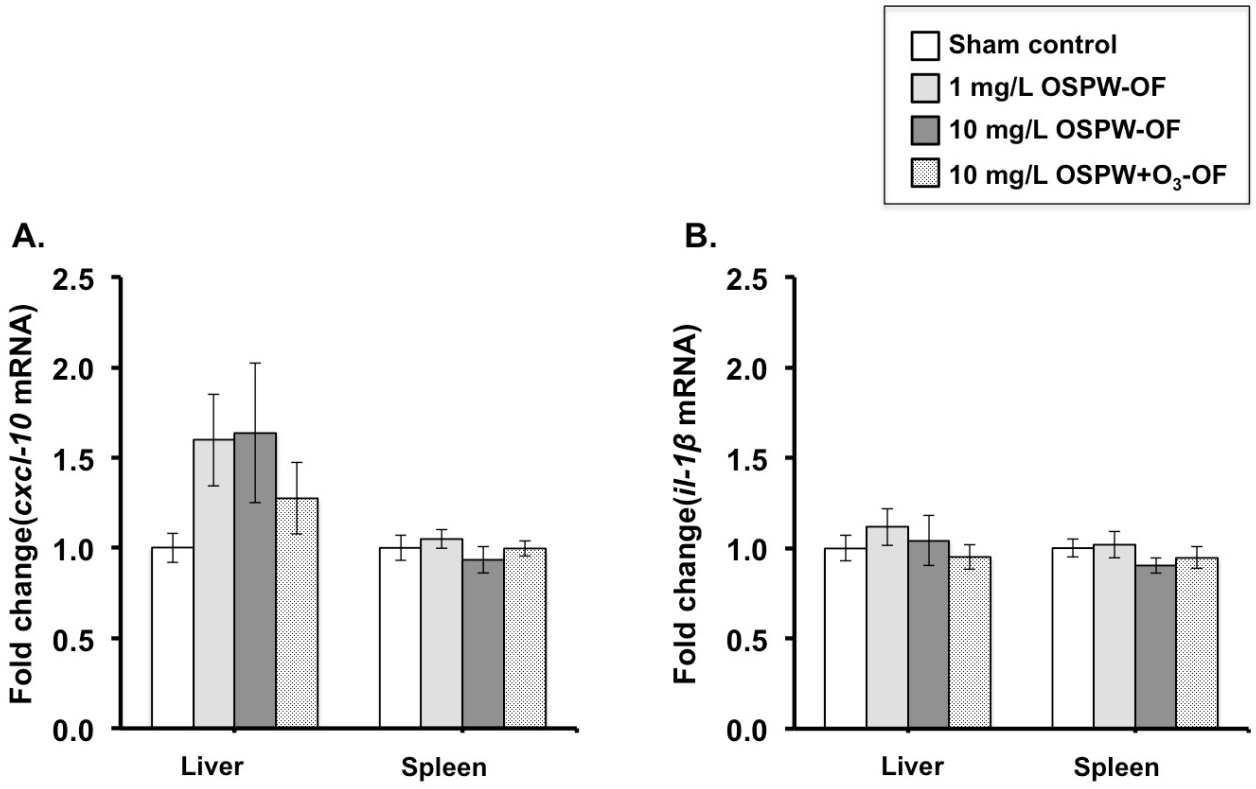

Figure 55. Effects of OSPW-OF sub-chronic exposures on the expression of cytokine genes in Balb/c mice. (A) *cxcl-10* and (B) *il-1β* mRNA expression levels were examined in Balb/c liver and spleen tissues by quantitative PCR after six gavage exposures up to gestational day 42. For each experimental group; sham control (0 mg/L; n=9), OSPW-OF 1 mg/L (n=10), OSPW-OF 10 mg/mL (n=9), and OSPW-O_3-OF 10 mg/L (n=11). Each bar represents the mean ± SEM for each group. P values were computed using one-way ANOVA followed by Dunnett's multiple comparisons test. *p<0.05 when comparing to sham control.

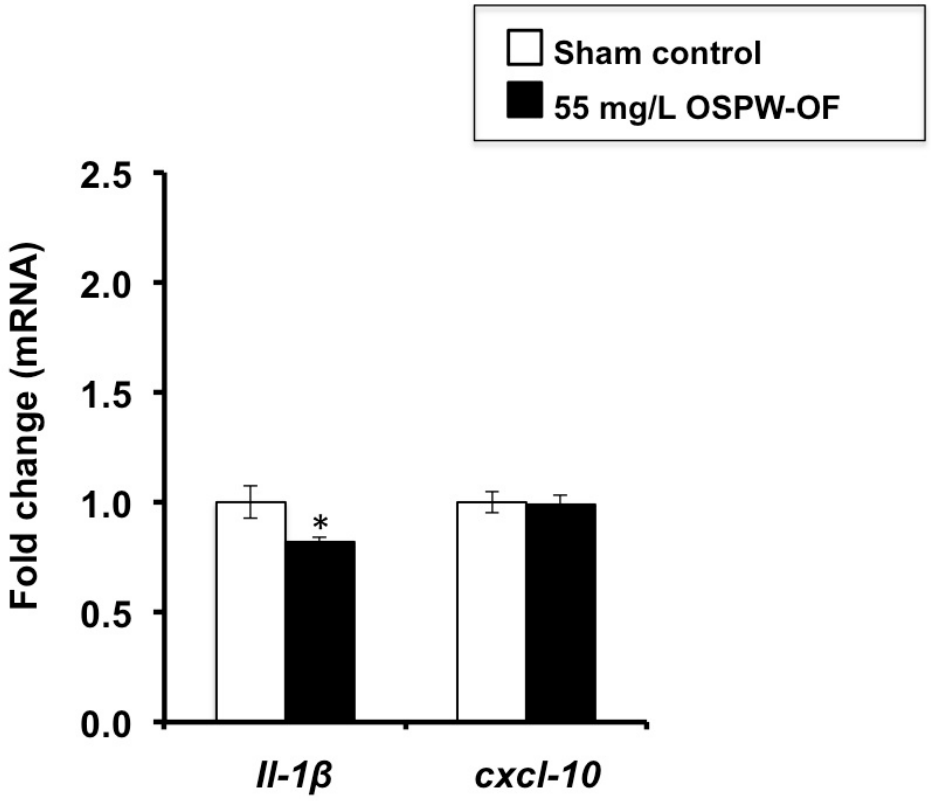

Figure 56. Effects of high dose OSPW-OF sub-chronic exposures on the expression of cytokine genes in Balb/c mice. *il-1β* and *cxcl-10* mRNA expression levels were examined in Balb/c liver tissue by quantitative PCR after six gavage exposures up to gestational day 42. For each experimental group; sham control (0 mg/L; n=7), and OSPW-OF 55 mg/L (n=5). Each bar represents the mean ± SEM for each group. P values were computed using one-way ANOVA followed by Dunnett's multiple comparisons test. *p<0.05 when comparing to sham control.

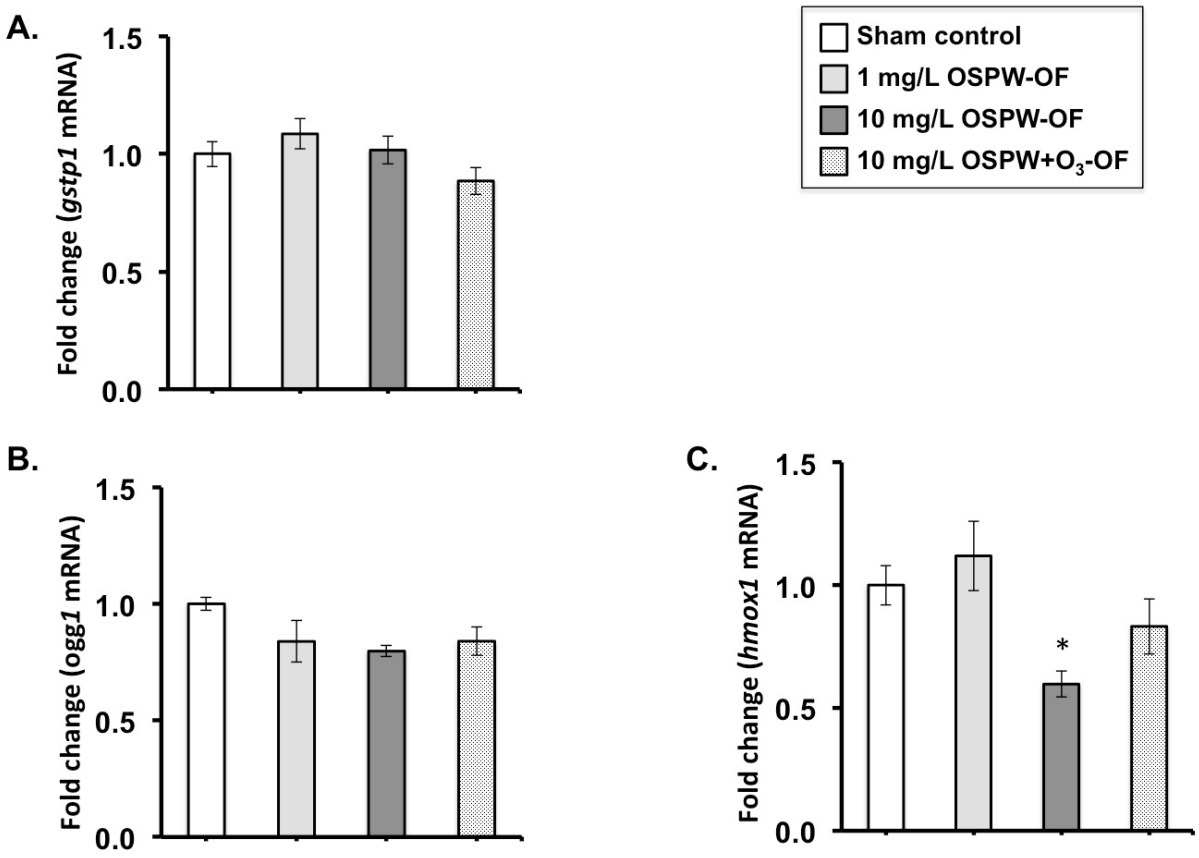

Figure 57. Effects of OSPW-OF sub-chronic exposures on the expression of stress genes in the liver of Balb/c mice. (A) *gstp1*, (B) *ogg1*, and (C) *hmox1* mRNA expression levels were examined by quantitative PCR after six gavage exposures up to gestational day 42 in the liver tissue of exposed mice. For each experimental group; sham control (0 mg/L; n=9), OSPW-OF 1 mg/L (n=10), OSPW-OF 10 mg/mL (n=9), and OSPW-O_3-OF 10 mg/L (n=11). Each bar represents the mean ± SEM for each group. P values were computed using one-way ANOVA followed by Dunnett's multiple comparisons test. *$p<0.05$ when comparing to sham control.

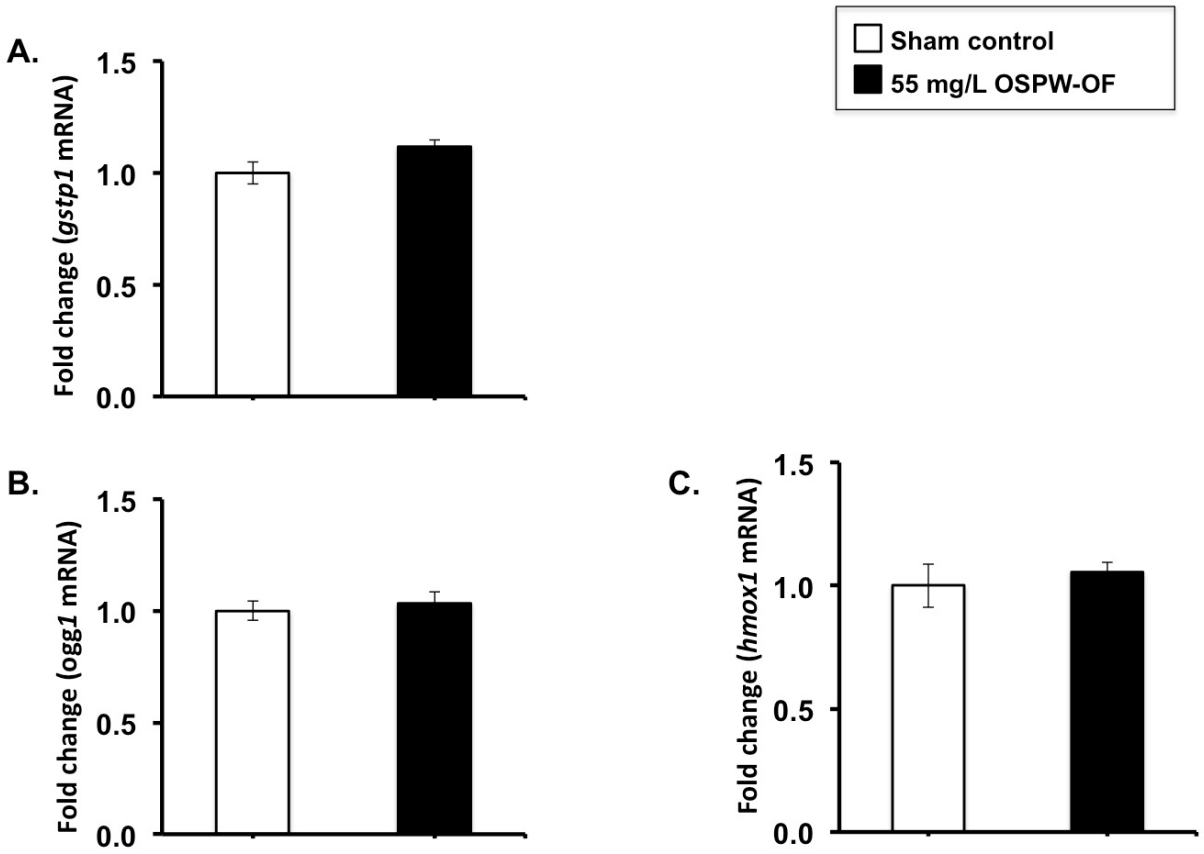

Figure 58. Effects of high dose OSPW-OF acute exposures on the expression of stress genes in the liver of Balb/c mice. (A) *gstp1*, (B) *ogg1*, and (C) *hmox1* mRNA expression levels were examined by quantitative PCR after six gavage exposures up to gestational day 42 in the liver tissue of exposed mice. For each experimental group; sham control (0 mg/L; n=7), and OSPW-OF 55 mg/L (n=5). Each bar represents the mean ± SEM for each group. P values were computed using one-way ANOVA followed by Dunnett's multiple comparisons test. *p<0.05 when comparing to sham control.

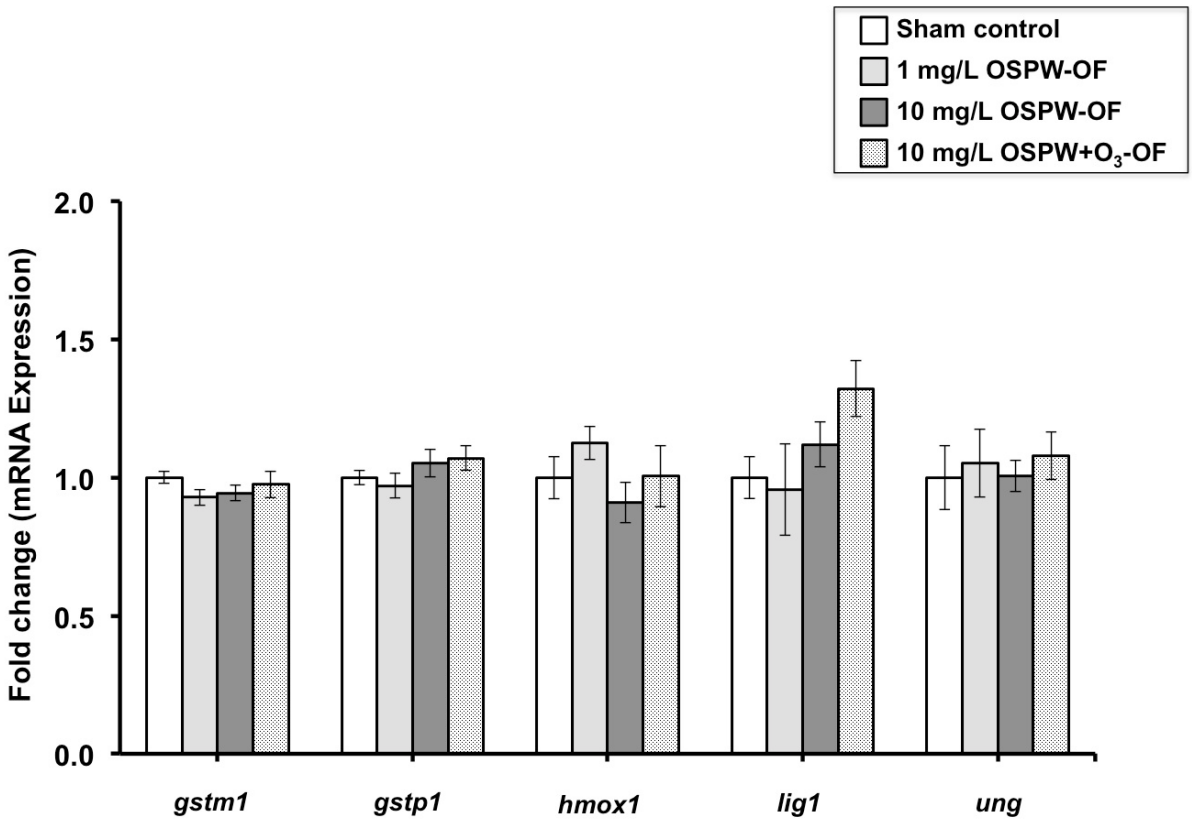

Figure 59. Effects of OSPW-OF sub-chronic exposures on the expression of stress genes in the spleen of Balb/c mice. The indicated stress gene mRNA expression levels were examined by quantitative PCR after six gavage exposures up to gestational day 42 in the spleen tissue of exposed mice. For each experimental group; sham control (0 mg/L; n=8), OSPW-OF 1 mg/L (n=10), OSPW-OF 10 mg/mL (n=6), and OSPW-O_3-OF 10 mg/L (n=10). Each bar represents the mean ± SEM for each group. P values were computed using one-way ANOVA followed by Dunnett's multiple comparisons test. *$p<0.05$ when comparing to sham control.

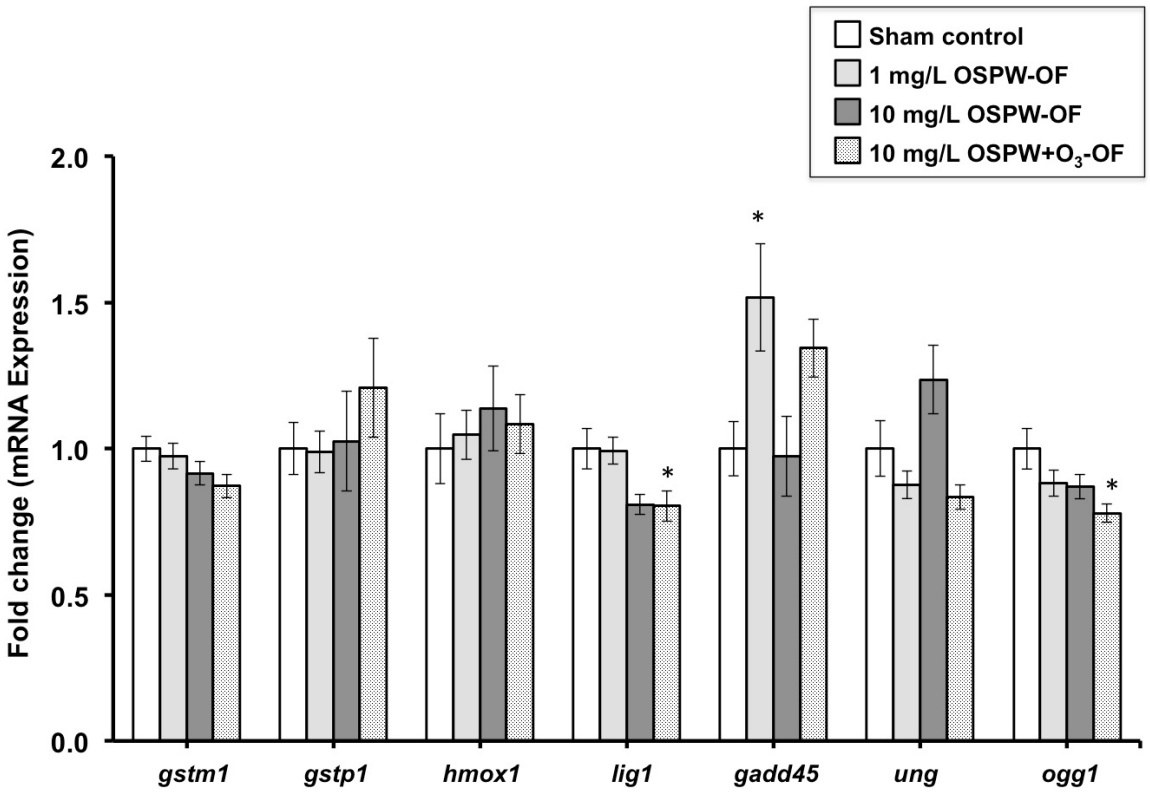

Figure 60. Effects of OSPW-OF sub-chronic exposures on the expression of stress genes in the liver of Balb/c pups. The indicated stress gene mRNA expression levels were examined by quantitative PCR after six gavage exposures up to gestational day 42. For each experimental group; sham control (0 mg/L; n=8), OSPW-OF 1 mg/L (n=10), OSPW-OF 10 mg/mL (n=6), and OSPW-O_3-OF 10 mg/L (n=10). Each bar represents the mean ± SEM for each group. P values were computed using one-way ANOVA followed by Dunnett's multiple comparisons test. *$p<0.05$ when comparing to sham control.

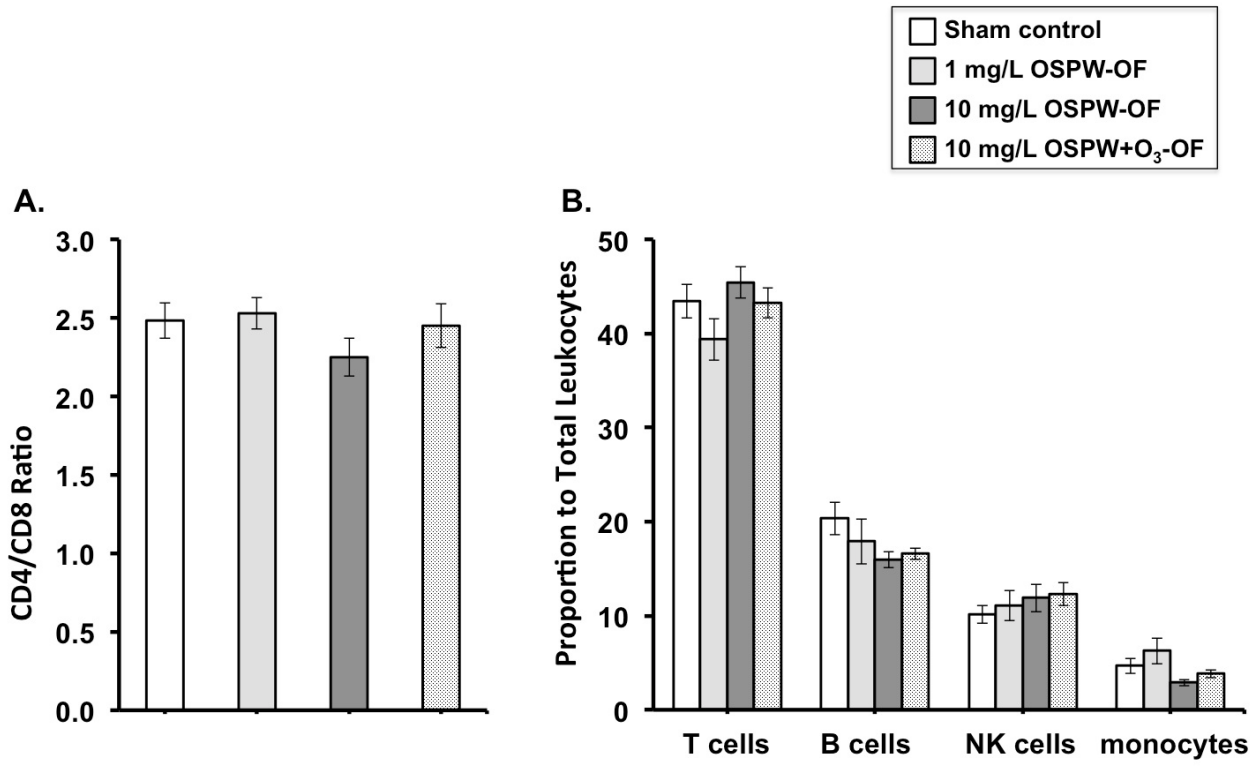

Figure 61. Effects of OSPW-OF acute exposures on peripheral blood immune cell numbers in Balb/c mice. Pregnant mice were exposed for six weeks to sham control (n=15), 1 mg/L OSPW-OF (n=9), 10 mg/L OSPW-OF (n=14), or 10 mg/L OSPW-OF-O_3 with (n=15). Peripheral blood mononuclear cells derived from whole blood of the experimental animals each were assessed by staining for the (A) CD4/CD8 ratio (CD45+CD3+CD4+/ CD45+CD3+CD8+), and (B) the proportions of T cells (CD45+CD3+), NK cells (CD45+CD3-DX5-), B cells (CD45+C3-B220+) and monocytes (CD45+CD3-CD11b+Ly6G-) in total leukocytes using BD LSR-Fortessa at Flow Cytometry Facility (University of Alberta). Results are mean ± SEM of the indicated mice each group. P values were computed using one-way ANOVA followed by Dunnett's multiple comparisons test. *$p<0.05$ when comparing to sham control.

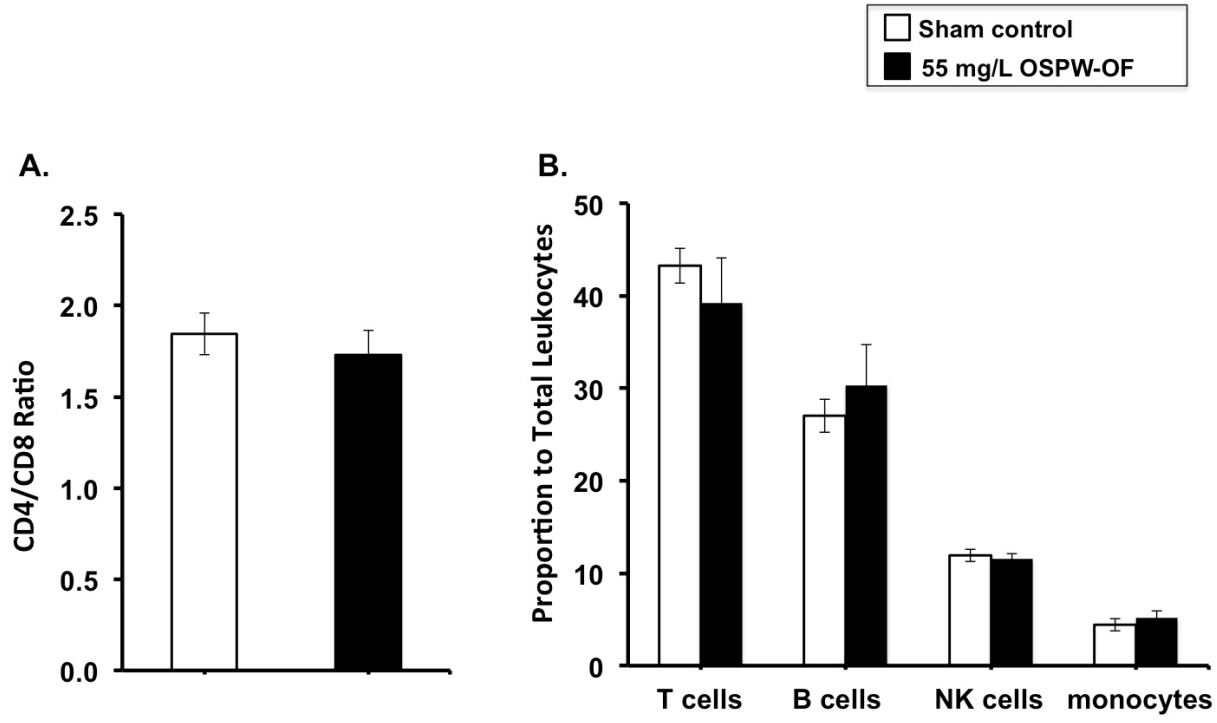

Figure 62. Effects of high dose OSPW-OF acute exposures on peripheral blood immune cell numbers in Balb/c mice. Pregnant mice were exposed for six weeks to sham control (n=6), or 55 mg/L OSPW-OF (n=5). Peripheral blood mononuclear cells derived from whole blood of the experimental animals each were assessed by staining for the (A) CD4/CD8 ratio (CD45+CD3+CD4+/ CD45+CD3+CD8+), and (B) the proportions of T cells (CD45+CD3+), NK cells (CD45+CD3-DX5-), B cells (CD45+C3-B220+) and monocytes (CD45+CD3-CD11b+Ly6G-) in total leukocytes using BD LSR-Fortessa at Flow Cytometry Facility (University of Alberta). Results are mean ± SEM of the indicated mice each group. P values were computed using one-way ANOVA followed by Dunnett's multiple comparisons test. *$p<0.05$ when comparing to sham control.

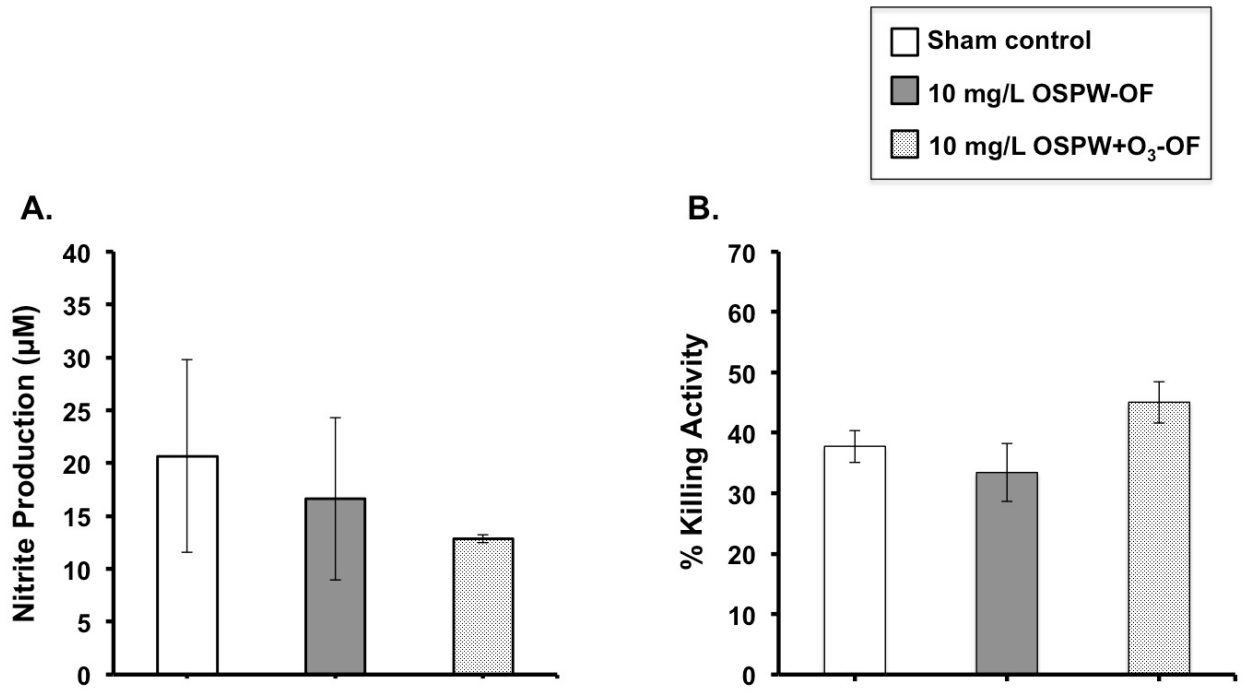

Figure 63. Effects of OSPW-OF acute exposures on *ex vivo* immune cell effector functions in Balb/c mice. Pregnant mice were exposed for six weeks to sham control (n=5), 10 mg/L OSPW-OF (n=4), or 10 mg/L OSPW-OF-O_3 (n=4). (A) Peritoneal macrophages were isolated from the exposed mice and then activated with bacterial lipopolysaccharide (LPS) for 18 h, prior to determination of their nitrite production levels using the Griess reaction (A). Results are mean ± SEM of the indicated mice each group. (B) Splenic natural killer cells were also purified from mice using NK negative isolation kit (Stemcell Technologies, Canada). The target killing activity (i.e., cytotoxicity) of the NK cells was then evaluated using Calcein AM assay. Briefly, NK cells were mixed with Calcein AM-labeled target B cells for 4h. The release of fluorescent calcein from the killed targets then was determined in the cell supernatants using EnSpire 2300 multimode plate reader (PerkinElmer, USA). Results are expressed as percentage of specific killing and demonstrated as mean ± SEM of the indicated mice each group. P values were computed using one-way ANOVA followed by Dunnett's multiple comparisons test. *$p<0.05$ when comparing to sham control.

A.

Tissue	OSPW-OF		Summary
	1 and 10 mg/L	55 mg/L	
Liver	No microscopic changes relative to control	**Mild lipid vacuolation** and **cytoplasmic stippling** (cytoplasmic effects)	The intestine, kidney, placenta, brain and lungs of mice exposed to OSPW-OF have no significant microscopical changes compared to control. There were some **mild effects on the livers and spleens of some animals from 55mg/L group**, but they were suggested to be normal physiologic reactions, not pathologic.
Spleen	No microscopic changes relative to control	Mild hyperplasia of lymphoid germinal centers (a nonspecific change indicating antigenic stimulation)	
Intestine	No microscopic changes relative to control	No microscopic changes relative to control	
Kidney	No microscopic changes relative to control	No microscopic changes relative to control	
Placenta	No microscopic changes relative to control	No microscopic changes relative to control	
Brain	No microscopic changes relative to control	No microscopic changes relative to control	
Lung	No microscopic changes relative to control	No microscopic changes relative to control	

B.

Tissue	OSPW-OF	Summary
	55 mg/L	
Liver	No microscopic changes relative to control	No significant difference was found between the treatment and control groups. It was concluded that exposure of OSPW-OF at this dose had no microscopic anatomic effects on mice.
Spleen	No microscopic changes relative to control	
Intestine	No microscopic changes relative to control	
Kidney	No microscopic changes relative to control	
Brain	No microscopic changes relative to control	
Lung	No microscopic changes relative to control	

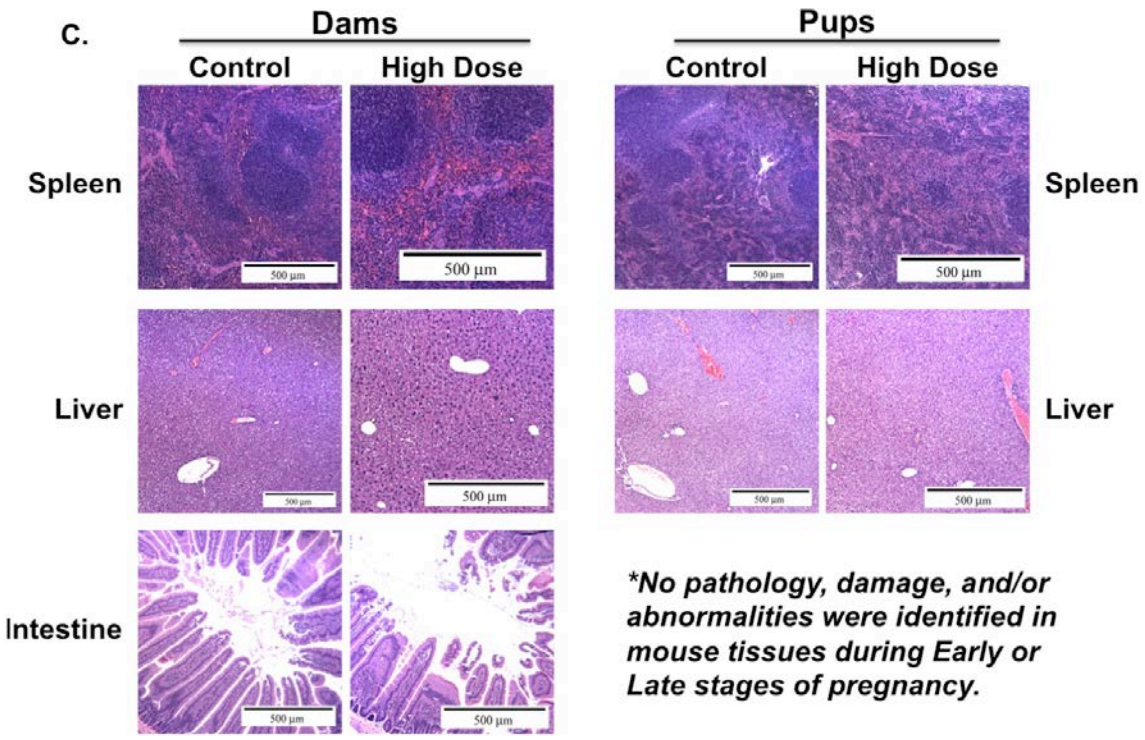

Figure 64. Pathological report summary of the histological effects of OSPW-OF acute exposures in Balb/c mice. Pathological report following acute (A) and sub-chronic (B) exposures to various oral doses of OSPW-OF doses based on NA content ranging from 1 mg/L to 55 mg/L. (C) Representative tissue histological images from female mice (Dams) and pups following sub-chronic exposures in pregnant Balb/c mice.